Technische Universität München
Fakultät für Chemie
Professur für Molekulare Katalyse

Macrocyclic Tetra-Dentate NHC Complexes for Catalysis and Medicinal Chemistry

Marco A. Bernd

Dissertation

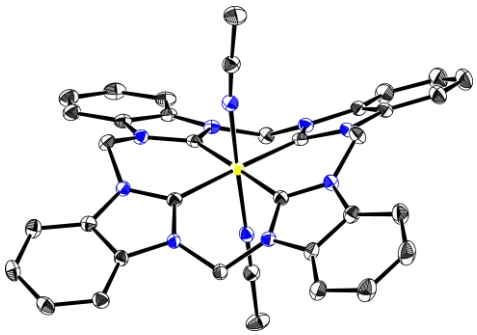
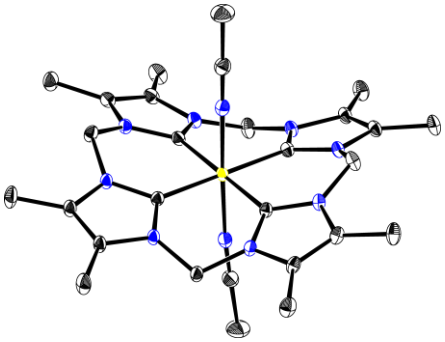
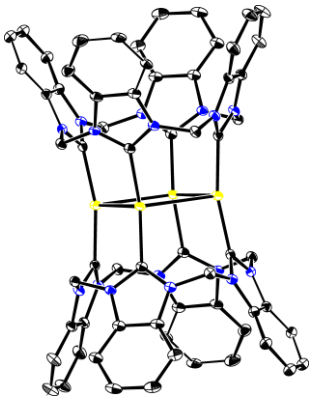
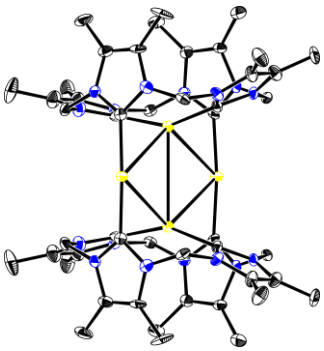

Technische Universität München

Fakultät für Chemie

Professur für Molekulare Katalyse

Macrocyclic Tetra-dentate NHC Complexes for Catalysis and Medicinal Chemistry

Marco Alexander Bernd

Vollständiger Abdruck der von der Fakultät für Chemie der Technischen Universität München zur Erlangung des akademischen Grades eines

Doktors der Naturwissenschaften (Dr. rer. nat.)

genehmigten Dissertation.

Vorsitzender:	Prof. Dr. Matthias J. Feige
Prüfer der Dissertation:	1. Prof. Dr. Fritz E. Kühn
	2. Prof. Dr. Tom Nilges

Die Dissertation wurde am 2. Dezember 2020 bei der Technischen Universität München eingereicht und durch die Fakultät für Chemie am 13. Januar 2021 angenommen.

Even a fool knows you can't touch the stars,

but it won't keep the wise from trying.

Harry Anderson

Die vorliegende Arbeit wurde im Zeitraum von Oktober 2017 bis November 2020 im Fachbereich Professur für Molekulare Katalyse der Technischen Universität München angefertigt.

Mein erster und besonderer Dank gilt meinem Doktorvater

Herrn Prof. Dr. Fritz E. Kühn

Für die reibungslose Aufnahme in seiner Arbeitsgruppe, das mir entgegenbrachte Vertrauen und die Möglichkeit eine spannende Thematik zu bearbeiten. Weiterhin bin ich für die forscherische Freiheit am Arbeitskreis dankbar, die für ein besonderes, angenehmes und produktives Forschungsumfeld schafft.

DANKSAGUNG

Diese Arbeit wurde durch die direkte oder indirekte Hilfe vieler Personen ermöglicht oder erheblich erleichtert. Im folgendem möchte ich mich daher bei allen Personen bedanken, die mich auf meinem Weg unterstütz haben.

Zuerst möchte ich mich bei **Robert Reich** bedanken für seiner organisatorische Arbeit am Arbeitskreis und für seine wissenschaftlichen Beträge in dem von ihm organisierten wöchentlichen Seminaren oder bei Diskussionen im Kaffeeraum. Vieles wäre durch deine Erfahrung und deine Beiträge nicht möglich, bzw. wäre nur mit deutlich mehr Aufwand zu erreichen.

Ein besonderer Dank geht an Frau **Ulla Hifinger**, ohne die unsere Arbeitsgruppe bei weiten nicht so gut funktionieren würde. Danke für die Geduld und Freundlichkeit bei der Hilfe von organisatorischen Belangen.

Für die Einführung in die Thematik der Tetra-NHCs und der Vermittlung aller nötigen Kniffes und Tricks in synthetischer Hinsicht möchte ich mich herzlich bei **Markus Anneser** bedanken. Dein chemisches Verständnis, deine offene und herzliche Art machten die Arbeit und Diskussionen mit dir sehr angenehm. Die abendlichen Diskussionen bei Whiskey oder Bier werde ich vermissen. Durch die Einführung in diese Thematik hast du zum Fundament dieser Arbeit beigetragen.

Weiterhin danke ich **Florian Dyckhoff** und **Jonas F. Schlagintweit** für die gute Zusammenarbeit, welche in einer Publikation mündete, die ich für diese Arbeit zentral halte. Die guten Diskussionen und Anregungen bzgl. Epoxidationskatalyse oder dem Design von etwaigen Komplexen haben diese Arbeit sehr unterstützt. Danke für die Zeit im Labor oder am Feierabend, als auch auf dem gemeinsamen Urlaub in Kalifornien.

Genauso gilt mein Dank **Elisabeth Bauer**. Dank deiner Mithilfe konnten wir zwei Publikation bis zur Veröffentlichung bringen. Die Zusammenarbeit mit dir empfand ich als sehr angenehm und man konnte sich stets aufs dich verlassen.

Weiterhin danke ich **Alexander Böth** und **Ben Hofmann** für das Einbringen ihrer theoretischen Kenntnisse in Bezug auf DFT Rechnungen, welche für das Verständnis von katalytischen Problemen sehr hilfreich waren. Im speziellem möchte ich **Alex** für seine gute Freundschaft danken und für all den Unsinn, den wir zusammen durchlebt haben. **Ben** möchte ich speziell für sein offenes Ohr und sein scheinbar grenzenloses chemisches Wissen danken, dass er stets freudig geteilt oder am Whiteboard visualisiert hat.

Für unzählige Auswertungen von Kristallstrukturen möchte ich ebenfalls **Jens Oberkofler** danken. Dein Schnalzen sowie Murren wenn ich dich erneut mit XRD Aufträgen überschüttet habe war stets Musik in meinen Ohren.

Dann danke ich noch meinen Laborkollegen: **Lorenz Pardatscher** für die gute Freundschaft und Wissbegierigkeit gegenüber dem Medium Internet, welches ich dir meist nicht auf dem einfachsten Weg nähergebracht habe. **Sebastian Hölzl** für deine gute Laune und Stimmung, falls mal wieder Sauerstoff an deine Proben kam. **Daniela Hey**, **Michael Sauer**, **Nadine Tappe** und **Christiane Egger** danke ich für die gute Stimmung im unteren Labor und die offene und direkte Art.

Ich danke ebenso den Leuten aus dem oberen Labor. Hier speziell **Christian Jakob** und **Eva Esslinger**, danke ich für die gute Zeit im und außerhalb vom Labor. Weiterhin danke ich **Bruno Dominelli**, **Alexander Imhoff**, **Andreas Hinterberger**, **Pauline Fischer**, **Nicole Dietl**, **Felix Kaiser**, **Tommy Hofmann**, **Dawen Xu**, **Han Li** und **Kevin Yang**. Es hat mir viel Freude bereitet mit euch allen in einer so großartigen Gruppe zu arbeiten.

Wenn auch recht kurzfristig möchte ich meinen letzten Forschungspraktikanten **Wolfgang Büchele**, aka. **Yogi**, danken. Durch deine selbstständige und genaue Arbeit ist sehr angenehm dich zu betreuen und ich hoffe, dass du meine Thematik in Form einer Masterarbeit und Doktorarbeit weiterführen wirst.

Ich danke meinen **Eltern** für das Vertrauen und die Unterstützung, die ich seit je her genießen darf. Durch euch war es mir möglich das Studium der Chemie aufzunehmen, abzuschließen, meine Promotion zu beginnen und mit dieser Arbeit abzuschließen. Ihr habt mich bedingungslos unterstützt und mir jegliche Freiheit gewährt wodurch ich mich selbst zu entfalten konnte. Durch eure Anleitung und die Vermittlung eurer Werte bin zu der Person geworden, die ich heute bin.

Zuletzt möchte ich mich bei meiner Freundin **Friederike** bedanken. Du gibst mir Kraft, Motivation und den Ausgleich, den ich im Leben brauche. Du machst mich glücklich. Im Rückblick auf unsere drei gemeinsamen Jahre freue ich mich auf unsere gemeinsame Zukunft.

KURZZUSAMMENFASSUNG

Diese Arbeit handelt von der Erweiterung der metalloganischen Chemie um makrozyklische tetradentate *N*-heterozyklische Carben Komplexe. Hierbei wird die Synthese von fünf neuen bioinspirierten 16-gliedrigen makrozyklischen tetradentaten NHC Liganden beschrieben, welche für die Synthese von neuen Übergangsmetallkomplexen verwendet werden. Zwei Ligand Systeme, welche auf 4,5-Dimethylimidazol bzw. Benzimidazol basieren, werden zur Synthese von neuen Fe^{II}- und Fe^{III}-Komplexe verwendet. Die Charakterisierung der Komplexe erfolgt mittels NMR-Spektroskopie, ESI-MS, Cyclovoltammetrie, Elementaranalyse und der Röntgenstrukturanalyse, falls geeignete Einkristalle der entsprechenden Verbindungen gezüchtet werden konnten. Die Komplexe sind derartig gestaltet, dass sie das aktive Zentrum von CYP-Enzymen imitieren, jedoch auf NHCs basieren. Daher werden diese Komplexe in der katalytischen Epoxidierung von *cis*-Cycloocten und anderen Olefinen getestet. Hierbei wird die Wirkung der unterschiedlichen Elektronendichte-Donierung der Liganden auf die Eisenzentren im Vergleich zum Imidazol-basierten System untersucht. Die methylsubstituierten Komplexe zeigen eine hohe Anfangsaktivität in der katalytischen Epoxidierung, welche jedoch durch eine erheblich geringere Stabilität kompensiert wird, wodurch unvollständige Umsätze resultieren. Beide Effekte können durch die vergleichsweise höhere Elektronendichte an den Eisenzentren erklärt werden, die durch den +I-Effekt der Methylgruppen induziert wird. Die Benzimidazol-basierten Komplexe zeigen hingegen eine geringere Aktivität und dementsprechend eine höhere Stabilität. Dies resultiert aus der geringeren Donorstärke des Liganden im Vergleich zu den Imidazol oder 4,5-Dimethylimidazol basierten Systemen. Diese geringere Aktivität ist für die Epoxidierung von unreaktiveren Substraten als *cis*-Cycloocten von Vorteil. Die elektronischen Effekte der Liganden auf das jeweilige Metallzentrum konnten mit Hilfe von Dichtefunktionalberechnungen verifiziert werden.

Diese makrozyklischen Ligand Systeme wurden ebenfalls zur Synthese neuer Komplexe mit Metallen der Nickel- und Kupfergruppe verwendet, welche in Studien zur Wachstumshemmung von Krebszellen evaluiert wurden. Für diese Studien wurden Imidazol- und Benzimidazol-basierte Komplexe verwendet. Die Gold oder Nickel(II) Komplexe zeigten schwache inhibitorische Wirkung gegen die getesteten Krebszell-Linien. Die Palladium(II) und Platin(II) Komplexe wiesen im Allgemeinen gute inhibitorische Aktivitäten auf, wobei die Benzimidazol-basierten Komplexe in bestimmten Zelllinien keine Aktivität aufwiesen. Eine vergleichsweise höhere Aktivität der Benzimidazol- zu Imidazol-basierten Komplexen kann auf deren höherer Lipophilie zurückgeführt werden. Zusätzlich wurden die Benzimidazol-basierten Komplexe mit Metallen der Nickelgruppe auf deren Photolumineszens Eigenschaften untersucht. Hierbei konnte für den Palladium(II) Komplex starke Phosphoreszenz Eigenschaften nachgewiesen werden.

Die verbliebenen drei Liganden wurden für die Synthese neuer Eisenkomplexe verwendet. Zwei Liganden basieren dabei auf 4,5-Diphenylimidazol bzw. 4,5-Bis(*para*-fluorphenyl)imidazol. Diese sollen als Teil einer zukünftigen Testreihe zur Untersuchung der Epoxidationsaktivität verwendet werden. Hierbei steht die sinkende Donorstärke der Liganden auf Grund von zunehmender Fluorierung im Fokus. Der verbleibende Ligand ist Imidazol-basiert, enthält jedoch im Gegensatz zur literaturbekannten Variante deuterierte Methylenbrücken. Die hieraus hergestellten Eisen-Komplexe dienen für zukünftige Studien zur Untersuchung von Mechanismen der Katalysatordeaktivierung unter oxidativen Bedingungen.

ABSTRACT

In this thesis, the synthesis of five new sets of bio-inspired ligand systems comprising of 16-membered macrocyclic tetradentate *N*-heterocyclic carbenes is reported. The ligands were utilized in the synthesis of novel transition metal complexes. Two ligand systems incorporating solely 4,5-dimethylimidazole or benzimidazole as NHC moieties were used in the synthesis of novel Fe^{II} and Fe^{III} complexes. These complexes are fully characterized by means of NMR spectroscopy, ESI-MS, circular voltammetry, elemental analysis and single crystal X-ray diffractometry, if suitable crystals of the respective compounds could be obtained. All four complexes are designed to mimic the active site of CYP enzymes based on NHCs. These complexes are utilized in the investigation of the effect of electron donating and withdrawing substituents at the NHC backbone position and the impact on catalytic epoxidation of *cis*-cyclooctene and other olefins, compared to the unsubstituted imidazole-based complexes. The methyl-substituted complexes show high activity in epoxidation reactions, which is compromised due to considerably lower stability leading to rapid degradation of the complexes. Both effects can be attributed to the increased electron density at the iron centers, which is induced by the +I effect by the methyl groups. The benzimidazole based complexes exhibits lower activity and higher stability, resulting from the electron withdrawing effect of the expanded aromatic system. This lower activity seems to be beneficial in the epoxidation of less reactive substrate than *cis*-cyclooctene. The described electronic effects are verified using density functional calculations.

These macrocyclic ligand systems are also utilized for the synthesis of novel group 10 and 11 complexes, which were applied for antiproliferative studies on cancer cells. Here, the imidazolyl- and benzimidazolyl-based complexes showed no remarkable activity for gold or Ni^{II} complexes. The Pd^{II} and Pt^{II} complexes show generally good activity, with the benzimidazolyl complexes show even higher activity but inactivity in certain cell lines. This higher activity can be attributed to the higher lipophilicity compared to imidazolyl based complexes. The benzimidazolyl-based complexes harboring group 10 elements are additionally investigated for photoluminescence properties, resulting in the detection of high phosphorescence for the Pd^{II} complex.

Furthermore the synthesis of novel iron complexes utilizing the remaining three ligands are reported. Two of these ligands incorporate 4,5-diphenylimidazole and 4,5-bis(*para*-fluorophenyl)imidazole as NHC moiety and are designed for investigating the effects of successive fluorination and the impact on epoxidation activity. The remaining ligand is based on imidazole moieties but contains deuterated methylene bridges. The corresponding iron complexes are designed for future kinetic studies to investigate a possible catalyst degradation pathway in epoxidation catalysis.

List of Abbreviations

BPMCN	*N,N'*-bis(2-pyridylmethyl)-*N,N*-dimethyl-trans-1,2-diaminocyclohexane
bpmen	*N,N'*-bis(2-pyridylmethyl)-1,2-diaminoethane
cisplatin	*cis*-diamminedichloridoplatinum(II)
CV	cyclic voltammetry
cyclam	1,4,8,11-tetraazacyclotetradecane
CYP	cytochrome P450 oxidase
DCM	dichloromethane
dG	deoxyguanosine residue
DFT	density-functional theory
DLC	delocalized lipophilic cations
DMSO	dimethyl sulfoxide
ESI-MS	electrospray ionization mass spectrometry
EtOH	ethanol
Et_2O	diethyl ether
G4-DNA	guanine quadruplex
h	hour
HeLa	human cervical cancer cell line
HIV	human immunodeficiency viruses
HMDS	hexamethyldisilazane
HPPO	hydrogen peroxide to propylene oxide
IC_{50}	half maximal inhibitory concentration
MeCN	acetonitrile
MeOH	methanol
min	minute
MTBE-MO	methyl *tert*-butyl ether-propylene oxide
MTO	methyltrioxorhenium
MTT	3-(4,5-dimethylthiazol-2-yl)-2,5-diphenyltetrazolium bromide
NADPH	reduced nicotinamide adenine dinucleotide phosphate
NHC	*N*-heterocyclic carbene
NMR	nuclear magnetic resonance
OTf	trifluoromethanesulfonate
PBATA	(((5-methyl-2-oxido-1,3-phenylene)bis(methylene))bis(azanetriyl))tetraacetate
PDP	2-((-2-(-1-(pyridin-2-ylmethyl)pyrrolidin-2-yl)pyrrolidin-1-yl)methyl)pyridine
Prx	peroxiredoxin
PyTACN	1-(2-pyridylmethyl)-4,7-dimethyl-1,4,7-triazacyclononane
ROS	reactive oxygen species
SARS-COV-2	severe acute respiratory syndrome coronavirus 2
SC-XRD	single crystal x-ray diffraction
sMMO	soluble methane monooxygenases
SM-PO	styrene monomer-propylene oxide
TEP	Tolman electronic parameter
THF	Tetrahydrofuran
TM	transition metal
tmc	1,4,8,11-tetramethyl-1,4,8,11-tetraazacyclotetradecane
tmima	tris((1-methylimidazol-2-yl)methyl)amine)

TOF	turnover frequency
TON	turnover number
tpa	tris(2-pyridylmethyl)amine
Trx	thioredoxin
TrxR	thioredoxin reductase
TS-1	titanium silicalite-1
UV/Vis	ultraviolet/visible spectroscopy
XRD	x-ray diffraction
WWI	world war I
$\Delta\psi_m$	mitochondrial membrane potential

CONTENT

1 INTRODUCTION

1.1 Overview of carbene as a ligand

Carbenes are electron-deficient carbon compounds with two non-bonding electrons and two substituents.[1] The non-bonding electrons may be present in the same orbital with antiparallel spins or in different orbitals with parallel spins in the ground state (see figure 1). The applicability of such carbenes as ligands forming stable transition complexes has been reported for the first time in 1964 by E. O. Fischer.[2] Such Fischer-carbene complexes are singlet state carbenes, due to a significant gap between their singlet and triplet ground state, and bear usually an π-donating substituent in α-position (*e.g.* amino, alkoxy, ...). The resulting metal-carbene is based on the interaction of two closed-shell singlet fragments. The bond arises from σ-based carbene-metal donation and from metal-carbene π-back donation. The electrons are polarized towards the metal, making the carbene electrophilic. The carbon-metal shows a partial double bond character due to the π-back bonding of the metal to the carbene. This character diminishes towards a single bond character, the higher the stabilization of the carbene becomes by its α-substituents. Fischer-carbenes usually coordinate to metals in low oxidation state.[3-7] Ten years after the discovery of carbene complexes by E. O. Fischer, R. R. Schrock reported a type of carbene complex whose electronic structure vastly differs from Fischer-carbenes (see figure 1).[8] These complexes are poorly stabilized carbenes, as the neighboring alkyl- or alkylidene groups are unable to stabilize the carbene significantly. Therefore, the gap between its singlet and triplet ground state is small, resulting in an occupation of the triplet state. The resulting metal-carbene bond has high covalent character due to the coupling of two triplet fragments. The electrons are equally distributed between the carbene and the metal forming a true double bond. Schrock carbene complexes display a nucleophilic carbon-metal bond, which is formed with early transition metals in high oxidation states.[3-5, 7] Both types of carbenes are highly important for organometallic synthesis and are applied as catalysts in several industrial processes, as they accelerate reactions like cycloaddition, benzannulation, and several nucleophilic substitutions for Fischer-carbenes[9] and most significantly olefin metathesis for Schrock-carbenes. In 2005, the development of the metathesis method was awarded with a Nobel prize.[10-12]

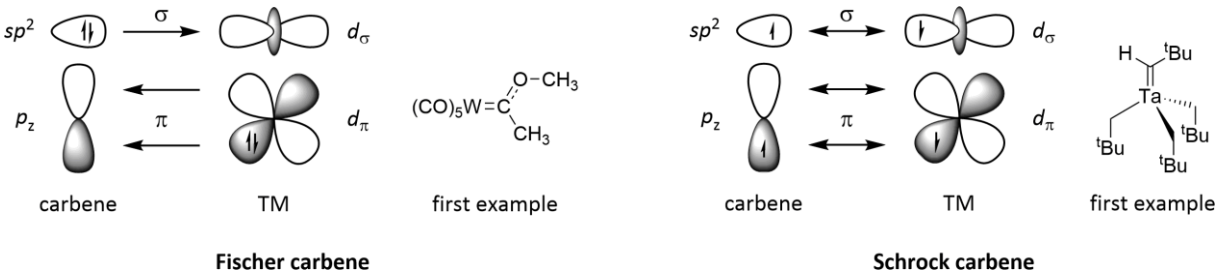

Figure 1: Schematic representation of the important orbital interactions in Fischer-type carbene (left) and Schrock-type carbenes (right) with transition metals and their first published example.[2, 4, 8]

1.2 NHCs and its development as a ligand system

N-heterocyclic carbenes (NHC) are a relatively new class of ligands for mainly transition metals. They consist of a cyclic carbene structure with at least one α-amino substituent[6], although two α-amino substituents are more common. This ligand class is the result of developments regarding Fischer-type carbene chemistry. Due to the high degree of stabilization the carbene receives *via* donation from the neighboring groups into its empty p-orbital, they require little to no π-backdonation from the metal. Therefore, NHCs can be seen as Fischer-type carbenes.[3] The first reports for NHC ligands were published by Wanzlick in the early years of 1960,[13-14] followed by the first NHC complexes in the year 1968 by Wanzlick[15] and Öfele[16]. After these initial studies Lappert *et al.* discussed the potential of *N*-heterocyclic carbenes as ligands in the 1970s.[17-20] The difficulty in consistently generating and isolating carbene complexes as well as the lack of applications stalled the development of this new ligand class. The break-through took place in 1991, when Arduengo *et al.* isolated the first free *N*-heterocyclic carbene.[21-24] The approach was based on the cyclic imidazole structure as the carbene core structure, which has been reported to be beneficial to generate stable carbene complexes.[15, 17-20] The innovative feature included the utilization of adamantyl substituents at the amino groups, sterically shielding the subsequently generated carbene from dimerization *via* the Wanzlick equilibrium.[4, 14] Through this approach, it was possible to stabilize the free carbene (see figure 2, Arduengo's carbene) in solution under inert conditions, which was unheard of before this point. These results brought NHCs back into the focus of a broad scientific community, as it was now easily possible to generate NHC complexes through addition of a suitable metal precursor to such a free carbene. Later developments broadened the scope of appliable ligand precursors. An *in-situ* deprotonation of azolium salts in presence of a suitable transition metals could generate carbene complexes in an easily and accessible way. Subsequently, NHCs proofed to be powerful ligands for homogeneous catalysis and found a myriad of applications in other fields of chemistry, like organometallic materials (metal-organic frameworks, liquid crystals, coordination polymers, photoactive materials, …) or metallopharmaceuticals.[25]

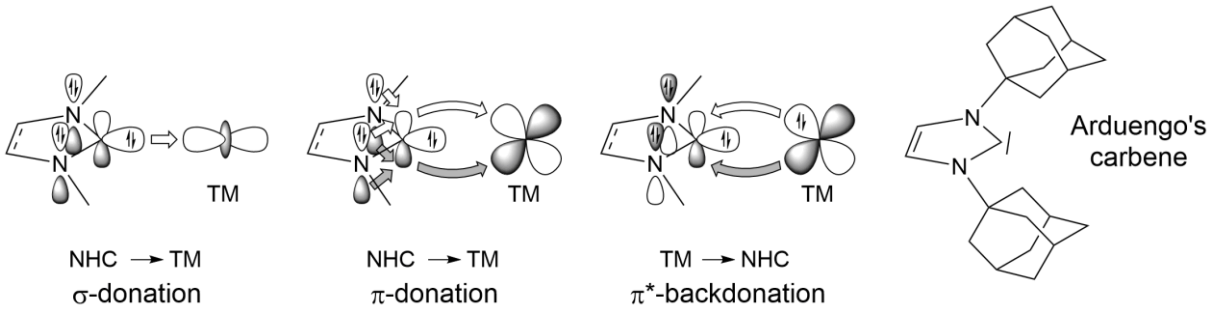

Figure 2: The three dominant orbital interactions between a NHC and a transition metal forming a carbene-metal bond, including σ-donation from the NHC to the metal (left), delocalization of the NHC π-system *via* the empty p-orbital of the carbene into an unoccupied metal orbital (2nd from left) and π-backdonation from an occupied d-orbital of the metal to the empty p-orbital of the carbene (3rd from left).[26] The first stable free NHC, reported by Arduengo, is depicted on the right side.[21]

The classic point of view put NHCs and its bonding property in correspondence to electron-rich phosphanes (e.g. trialkylphosphanes, possessing strong donor capabilities and negligible π-accepting abilities) due to theoretical studies on the electronic structure.[1] Furthermore, NHCs are able to bind metal centers incapable of π-backdonation, like main group elements or rare earth metals, which has been pleaded as an empirical finding of their pure-donor capability for some time. Such complexes (*e.g.* with Mg, B, Al, Ga, Th, Si, Y, Sm, Ba)[27-35] can be viewed as donor-adducts, similar to ammonia or ether complexes. Investigations on complexes harboring alkaline earth metals *via* NMR spectroscopy and x-ray diffractometry showcased a range from covalent bonding with lighter elements (*e.g.* Mg) to a high degree of ionic bonding for heavier elements (*e.g.* Ba). As π-backdonation is impossible for these cases, π-donation from the substituents (usually *N*-donors) of the carbene into the empty p-orbital was assumed to render such complexes kinetically stable. Therefore, it was assumed that NHCs resemble an amplification of Fischer-carbenes in terms of decreased π-backbonding compared to Schrock-carbenes. This was confirmed by early theoretical studies that computed a high electron donation from the α-amino substituent into the unoccupied p-orbital of the carbene. Therefore the requirement of metal to carbene π-backdonation was presumed to be negligible.[1, 26]

NHCs can be utilized as strong ligands or replace phosphane ligands in already investigated fields, as they offer similar donor strength combined with several advantages. The most profound are easier modifiability to tune their steric and electronic features, higher air and thermal stability and lower toxicity. Furthermore, NHCs do not tend to dissociate from the metal center, preventing degradation of the complexes and therefore do not require an excess of ligand when applied in catalysis.[36] Among a high variety of possible frameworks for NHCs, five-membered rings, imidazol-2-ylidene and imidazolin-2-ylidene, are the most common motifs used to generate NHC-complexes. Other frameworks are seen rarely and often resemble a special application.[4] Within these five membered ring structures, saturated NHCs based on imidazolin-2-ylidene skeletons have higher basic character, and therefore higher donation capabilities than unsaturated NHCs based on imidazol-2-ylidene.[37]

Modification of the NHC ligand system can be easily performed *via* modifying the *N*-substituents, also known as the “wingtip” positions, or modifying the saturated or unsaturated positions of the five-ring motif, also known as the “backbone” positions.[5, 36, 38-40] Modification of the *N*-substituents allows for the modulation of the electronic properties as well as the steric properties of the carbene and consequently the coordinated metal. Addition of electron withdrawing groups at this position results in decreased donation of the amines to the empty p-orbital of the carbene, decreasing the donation capabilities to the metal center. This effect also applies *vice versa*. Applying substituents with steric demand results in carbenes with less compulsion to dimerize as part of the Wanzlick equilibrium. Furthermore, the steric effect may shield the coordinated metal and/or influence other ligands.[1, 4, 41-43] Modification of the “backbone” position mainly influences the electronic properties of

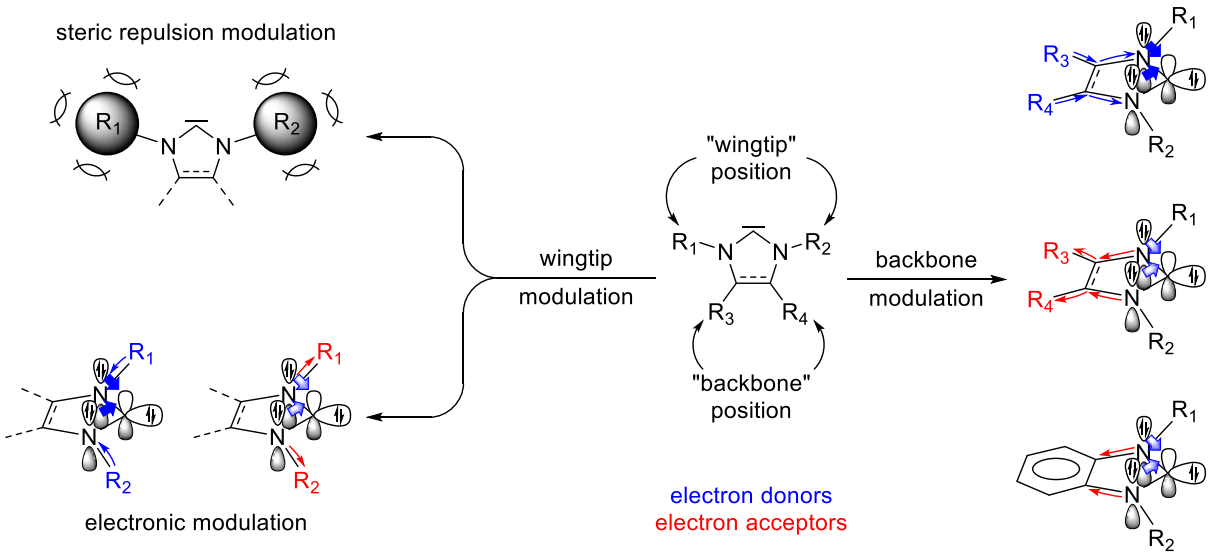

Figure 3: Major modification possibilities for NHCs, based upon 5 membered ring systems. The "wingtip" offers steric and electronic modification. Modification of the "backbone" primarily results in modulation of electronic properties, as steric effects do not directly impact the metal center and only slightly other coordinated ligands.[1]

the carbene, as these substituents usually do not interfere sterically with the metal center. Addition of electron donating groups at the backbone increases the electron density at the carbene and consequentially at the metal center. Electron withdrawing groups have the opposite effect, as well as enlarging the aromatic functionality, as it is the case for benzimidazole.[1, 37, 44] According to these properties NHCs were utilized by numerous research groups in homogeneous catalysis and pushed their development from a relatively new field to a widely applied ligand system on equal with cyclopentadienyl and/or phosphanes.[6, 40, 45-48]

More recent investigations on the electronic properties of NHCs led to the conclusion that their π-accepting capability cannot be neglected. Several reports have shown that the empty π, π* orbital of the NHC can contribute to the carbene-metal bond.[1] Although there have been earlier reports suggesting this situation, wide acceptance followed after Meyer *et al.* demonstrated the existence of π-backbonding by computational analysis of an tripolar Ag^{I}-NHC complex and the subsequent Cu^{I} and Au^{I} derivatives.[49] Here, the π-backbonding was estimated to contribute to 15-30 % of the overall orbital interactions.[1]

In general, NHCs give access to a ligand format, of which the synthesis is usually remarkably easy. They offer a stabilization of a vast range of transition metals in various oxidation states as well as main group elements and a high diversity in the steric and electronic properties. Through these properties, the ligand can be fine-tuned almost at wish.[37]

1.3 Epoxidation catalysis

1.3.1 Out-dated and state of the art industrial synthesis

Epoxides are strained three-membered heterocycles, consisting of two carbon atoms and one oxygen atom. The interest in such compounds lies in its reactivity, as the strained three-membered ring can be regio- and stereoselectively opened by a wide variety of nucleophiles, depending on the environment. The resulting 1,2 functionality is a common biological motif and thereby has a major significance for the organic synthesis of fine and bulk chemicals. Although there are other means of synthesis, the most common one is the oxidation of alkenes.[50] As oxidants, hydrogen peroxide, peracids, alkyl hydroperoxides or oxygen are applied, usually in the presence of a TM catalyst.[51]

The demand on global scale is by far greatest for ethylene oxide and propylene oxide, the simplest representatives of this compound class. Both of them are mainly used in polymer industry for the synthesis of polyglycols or polyurethanes. Other applications are as surfactants, epoxy resins or for the synthesis of organic carbonates.[51-54] Ethylene oxide can be synthesized *via* the direct oxidation of ethylene, employing oxygen from air or pure oxygen as oxidant. The reaction is catalyzed *via* a heterogeneous catalyst system based on silver nanoparticles supported on various matrices, depending on the process.[55] This process can only be performed for substrates without an allylic stabilization of the olefin. Applying propylene to this process results in the formation of acrolein or acrylic acid as main products.[56]

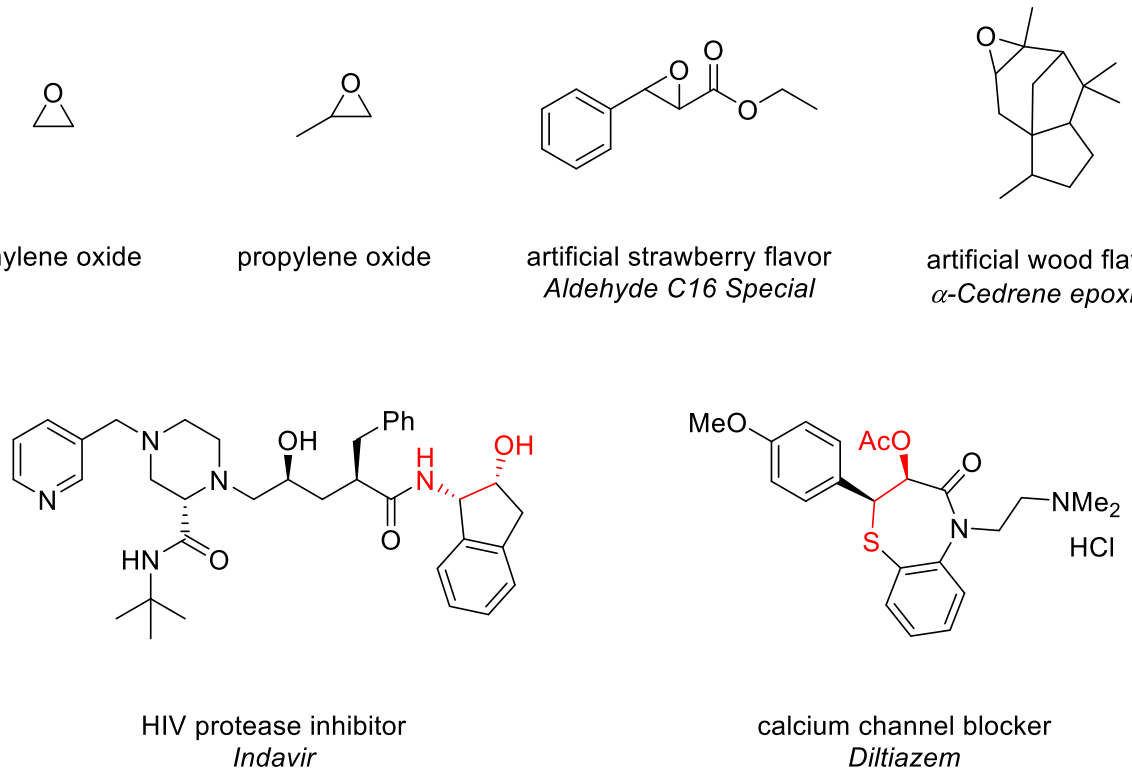

Figure 4: Examples of epoxides for polymer industry (top left), fragrances/flavors (top right) and pharmaceuticals, which include an epoxide as synthesis step (bottom, former epoxide marked red).[57-58]

The chlorohydrin route is a two-step process, applying propylene, chlorine and water, of which the latter two generate hypochlorous acid as an intermediate, to obtain the respective propylenchlorohydrin isomers. The second step is the dehydrochlorination of these isomers with calcium- or sodium hydroxide to obtain propylene oxide, which is purified *via* distillation.[56, 59]

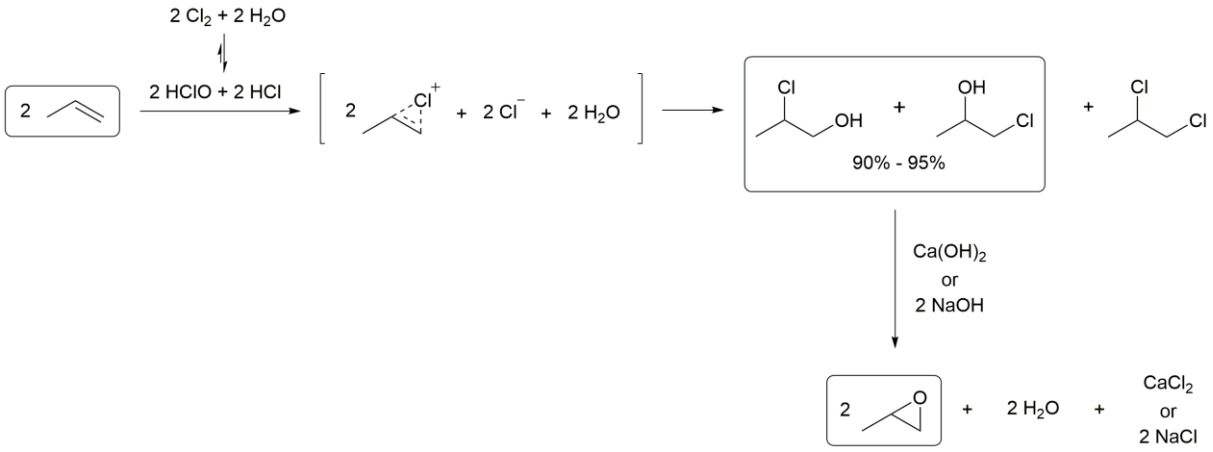

Scheme 1: Chlorohydrin process depicted for the production of propylene oxide as example.[59]

The major disadvantage of the chlorohydrin process is the disposal problem of the unwanted side products. 1,2-dichloropropane has little usage and is accounted generally as a loss in yield and high effort has to be made to remove all remaining hydrocarbons from the residue brine solution (~5 w%) before it can be discarded into the wastewater stream. The separation of calcium or sodium chloride is not economically feasible, due to its low value. The disposal problems can be circumvented at large-scale production plants (>100 000 tons/y), as they are often integrated within chlorine production plants and can recycle the chlorine salts *via* electrolysis and convert the 1,2-dichloropropane to propene for recycling or propane for combustion.[56, 59]

Due to the highly corrosive nature of this process and the generation of side products, focus was shifted on the development of more efficient pathways for epoxidation. The utilization of hydrogen peroxide would be beneficial as this would be highly atom-economic due to water being the only side product. However, the oxidation potential of hydrogen peroxide using conventional catalysts, available at that time, was not sufficient for this reaction.[59] Therefore, processes were developed utilizing organic peroxides readily converting olefins to epoxides. Examples would be the SM-PO (styrene monomer) and MTBE-PO (methyl *tert*-butyl ether) processes, named after the coupling product which is generated from the side products of the processes. [59-60]

As the economic efficiency of the production of propylene oxide was dependent on the market situation of the side products, a great interest was put in the development of coproduct-free processes. The cumol process also utilizes organic peroxides, but the side product, a hydroxide species, can be recycled *via* reduction with hydrogen gas. The next development step sought to find a process,

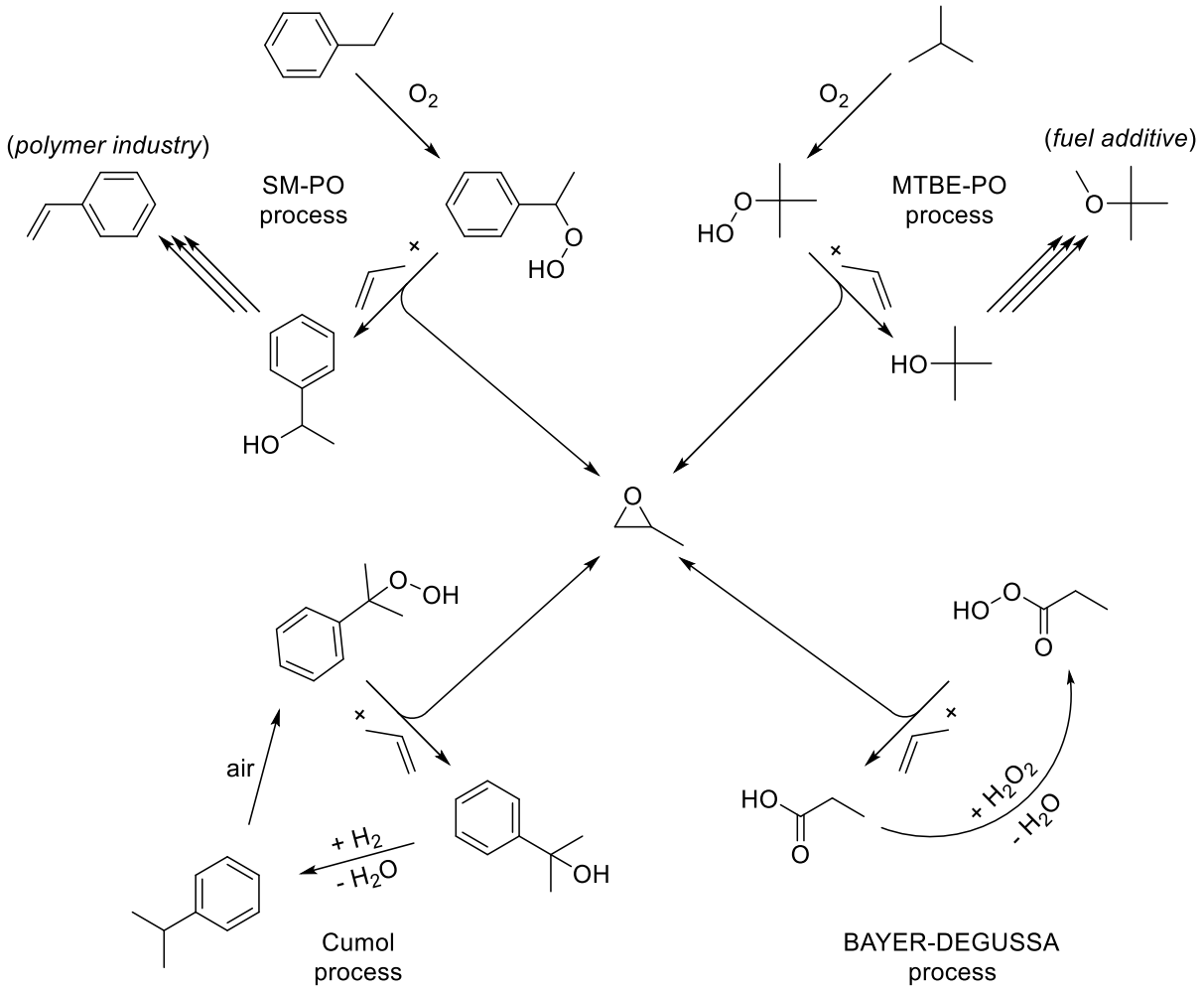

Scheme 2: Different processes for the synthesis of propylene oxide utilizing coupling reagents.[59]

to transfer an oxygen to propylene, without any reduction of the side product being required. This was realized with the Bayer-Degussa process utilizing propionic acid. The propionic acid is converted with hydrogen peroxide to the corresponding peracid, which transfers an oxygen atom to the olefin. Upon oxygen transfer the propionic acid is reformed.[59]

All processes utilizing a coupling agent have the disadvantage that side reactions like ring opening of the epoxide may occur. To circumvent this, a process without nucleophilic species would be required. This was achieved with the direct conversion of propylene with hydrogen peroxide using titanium silicalite-1 (TS-1) as catalyst in the HPPO (hydrogen peroxide to propylene oxide) process. The titanium atoms form a hydroperoxide complex with hydrogen peroxide at the active center, which is stabilized by protic solvents, preferably methanol. This complex is able to transfer an oxygen atom to the double bond of an olefinic molecule. The reaction takes place within the network of pores, which have a hydrophobic character suppressing side reactions almost completely resulting in selectivity to propylene oxide of more than 98%. The selectivity towards the target molecule depends on the tunable diameter of the pores, acting as a molecular sieve.[59, 61-62]

1.3.2 Homogeneous systems

Homogeneous epoxidation catalysts are scarce in industrial scale production processes, as the metal precursors are usually expensive, and the synthesis may include multiple steps. Furthermore, homogeneous systems often entail a challenging separation from the product stream and usually can rarely be reused, due to low overall stability. On the other hand, homogeneous systems offer superior activity, selectivity, tolerance for intricate olefin systems as well as functional groups and have a rather large substrate scope. [63] Furthermore, the defined structure of homogeneous catalysts allow for easier mechanistic investigations compared to heterogeneous systems, as no surface effects and less diffusion effects have to be considered. Numerous homogeneous catalysts are known, which typically are based on early transition metals. Whereas there are complexes based on Ti-, V-, Cr-, W-, Mn-, Co-, Ru- and Mo-catalysts, a detailed focus will be set on rhenium and iron complexes in the following chapters.[64-70]

The most prominent organometallic rhenium complex is methyltrioxorhenium(VII) (MTO), which shows tremendous versatility as oxidation catalyst. MTO was first reported in 1978,[71] in-depth investigations of this compound as catalyst for oxidation reactions was later reported by the groups of Herrmann and Espenson. Beside its catalytic oxidative reactivity for alkynes, sulfides, phosphines and halides, MTO was particularly investigated as epoxidation catalyst under mild reaction conditions. The generally accepted mechanism proposed by Herrmann *et al.* involves two separate reaction cycles including the formation of a mono- or bis(η_2-peroxo) species. These peroxo species react with an olefin double bond consecutively converting it to the corresponding epoxide (see scheme 3).[72-75]

Other reactions which can be catalyzed by MTO are the formation of aldehydes/ketones/acids from olefins, the oxidation of aromatic compounds, aldehyde olefination and olefin metathesis.[76] Efforts have been made to modify the alkyl group of the MTO structure to investigate possible beneficial or stabilizing effects on the catalysts system. It has been reported that the elongation of the alkyl chain enables β-H elimination or radical decomposition, both inactivating the catalyst system.[70] Although MTO offers appealing activity in epoxidation catalysis, rhenium as the starting material and the sophisticated complex synthesis are rather expensive to see a broad industrial scale application.

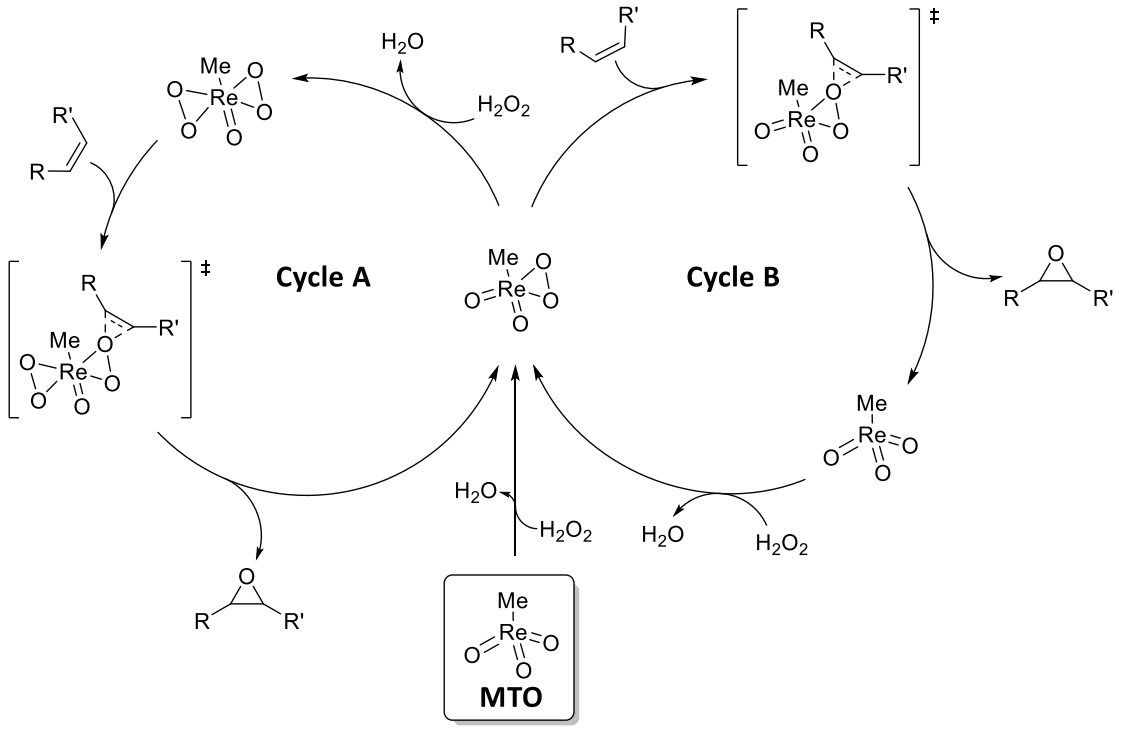

Scheme 3: Mechanism of epoxidation reaction catalyzed by MTO. Two active species (mono-η_2-peroxo, cycle B; bis-η_2-peroxo, cycle A) are able to transfer oxygen to the respective olefin.[75]

1.3.3 Iron complexes in epoxidation catalysis

Although metals like molybdenum or rhenium are well established as oxidation or epoxidation catalysts, there have been ambitions to implement catalysts based on inexpensive and more abundant metals. Also, the aspect of toxicity and resulting safety requirements for employees in an industrial scale production that must be considered results in a motivation to develop biological and more environmentally benign catalysts.[64, 75] In nature, certain enzymes have the ability to catalyze epoxidation reactions under relatively mild and aerobic conditions.[77] The general progress in biological investigation and the resulting understanding of enzymes and the motif of their active centers gave starting points for catalyst development in the last decades. Thus, the development of biomimetic catalysts based on cheaper, abundant and "non-toxic" metals, manganese and iron in particular, have attracted attention in recent years.[78-83] Important examples for iron-based oxidation enzymes are soluble methane monooxygenases (sMMO)[84-87] and cytochrome P450 oxidases (CYP).[88-92] These enzymes are able to oxidize very challenging substrates, for example the conversion of methane to methanol for sMMO[87] or alkanes, alkenes and aromatic compounds for CYP[88, 90]. The structure of the active site of sMMO (see figure 5, right side) is a diferric cofactor, where both Fe^{III} centers display an octahedral coordination and are bridged *via* a hydroxide and two carboxylates, an acetate and a glutamate. The remaining coordination sites are occupied by *O*-donors (water,

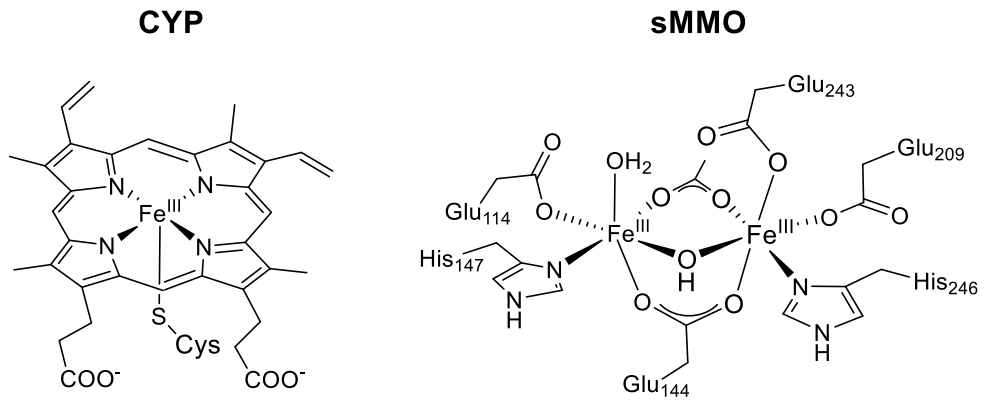

Figure 5: Depiction of the active center of cytochrome P450 enzyme (CYP, left)[88] and soluble methane monooxygenases (sMMO, right)[93].

glutamate) and *N*-donors (histidine).[93] The structure of the active site of the CYP family exhibits a cofactor, containing only a single iron center. This Fe^{III} center is coordinated by a heme ligand in all four equatorial positions and additionally by a cysteine in axial position, anchoring the complex to the protein (see Figure 5, left side). This *S*-donor cysteine, due to its *trans*-effect, has a significant influence on the cofactor's ability for coordinating and subsequently reducing molecular oxygen, and stabilizing the high valent radical species occurring in the mechanistic cycle.[84]

The family of CYPs is comparably versatile, as it is capable to oxidize a broad range of substrates. The generally accepted mechanism was proposed by Groves *et al.* in the 1970s and the epoxidation revolves around isolable intermediates of the active center (see Scheme 4, intermediates marked blue).[94-96] The Fe^{III}-heme complex is reduced *via* interaction with another protein and NADPH to its Fe^{II} derivative, which coordinates oxygen and forms a Fe^{III}-hydroperoxo species. This species can also be formed by direct coordination of hydrogen peroxide to the Fe^{III}-heme complex. The subsequent heterolytic cleavage of the peroxo bond results formally in a Fe^{V}-oxo species, which is considered the active species. This high valent species is stabilized by a delocalization of a positive charge into the porphyrin ligand system, forming a Fe^{IV}-oxo species along a cationic porphyrin radical ligand. This non-innocence of the ligand system plays a central role in the substrate oxidation. Non-innocence describes the ability of a ligand system to alter the metal's oxidation state *via* redox activity. The iron-oxo species subsequently transfers an oxygen atom directly to the olefin, forming the epoxide.[88, 97-101]

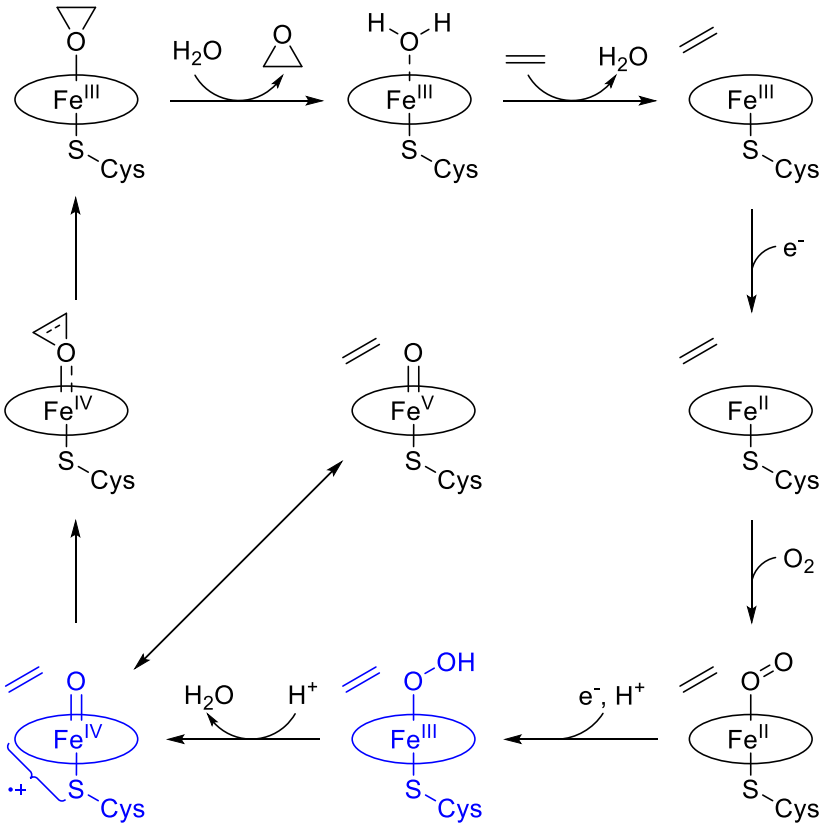

Scheme 4: Simplified epoxidation mechanism of cytochrome P450 enzymes utilizing molecular oxygen as oxidant. Isolable intermediates are marked blue.[88, 98]

Due to the ability of biological iron-based oxidase enzymes to utilize oxygen for the oxidation of various substrates and simultaneously achieving high selectivity, major efforts have been focused into development of a wide variety of complexes, mimicking the active center of enzymes. Especially porphyrins were studied in detail, as this ligand is an essential motif in biological systems with a wide range of reactivities. Among others, porphyrins are essential for the function of photosynthesis[102], oxygen transport[103] and energy supply[104] in biological systems. This resulted, besides the development of a wide range of new biomimetic iron-based compounds, in further investigations on mechanisms.

The development of biomimetic complexes can be separated into two major classes, heme and non-heme systems. While the former one focusses solely on complexes ligating porphyrin systems or close derivatives, the second one may include a huge variety of ligands consisting of *N*-, *O*-, *S*- or *C*-donors.[81]

1.3.3.1 Heme systems

Heme systems consist of iron complexes bearing porphyrin ligands with modulated electronic properties compared to the biological systems. These complexes catalyze, amongst other reactions, the epoxidation of various olefins as well as the hydroxylation of alkanes, applying for example iodosylbenzene as the oxidant. The reactivity mainly depends on the electronic structure of the porphyrin ligand. Applying electron withdrawing groups results in an electron-deficient iron center, which therefore exhibit a higher oxidizing power and higher reactivities in hydrocarbon oxygenation reactions.[105] To prevent decomposition of these complexes, steric substituents are usually introduced at the *meso* positions (see figure 6) to suppress ligand oxidation or formation μ_2-oxo bridged dimers.[82, 105-108]

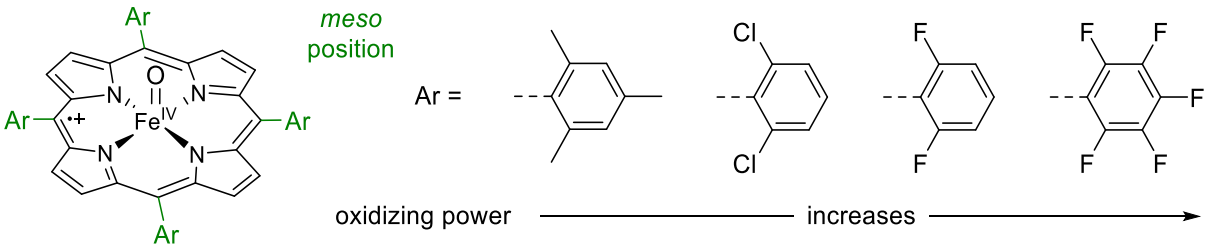

Figure 6: Possible modifications at the meso-position of a porphyrin and the resulting influence on catalytic reactivity.[105]

Furthermore, the choice of the axial ligand as well as the solvent in the catalytic reaction have a distinct influence on the reactivity of the complexes towards alkane hydroxylation and oxo-transfer reactions. With higher donation ability of the axial ligands the Fe-oxo bond length increases in the corresponding transition state, due to a weakening of the Fe-oxo bond. This improves oxo transfer reactions or enhances H-abstraction due to a strengthening a possible FeO-H bond,.[108]

1.3.3.2 Non-heme systems

Although non-heme iron complexes are not strictly defined to a certain structural feature, non-heme often refers to complexes bearing a tetra-dentate ligand, resembling the bonding mode of the porphyrin structure. These chelators may include various chemical structures, being able to bind to the iron center, *e.g. N*-, *O*-, *C*- or *S*-donors. The by far most studied type of non-heme ligand system bears a high number of *N*-donors or consists exclusively of such, as well as two labile ligands (*e.g.* coordinating solvents or weakly coordinating counter ions). [81, 109-111] Amines, pyridines, pyrrolidines and pyrroles are commonly applied as *N*-donors.[81] Although some of these complexes apply oxidants like molecular oxygen or organic peroxides,[75, 81, 112] the majority utilizes hydrogen peroxide,[81, 113] as it is ecological benign, forming water as the only stoichiometric side product.[81, 110, 114-116]

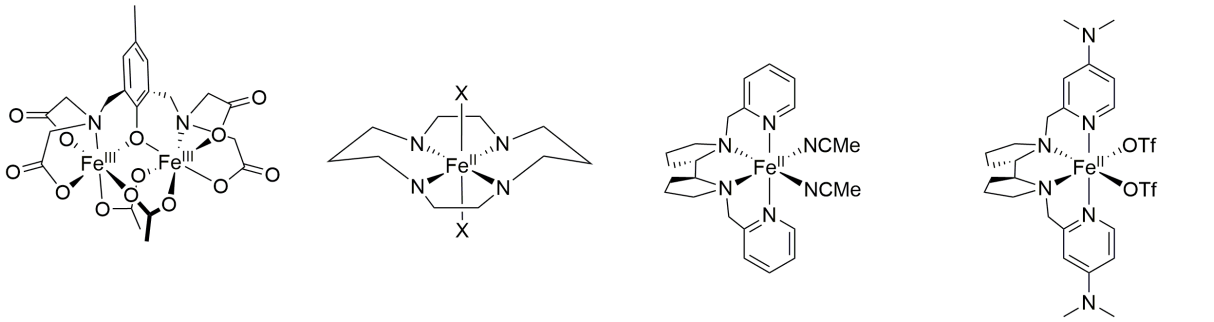

Figure 7: Examples of non-heme iron catalysts for oxidation reactions.[117-120]

The first non-heme iron complex was reported by Que *et al.* in 1986.[117] The complex is inspired from the active site of sMMO and harbors two iron centers, bridged by a phenolate based tetraacetate moiety and two acetates (see figure 7, $(Fe^{III})_2$PBATA$(OAc)_2$).[117] In 1991 Nam *et al.* reported the first *in-situ* generation of an epoxidation catalyst with a single iron center using the cyclam ligand system (see figure 7, *trans*-Fe^{II}(cyclam)).[118] This catalytic system could convert various olefins to epoxides using a 30% aqueous solution of hydrogen peroxide.[118]

In the following years, tetradentate amino-imine ligands (see figure 8 for selected examples) stood in the focus of research, especially by Que *et al.*, to investigate the respective structure-reactivity relationship. This contributed important work in the exploration of the mechanisms of Fe^{II}-catalyzed epoxidation reactions utilizing hydrogen peroxide.[82, 109-110, 114, 121-129] Based on these investigations, Chen and White reported stereoselective oxidation catalyst for natural products in 2007 (see figure 7, *cis*-Fe^{II}(*S*,*S*-PDP)$(CH_3CN)_2$). This concept was then exerted by other groups for the stereoselective epoxidation of olefins (for example see figure 7, *cis*-Fe^{II}(*S*,*S*-Me2N-PDP)$(OTf)_2$).[120]

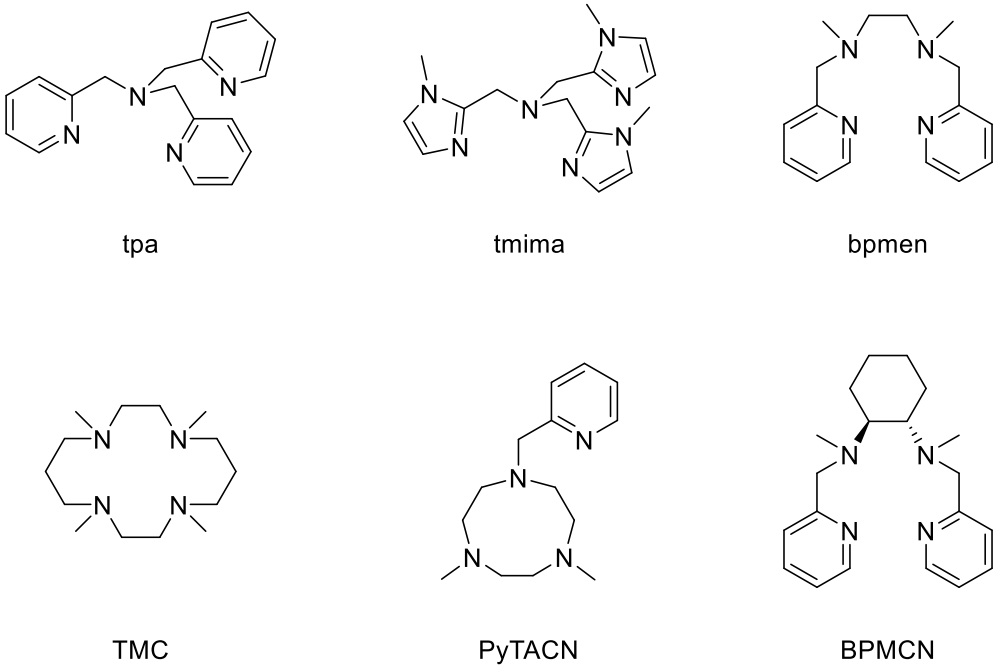

Figure 8: Examples of various ligands for non-heme metal complexes offering *cis*- or *trans*-labile coordination.[81, 105, 130]

The investigations revealed a mechanism for non-heme complexes remotely similar to that of cytochrome P450. The generally accepted mechanism includes a high valent Fe^{IV} or Fe^{V} oxo species as active species. The generation of such high-valent species is depicted in scheme 5.

If a Fe^{II} species is applied as a pre-catalyst, the first step is a one-electron oxidation with subsequent exchange of a labile ligand with a hydroperoxide, forming a Fe^{III}-hydroperoxo species (*1*).[81, 111, 131] This intermediate (*1*) can either directly react with a substrate, which is quite rare, or initiate various routes to form high-valent Fe^{IV}-oxo or Fe^{V}-oxo species, which commonly act as active species for epoxidation.[81, 83, 111] The homolytic cleavage of the peroxide forms a Fe^{IV} species and a hydroxyl radical (*2*). This pathway is often sought to be suppressed or minimized, as hydroxyl radicals are bound to act as initiators for radical chain reactions, leading to lower selectivity for oxidation or epoxidation. However, some ligands are able to donate an electron to the iron center, if their structure allow a delocalization of the lost electron, generating a hydroxide anion instead of a radical alongside a $(L^{+\cdot})Fe^{IV}$ species (*3*). As the hydroxide anion is unable to initiate radical chain reactions, this pathway offers higher selectivities *via* homolysis. Heterolytic bond cleavage generates a Fe^{V}-oxo species (*4*) alongside a hydroxide anion. This pathway also benefits in terms of selectivity, as no radicals are generated, but is only accessible if the ligand system can stabilize a high valent Fe^{V} intermediate.

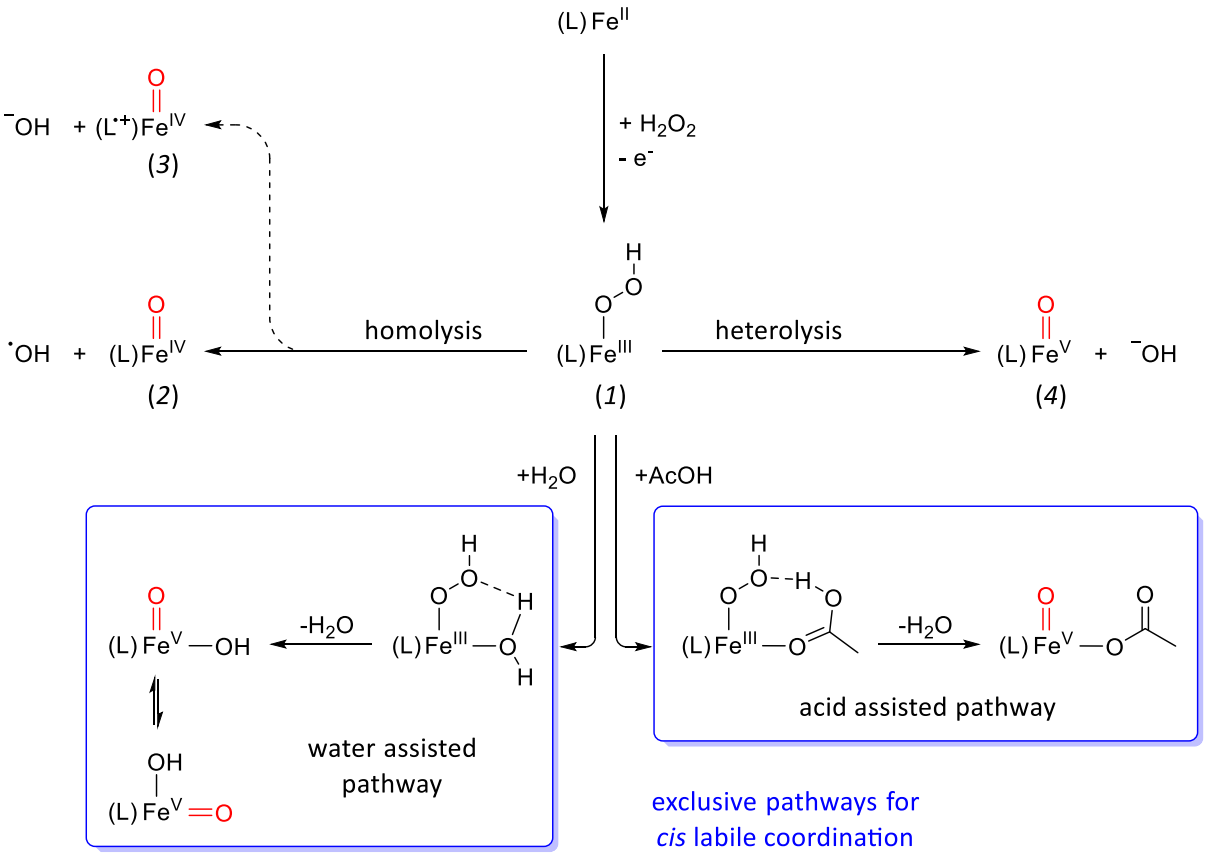

Scheme 5: Different pathways for the formation of high-valent iron oxo species in the reaction of biomimetic iron complexes with hydrogen peroxide. Water and acid assisted (*e.g.* acetic acid) pathways for heterolytic elimination of water are marked blue and are only feasible for complexes with *cis*-labile ligands. [82, 105, 130]

The heterolysis can be promoted by water or organic acids but is only applicable for complexes bearing *cis*-labile coordination sites, as the additives need to coordinate in close proximity to the peroxide.[109-110] These coordinating additives act as a proton shuttle and form a 5- or 6-membered ring intermediate, thereby accelerating hydroxide elimination through protonation to yield water.[82, 110, 114] The acid assisted pathway offers benefits compared to the solely water assisted pathway, as it promotes the heterolytic elimination of water more efficiently. Additionally, this pathway increases the selectivity to epoxides by competing with water for free coordination sites. This decreases epoxide ring-opening and subsequently reduces diol formation.[81, 114, 131] Complexes with *trans*-labile coordinative sites generally exhibit high selectivity towards epoxides, as water cannot be in close proximity to the epoxide while coordinating to the iron center at the same time. [81, 113-114, 131-132]

Aside from Brønsted acids, the utilization of Lewis acids as accelerating additives for iron complexes in hydroxylation and epoxidation catalysis was established in recent years. $Sc(OTf)_3$ is the most commonly applied, as it offers a high Lewis acidic character and as it is also applicable for complexes offering *trans*-labile coordination sites. Furthermore, its weakly coordination anions do not compete for coordination sites. The accelerating properties stem from the possibility of generating protons from present water in the catalysis or directly interacting with the Fe^{III}-hydroperoxo species and facilitate the elimination of hydroxyl groups. It is still highly debated whether Sc^{3+} is truly an innocent additive, as crystal structure analysis and DFT calculations suggest that Sc^{3+} is able to bind to oxygen or nitrogen atoms in several iron- and cobalt-oxo complexes. Such an interaction may modify the electronic structure of a respective complex or even change the oxidation state of the metal center, questioning the applicability of the prevailing catalytic mechanism.[133-140]

To further improve the catalytic activities, ligands were modified to better stabilize the high-valent iron-oxo intermediates. The requirements for such a ligand would be high donating capabilities for stabilizing high-valent states, π-backdonation capabilities to form a more rigid bond, which is less susceptible towards dissociation and subsequent oxidation, leading to degradation of the complex. This is where NHCs entered the stage as ligands for non-heme epoxidation catalysis starting in the 1990s, due to the first report of successful catalytic testing.[48, 141-142] The growing interest in iron-NHC complexes was also support by the relatively easy access of these compounds *via* various synthetic routes. These routes usually start from imidazolium salts and yield the desired complex by direct metalation or by intermediates, which are further converted. The most utilized synthetic routes are depicted in scheme 6.

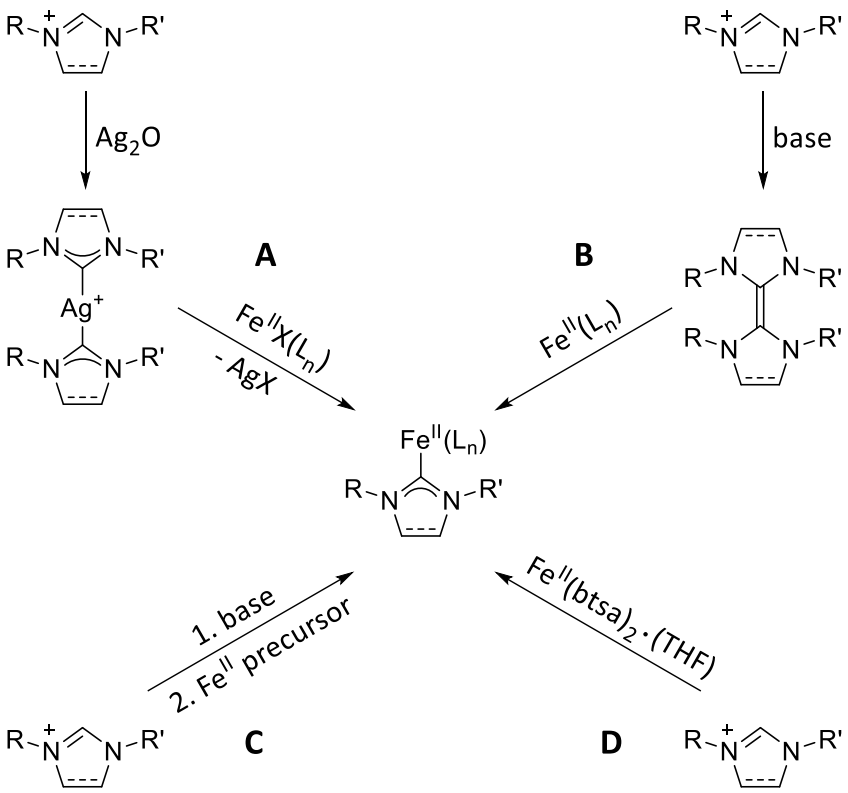

Scheme 6: Usual synthesis routes for the generation of Fe^{II}-complexes.[142]

The transmetalation route A is the most commonly applied synthesis method for generating NHC complexes for a broad amount of transition metals. This method requires a precursor complex, which offers an easy bond cleavage between the precursor metal and the NHC. The substituted metal cation preferably forms insoluble salts with certain anions for easy separation. The by far most common applied variety is the silver based transmetalation. Silver complexes can be easily synthesized by suspending an imidazolium salt solution with Ag_2O, which acts as base to generate *in-situ* carbenes and as metalation agent. The downsides of this method are, that silver complexes are usually light sensitive, silver salts may be difficult to separate during work-up and may oxidize the iron complexes during transmetalation due to the oxidative potential of Ag^{I}.[143] Metalation route B is based on the deprotonation of an azolium salt, forming an NHC dimer, into which the iron precursor inserts. This method is only feasible if the dimer's bond is labile enough for iron insertion. Route C utilizes the *in-situ* generation of an NHC with an external base, forming the complex with the iron precursor. Route D combines the application of a base and iron precursor of route C, as the base is present as internal anion of the metal precursor. The downside lies in the fixed applicable stoichiometry of base to metal due to its oxidation state. If the desired complex does not require this fixed ratio, one participant (base or metal) has to be applied in excess, requiring separation during work-up.[142]

The development further progressed from initial complexes, bearing mostly mono- or bidentate NHC ligands, to polydentate ligands, offering a higher chelating effect. A particular focus was set on the development on acyclic or macrocyclic tetradentate ligand motifs, which allows comparability to the respective class of pure *N*-donor non-heme complexes developed by Que, Nam, Costas and others.[142]

The first macrocyclic tetra-NHC iron complex was reported by Jenkins *et al.* in 2011 (see figure 9) and has been investigated for its ability to catalyze the aziridination of olefins by aryl azides.[144] In 2013, Meyer *et al.* reported the first isolation and characterization of an Fe^{IV}-oxo species bearing a tetra-NHC. This highlighted the capability of this ligand class to stabilize high-valent iron-oxo species and indicated the potential of such complexes for oxidation catalysis.[145] Starting in 2012, Kühn and coworkers reported a set of new NHC Fe^{II} complexes, exhibiting an acyclic tetradentate motif comprising of two imidazolylidene carbene-donors and two pyridine *N*-donors (Figure 9, **I**-**III**)).[146]

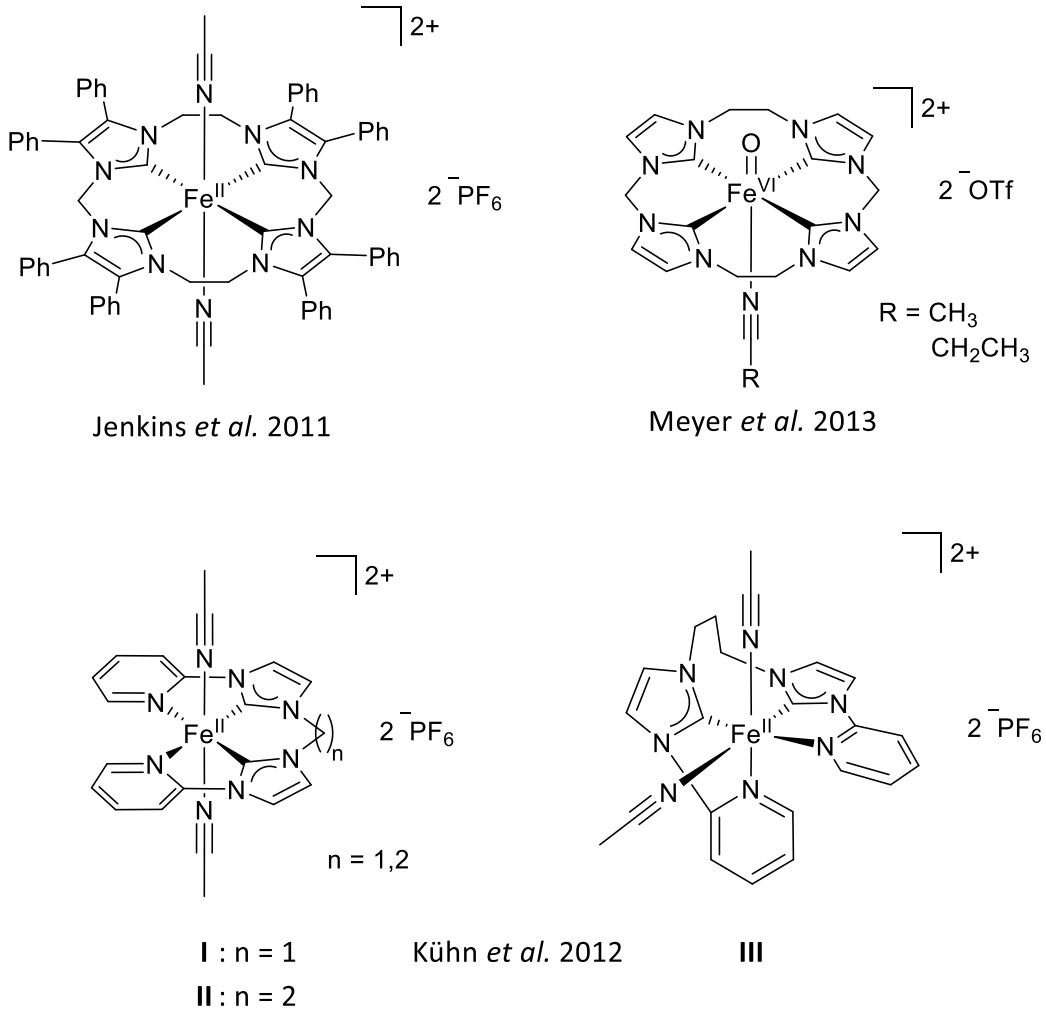

Figure 9: Structures of cyclic tetradentate iron-NHC complexes reported by Jenkins & Meyer and acyclic tetradentate iron-NHC/pyridine complexes reported by Kühn.[132, 144-146]

From these, complexes **I** and **II** exhibit a planar coordination sphere, whereas **III** exhibits a sawhorse coordination type. The coordination type depends on the length of the alkyl bridge between the NHC moieties. Methylene or ethylene bridges induce a more rigid structure which prefers in-plane coordination, as the longer and more flexible propylene bridge allows for an out-of-plane coordination. Complex **I** was applied in epoxidation catalysis.[132, 146] This complex showed promising activity, as its turnover frequency (TOF) of 2,600 h^{-1} at that time was in the higher regions of reported activities for non-heme iron complexes, without the application of additives.[75, 81, 132] Due to this promising result, the focus shifted towards purely carbene donor ligands. The complexes **IV** and **V** (see figure 10) were reported by Kühn *et al.* and possess purely NHC donors and exclusively methylene bridges. Both can be seen as bio-inspired complexes, as they share a structurally resemble to the porphyrin system. Complex **IV** can shift between *cis*- and *trans*-configuration due to its acyclic structure, whereas complex **V** can only assume and planar ligand coordination with the resulting *trans* labile coordination sites.[75, 81, 147-148]

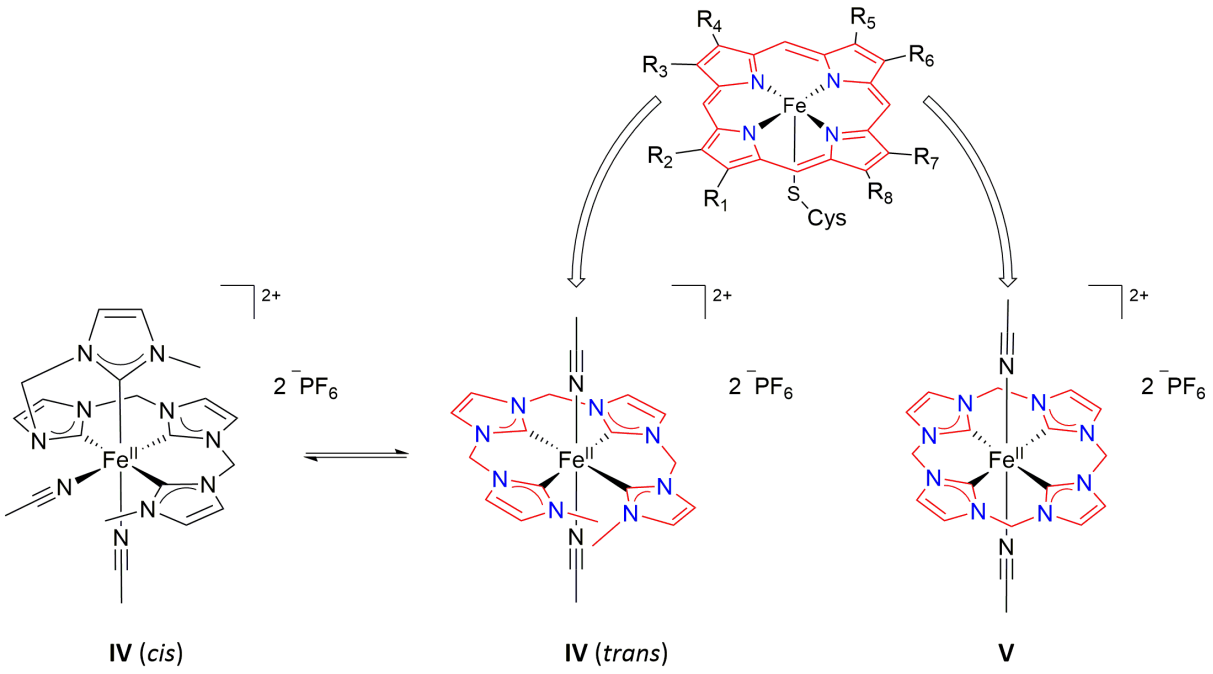

Figure 10: Square planar Fe^{II} complexes **IV** (*trans*) and **V**, showing structural resemblance to heme systems. Complex **IV** (*trans*) is in equilibrium with its *cis*-conformer at room temperature.[75, 81, 147-148]

Complex **V** showed unprecedented high activity in the epoxidation of *cis*-cyclooctene at ambient conditions with an initial TOF of 50,400 h^{-1} with a selectivity of >99% for the epoxide. This activity can be further enhanced if the Fe^{III} derivate **VI** is utilized as starting catalyst, raising the initial TOF to 183,000 h^{-1}. This is due to skipping of an *in-situ* initial one-electron oxidation step from **V** to **VI** by hydrogen peroxide, which is represented by an induction phase in catalysis. This prior oxidation may be performed *via* converting complex **V** with the stable radical thianthrenyl hexaflouoro-phosphate.[113, 147]

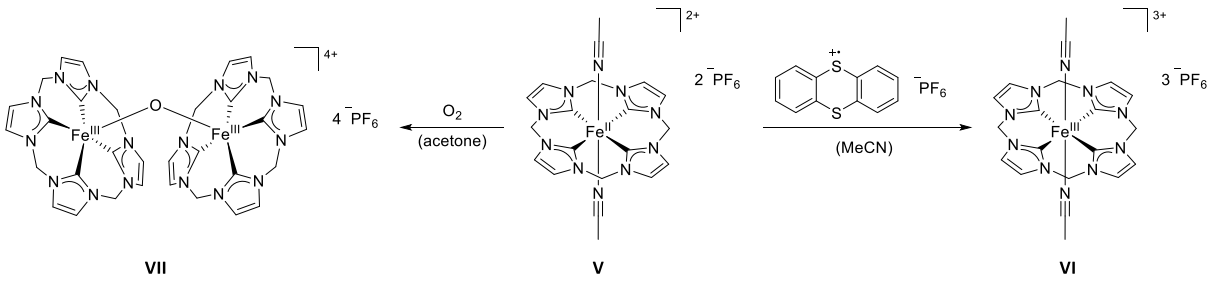

Scheme 7: Possible conversions of cyclic tetra-NHC Fe^{II} complex V to form the respective Fe^{III} complex or an oxo-bridged Fe^{III}-O-Fe^{III} dimer.[113, 149]

Although the complexes **V** and **VI** resemble a significant improvement in terms of reactivity compared to other non-heme iron epoxidation catalysts at that time, the limited stability under oxidative catalytic conditions is still a major issue. The complexes tend to rapidly degrade upon lack of substrate availability or if the substrate is more challenging olefins for epoxidation. Well known decomposition pathways of non-heme iron catalysts generally include the oxidation or dissociation of the ligand structure. Aside from that, the formation of an inactive μ_2-oxo bridged Fe^{III}-O-Fe^{III} dimer **VII** can also deactivate the catalyst system. The dimer **VII** can be selectively formed by dissolving complex **V** in acetone under aerobic conditions.[113, 149] This lability, the non-recyclability, the limited substrate scope and the high effort/price for ligand synthesis are the reasons why this complex system until now is not suitable for application in industry.

1.4 Medicinal chemistry

1.4.1 Cancer, a global challenge

According to the annual report of the American Cancer Society 2019 cancer is the second leading cause of death in the USA.[150] This is the result of the general advancement in medicine and pharmacy making classic causes of death, *e.g.* infections, cardiovascular diseases or diabetes less fatal. The pace of this advancement could not be abided for cancer, as such diseases are generally quite challenging to treat.[151]

Cancer generally can be described as malfunctioning cells, which proliferate uncontrolled, unable to form normal shaped or functioning tissue and instead form tumors which invade and destroy adjacent tissue.[152] The concept for tumor formation describes a multistep process, which is based on a Darwin-type of evolution, giving the mutated cells an advantage over healthy cells in terms of proliferation. The initiation of cancer cells basically consists of a mutation of former healthy cells as a result of genetic alteration. The primary or subsequent mutations are required to give the cells certain properties to form a tumor. These are, among others, self-induced grow signals, replicative immortality, the circumvention of programmed cell-death (apoptosis) to resist external control factors like growth inhibition. Furthermore, cancer cells require means to evade immune responses and to provide themselves with the required amount of oxygen and nutrients by growing blood vessels (angiogenesis) to sustain the increased metabolism. Such mutations of healthy cells may occur spontaneously or can be induced and/or promoted by physical, chemical or biological factors. Examples are the interaction of radiation with genetic material, the generation of hazardous radicals within or in close proximity to cells or infections with viruses, which inhibit tumor suppressor proteins.[153-157]

Tumor tissue generally does not consist solely of a cluster of primary cancer cells, as these represent the basis of a tumor. The cancer cells within the tumor differentiate into various types to build and promote a microenvironment beneficial for the tumor. Among others, the tumor, aside primary cancer cells, may consist of invasive cancer cells, cancer stem cells, immune and inflammatory cells, fibroblasts, pericytes and endothelial cells to form such a malignant microenvironment.[157] Cancer stem cells, although relatively rare, were found to have self-regenerating abilities and can therefore better resist therapeutic attempts and potentially lead to recurrence of cancer.[158] Tumors are most often a dynamic, heterogeneous tissue and have a complexity which is *on par* to that of healthy tissue, making cancer treatment challenging.[157]

1.4.2 Early chemotherapeutic cancer treatment

Chemotherapy is the concept of applying chemical substances to a patient to treat certain illnesses. In terms of cancer therapy, it usually consists of applying cytotoxic substances to the patient in hope of damaging cancer tissue in more substantial way than the healthy surrounding tissue. This may be achieved either by applying substances, which have an affinity for cancer cells due to certain overexpression of targetable moieties or *via* unselective distribution utilizing the fact that cancer in general has a higher metabolism and therefore have an increased intake of substances from the blood stream. This distribution gradient is utilized to damage cancer cells more significantly than healthy cells and therefore stop the tumor's growth or reduce its mass. Chemotherapy is a common method to treat cancer, aside radiation therapy and surgery and are often performed subsequentially as part of a therapy.[159-161]

The first reported case of anticancer chemotherapy was based on the utilization of nitrogen mustard, a deviation from the WWI chemical warfare agent mustard gas, to threat a severe case of lymphoma in 1942. The concept arose, as reports of soldiers affected by mustard gas (see figure 11) from WWI showed a severe decline in white blood cells – cells that, if mutated can cause the development of lymphoma. This first experimental treatment showed that the systematic administration of chemicals could induce tumor regression.[159-161] It was later found, that the mode of action lies in alkylation and cross-linking of deoxyguanosine residue (dG) in the DNA with available other nucleophiles like deoxyguanosine residues or amino acids like histidine, cysteine or lysine, being in close proximity from nearby proteins (see figure 12).

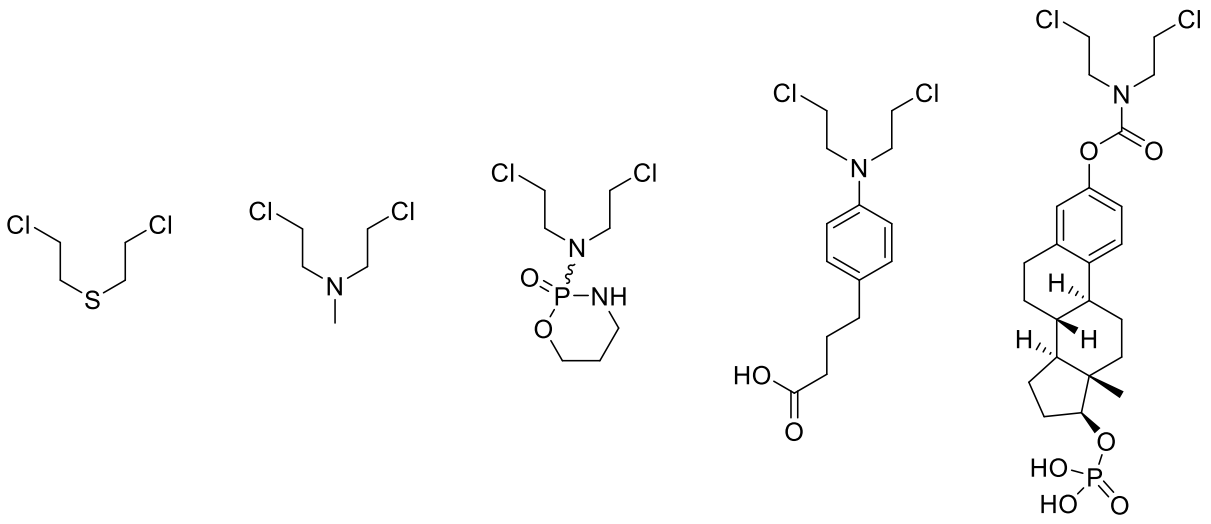

mustard gas | mechlorethamine | cyclo-phosphamide | chlorambucil | estramustine phosphate

Figure 11: Structure of mustard gas, its nitrogen based derivate mechlorethamine and further from this compound developed alkylating antineoplastic agents.[159, 162]

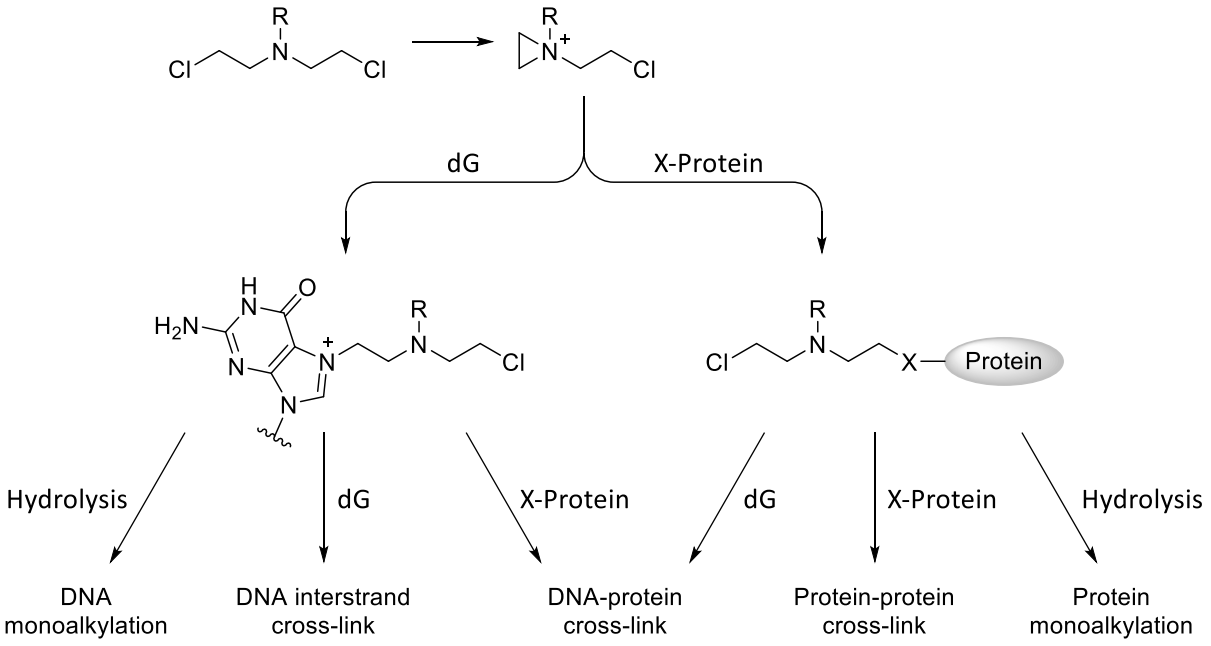

Figure 12: Proposed mechanism of nitrogen-mustard induced formation of DNA alkylation and crosslinking.[159, 163]

Such a DNA cross-link activates a signal cascade, which ultimately leads to apoptosis in the affected cells.[159, 163-166] Although other concepts for chemotherapeutic cancer treatment rose simultaneously, improved alkylation agents were developed, being stabilized *via* applying electron-rich substitutions to enable oral administration [*e.g.* cyclophosphamide, chlorambucil, estramustine phosphate (see figure 11)].[159, 162] Estramustine phosphate is an estrogen coupled nitrogen mustard derivate which still sees administration in complicated or progressed stages of prostate cancer.[162] Unfortunately, it became clear in the 1950s and 60s that all alkylating agents are only applicable against very specific types of cancer. Additionally they are highly toxic to developing bone marrow cells and would not cure any solid tumors on their own, even when administered over long periods.[167] Therefore it was necessary to find other drugs with higher success rate in curing cancer and an broader therapeutic spectrum.

1.4.3 Inorganic compounds for cancer treatment

The most significant breakthrough in cancer treatment of solid tumors was the discovery of the antiproliferative properties of cisplatin (*cis*-diamminedichloridoplatinum(II)) (see figure 13) by Rosenberg *et al* in 1965.[168] While investigating the effects of electric current on bacteria, he observed an interruption in replication activity. He later discovered that this effect was not dependent on the electric current, but rather on a chemical being released from the platinum electrodes.[169] Subsequent investigations on cisplatin revealed its cytotoxic properties and the Food and Drug Administration (FDA) approved its use for treatment of ovarian and testicular cancer in 1978.[167] Today, cisplatin and its close derivatives are the most widely utilized inorganic chemotherapeutic drugs administrated

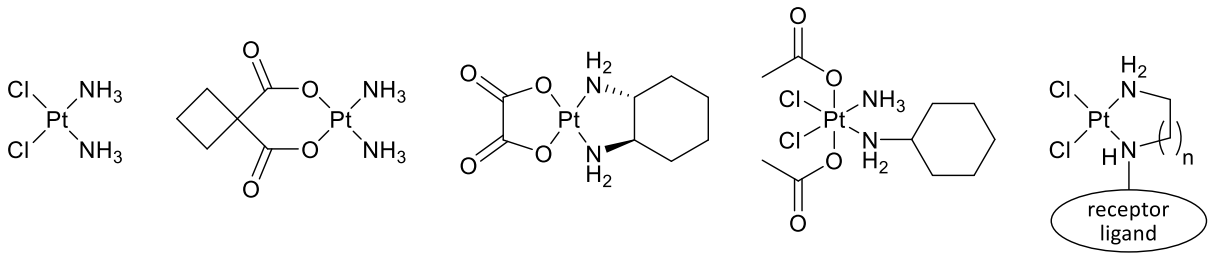

cisplatin carboplatin oxaliplatin satraplatin

Figure 13: Structures of cisplatin and its already applied derivatives carboplatin and oxaliplatin. Satraplatin, a Pt^{II} prodrug, was the first Pt^{IV} drug to reach the phase III in clinical trials.[170] Other developments include the linking of targeting of fluorescent groups, *e.g.* vitamin derivatives, estrogens or bile acid derivatives, to a cisplatin core.[171-172]

against solid tumors like lung, bladder, testicular, ovarian, colorectal cancer, among others.[173] The most common derivatives are carboplatin and oxaliplatin (see figure 13), which were approved in 1989 and 2002, respectively. Such derivatives usually aim to increase the stability of the compounds under physiological conditions, replacing the labile chlorine ligands with carboxylates or replacing the monodentate amines with bidentate diamines or stronger donating monodentate amine ligands.[173] The general mechanism for platinum based anti-cancer is most intensively studied for cisplatin and can be transferred onto its derivatives. The vast majority of Pt^{II} based complexes offer a square planar coordination sphere due to their electronic d^8 configuration.[174] As Pt^{IV}-based systems get reduced to Pt^{II} at some point before the mechanistic action, the same principles apply.[170] The square planar complex displays two *cis* amine ligands, which are considered persistent and two *cis*-standing leaving groups (chlorine, carboxylates). Upon administration of the drug into the blood stream, the local chloride concentration (~ 100 mM) preserves the drugs composition. The drug enters the cell *via* passive diffusion and/or active transportation by membrane proteins, mainly *via* the copper membrane transporter CTR1.[175-176] The cellular accumulations differ for the derivatives of cisplatin, as different membrane proteins are responsible for transfer into the cell.

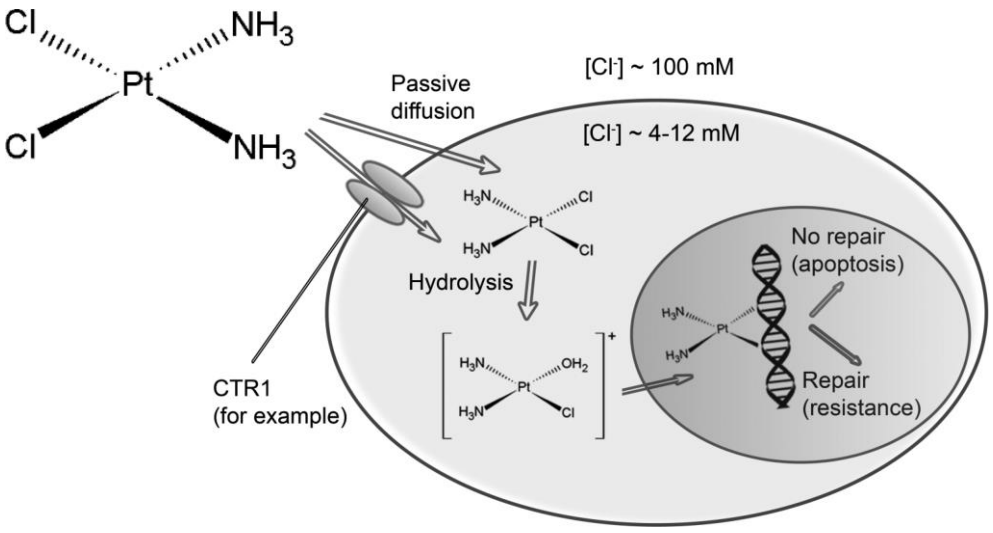

Figure 14: Mechanism of action for cisplatin for DNA binding.[176] Reprinted from Ref. [176] by permission of the American Chemical Society (see chapter 5.3).

In the cytoplasm, inside the cell, the local chloride ion concentration is too low (<20 mM) to maintain the coordinating ligands, resulting in the aquation of the complex, displacing a chloride by a water molecule, forming *cis*-$[Pt(NH_3)_2Cl(H_2O)]^+$. This reaction is considerably slower if a cisplatin derivate is applied, which coordinates carboxylates instead of chlorides, resulting in increased retention half-life times. Due to the positive charge of the hydrolyzed complexes, these compounds do not readily exit the cells again, as a transfer through the lipophilic cell membrane is unfavored. Furthermore, the aquated complex can enter the nucleus, where the positive charge attracts the complexes to the negatively charged nuclear DNA.[175-176] These hydrolyzed complexes are considered to be the active form, as they are potent electrophiles and the purine bases guanine or adenine replace the weakly coordinated water molecules readily in a nucleophilic attack of the N^7 position. The remaining chloride is subsequently replaced by another purine base to form a cross-link on the DNA. These cross-links may occur between purine bases on the same strand or on different strands, forming intrastrand or interstrand DNA cross-links, respectively (see figure 15). This process also occurs with cisplatin derivatives, although the ratio of cross-links and participated base pairs may vary.[175-176] These DNA adducts distort the DNA structure through bending and unwinding, which inhibits the DNA replication and transcription, causing a suspension in the cell cycle, which may induce pro-apoptotic signals. The cell counteracts the DNA platination *via* repair mechanisms, which are able to replace affected DNA regions through excision and replacement. DNA-protein cross-links can effectively shield platin induced DNA cross-links in close proximity from repair due to steric repulsion of the bulky repair proteins. If the DNA damage is too extensive to repair, apoptosis is induced, leading to cell death. Aside from direct interaction with DNA, cisplatin is also attributed to other cellular damages. The binding and possible inactivation of proteins can induce oxidative stress *via* mitochondria damage and dysfunction, glutathione depletion and lipid peroxidation.

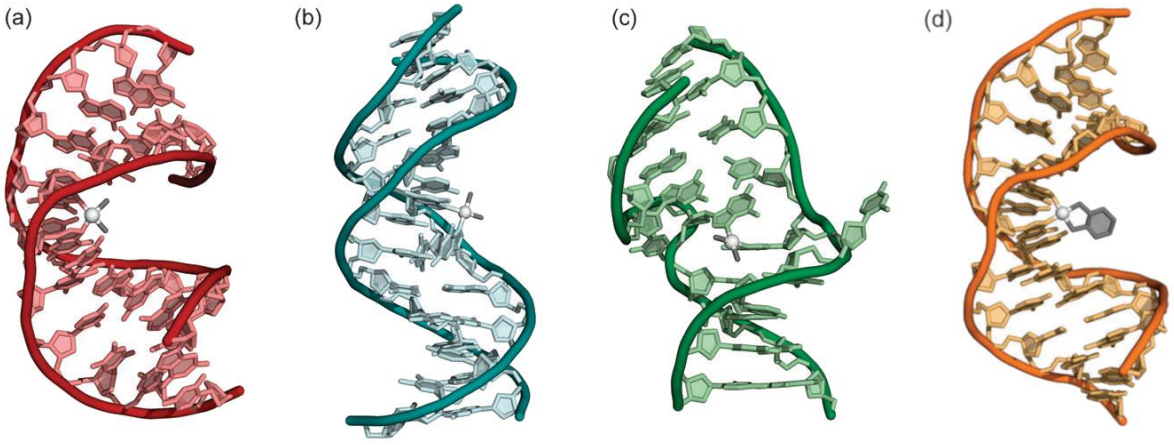

Figure 15: X-Ray crystal and NMR structures of double stranded DNA containing adducts of platinum anticancer agents: (a) Cisplatin 1,2-d(GpG)-intrastrand cross-link; (b) Cisplatin 1,3-d(GpTpG)-intrastrand cross-link; (c) Cisplatin interstrand cross-link. (d) Oxaliplatin 1,2-d(GpG)-intrastrand cross-link.[170] Reprinted and modified from Ref. [170] by permission of The Royal Society of Chemistry (see chapter 5.4).

Damages due to protein malfunctions may independently induce apoptosis aside DNA damages.[175, 177] These processes are highly unselective, as platinum-based drugs usually do not harbor a targeting group. Therefore, a distribution gradient may only be achieved due to the increased metabolism of cancer cells or due to overexpression of membrane transport proteins compatible to the administered drug. Every platinum-based drug has a dose-limiting toxicity, at which point a severe side effect may compromise the success of the treatment. The most prominent side effect of cisplatin is its quite intense nephrotoxicity (damaging of kidneys).[178] In the case of carboplatin, the bidentate dicarboxylate functions as leaving group instead of the chlorides of cisplatin. The reactivity is considerably lower, as bidentate carboxylates are more stable ligand compared to chlorides and such derivates therefore depict slower kinetics in DNA binding. This reduced reactivity limits side reactions with proteins, increasing its retention half-life to 30 h for carboplatin in the cytoplasm compared to 1.5 - 3.6 h for cisplatin. This lower reactivity also greatly reduces side effects like nephrotoxicity at the cost of other side effects. Carboplatin has a suppressive effect on blood cell production, whereas oxaliplatin can be severely neurotoxic. The lower reactivity also reduces the effectiveness of the drug. Therefore, higher dosages are required to achieve the same effect compared to cisplatin. For carboplatin, the dosage ratio is 4:1. This reduced effectiveness is partly due to its inertness, resulting in higher drug amounts leaving the body *via* urine.[178-179]

A major setback in the curing of cancer with platinum-based chemotherapeutics is the development of resistances resulting in therapeutic failure, which until now are an unavoidable issue. These resistances usually appear during or after a prolonged treatment, as a result of adaptive mutation of the cancer cells. The development of resistance to cisplatin usually also applies to other platinum-based chemotherapeutics, due to their similar mode of action.[180] To prevent that, one strategy is to administer platinum-based chemotherapeutics together with other anti-cancer drugs, addressing other mechanisms.[175]

1.4.4 Gold complexes in anticancer therapy

The utilization of gold-based drugs for medical purposes has a relatively long history and date back to medieval physicians (*e.g.* Paracelsus) applying ointments of colloidal gold for various skin conditions, and even earlier than that.[181-182] In 1890, Robert Koch discovered that a solution of gold cyanide inhibits the growth of tuberculosis bacteria *in vitro*. Although he could not confirm his results in animal testing, some years later other gold compounds like potassium tetrachloroaurate or sodium aurothiomalate were reported to be beneficial against tuberculosis and syphilis.[181] In the following years (1925-1935), the intravenous administration of Au^{I} thiolate salts, despite the lack of scientific evidence for antitubercular benefits, gave rise to reports about reduced joint pain in patients. This led to Forestier discovering the beneficial aspects of gold compounds for treatment of rheumatoid arthritis.[181-183]

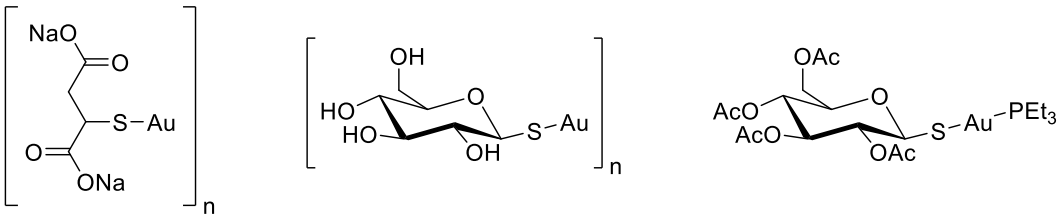

sodium aurothiomalate
Myocrisin

aurothioglucose
Solganol

auranofin
Ridaura

Figure 16: Chemical structure of gold(I) thiolates Myocrisin and Solganol, both of which are polymers and Auranofin.

Further development gave rise to gold thiolates as drugs for treating rheumatoid arthritis (*e.g.* Myocrisin and Solganol, see figure 16) and approval by the FDA. Due to severe side effects of these gold thiolates and the requirement for intravenously injection, Sutton *et al.* developed auranofin in the early 1970s, which induces less side effects and can be administered orally.[182, 184] In the late 1970s, before the approval of the FDA for anti-rheumatic application of auranofin, Lorber *et al.* discovered an inhibitory effect of auranofin on HeLa cells.[185] Subsequently further studies expanded the antiproliferative applicability to various cancer cell lines, including cisplatin resistant cancer cell lines, *in vitro* and also *in vivo*.[186-187] This led to the broad screening of gold complexes harboring various types of ligands for their anticancer potential. Meanwhile, more broad screening of auranofin for possible applications uncovered anti-parasitic,[188] anti-viral (tested against HIV)[189] and anti-bacterial[190] properties. In lights of current events, a recent study found an inhibition of SARS-COV-2 replication in human cells by auranofin.[191]

Gold complexes for therapeutic applications commonly occur in the oxidation states +III and +I. In recent years, gold nanoparticles with defined dimensions and surface structures have gained increasing interest as drug delivery systems, in photodynamic therapy or as therapeutic agent.[192] Au^{III} complexes are isoelectric to Pt^{II} compounds, making them highly interesting for anti-cancer studies.

A problem of Au^{III} complexes is their poor stability under physiological conditions, as they can be reduced to Au^{I} by thiols like glutathione or albumin. This may give rise to enhanced cytotoxicity, as oxidative stress is induced on forming an reduced Au species, which itself may be cytotoxic. The downside is an increased Au^{III} drug deactivation in cells and an higher challenge for studying the drugs interaction relationship, as multiple oxidation states of gold compounds can be present within the cell.[193-195] This instability can be overcome *via* applying a ligand system being able to stabilize the Au^{III} center. Due to its relative oxidation stability under physiological conditions, Au^{I} compounds are the predominantly applied for therapy studies.

Auranofin and its phosphine bearing analogues have shown to primarily cause apoptosis *via* a mitochondrial pathway, which resulted in the acceptance that gold complexes in general are active as antimitochondrial agents.[196-197] A defining reactivity of gold complexes under physiological conditions bearing at least one labile ligand is their high affinity to thiol and selenol groups (*e.g.* cysteine and selenocysteine).

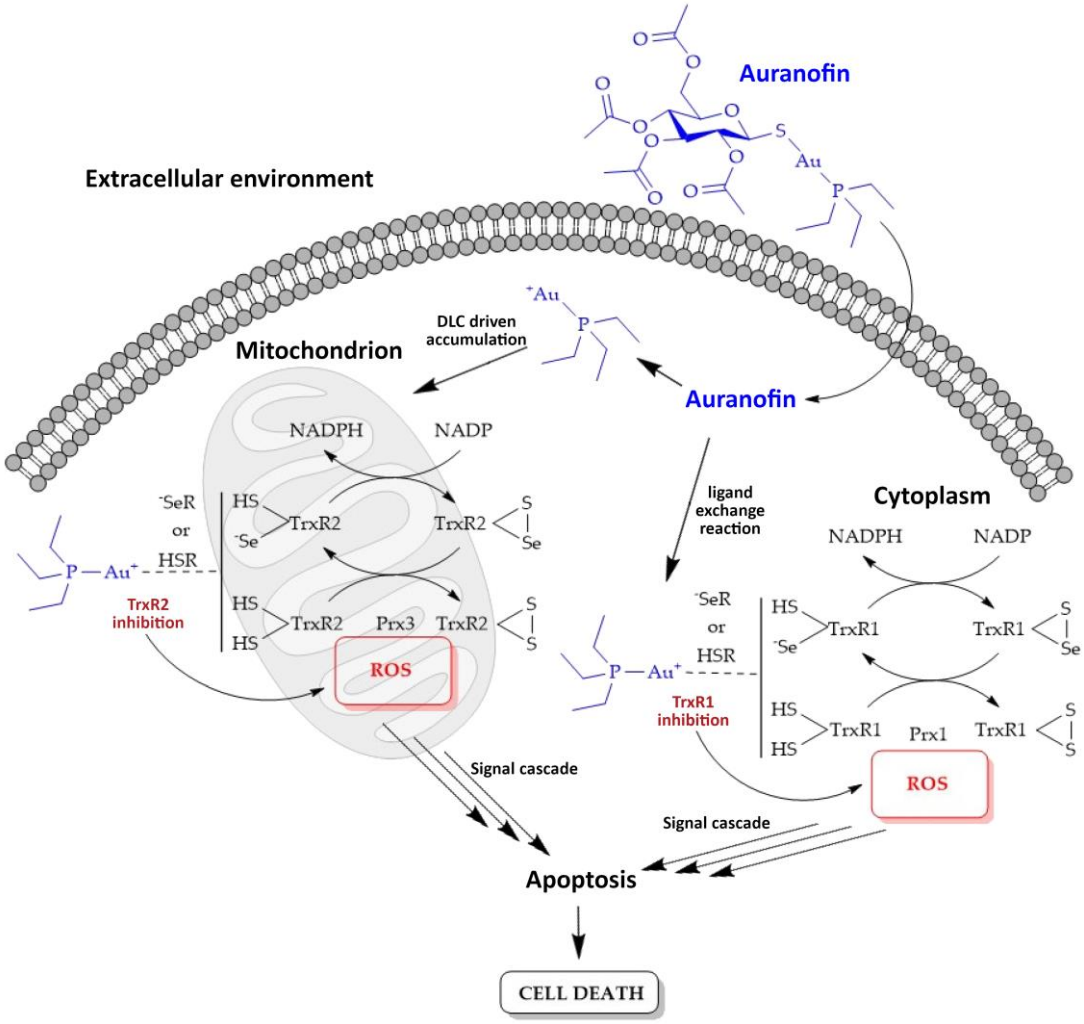

Figure 17: Simplified scheme of auranofin's mechanism to induce apoptosis *via* TrxR inhibition in cytoplasm and mitochondria.[198] Reprinted and modified from open access Ref. [198] by permission of the Creative Commons Attribution License [Attribution 4.0 International (CC BY 4.0)] (see chapter 5.5).

It was discovered that Au^{I} phosphines are potent inhibitors of the redox active enzyme thioredoxin reductase (TrxR). This enzyme is over-expressed in certain types of cancer, contains an easily accessible selenocysteine residue on its flexible *C*-terminal arm and cysteine rich sequences at the *N*-terminal active site.[199] Aside from TrxR, the thioredoxin systems consist of thioredoxin (Trx) and NADPH, regulating crucial cell functions and the catalytic reduction of a variety of proteins. This includes peroxiredoxin (Prx), which is required for the reductive disposal of H_2O_2, a reactive oxygen species (ROS) formed in the respiratory chain.[200] Three isoforms of TrxR are known, which are mainly present in cytosol (TrxR1), mitochondria (TrxR2) and testis (TrxR3). By binding to the selenocysteine or cysteine of these proteins, the switching redox cycles are disrupted, halting the enzymatic cascade. This leads to a redox de-equilibrium, inducing, among other effects various apoptotic pathways. The apoptosis can be induced *via* the excessive accumulation of ROS or subsequent effects, depending on the inhibited isoform of TrxR.[197, 201-209] This concept is depicted in a simplified way in figure 17. As auranofin readily undergoes ligand exchange, it can react with sulfur containing proteins in the blood stream before entering the cell. Therefore, a lot of effort has been directed to stabilize the complex against premature reaction, to prevent inactivation, and to increase cellular accumulation. Following knowledge of ligands behavior derived from catalyst development, both ligands, but preferably the phosphine ligand, have been replaced with NHCs to increase the complexes stability and to fine tune the sterics and their lipophilicity.[40, 210] NHCs showed to be excellent scaffolds in medicinal chemistry due to their trivial modifiability. This allows for the preparation of wide ligand libraries with relative ease, enabling the determination of optimal ligand properties with small effort. Additionally Au-NHC complexes show great stability in biological media by stalling ligand dissociation reactions. Very high antitumor activities have been reported for neutral and cationic Au-NHC complexes compared to the reference cisplatin or auranofin.[211]

A concept for selectively targeting mitochondria is the exploitation of its mitochondrial membrane potential ($\Delta\psi_m$). This electrical potential is a result of the respiratory chain of the mitochondria, as they establish a proton gradient between their inner membrane and their internal matrix. The inner matrix has a negative electronic potential, due to protons being transferred into the intermembrane space. Lipophilic cations which can delocalize its charge [*i.e.* delocalized lipophilic cations (DLC)] are drawn to the inner membrane due to coulomb interactions. Their lipophilicity enables them to penetrate the hydrophobic plasma and mitochondrial membranes and to accumulate in the mitochondria. It has been reported that the $\Delta\psi_m$ is higher in certain cancer cells compared to healthy cells, giving an exploitable target for cancer treatment.[212-213] Aside targeting mitochondria and the TrxR system, a direct interaction of gold complexes with genetic material is possible for quadruplex DNA aside double helical DNA.[214-218] This type of genetic secondary structure is formed in DNA regions with guanine rich sequences and can form from a singular, two or four strands. This structure often occurs at the end of

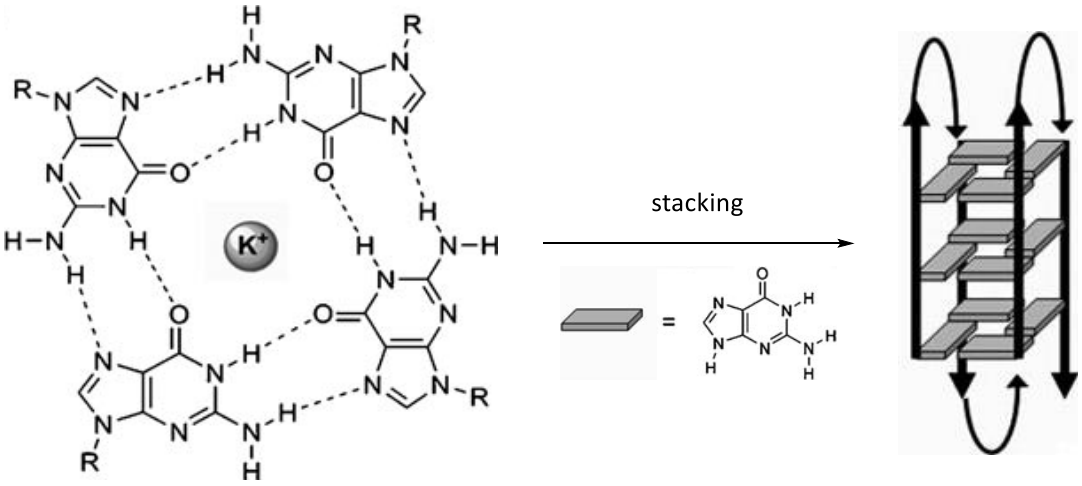

Figure 18: Four guanine bases forming a guanine tetrad with central monovalent cation (here potassium), stacking to form a guanine quadruplex formed from a singular DNA strand.[215] Reprinted and modified from Ref. [215] by permission of John Wiley and Sons (see chapter 5.6).

chromosomes, due to the guanine rich, repetitive sequences in the telomeric regions or in regions of transcriptional regulation. The structure is based on the association of four guanine residues *via* Hoogsteen hydrogen bonding and form a square planar guanine tetrad. These tetrads stack on top of each other due to π-interactions to form a guanine quadruplex (G4-DNA) and incorporate monovalent cations in the central cavity (see figure 18).[215]

Quadruplex DNA is prominently present in telomeric regions of the DNA and cancer cells tend to have overexpressed telomerase systems.[219-220] Various publications showed that the chromosome shortens upon DNA replications, prior to cell division. The length of telomers is maintained by the activity of telomerases, which is regulated in normal cells. However, cancer cells counteract such a progressive loss of the telomere length unregulated and therefore obtain limitless replication potential. Telomerase systems are overexpressed in about 85-90% of all cancer cell types.[221-224] The telomerase activity can be inhibited *via* the stabilization of G4-DNA structures, as this structure cannot be processed by the telomerase, leading to apoptosis. Therefore, targeting G4-DNA can improve selectivity towards cancer cells against regular cells.[221-223]

Multiple complexes, harboring different transition metals and ligand types, and organic compounds have been reported to stabilize G4-DNA structures. [215, 217-218, 225-227] If planar or linear compounds are applied, the interaction usually occurs *via* external stacking to the tetrads or intercalation between the tetrad layers.[226-229] It has been shown that the interaction mainly relies on π-π interactions of the compound with the guanine residues.[227] Aside from the classic metals, coordinated in biological systems, the scope of application could be expanded by the utilization of other late transition metals. Additional applications lie in the field of medicinal imaging or drug transportation.[227, 229-231]

2 OBJECTIVE

The high activity in epoxidation catalysis of the non-heme iron complexes **V** and **VI,** reported by Kühn and coworkers are a promising starting point for further investigations of cyclic tetra-NHC iron complexes.[113, 147] Therefore, the catalytic system may be improved *via* modifying the ligand system. Increasing or decreasing the electron donation towards the iron center is prone to have a defined effect on the catalyst system. Such modifications may further increase the catalytic activity or decrease the lability of the system. This could enable catalysis at elevated temperatures or the conversion of more challenging substrates. Deuteration experiments of complexes **V** and **VI** and subsequent kinetic studies would give insights into possible degradation pathways.

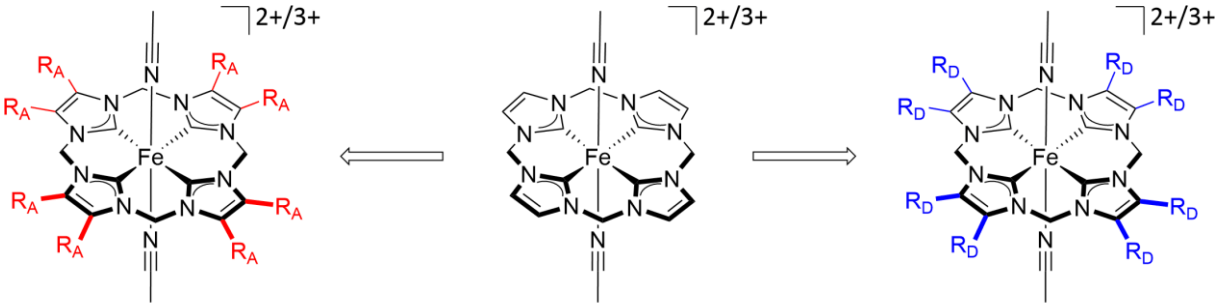

Figure 19: Chemical structure of complexes **V** or **VI** and possible derivative structures with electron accepting (R_A, red) and donating substituents (R_D, blue).

Macrocyclic square-planar tetra-dentate NHC complexes remotely resemble porphyrin systems in structure. Such complexes could offer beneficial properties in biological applications, for example as drug for anti-cancer treatment. There are numerous examples for square-planar complexes harboring group 10 and 11 elements which have been already successfully tested.[232] Therefore, ligand systems which are primarily developed for iron-based epoxidation catalysis can also be utilized to synthesize new group 10 or 11 complexes and apply those for biological testing to provide valuable information about activity-structure relationships.

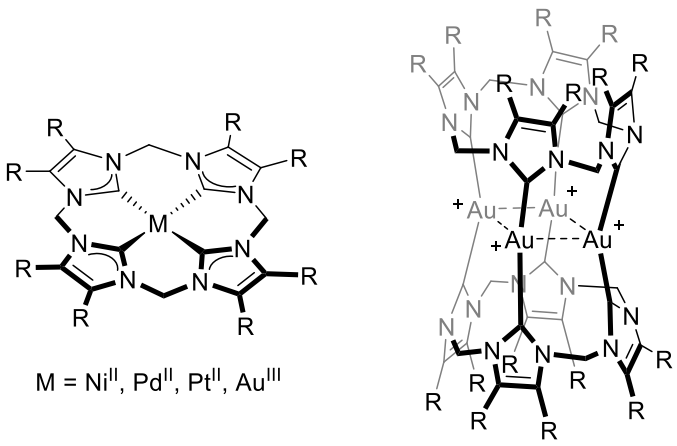

Figure 20: Chemical structures of macrocyclic tetra-NHCs ligands with square planar coordinating metal ions and linear coordinating Au^I, based on already reported structures.[233]

3 Results

3.1 Publication Summaries

3.1.1 Tuning the electronic properties of tetradentate iron-NHC complexes: Towards stable and selective epoxidation catalysts

Marco A. Bernd,[‡] Florian Dyckhoff,[‡] Benjamin J. Hofmann, Alexander D. Böth, Jonas F. Schlagintweit, Jens Oberkofler, Robert M. Reich and Fritz E. Kühn

[‡] M. A. Bernd and F. Dyckhoff contributed equally to this work.

Journal of Catalysis **2020**, *391*, 548–561

The iron(III) complex system *trans*-diacetonitrile[calix[4]imidazolyl]iron(III) hexafluorophosphate, reported in 2015 by Kühn *et al.* offers appealing activity in the epoxidation of *cis*-cyclooctene.[113] To further investigate this catalyst system and to determine a path for further investigations, this article addresses the modification of the macrocyclic ligand system in both possible ways in terms of electron donating capabilities. The synthesis of the new macrocyclic 4,5-dimethylimidazolium based ligand is reported alongside the synthesis of its Fe^{II} (**1a**) and Fe^{III} (**1b**) complexes. Two novel Fe^{II} (**2a**) and Fe^{III} (**2b**) complexes are reported harboring a macrocyclic benzimidazolylidene ligand. All novel compounds are characterized *via* NMR spectroscopy, ESI-MS and elemental analysis. SC-XRD structures were acquired if suitable crystals could be obtained. Furthermore, complexes are additionally characterized by of CV, UV/Vis and tested as catalysts in the epoxidation of *cis*-cyclooctene. Their different electronic properties on the respective iron centers are demonstrated *via* cyclic voltammetry, displaying lower

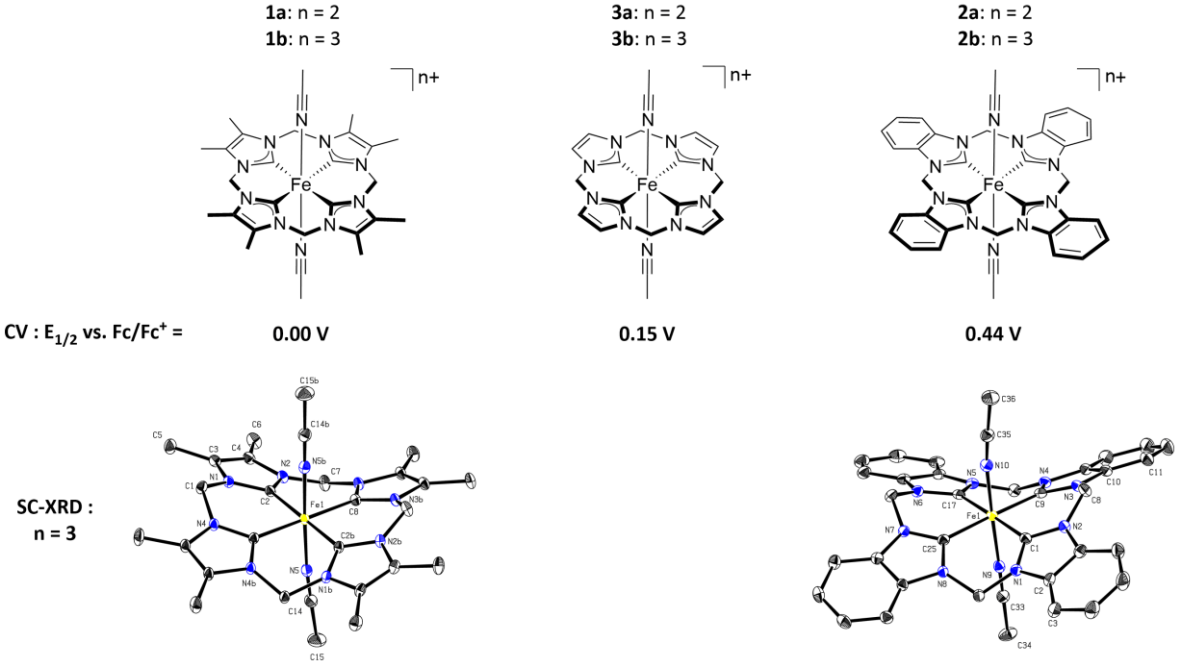

Figure 21: Chemical structures of complexes **1a**/**b** and **2a**/**b** compared to already reported complexes **3a**[147]/**b**[113]. Half-cell potentials are given with comparison to complex system **3a**/**b**, additionally SC-XRD structures of **1b** and **2b** are depicted.

(**1a**/**1b**: 0.00 V vs. Fc/Fc^+) and higher (**2a**/**2b**: 0.44 V vs. Fc/Fc^+) half-cell potentials compared to the referencing system (**3a**/**3b**: 0.15 V vs. Fc/Fc^+), aligning with the trend of the TEP of the monodentate congeners. As previously reported for complex **3a**, catalytic activity and stability of **1a** and **2a** are increased *via* addition of a Lewis acid ($Sc(OTf)_3$). Complexes **1a** and **1b** display only a low overall catalytic performance due to stability issues, **2a** and **2b** display a remarkable higher stability (TON up to 1,000 at 20 °C), but are considerably less active compared to **3a** and **3b**. Catalytic experiments at elevated temperatures of catalyst **2b** highlight its remarkable stability resulting in the highest reported TONs (360) at 80 °C for a non-heme iron epoxidation catalyst. Due to this high stability, complex **3b** is capable of catalyzing the epoxidation of more challenging substrates in comparison to the other complexes. The results of the catalytic survey do not align with the predictions made based on TEP or CV, especially for the complex **3b** showing the overall highest activity. DFT calculations reveal a significant π-interaction in compounds **1b** and **2b**, in contrast to the unsubstituted complex **3b**. Such π-interactions have not been calculated for monodentate NHC complexes and are likely derived from the rigid cyclic tetra-NHC structure. This results in electron density deflection from the iron center in complex **1b**, compensating the donating effect of the methyl groups and resulting in lower activity than **3b**.

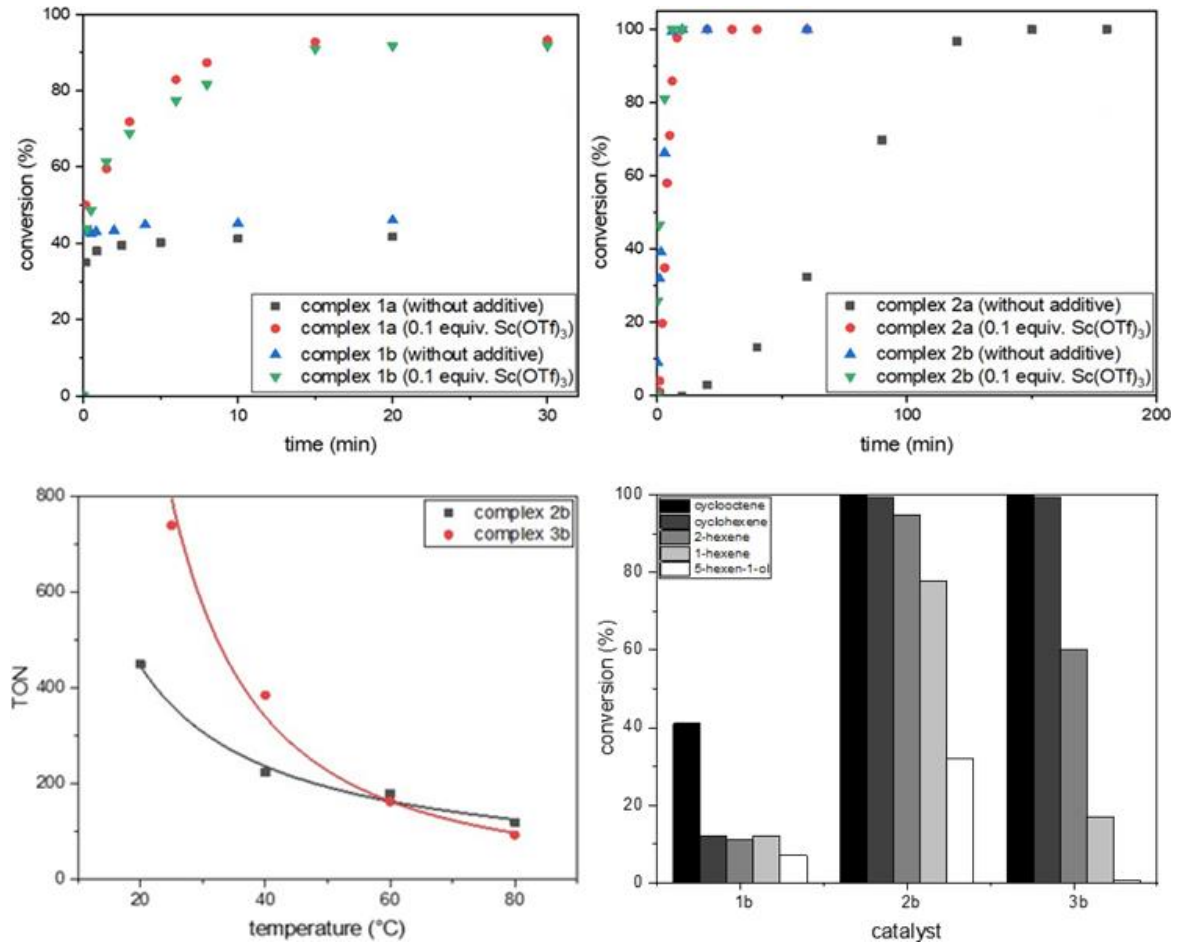

Figure 22: *Top*: Catalytic data of **1a**/**b** and **2a**/**b** with and without $Sc(OTf)_3$ as additive. *Bottom left*: Comparative graph of **2b** and **3b** temperature dependent stability, measured *via* TON. *Bottom right*: Conversion rates of various substrates for **1b**, **2b** and **3b.**

3.1.2 Synthesis, characterization, and biological studies of multidentate gold(I) and gold(III) NHC complexes

Elisabeth B. Bauer,[‡] Marco A. Bernd,[‡] Max Schütz, Jens Oberkofler, Alexander Pöthig, Robert M. Reich and Fritz E. Kühn

[‡] E. B. Bauer and M. A. Bernd contributed equally to this work.

Dalton Transactions **2019**, *48*, 16615–16625

This publication evaluates the anti-cancer activity of multidentate NHC Au^{I} and Au^{III} complexes, harboring macrocyclic or open-chain multidentate NHC ligands. Although some complexes were already known in literature, no testing for biological activity have been reported so far. The synthesis of novel compounds **1**, **2**, **3** and **L2** is described and the characterization is performed *via* ^{1}H and ^{13}C NMR spectroscopy, ESI-MS, XRD crystallography and elemental analysis. Additionally, the redox activity of complex **1** is investigated using cyclic voltammetry. The SC-XRD structures of **2** and **3** are particularly interesting, as both complexes show a composition of M_4L_2 and harbor monovalent, linear coordinating metal centers, but the Ag^{I} complex forms a tubular like structure, whereas Au^{I} forms only two C-Au^{I}-C inter-ligand connections and two intra-ligand connections. The complexes **1**, **3**, **4**, **5** and **6** are evaluated for their antiproliferative properties in MTT assays. The obtained IC_{50} values indicate that complex **5** is the most active complex in the cancer cell lines MCF-7 and A2780cisR cells.

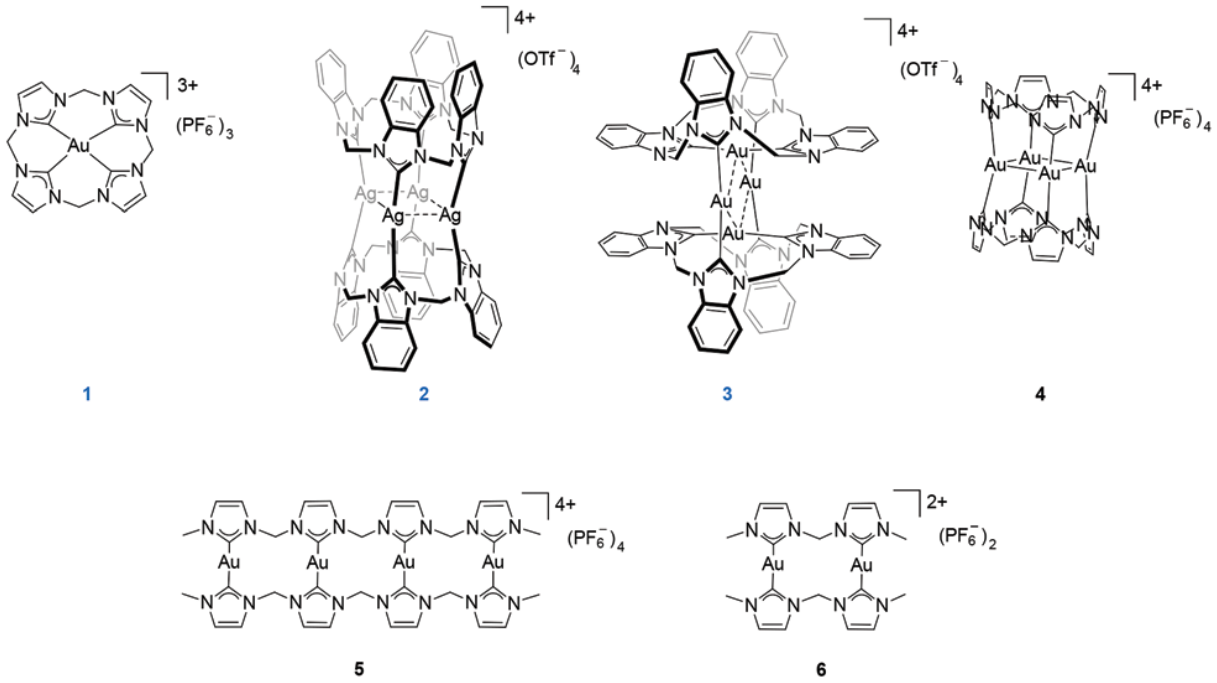

Figure 23: Chemical structural of complexes **1**-**6**. Complexes **1**-**3** are novel compounds (marked blue). Complex **2** is not tested in MTT assays due to inherent light sensitivity.

Complexes **1**, **4**, and **6** display relatively high IC_{50} values (43 - 80 µM) or no activity at all. A reason for these comparatively high IC_{50} values might be a reduced stability of these complexes under physiological conditions. However, stability studies preceding the MTT assay showed no entire instability in the cell culture medium, as though some degree of decomposition depending on the particular complex is noticeable within the incubation periods. In these studies complex **1** depicts an unusual proton exchange by deuterium at the methylene bridges. This exchange shows the possibility of an nucleophilic attack leading to decomposition of the complex. The IC_{50} values of the Au_4L_2 complexes **3** and **4** show that the increased lipophilicity improves the antiproliferative properties in HeLa and A2780cisR cell lines.

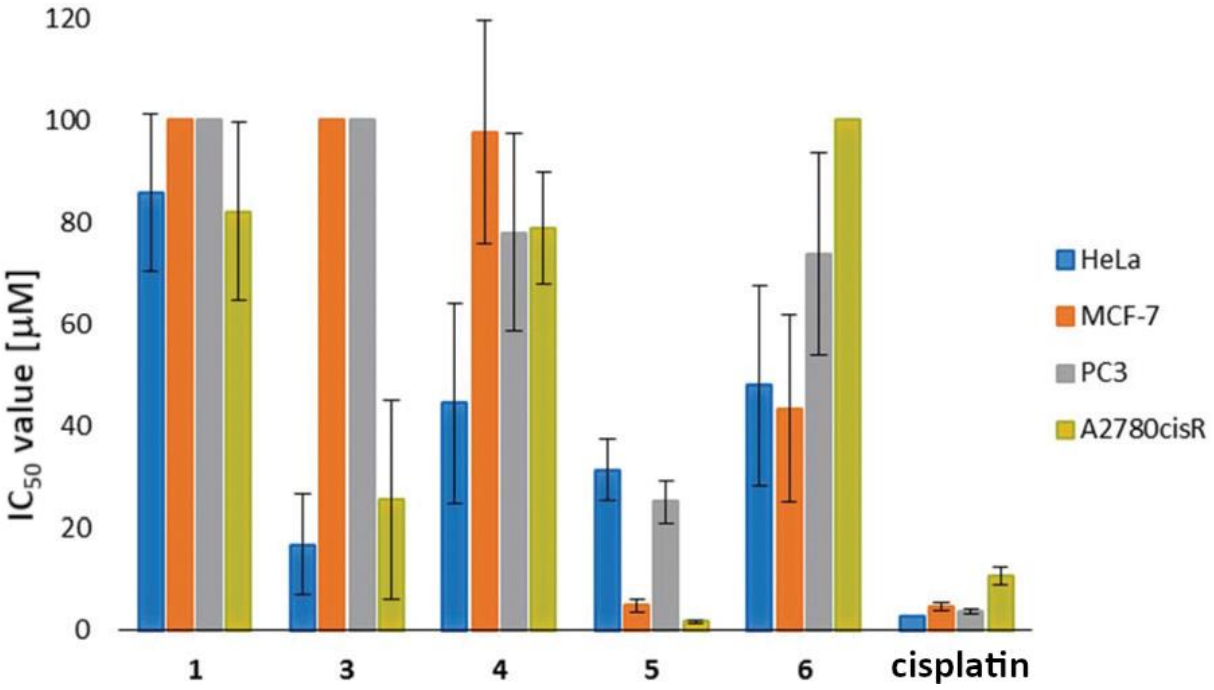

Figure 24: Graphic representation of the IC_{50} values [µM] with error range determined *via* MTT assays with an incubation time of 48 h for the different NHC gold complexes **1**, **3**-**6** and cisplatin in HeLa, MCF-7, PC3, and A2780cisR cancer cell lines.

3.1.3 Macrocyclic NHC complexes of group 10 elements with enlarged aromaticity for biological studies

Marco A. Bernd,[‡] Elisabeth B. Bauer,[‡] Jens Oberkofler, Andreas Bauer, Robert M. Reich and Fritz E. Kühn

[‡] M. A. Bernd and E. B. Bauer contributed equally to this work.

Dalton Transactions **2020**, *49*, 14106-14114

This publication investigates square planar macrocyclic tetradentate NHC complexes of Ni^{II}, Pd^{II} and Pt^{II} for their antiproliferative properties against cancer cells utilizing MTT assays. The ligands are designed to mimic porphyrin system and are based on imidazolium and benzimidazolium. Complexes **A-C** harbour the macrocyclic imidazolyl ligand and are already known in literature[233] but have not been tested for antiproliferative properties. A new synthetic route is reported and novel complexes **D-F** incorporate a macrocyclic benzimidazolyl ligand and are characterized *via* NMR spectroscopy, ESI-MS, elemental analysis, XRD crystallography and UV/Vis spectroscopy. It has been predicted by DFT calculations in literature[234] that the Pt^{II} containing complex **F** should exhibit phosphorescence. Therefore, photometric evaluation of complexes **D-F** is conducted. The predicted phosphorescence of complex **F** could not be verified, however the Pd^{II} containing complex **E** shows high phosphorescence.

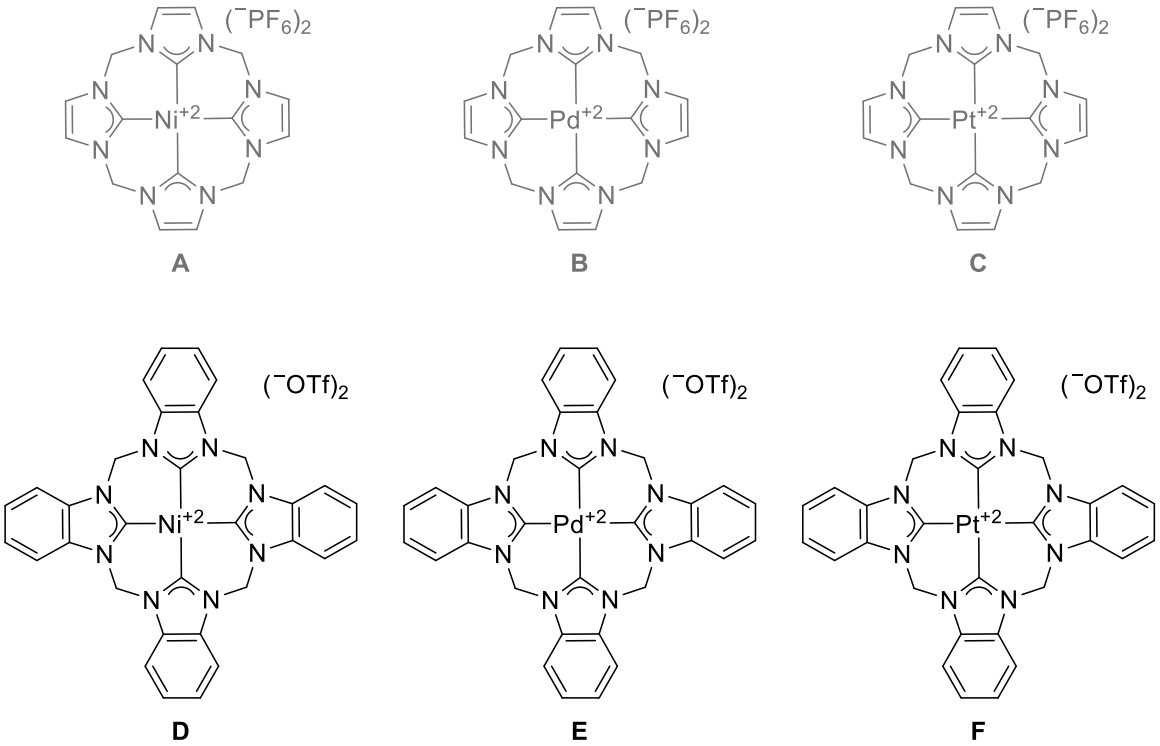

Figure 25: Chemical structures of literature known macrocyclic NHC complexes **A-C** and novel complexes **D**-**F**, incorporating group 10 metals.

The complexes **A**-**F** are evaluated for their stability in DMSO/cell culture medium prior to evaluation of their antiproliferative properties in MTT assays. The obtained IC_{50} values portray that both Ni^{II} complexes **A** and **D** exhibit very poor to no activity in all cancer cell lines, whereas the Pd^{II} (**B**/**E**) and Pt^{II} (**C**/**F**) complexes exhibit good activity in the tested cancer cell lines. The exceptions are complexes **E** and **F**, which show no activity in MCF-7 cells. The highest activity is shown by complex **E** in A2780cisR cells and HeLa cells. The IC_{50} values for both imidazolyl based complexes **B** and **C** are very similar, as are the values for the benzimidazolyl complexes **E** and **F**. This indicates that the biological activity is mainly depended on the present ligand system, as the differences between the according Pd^{II} and Pt^{II} complexes is not significant. The smaller IC_{50} values of **E** and **F** compared to **B** and **C** in HeLa and A2780cisR cell lines indicate that the increased lipophilicity improves the antiproliferative properties, which stands in contrast to the inactivity of **E** and **F** in MCF-7 cells. Furthermore, complexes **E** and **F** offer luminescence properties without an additional marker as proven by UV/Vis and photometric evaluation.

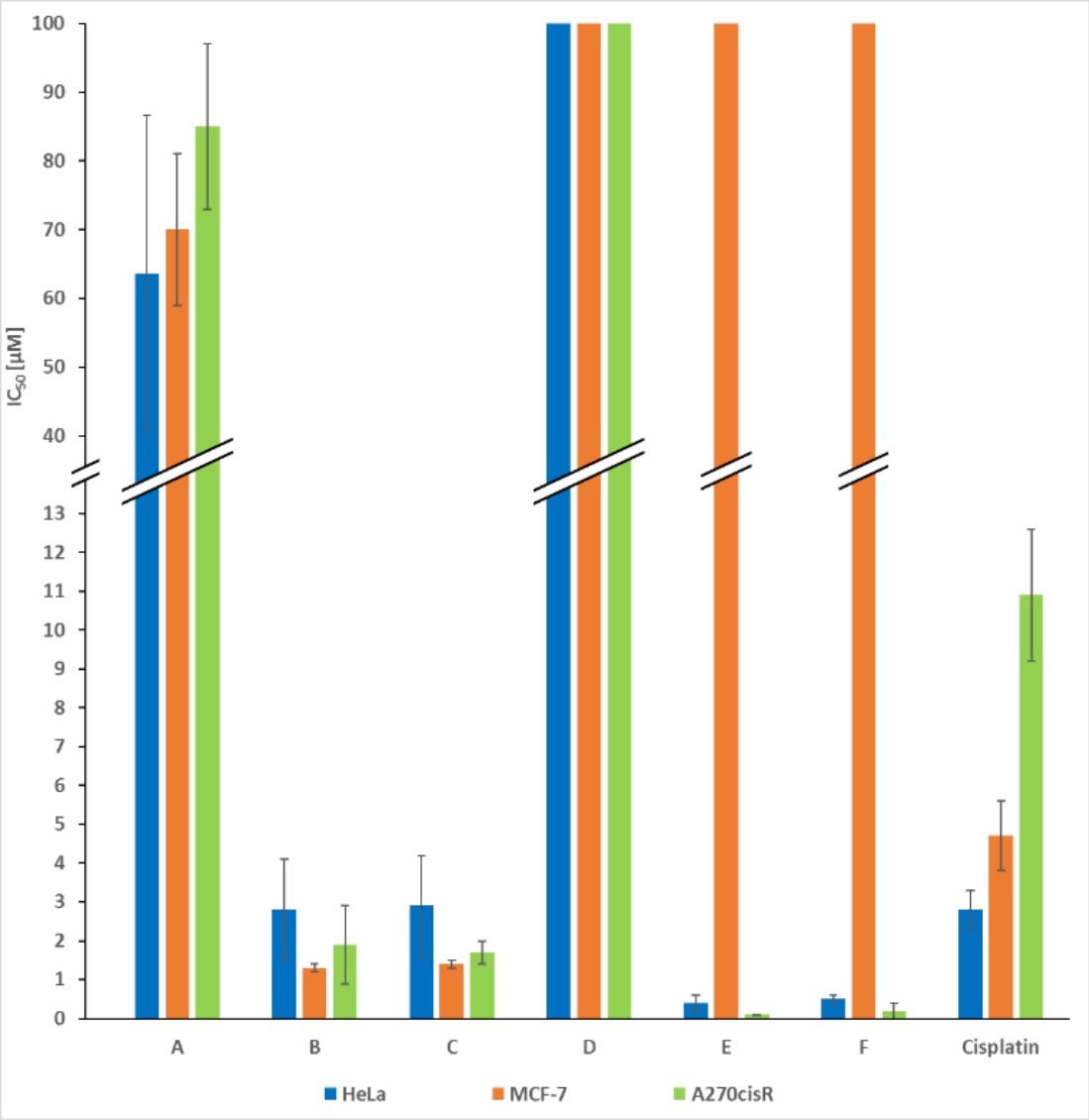

Figure 26: Graphical representation of the IC_{50} values [µM] determined for the complexes **A**-**F** in HeLa, MCF-7 and A2780cisR cells *via* the MTT assay with an incubation time of 48 h.

3.2 Unpublished Results

3.2.1 Investigation of ligand fluorination for epoxidation catalysis

The publication "Tuning the electronic properties of tetradentate iron-NHC complexes: Towards stable and selective epoxidation catalysts",[235] which is part of this thesis, gives evidence that decreasing the donor strength of macrocyclic tetra-NHC ligands is beneficial for iron-based epoxidation catalysis. Therefore, a ligand system capable of harboring an increasing amount of fluorine atoms was set out for development. The system was chosen to resolve around 4,5-diphenylimidazole, as the utilization of backbone fluorinated or CF_X substituted derivatives of imidazole induces challenges in the macrocyclization step, which could not be circumvented. This is due to a decrease in nucleophilicity induced by fluorination of the amine/imine functionalities of the imidazole-based building blocks. This interferes with the macrocyclization step, being based on an nucleophilic substitution reaction. For this ongoing project the two ligands Calix[4](4,5-diphenylimidazolium) triflate (**^{Ph}L OTF**) and Calix[4](4,5-bis(*para*-fluorophenyl)-imidazolium) triflate (**$^{p\text{-}F\text{-}Ph}$L OTf**) are successfully synthesized and utilized in the synthesis of the respective Fe^{II} complexes.

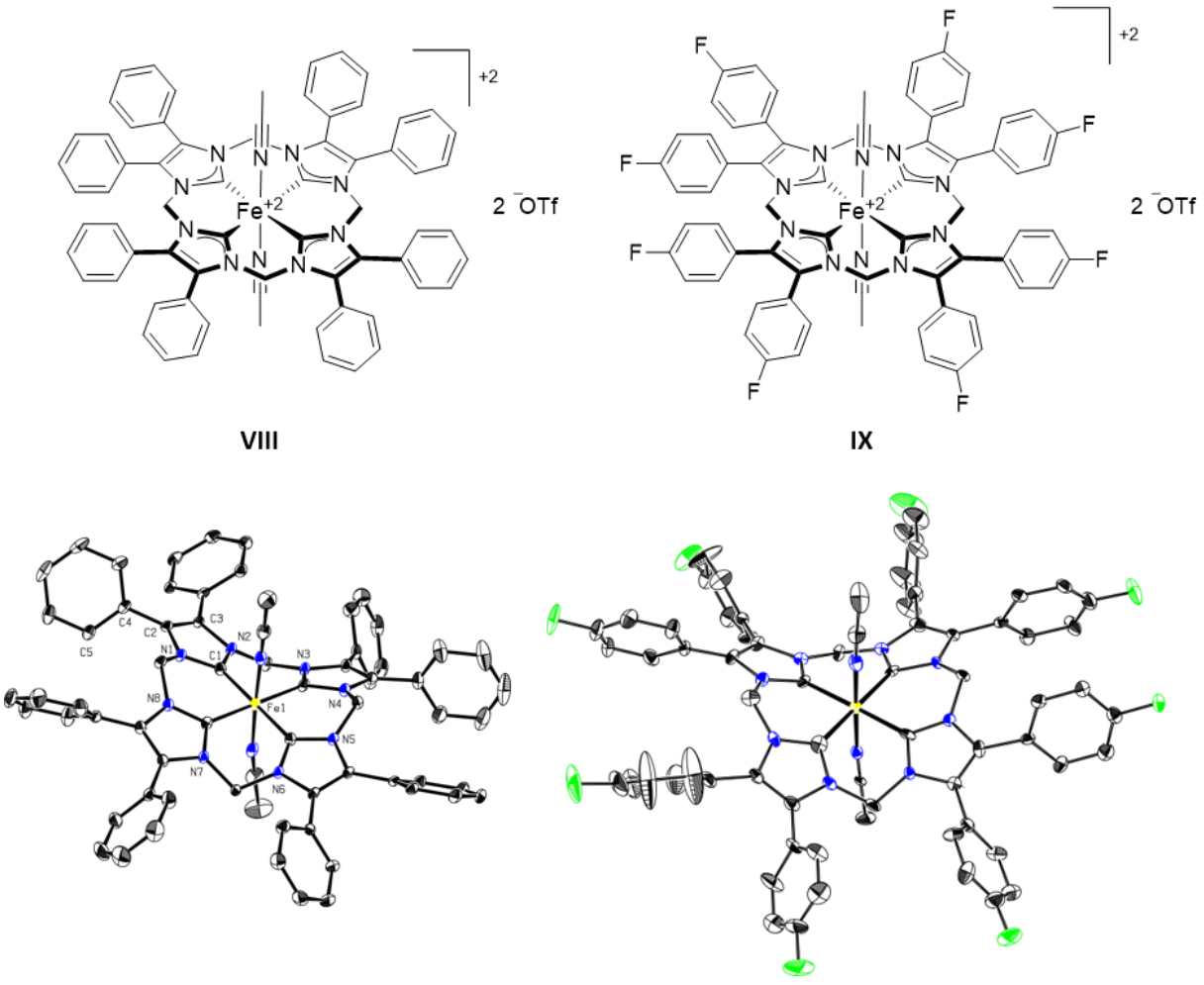

Figure 27: Chemical structure an ORTEP style representation of unpublished Fe^{II} complexes **VIII** and **IX**. The SC-XRD structure of **IX** is only preliminary, due to twinning of the crystals. Thermal ellipsoids are shown at a 50% probability level, hydrogen atoms are omitted for clarity. Element colors: black - carbon, blue – nitrogen, green – fluorine, yellow – iron.

Synthesis of 4,5-bis(*para*-fluorophenyl)imidazole is performed *via* a literature known synthesis, combining two steps in a one-pot synthesis,[236] whereas 4,5-diphyenimidazole is commercially available. Starting from the basic imidazole building blocks, the syntheses for dimerization, macrocyclization and metalation are performed in accordance to literature for imidazole derivatives.[147, 237] The poor solubility of both imidazolium macrocycles in water makes the anion exchange to hexafluorophosphate unfavorable. Therefore, the corresponding Fe^{II} complexes are synthesized bearing a triflate anion. This does not harm comparability to similar systems, as shown for the macrocyclic iron complexes incorporating benzimidazole NHC moieties.[235]

Single crystals for determining the structure by SC-XRD were obtained *via* slow diffusion of diethyl ether into an acetonitrile solution of the respective complex. Here, the acquired diffraction data set of **IX** could not yet been refined to satisfying values, rendering the reported values for bond distances questionable. The acquired structure for **IX** can therefore only be utilized to confirm the synthesis method.

CV experiments of **VIII** and **IX** were conducted to determine the half-cell potential of these complexes compared to **V**/**VI**[147] ($E_{1/2}$(**V**/**VI** vs. Fc/Fc^+) = 0.15 V) and **2a**/**2b** ($E_{1/2}$(**2a**/**2b** vs. Fc/Fc^+) = 0.44 V)and in relation to each other. Both complexes **VIII** and **IX** show a reversable one-electron oxidation. Complex **VIII** shows a half-cell potential $E_{1/2}$(vs. Fc/Fc^+) of 0.19 V, whereas complex **IX** shows a half-cell potential $E_{1/2}$(vs. Fc/Fc^+) of 0.21 V. The higher half-cell potential of **IX** can be explained through the -I effect of the fluorine-substitution, decreasing the electron density at the iron center, making an oxidation slightly comparably unfavorable. This finding is in accordance to the assumptions for the fluorine substitution. It is assumed that this trend should continue for complexes with higher degree of fluorine substitution than **IX**. The determined half-cell potentials are between **V**/**VI** and **2a**/**2b**, demonstrating that this system in general is interesting for evaluation in epoxidation catalysis. Complexes **VIII**, **IX**, or other derivatives bearing multiple fluorine atoms on each phenyl ring may offer high activity in epoxidation catalysis, comparable to **V**/**VI** but also show sufficient stability as **2a**/**2b** due to the lower donation capabilities of the respective ligand system.

Preliminary results suggest that the π-system of the phenyl rings do not interact with the π-system of the imidazole moieties. This can be seen from the CV, which would detect higher half-cell potentials, due to the aromatic system dispersing electron density from the iron center *via* their -M effect. The SC-XRD additionally shows that the phenyl rings do not align with the imidazolyl, due to steric repulsion, rendering a π-interaction highly unfavorable. This results in the -M effect of the phenyl rings to be highly suppressed, as the phenyl π-system can only interact with the π-system of the 4,5-imidazolyl positions if both systems are aligned.

3.2.2 Synthesis of deuterated derivative of macrocyclic imidazolyl-based Fe^{II} and Fe^{III} complexes

The primary degradation pathway for macrocyclic tetra-NHC iron complexes under oxidative conditions is still unknown. Therefore, the synthesis of the deuterated pre-ligand calix[4]imidazolium-d_8 hexafluorophosphate (**L-*d*$_8$ PF$_6$**) was developed, which is a derivative of a literature known compound.[147] The deuterium atoms are placed at the methylene bridges, replacing -CH_2- with -CD_2- groups. This ligand was utilized for the synthesis of the corresponding Fe^{II} (**X**) and Fe^{III} (**XI**) complexes for future investigations. Here, the focus lies on the investigation of a possible degradation pathway in the catalytic epoxidation of *cis*-cyclooctene using hydrogen peroxide.

The success of deuteration was monitored during the synthesis steps *via* the residue proton signals of the corresponding chemical groups, the $^1J_{D\text{-}13C}$ coupling in ^{13}C NMR spectroscopy, ^2H NMR spectroscopy, ESI-MS and high-resolution mass spectroscopy. To evaluate whether the deuterium atoms interfere unexpectedly with the electron density of the iron center, CV measurements were conducted. Here, no difference to the half-cell potential to **V**/**VI**[147] could be detected. Complexes **X** and **XI** were utilized in the catalytic epoxidation utilizing *cis*-cyclooctene as model substrate and compared to its non-deuterated derivatives. If a degradation pathway would include the oxidation of the methylene bridges, the kinetic isotope effect would stabilize the complexes **X** or **XI** in comparison to **V** or **VI**.

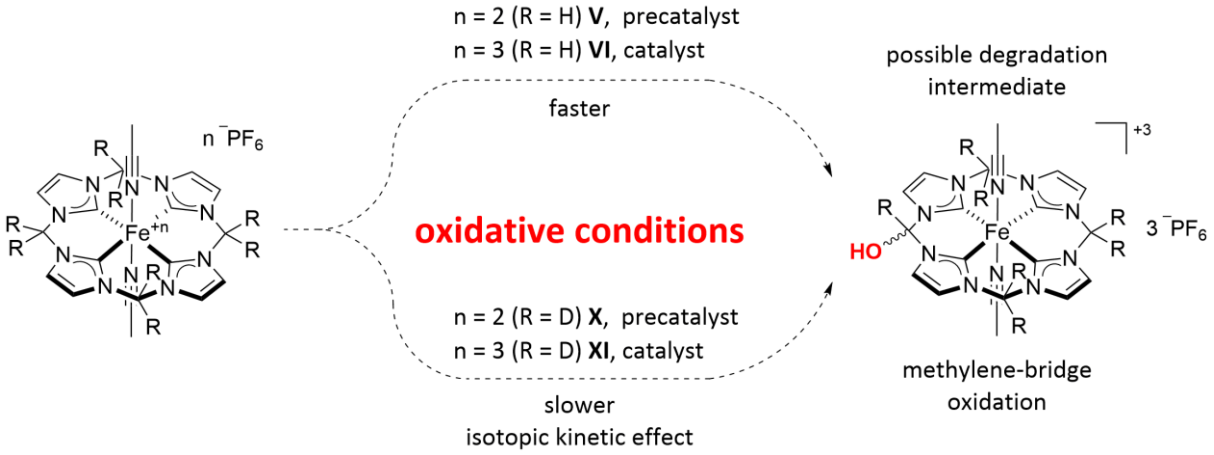

Figure 28: Chemical structure of the Fe^{II} complex **X** (R = D, n = 2) and the corresponding Fe^{III} derivative **XI** (R = D, n = 3) and to be investigated possible degradation pathway for macrocyclic tetra-NHC iron complexes under oxidative conditions.

A turn-over number comparison at 20 °C shows no distinctive difference in the stability of the complexes. Here, complex **VI** is reported to show a TON of 740 regularly and 1230 with the presence of $Sc(OTf)_3$,[238] complex **XI** shows a TON of 760 regularly and 1250 in the presence of $Sc(OTf)_3$. These values are too similar for a discrete degradation pathway which requires the oxidation of the methylene bridges. Therefore, it can be assumed that no significant amount of methylene oxidation initiates degradation of the complexes under oxidative conditions.

3.2.3 Complexes for further biological studies

Furthermore, multiple group 10 and 11 complexes have been synthesized applying the ligand Calix[4](4,5-dimethylimidazolium) triflate or hexafluorophosphate.[235] These complexes are designed for future biological studies in comparison to the publications implemented in this thesis.[239-240]

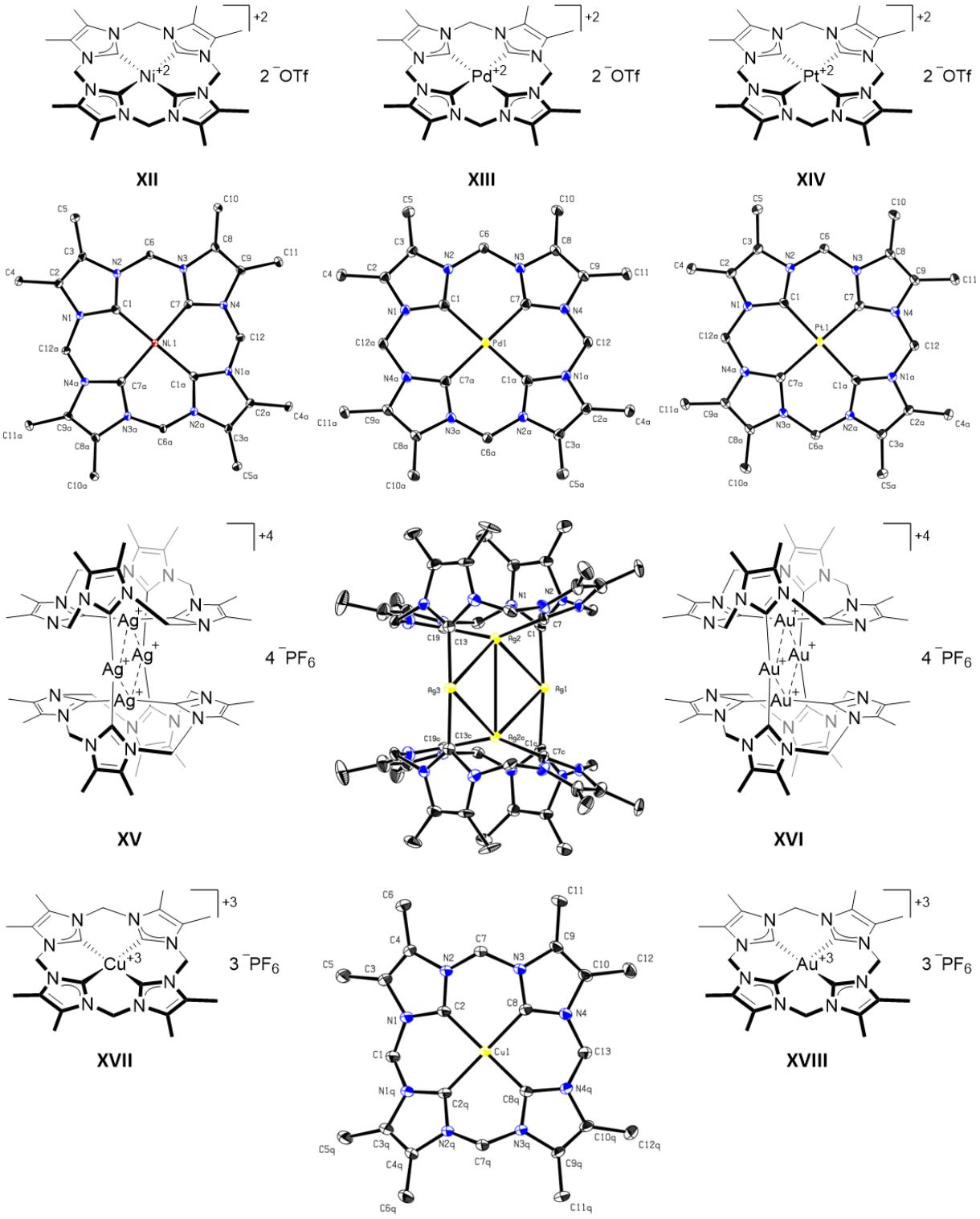

Figure 29: Chemical structures of synthesized complexes harboring Calix[4](4,5-dimethylimidazolium) OTf^- or PF_6^- as ligand. Acquired SC-XRD structures are depicted. All complexes are determined for biological testing. Acquired SC-XRD structures are depicted in ORTEP style for complexes **XII**, **XIII**, **XIV**, **XV** and **XVII**. Thermal ellipsoids are shown at a 50% probability level, hydrogen atoms are omitted for clarity. Non-metal element colors: black – carbon, blue – nitrogen.

This series include various square planar complexes as well as complexes of the composition M_4L_2, due to linear coordination. The Cu^{III} complex is of particular interest, due to its air and water stability. This complex is similar to an example in literature,[241] both of which have not been tested for biological applications. Furthermore, the Au^{III} complex is of high interest, as Au^{III} compounds have gained much focus in recent year in the field of anti-cancer drug development.[242]

4 Conclusion and Outlook

This thesis focusses on the synthesis of macrocyclic tetra-dentate *N*-heterolytic carbene ligand systems, which are exclusively methylene bridged. These ligands are utilized for the synthesis of various late transition complexes. These complexes have been generally characterized by means of ^{1}H and ^{13}C NMR spectroscopy, ESI-MS, SC-XRD (if suitable crystals could be obtained) and elemental analysis. If required, further characterization was performed *via* UV/Vis spectroscopy and CV. The complexes were investigated for applicability in different fields, depending on the transition metal present in the complex.

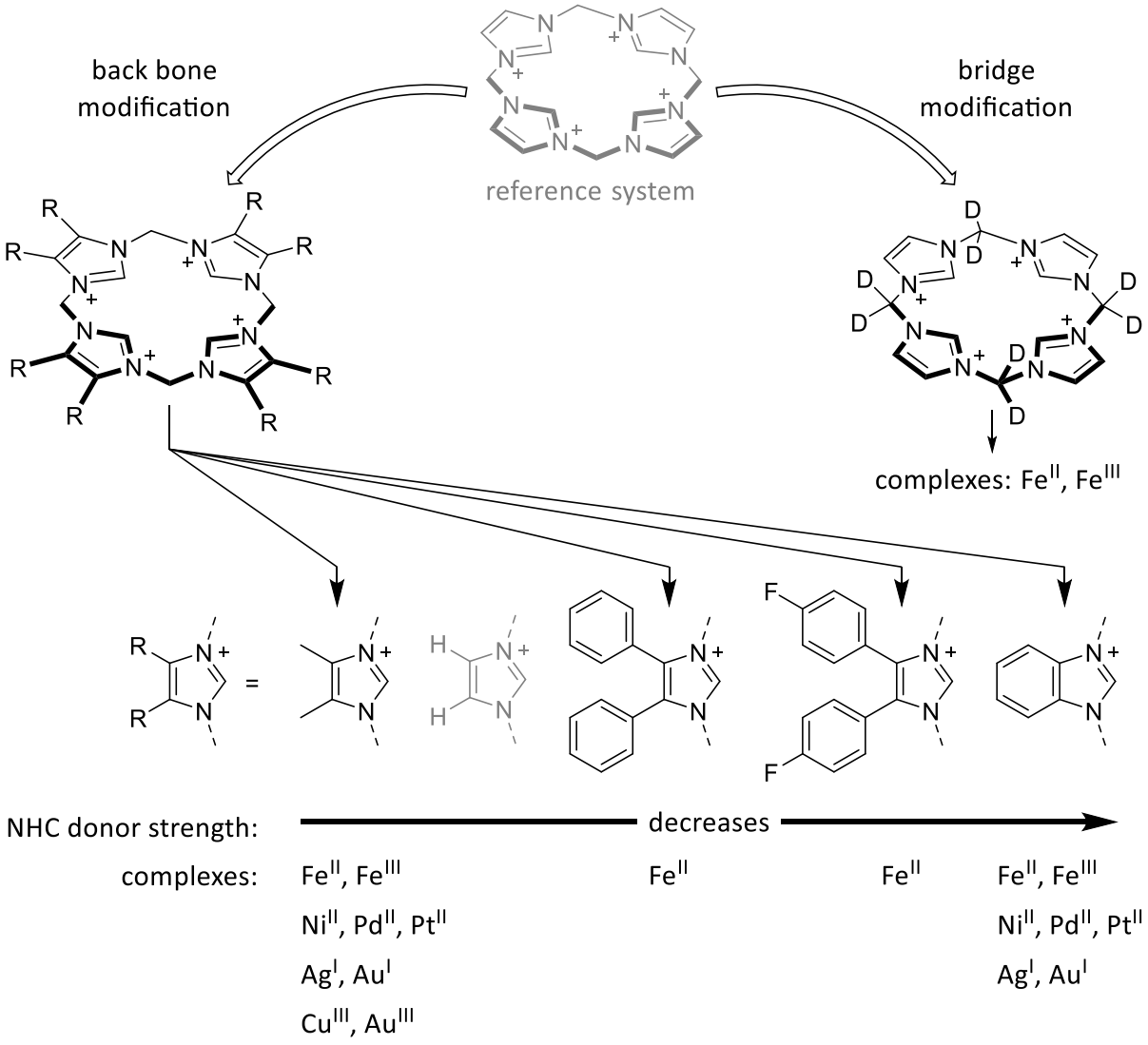

Figure 30: Ligand modification performed in this work and the subsequently synthesized complexes.

The benchmark ligand system based on imidazole units has been modified to vary the donating capabilities of the ligand system. Therefore, the ligand based on benzimidazolium offers decreased donation and 4,5-dimethylimidazolium increased donation capabilities. Both of these ligands have been primarily utilized for the synthesis of Fe^{II} and Fe^{III} complexes. These complexes have been investigated for their applicability as catalysts in epoxidation catalysis in comparison to the bench-mark imidazolyl-based complexes. The purpose was to investigate the role of varying the electron density at the iron center of the complexes and the corresponding effect on catalyst performance. The results show that an increased electron donation to the iron center decreases the stability of the complexes under oxidative conditions and therefore is disadvantageous for the epoxidation reaction. In contrast, the decreased electron density at the iron center greatly increases the catalysts stability at the cost of an overall lower activity. The decreased activity of the catalyst seems to be beneficial in the epoxidation of more challenging olefins as substrates compared to *cis*-cyclooctene.

Further studies should focus on the investigation of modified catalyst systems with decreased electron density compared to the imidazole-based reference system, as this seems to be beneficial for overall applicability. Iron complexes harboring a naphtho[2,3-d]imidazolium-based ligand would be of particular interest. It would provide information if the trend seen for the benzimidazolyl system would continue by further enlarging the aromatic system. This may increase stability and therefore show even better performance for challenging substrates. Also, the aromatic moieties of this naphthoimidazolium-based ligand or the benzimidazolium-based ligand give a possible target for modification. It is deemed possible to perform an electrophilic aromatic substitution *via* a Friedel-Crafts acylation. Therefore, an immobilization of the respective complex system should be feasible. This may increase the stability of the complex system, as it is still unknown whether degradation occurs *via* interaction of two complex systems in close proximity under oxidative conditions. Furthermore, the ligand **^{Ph}L OTf** offers a suitable system for investigating the modulation of donating capabilities by progressive fluorination. CV indicates that complex **VIII** offers a similar half-cell potential as the bench-mark system **V**/**VI**. Complex **IX** has an increased half-cell potential due to the presence of fluorine. Therefore, by adding another derivative harboring multiple fluorine/phenyl would give a library for testing the effect of progressive fluorination on catalyst performance in epoxidation. These possible future developments in the field of epoxidation catalysis utilizing macrocyclic Fe-NHC complexes are summarized in figure 31.

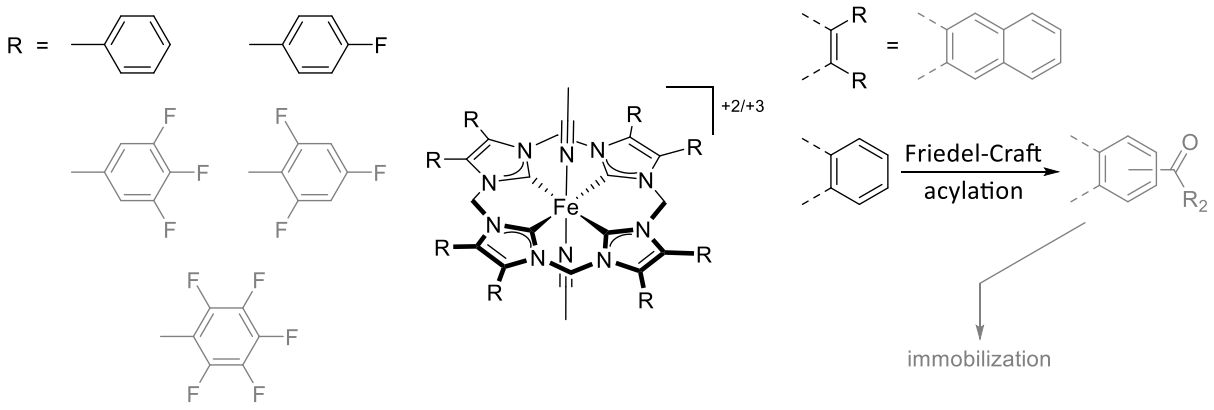

Figure 31: Possible future project concerning the development of iron-based epoxidation catalysis. Blackened regions depict compounds with assured synthetic success, greyed are deemed possible.

Macrocyclic tetra-NHC complexes based on imidazolyl and benzimidazolyl ligands have been synthesized harboring group 10 and 11 metals. These complexes were structurally compared and applied in biological testing for the antiproliferative effects on cancer cells. For group 11 elements, the synthesis of the Au^{III} complex **1** was successful. Together with the new Au^{I} complex **3** and other previously published gold-NHC-complexes, these compounds were investigated for stability in cell culture medium as well as in solution with presence of GSH. All complexes showed sufficient stability for further cell tests. While performing the stability studies, an unexpected proton to deuterium exchange due to the deuterated NMR solvent was observed for complex **1**. The complexes were subsequently tested for their antiproliferative properties in multiple cancer cells using the MTT assay method. This study shows that the open-chain complex **5** offers the overall best activity with a high selectivity for the MCF-7 and A2780cisR cancer cell lines. A second study covered the biological testing of square planar complexes based on macrocyclic tetra-dentate imidazolyl and benzimidazolyl ligands harboring divalent group 10 metals. The benzimidazolyl complexes are novel, the imidazolyl complexes are literature known, whereas new synthetic routes for the latter are reported. A photometric evaluation of benzimidazolyl complexes **D**-**F** was performed, due to theoretical studies predicting phosphorescence for the respective Pt^{II} complex. The phosphorescence of the Pt^{II} complex could not be verified, however the Pd^{II} complex **E** showed high phosphorescence. Prior to cell testing, all six complexes were evaluated for their stability in DMSO/cell culture medium and in the presence of GSH. The antiproliferative properties were determined in MTT assays. The obtained IC_{50} values show that the Pd^{II} (**B**/**E**) and Pt^{II} (**C**/**F**) complexes exhibit good activity in the tested cancer cell lines, with the exception of the benzimidazolyl complexes **E** and **F** in MCF-7 cells. The difference in inhibitory activity between Pd^{II} or Pt^{II} is not significant in most cell lines in contrast to the Ni^{II} complexes, which exhibiting poor to no activity in all cancer cell lines. The increased lipophilicity of benzimidazolyl based complexes improves the antiproliferative properties, if a significant activity is present, compared to imidazolyl based complexes.

Future studies in the field of medicinal chemistry utilizing complexes harboring macrocyclic tetradentate NHCs should include the investigation of distribution studies of the benzimidazolyl complexes **E** & **F** utilizing their luminescence properties. Therefore, these compounds may also be investigated for applicability in photodynamic light therapy. Furthermore, studies whether these square planar complexes can stabilize G-quadruplex DNA are of interest to determine possible mode of actions. Additionally, the unpublished complexes **XII**-**XVIII** based on 4,5-dimethylimidazole are of interest for biological testing. For a complete study, the "library" of possible group 10 and 11 complexes should be completed which includes the Cu^{I} complex.

5 EXPERIMENTAL

5.1 General remarks

Unless otherwise stated, all manipulations were performed under an argon atmosphere using standard Schlenk and glovebox techniques. Solvents were obtained water- and oxygen-free from an MBraun solvent purification system and stored over molecular sieves 3 Å. DMSO was dried being refluxed over CaH_2 and distilled prior being stored over molecular sieve 4 Å, MeCN-d_3 was refluxed over phosphorus pentoxide and distilled prior to use. [Fe(HMDS)$_2$(THF)][243], thianthrenyl hexafluorophosphate[244] and calix[4](4,5-dimethylimidazolium) triflate and hexafluorophosphate[235] were synthesized according to literature procedures. Methylene-d_2 bis(trifluoromethansulfonate) (Me-d_2(OTf)$_2$) was synthesized corresponding to literature,[147] utilizing paraformaldehyde-d_2 instead of regular paraformaldehyde. CD_2Cl_2 (99.80% D) was purchased from Euriotop with and paraformaldehyde-d_2 (98% D) from Sigma-Aldrich. All other reagents were purchased from commercial suppliers and used without further purification. NMR spectra were recorded on a Bruker Avance DPX 400 (^{1}H NMR, 400.13 MHz; ^{13}C NMR, 100.53 MHz) and Bruker Avance III 400 (^{2}H NMR, 61 MHz; ^{19}F NMR, 471 MHz). Chemical shifts are reported relative to the residual signal of the deuterated solvent. For ^{2}H NMR spectra, chemical shifts are reported relative to the added standard of deuterated solvent diluted in the equivalent non-deuterated solvent. For ^{19}F NMR spectra, chemical shifts are referenced towards hexafluoro benzene (-164.9 ppm) if non-anion signals are of interest. Elemental analyses (C/H/N) were performed by the microanalytical laboratory at Technische Universität München. The calculated results for the elemental analysis of deuterated compounds are stated as non-deuterated components, as the detection is performed *via* gas chromatography with subsequent thermal conduction. With this setup, no differentiation can be made between the proton and deuterium content. Therefore, this method is only liable to confirm the absence of major contaminations. Electrospray ionization mass spectrometry (ESI-MS) data were acquired on a Thermo Fisher Ultimate 3000 using formic acid as eluent additive, high resolution mass spectrometry (HR-MS) data were acquired on a Thermo Fisher Exactive Plus Orbitrap. CV measurements were recorded using a Metrohm Autolab potentiostat employing a gastight three-electrode cell under an argon atmosphere. A glassy carbon electrode was used as the working electrode and polished before each measurement. A graphite stick was used as the counter electrode. The potential was measured against Ag/AgCl (3.4 M KCl) with a scan rate of 100 mV/s and ferrocene was applied as an internal standard. Tetrabutylammonium hexafluorophosphate (100 mM in MeCN) was used as the electrolyte. The concentration of the complexes was about 5 mM.

5.2 X-ray crystallographic measurements

Data was collected on a single crystal x-ray diffractometer equipped with a CMOS detector (Bruker APEX III, κ-CMOS), an IMS microsource with MoK_α radiation (λ = 0.71073 Å) and a Helios optic using the APEX3 software package.[245] Measurements were performed on single crystals coated with perfluorinated ether. The crystals were fixed on top of a KAPTON micro sampler and frozen under a stream of cold nitrogen. A matrix scan was used to determine the initial lattice parameters. Reflections were corrected for Lorentz and polarization effects, scan speed, and background using SAINT.[246] Absorption correction, including odd and even ordered spherical harmonics was performed using SADABS.[247] Space group assignment was based upon systematic absences, E statistics, and successful refinement of the structure. The structures were solved using SHELXS or SHELXT with the aid of successive difference Fourier maps, and were refined against all data using SHELXT in conjunction with SHELXE.[248-250] Hydrogen atoms were calculated in ideal positions as follows: Methyl hydrogen atoms were refined as part of rigid rotating groups, with a C–H distance of 0.98 Å and $U_{iso(H)} = 1.5\ U_{eq(C)}$. Other hydrogen atoms were placed in calculated positions and refined using a riding model, with methylene and aromatic C–H distances of 0.99 Å and 0.95 Å, respectively, and other C–H distances of 1.00 Å, all with $U_{iso(H)} = 1.2\ U_{eq(C)}$. Non-hydrogen atoms were refined with anisotropic displacement parameters. Full-matrix least-squares refinements were carried out by minimizing $\Sigma_w(F_o^2 - F_c^2)^2$ with the SHELXL weighting scheme.[248] Neutral atom scattering factors for all atoms and anomalous dispersion corrections for the non-hydrogen atoms were taken from *International Tables for Crystallography*.[251] A split layer refinement was used for disordered groups and additional SIMU, DELU, RIGU, ISOR and SAME restraints were used, if necessary. Images of the crystal structures were generated with PLATON.[252]

5.3 Synthetic procedures

5.3.1 1,1'-Methylenebis(4,5-diphenylimidazole) ($^{Ph}Im_2Me$)

This synthesis was conducted in accordance to literature.[237]

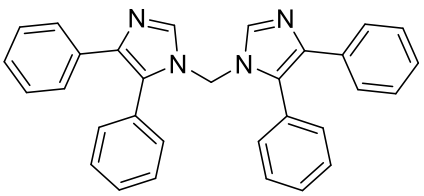

$^{Ph}Im_2Me$

Diphenylimidazole (20.82 g, 94.52 mmol, 1.0 eq.) is suspended with finely ground KOH (85%, 9.5 g, 143.93 mmol, 1.5 eq.) in 160 mL MeCN. The resulting blue suspension is stirred for 15 min and CH_2Br_2 (3.65 mL, 9.04 g, 52.0 mmol, 0.55 eq.), diluted in 5 mL MeCN, is added slowly. After stirring for 5 days at room temperature 25 mL ice cold H_2O is added, precipitating a white solid. The white solid is filtered and washed two times with H_2O. After drying in vacuum, the product is obtained as a white solid in 87% yield (18.50 g, 40.88 mmol).

The analytic data is in accordance with literature.[237]

^{1}H NMR (400 MHz, $CDCl_3$) δ(ppm) = 7.57 - 7.46 (m, 6H, C_{phenyl}), 7.43 (dd, *J* = 8.2, 1.4 Hz, 4H, C_{phenyl}), 7.24 - 7.10 (m, 10H, C_{phenyl}), 6.77 (s, 2H, N-C*H*-N), 5.70 (s, 2H, -C*H*$_2$-).

^{1}H NMR (400 MHz, DMSO-d_6) δ(ppm) = 7.55 - 7.40 (m, 6H, C_{phenyl}), 7.34 - 7.27 (m, 4H, C_{phenyl}), 7.20 - 7.06 (m, 12H, C_{phenyl} + N-C*H*-N), 5.96 (s, 2H, -C*H*$_2$-).

^{13}C NMR (101 MHz, DMSO-d_6) δ(ppm) =137.29, 137.16, 134.21, 130.46, 129.34, 129.16, 129.07, 128.04, 127.15, 126.32, 125.90, 53.45 (-*C*H$_2$-).

Elemental analysis: for $C_{31}H_{24}N_4$ anal. calcd.: C 82.27; H 5.35; N 12.38; S 0.00.
found: C 81.89; H 5.22; N 12.28; S 0.00.

5.3.2 Calix[4](4,5-diphenylimidazolium) triflate (^{Ph}L OTf)

This synthesis was conducted in accordance to literature for similar compounds.[147, 235, 239]

^{Ph}**Im$_2$Me** (2.0 g, 4.42 mmol, 2 eq.) is dissolved in 600 mL dry MeCN and cooled to -30 °C. Methylene bis(trifluoromethanesulfonate) (1.45 g, 4.64 mmol, 2.1 eq.) is diluted in 40 mL MeCN and slowly added to the cooled solution. After complete addition, the mixture is stirred and allowed to warm to room temperature overnight. The solvent is removed in vacuum and the resulting yellow solid is washed three times consecutively with THF with decreasing amounts of volume (10 mL, 7 mL, 5 mL). After this, the solid is additionally washed three times with MeCN (5 mL, 1 mL, 1 mL). After drying in vacuum the product is obtained as a white solid (846.0 mg).

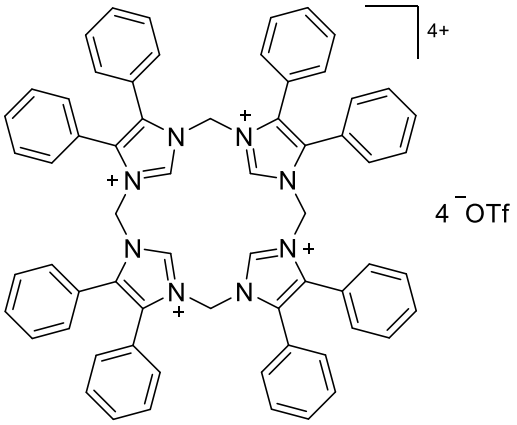

^{Ph}**L OTf**

ESI-MS: m/z [(**^{Ph}L OTf**) -1OTf$^-$ +MeCN]$^+$ calc: 1420.31, found: 1419.43; [(**^{Ph}L OTf**) -1OTf$^-$]$^+$ calc: 1379.29, found: 1379.41; [(**^{Ph}L OTf**) -2OTf$^-$ +MeCN]$^{3+}$ calc: 635.68, found: 635.56; [(**^{Ph}L OTf**) -2OTf$^-$]$^{2+}$ calc: 615.17, found: 615.44; [(**^{Ph}L OTf**) -3OTf$^-$]$^{3+}$ calc: 360.46, found: 360.70; [(**^{Ph}L OTf**) -4OTf$^-$]$^{4+}$ calc: 233.11, found: 233.16.

5.3.3 *trans*-Diacetonitrile[calix[4](4,5-diphenylimidazoyl]iron(II) triflate (VIII)

This synthesis was conducted in accordance to literature for similar compounds.[147, 235]

A Schlenk tube is charged with [Fe(HMDS)$_2$(THF)] (300.0 mg, 669.1 µmol, 2.15 eq.) dissolved in 20 mL of dry and degassed MeCN. The solution is frozen using liquid nitrogen cooling and a magnetic stirrer is placed on top the frozen solution. In a separate Schlenk tube, **^{Ph}L OTf** (476.0 mg, 311.2 µmol, 1.0 eq.) is dissolved in 60 mL MeCN, cooled to -45 °C and added onto the frozen [Fe(HMDS)$_2$(THF)] solution using a transfer cannula. The mixture is stirred and allowed to slowly warm to room temperature overnight (18 h total). The volume of the mixture is reduced to 20 mL solvent in vacuum and filtered over dried silica (~10 g) under inert conditions. The column is eluted with 160 mL MeCN, the volume is reduced to 15 mL and filtered. The solvent is reduced to 3 mL and a yellow solid is precipitated upon addition of 30 mL Et_2O. The yellow solid is purified *via* consecutively suspending it in 0.5 mL MeCN, adding 5 mL Et_2O and separating the precipitate *via* centrifugation. The product is obtained as yellow solid after washing with 5 mL Et_2O and drying in vacuum in 34% yield (144.6 mg, 106.0 µmol).

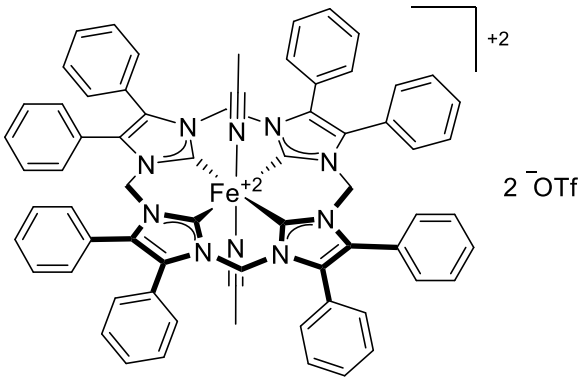

VIII

^{1}H NMR (400 MHz, CD_3CN) δ(ppm) = 7.41 (s, 40H, phenyl), 6.05 (s, 8H, -C*H*$_2$-), 1.96 (s, 6H, C*H*$_3$CN).

^{13}C NMR (126 MHz, CD_3CN) δ(ppm) = 206.21 (N-*C*-N), 133.31 (C_{phenyl}), 131.54 (C_{phenyl}), 130.53 (C_{phenyl}), 130.00 (C_{phenyl}), 127.91 (C_{phenyl}), 59.68 (-*C*H$_2$-).

^{19}F NMR (471 MHz, CD_3CN) δ(ppm) = -79.36 (s, OTf^-).

ESI-MS: m/z [(**VIII**) -2MeCN -1OTf^-]$^+$ calc: 1133.29, found: 1133.14; [(**VIII**) -2MeCN -2OTf^-]$^{2+}$ calc: 492.17, found: 492.44.

5.3.4 4,5-bis(*para*-fluorophenyl)imidazole (*p*-F-Ph**Im**)

This synthesis was conducted in accordance to literature, combining two synthesis steps into one.[236]

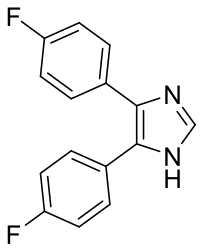

p-F-Ph**Im**

Thiamine hydrochloride (10.04 g, 30.0 mmol, 0.08 eq.) is dissolved in a mixture of 50 mL H_2O and 100 mL EtOH. 2.0 M NaOH solution is added dropwise until the pH stabilized at pH 9-10. To the yellow solution 4-Fluorbenzaldehyde (40.0 mL, 46.4 g, 373.85 mmol, 1.0 eq.) is added and the mixture is stirred at room temperature for 7 days. The white precipitate is filtered and washed with a EtOH : H2O (2:1) mixture. From the combined filtering solutions, EtOH is removed in vacuum and the remaining H_2O solution is extracted three times with 50 mL DCM. The DCM is removed *via* distillation and the resulting yellow oil is combined with the white precipitate and dissolved in 100 mL formamide. After refluxing the mixture for 3 h and cooling to room temperature, the sample is poured into 500 mL H_2O. The resulting gummy like precipitate is stirred vigorously for 2 days. The resulting powder is filtered and washed two times with H_2O. The powder is dried and washed consecutively with small amount of a mixture of THF : *n*-pentane (1:2), until the washing solutions show no discoloration. After drying in vacuum the product is obtained as a white powder in 29% yield (13.35 g, 52.1 mmol).

^{1}H NMR (400 MHz, DMSO-d_6) δ(ppm) = 12.52 (s, 1H, N*H*), 7.78 (s, 1H, NC*H*N), 7.45 (dt, $^4J_{19F\text{-}1H}$ = 20.4 Hz, $J_{1H\text{-}1H}$ = 7.2 Hz, 4H, HC-C*H*-C), 7.19 (dt, $^3J_{19F\text{-}1H}$ = 53.1 Hz, $J_{1H\text{-}1H}$ = 8.5 Hz, 4H, FC-C*H*-C).

^{13}C NMR (101 MHz, DMSO-d_6) δ(ppm) = 161.50 (d, $^1J_{19F\text{-}13C}$ = 243.9 Hz, *C*F), 160.94 (d, $^1J_{19F\text{-}13C}$ = 243.7 Hz, *C*F), 135.61 (N*C*HN), 135.18 (N-*C*-C), 131.74 (C-*C*-CH), 130.04 (d, $^3J_{19F\text{-}13C}$ = 7.8 Hz, HC-*C*H-C), 128.80 (d, $^3J_{19F\text{-}13C}$ = 7.3 Hz, HC-*C*H-C), 127.64 (C-*C*-CH), 125.26 (N-*C*-C), 115.72 (d, $^2J_{19F\text{-}13C}$ = 21.6 Hz, FC-*C*H-C), 115.08 (d, $^2J_{19F\text{-}13C}$ = 21.1 Hz, FC-*C*H-C).

^{19}F NMR (376 MHz, DMSO-d_6) δ(ppm) = -114.22 (C*F*), -116.16 (C*F*).

ESI-MS: m/z [(*p*-F-Ph**Im**) $+H^+]^+$ calc: 257.09, found: 257.17.

Elemental analysis: for $C_{15}H_{10}F_2N_2$ anal. calcd.: C 70.31; H 3.93; N 10.93; S 0.00.
found: C 70.17; H 3.88; N 11.13; S 0.00.

5.3.5 1,1'-Methylenebis(4,5-bis(*para*-fluorophenyl)imidazole) ($^{p\text{-F-Ph}}$Im$_2$Me)

This synthesis was conducted in accordance to literature.[237]

$^{p\text{-F-Ph}}$**Im** (5.14 g, 20.0 mmol, 1.0 eq.) is dissolved in 20 mL MeCN and finely ground KOH (85%, 2.00 g, 33.8 mmol, 1.5 eq.) is added. After stirring the mixture for 5 min at room temperature CH_2Br_2 (0.7 mL, 1.74 g, 10.0 mmol, 0.5 eq.) is added. The mixture is stirred at 50 °C for 4 days upon which 25 mL H_2O is added. The precipitate is filtered and washed two times with H_2O. After drying in vacuum the product is obtained as a white solid in 82% yield (4.33 g, 8.3 mmol).

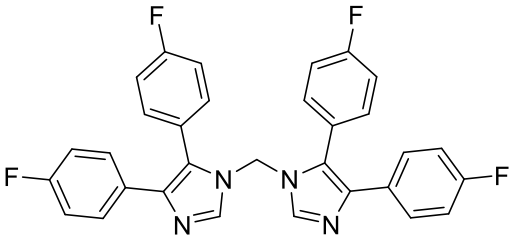

$^{p\text{-F-Ph}}$**Im$_2$Me**

^{1}H NMR (400 MHz, DMSO-d_6) δ(ppm) = 7.32 - 7.15 (m, 14H), 7.03 (t, J = 8.9 Hz, 4H), 6.03 (s, 2H, -CH_2-).

^{13}C NMR (101 MHz, DMSO-d_6) δ(ppm) = 162.41 (d, $^1J_{19F\text{-}13C}$ = 246.6 Hz, *C*F), 160.88 (d, $^1J_{19F\text{-}13C}$ = 243.5 Hz, *C*F), 137.57 (N-*C*H-N), 136.78 (N-*C*-C), 132.64 (d, $^3J_{19F\text{-}13C}$ = 8.6 Hz, HC-*C*H-C), 130.60 (d, $^4J_{19F\text{-}13C}$ = 3.0 Hz, C-*C*-CH), 127.82 (d, $^3J_{19F\text{-}13C}$ = 8.0 Hz, HC-*C*H-C), 125.80 (N-*C*-C), 125.37 (d, $^4J_{19F\text{-}13C}$ = 3.3 Hz, C-*C*-CH), 116.22 (d, $^2J_{19F\text{-}13C}$ = 21.6 Hz, FC-*C*H-C), 115.00 (d, $^2J_{19F\text{-}13C}$ = 21.4 Hz, FC-*C*H-C), 53.57 (-CH_2-).

^{19}F NMR (376 MHz, DMSO-d_6) δ(ppm) = -112.17 (C*F*), -115.87 (C*F*).

ESI-MS: m/z [($^{p\text{-F-Ph}}$**Im$_2$Me**) +H^+]$^+$ calc: 525.17, found: 525.03; [($^{p\text{-F-Ph}}$**Im$_2$Me**) +2H^+]$^{2+}$ calc: 263.09, found: 263.39.

Elemental analysis: for $C_{31}H_{20}F_4N_4$ anal. calcd.: C 70.99; H 3.84; N 10.68; S 0.00.
found: C 70.50; H 3.78; N 10.51; S 0.00.

5.3.6 Calix[4](4,5-bis(*para*-fluorophenyl)imidazolium) triflate ($^{p\text{-F-Ph}}$L OTf)

This synthesis was conducted in accordance to literature for similar compounds.[147, 235, 239]

$^{p\text{-F-Ph}}$**Im$_2$Me** (4.16 g, 7.94 mmol, 2.0 eq.) is dissolved in 700 mL dry MeCN and cooled to -45 °C. Methylene bis(triflate) (2.61 g, 8.34 mmol, 2.1 eq.) is diluted in 40 mL MeCN and slowly added to the cooled solution. After complete addition, the mixture is stirred and allowed to warm to room temperature overnight. The solvent is removed in vacuum and the resulting yellow solid is washed six times consecutively with THF with decreasing amounts of volume (10 mL, 5 mL, 4 mL, 4 mL, 2 mL). After drying in vacuum the product is obtained as a white solid (2.05 g).

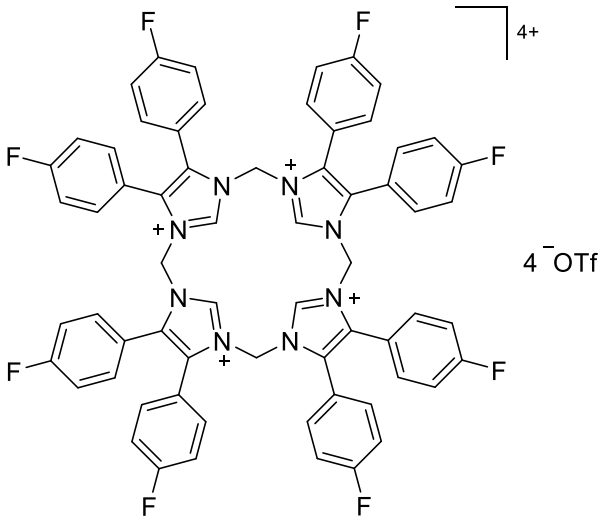

$^{p\text{-F-Ph}}$**L OTf**

ESI-MS: m/z [(**$^{p\text{-F-Ph}}$L OTf**) -4OTf$^-$]$^{4+}$ calc: 269.09, found: 269.

5.3.7 *trans*-Diacetonitrile[calix[4](4,5-bis(*para*-fluorophenyl)imidazoyl] iron(II) triflate (**IX**)

This synthesis was conducted in accordance to literature for similar compounds.[147, 235]

A Schlenk tube is charged with [Fe(HMDS)$_2$(THF)] (300.0 mg, 669.1 µmol, 2.15 eq.) dissolved in 30 mL of dry and degassed MeCN. The solution is frozen using liquid nitrogen cooling and a magnetic stirrer is placed on top the frozen solution. In a separate Schlenk tube, **$^{p\text{-F-Ph}}$L OTf** (520.3 mg, 310.8 µmol, 1.0 eq.) is dissolved in 80 mL of MeCN, cooled to -45 °C and added onto the frozen [Fe(HMDS)$_2$(THF)] solution using a transfer cannula. The mixture is stirred and allowed to slowly warm to room temperature overnight (18 h total). The volume of the mixture is reduced to 25 mL solvent *in vacuo* and filtered over dried silica (~10 g) under inert conditions. The column is eluted with 120 mL MeCN, the volume is reduced to 15 mL and filtered. The solvent is reduced to 3 mL and a white solid is precipitated upon addition of 30 mL Et_2O. The solid is discarded and additional 10 mL Et_2O is added to the filtrate and stirred for 1 h to precipitate a yellow solid. The solid is again dissolved in 1 mL MeCN and precipitated again *via* addition of 50 mL Et_2O. After washing the solid with 5 mL Et_2O and drying in vacuum, the product is obtained as a yellowish solid in 4% yield (18.7 mg, 12.4 µmol).

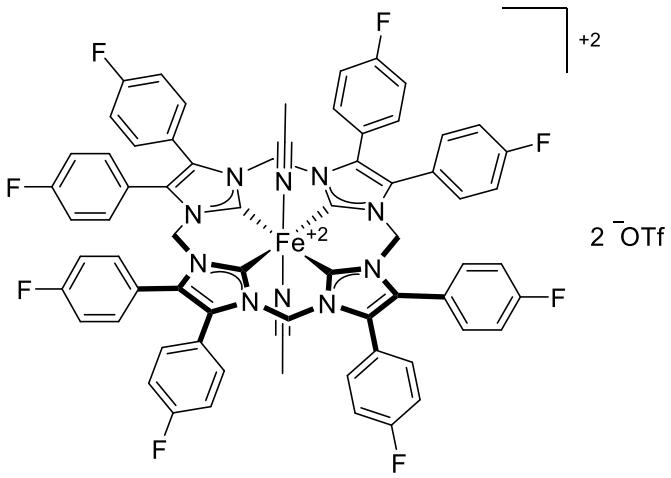

IX

^{1}H NMR (400 MHz, CD_3CN) δ(ppm) = 7.43 - 7.37 (m, 16H, HC-C*H*-C), 7.22 - 7.14 (m, 16H, FC-C*H*-CH), 5.99 (s, 8H, -CH_2-), 1.96 (s, 6H, CH_3CN).

^{13}C NMR (101 MHz, CD_3CN) δ(ppm) = 206.18 (N-*C*-N), 164.23 (d, $^1J_{19F\text{-}13C}$ = 248.6 Hz, *C*F), 133.89 (d, $^3J_{19F\text{-}13C}$ = 8.7 Hz, HC-*C*H-C), 132.59 (N-*C*-C), 124.04 (d, $^4J_{19F\text{-}13C}$ = 3.4 Hz, HC-*C*-C), 117.08 (d, $^2J_{19F\text{-}13C}$ = 22.1 Hz, FC-*C*H-CH), 59.74 (-CH_2-).

^{19}F NMR (376 MHz, CD_3CN) δ(ppm) = -76.74 (s, 6F, OTf^-), -109.97 (tt, $^3J_{29F}$ = 8.9 Hz, $^4J_{1H\text{-}19F}$ = 5.4 Hz, 8F, -C*F*).

ESI-MS: m/z [(**IX**) -OTf^-]$^+$ calc: 1277.21, found: 1277.07; [(**IX**) -2OTf^-]$^{2+}$ calc: 564.13, found: 564.73.

Elemental analysis: for $C_{70}H_{46}F_{14}FeN_{10}O_6S_2$ anal. calcd.: C 55.71; H 3.07; N 9.28; S 4.25.
found: C 54.79; H 3.00; N 9.63; S 4.32.

5.3.8 Sodium imidazolide

This synthesis was conducted in accordance to literature.[253]

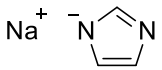

Imidazole (20.0 g, 294 mmol, 1.00 eq.) is melted at 110 °C in an open vessel and fine ground NaOH (11.2 g, 279 mmol, 0.95 eq.) is slowly added. The reaction is maintained at 110 °C for 4 h while stirring, allowing the generated water steam to leave the reaction vessel. After cooling to room temperature, the crude product is subsequently washed with 5 mL H_2O, two times 50 mL THF and 50 mL *n*-pentane . After drying in *vacuo* the product is obtained as a pale orange solid in 86% yield (21.6 g, 240 mmol).

^{1}H NMR (400 MHz, DMSO-d_6) δ(ppm) = 7.13 (s, 1H, NC*H*N), 6.70 (s, 2H, NC*H*C).

Elemental analysis: for $C_3H_3N_2Na$ anal. calcd.: C 40.01; H 3.36; N 31.11; S 0.00.
found: C 39.98; H 3.44; N 31.28; S 0.00.

These data are in alignment with literature.[253]

5.3.9 Di(imidazol-1-yl)methane-d$_2$ (**Im$_2$Me-*d$_2$***)

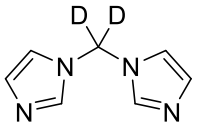

Im$_2$Me-*d$_2$*

Sodium imidazolide (6.53 g, 72.5 mmol, 1.0 eq.) is dissolved in 55 mL dry DMSO. CD_2Cl_2 (8.1 mL, 9.45 g, 108.72 mmol, 1.75 eq.) is added and the mixture is stirred for 19 h at 40 °C. DMSO is removed from the resulting orange suspension *via* vacuum distillation and the residue is suspended in 40 mL MeCN. After filtration and washing of the solid four times with 20 mL MeCN, the combined organic solutions are reduced to 20 mL volume. Upon addition of Et_2O a pink solid precipitate. The crude product is dissolved in 70 mL MeCN and filtered over silica, using 100 mL MeCN as a eluent. The solvent is removed in *vacuo*, the resulting white solid again dissolved in 20 mL acetone and precipitated with 40 mL *n*-pentane. The product is obtained as a white solid in 75% yield (4.09 g, 27.2 mmol).

The deuterium content at the methylene bridge is >99% (determined *via* ^{1}H NMR spectroscopy).

^{1}H NMR (500 MHz, $CDCl_3$) δ(ppm) = 7.64 (s, 2H, N-C*H*-N), 7.09 (s, 2H, N-C*H*-CH), 6.98 (t, *J* = 1.2 Hz, 2H, N-C*H*-CH), 5.98 (t, residual H, $^2J_{H\text{-}D}$ = 1.81 Hz, -C*D$_2$*-).

^{1}H NMR (500 MHz, CD_3CN) δ(ppm) = 7.73 (s, 2H, N-C*H*-N), 7.18 (s, 2H, N-C*H*-CH), 6.95 (s, 2H, N-C*H*-CH), 6.06 (t, residual H, $^2J_{H\text{-}D}$ = 2.1 Hz, -C*D$_2$*-).

^{13}C NMR (126 MHz, CD_3CN) δ(ppm) = 138.06 (N-*C*H-N), 130.71 (CH-*C*H-N), 119.56 (N-*C*H-CH), 56.09 (tt, $^1J_{D\text{-}13C}$ = 23.6 Hz, -*C*D$_2$-).

^{2}H NMR (61 MHz, CH_3CN) δ(ppm) = 6.05 (s, 2D, -C*D$_2$*-).

ESI-MS: m/z [**Im$_2$Me-*d$_2$*** +1H$^+$]$^+$ calc: 151.09, found: 150.93.

Elemental analysis: for $C_7H_8N_4$ anal. calcd.: C 56.74; H 5.44; N 37.81; S 0.00.
found: C 55.67; H 5.28; N 36.76; S 0.00.

5.3.10 Calix[4]imidazolium-d$_8$ triflate (L-*d*$_8$ OTf)

The synthesis is performed according to literature procedures[147] utilizing deuterated starting materials, **Im$_2$Me-*d*$_2$** and **Me-*d*$_2$(OTf)$_2$**.

Im$_2$Me-*d*$_2$ (733.9 mg, 4.89 µmol, 2.0 eq.) is dissolved in 500 mL dry MeCN and cooled using an ice-bath. **Me-*d*$_2$(OTf)$_2$** (1.54 g, 4.89 µmol, 2.0 eq.) are dissolved in 40 mL dry MeCN and slowly added towards the former solution within 1 h. The mixture is allowed to warm to room temperature and stirred for 20 h. The solvent is removed and the crude product washed two times with 2 mL acetone. After drying in vacuum the product is obtained as a white solid in 72% (1.64 g, 1.76 µmol) yield.

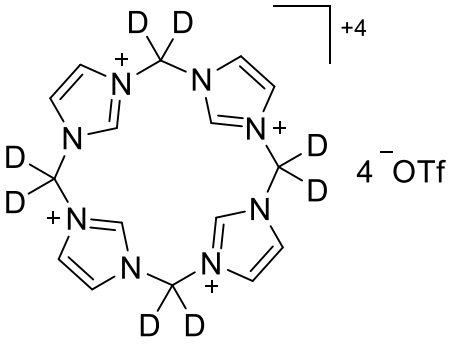

L-*d*$_8$ OTf

The deuterium content on the methylene bridges is >98% (determined *via* ^{1}H NMR spectroscopy).

^{1}H NMR (500 MHz, DMSO-d_6) δ(ppm) = 9.69 (t, *J* = 1.5 Hz, 4H, N-C*H*-N), 8.01 (d, *J* = 1.6 Hz, 8H, N-C*H*-CH), 6.83 (s, residual H, -CD_2-).

^{13}C NMR (126 MHz, DMSO-d_6) δ(ppm) = 137.84 (N-*C*H-N), 120.64 (q, $^1J_{19F\text{-}13C}$ = 322.1 Hz, OTf), 123.61 (N-*C*H-C), 58.84 (m, $^1J_{D\text{-}13C}$, -*C*D_2-).

Elemental analysis: for $C_{20}H_{20}F_{12}N_8O_{12}S_4$ anal. calcd.: C 26.09; H 2.19; N 12.17; S 13.93.
found: C 25.80; H 2.12; N 11.80; S 13.82.

5.3.11 Calix[4]imidazolium-d$_8$ hexafluorophosphate (**L-*d*$_8$ PF$_6$**)

The anion exchange is performed according to literature procedures[147] for non-deuterated compounds.

L-*d*$_8$ OTf (1.55 g, 1.67 mmol, 1.0 eq.) is dissolved in 30 mL H_2O and added to a solution of NH_4PF_6 (1.36 g, 8.35 mmol, 5 eq.) in 25 mL water. The precipitated white solid is isolated *via* centrifugation and washed four times with 5 mL H_2O. After drying in *vacuo*, the product in obtained as a white solid in 92% yield (1.40 g, 1.53 mmol).

The deuterium content on the methylene bridges is >98% (determined *via* ^{1}H NMR spectroscopy).

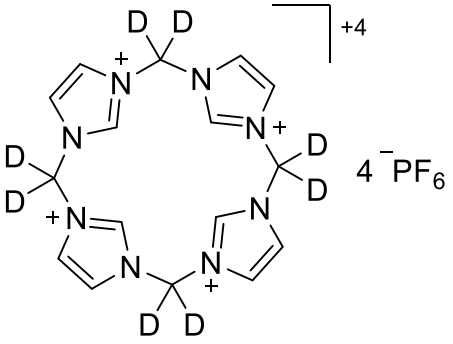

L-*d*$_8$ PF$_6$

^{1}H NMR (500 MHz, DMSO-*d*$_6$) δ(ppm) = 9.68 (s, 4H, N-C*H*-N), 8.00 (d, *J* = 1.3 Hz, 8H, N-C*H*-C), 6.83 (s, residual H, -C*D*$_2$-).

^{13}C NMR (126 MHz, DMSO-*d*$_6$) δ(ppm) = 137.76 (N-*C*H-N) , 123.63 (N-*C*H-C) , 58.85 (m, -*C*D$_2$-).

^{19}F NMR (471 MHz, DMSO-*d*$_6$) δ(ppm) = -70.14 (d, $^1J_{31P\text{-}19F}$ = 711.4 Hz, PF_6^-), -77.73 (s, residue signal, OTf).

^{1}H NMR (500 MHz, CD_3CN) δ(ppm) = 9.10 (s, 4H, N-C*H*-N), 7.76 (d, *J* = 1.6 Hz, 8H, N-C*H*-C), 6.63 (s, residual H, -C*D*$_2$-).

^{13}C NMR (126 MHz, CD_3CN) δ(ppm) = 138.57 (N-*C*H-N), 125.33 (N-*C*H-C), 60.30 (tt, $^1J_{D\text{-}13C}$ = 26.2 Hz, -*C*D$_2$-).

^{19}F NMR (471 MHz, CD_3CN) δ(ppm) = -72.40 (d, $^1J_{31P\text{-}19F}$ = 707.3 Hz, PF_6^-), -79.08 (s, residue signal, OTf).

^{2}H NMR (61 MHz, CH_3CN) δ(ppm) = 6.65 (s, -C*D*$_2$-).

ESI-MS: m/z [**L-d$_8$ PF$_6$** -1PF_6^-]$^+$ calc: 767.12, found: 766.89.

Elemental analysis: for $C_{16}H_{20}F_{24}N_8P_4$ anal. calcd.: C 21.25; H 2.23; N 12.39; S 0.00.
found: C 20.35; H 2.53; N 11.47; S 0.18.

5.3.12 trans-Diacetonitrile[calix[4]imidazoyl-d$_8$]iron(II) hexafluorophosphate (X)

The synthesis is performed according to literature procedures[147] utilizing the deuterated ligand **L-*d*$_8$ PF$_6$**.

[Fe(HMDS)$_2$(THF)] (420.0 mg, 938 µmol, 2.1 eq.) is dissolved in 40 mL MeCN and frozen applying liquid nitrogen cooling. On top of that frozen solution, a cooled (-40 °C) solution of **L-*d*$_8$ PF$_6$** (399.8 mg, 438.4 µmol, 1.0 eq.) in 40 mL MeCN with a stirring bar is placed. The mixture is allowed to slowly warm to room temperature and stirred for 3 days. The resulting dark solution is reduced to approximately 15 mL volume in *vacuo* and filtered over a short plug of dried silica under argon and is eluted with 120 mL MeCN. The solvent is removed in vacuum and the residue re-dissolved in 4.5 mL MeCN. Precipitation with 20 mL Et_2O lead to a yellow solid with brownish contamination. The crude product is washed two times with 0.2 mL MeCN and consecutively washed two times with a mixture of in 0.2 mL MeCN and 2 mL Et_2O. After a final washing step with Et_2O and drying in vacuo the product is obtained as a yellow solid in 56% yield (185.8 mg, 245.7 µmol).

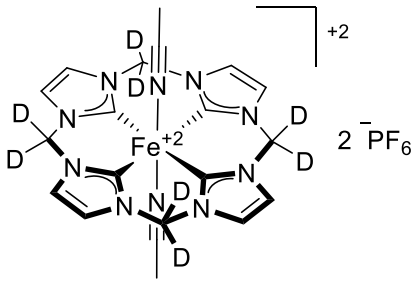

X

The deuterium content on the methylene bridges is >98% (determined *via* ^{1}H NMR spectroscopy).

^{1}H NMR (400 MHz, CD_3CN) δ(ppm) = 7.59 (s, 8H, N-C*H*-C), 6.30 (s, residual H, -C*D*$_2$-), 1.96 (s, 6H, C*H*$_3$CN).

^{13}C NMR (126 MHz, CD_3CN) δ(ppm) = 205.26 (N-*C*-N), 129.91 (D_3C-*C*-N···Fe), 122.83 (N-*C*H-C), 63.81 - 62.52 (m, $^1J_{D\text{-}13C}$, -*C*D_2-), 4.37 - 3.56 (m, $^1J_{D\text{-}13C}$, D_3*C*-CN···Fe).

^{2}H NMR (61 MHz, CH_3CN) δ(ppm) = 6.31 (s, 8D, -C*D*$_2$-).

ESI-MS: m/z [**X** -2MeCN -1PF_6^-]$^+$ calc: 529.10, found: 528.82, [**X** -2MeCN -2PF_6^- +1$HCOO^-$]$^+$ calc: 429.13, found: 428.92, [**X** -2MeCN -2PF_6^-]$^+$ calc: 192.07, found: 192.17.

Elemental analysis: for $C_{20}H_{22}F_{12}FeN_{10}P_2$ anal. calcd.: C 32.10; H 2.96; N 18.72; S 0.00.
found: C 31.13; H 2.93; N 17.80; S 0.00.

5.3.13 trans-Diacetonitrile[calix[4]imidazoyl-d_8]iron(III) hexafluorophosphate (**XI**)

The synthesis is performed according to literature procedures[113] utilizing the deuterated complex **X** as starting material.

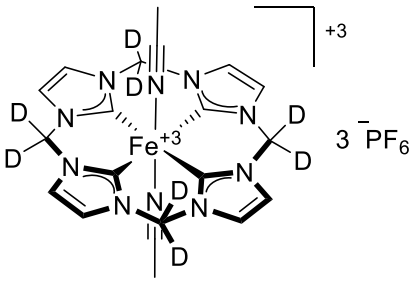

XI

X (103.5 mg, 136.8 µmol, 1.0 eq.) is dissolved in 12 mL MeCN and cooled to -40 °C. Thianthrenyl hexafluorophosphate (58.3 mg, 161.4 µmol, 1.15 eq.) dissolved in 11 mL MeCN is added. The mixture is allowed to warm to room temperature and stirred for 1 h. The resulting violet solution is reduced to 5 mL volume and precipitated upon addition of 70 mL Et_2O. The filtered solid is washed two times with a mixture of 1 mL MeCN and 4 mL Et_2O and consecutively washed two times with 3 mL Et_2O. After drying in vacuo the product is obtained as violet solid in 84% yield (103.7 mg, 115.0 µmol).

Due to the paramagnetic nature of this compound the deuterium content cannot reliably determined *via* ^{1}H NMR spectroscopy. The deuterated species is the primary species found in HR-MS.

^{1}H NMR (400 MHz, CD_3CN) δ(ppm) = 108.69 (s, N-C*H*-CH), 44.54 (s, residual H, -C*D*$_2$-).

^{2}H NMR (61 MHz, CH_3CN) δ(ppm) = 43.60 (s, -C*D*$_2$-).

ESI-MS: m/z [**XI** -3PF_6^- -2MeCN +$HCOO^-$]$^{2+}$ calc: 214.57, found: 214.54; [**XI** -3PF_6^- -2MeCN +F^-+$HCOO^-$]$^+$ calc: 448.13, found: 448.07; [**XI** -2PF_6^- -2MeCN +F^-]$^+$ calc: 548.10, found: 547.81; [**XI** -2PF_6^- -2MeCN +$HCOO^-$]$^+$ calc: 574.10, found: 573.62; [**XI** -1PF_6^- -1MeCN]$^+$ calc: 715.09, found: 715.64.

Elemental analysis: for $C_{20}H_{14}D_8F_{18}FeN_{10}P_3$ anal. calcd.: C 26.89; H 2.48; N 15.68; S 0.00.
found: C 27.72; H 2.69; N 15.25; S 0.00.

5.3.14 Calix[4](4,5-dimethylimidazoyl)-nickel(II) triflate (**XII**)

This synthesis was conducted in accordance to literature for similar compounds.[240]

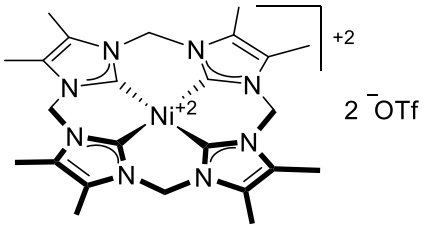

XII

Calix[4](4,5-dimethylimidazolium) triflate (281.21 mg, 194 µmol, 1.0 eq.) is dissolved in 10 mL dry DMSO together with $Ni(OAc)_2$ (34.7 mg, 196 µmol, 1.01 eq.) and NaOAc (158.9 mg, 1.94 mmol, 10.0 eq.). The mixture is stirred at 70 °C for 16 h. The DMSO is removed *via* vacuum distillation, a small amount of MeCN is added to precipitate a yellowish crude product upon addition of 48 mL Et_2O. The solid is suspended in 15 mL MeCN and filtered. The filtrate is filtered over a plug of alkaline aluminum oxide and eluted with 100 mL MeCN. The solvent of the filtrate is reduced to 5 mL and 15 mL Et_2O is added to precipitate a yellow solid. The solid is isolated *via* centrifugation and washed two times with 5 mL Et_2O. After drying in *vacuo* the product is obtained as slightly yellow solid in 65% yield (100 mg, 126.7 µmol).

^{1}H NMR (400 MHz, DMSO-d_6) δ(ppm) = 6.08 (s, 8H, -CH_2-), 2.40 (s, 24H, -CH_3).

^{13}C NMR (101 MHz, DMSO-d_6) δ(ppm) = 164.95 (N-*C*-N), 125.94 (N-*C*-CH_3), 57.86 (-*C*H_2-), 8.18 (-*C*H_3).

^{1}H NMR (400 MHz, CD_3CN) δ(ppm) = 5.92 (s, 8H, -CH_2-), 2.36 (s, 24H, -CH_3).

^{13}C NMR (101 MHz, CD_3CN) δ(ppm) = 167.15 (N-*C*-N), 127.20 (N-*C*-CH_3), 59.09 (-*C*H_2-), 8.93 (-*C*H_3).

ESI-MS: m/z [**XII** -2OTf^-]$^{2+}$ calc: 245.10, found: 245.31; [**XII** -1OTf^-]$^+$ calc: 639.16, found: 639.22.

Elemental analysis: for $C_{26}H_{32}F_6N_8NiO_6S_2$ anal. calcd.: C 39.56; H 4.09; N 14.20; S 8.12.
found: C 38.18; H 4.10; N 13.62; S 7.78.

5.3.15 Calix[4](4,5-dimethylimidazoyl)-palladium(II) triflate (**XIII**)

This synthesis was conducted in accordance to literature for similar compounds.[240]

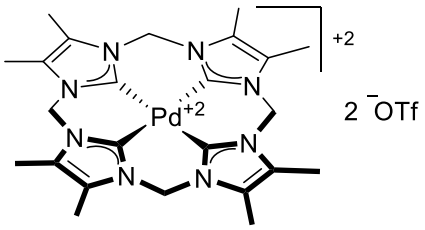

XIII

Calix[4](4,5-dimethylimidazolium) triflate (436.6 mg, 302.7 µmol, 1.0 eq.) is dissolved in 15 mL dry DMSO together with $PdCl_2(MeCN)_2$ (51.7 mg, 197.8 µmol, 0.65 eq.) and NaOAc (161.5 mg, 1.97 mmol, 6.5 eq.). The mixture is stirred at 70 °C for 17 h. The DMSO is removed *via* vacuum distillation, 5 mL MeCN is added to precipitate a yellowish crude product upon addition of 60 mL Et_2O. The solid is suspended in 15 mL MeCN and filtered over a plug of alkaline aluminum oxide and eluted with 100 mL MeCN. The solvent is reduced to 7 mL volume and 15 mL Et_2O is added to precipitate a white solid. The solid is isolated *via* centrifugation and washed two times with 5 mL Et_2O. After drying in *vacuo* the product is obtained as a white solid in 40% yield (101.2 mg, 120.9 µmol).

^{1}H NMR (400 MHz, DMSO-d_6) δ(ppm) = 6.34 (s, 8H, -CH_2-), 2.42 (s, 24H, -CH_3).

^{13}C NMR (101 MHz, DMSO-d_6) δ(ppm) = 161.73 (N-*C*-N), 126.03 (N-*C*-CH_3), 60.42 (-*C*H_2-), 8.06 (-*C*H_3).

^{19}F NMR (376 MHz, DMSO-d_6) δ(ppm) = -77.75 (OTf^-).

ESI-MS: m/z [**XIII** -2OTf^-]$^{2+}$ calc: 269.09, found: 268.77; [**XIII** -1OTf^-]$^+$ calc: 687.13, found: 687.21.

Elemental analysis: for $C_{26}H_{32}F_6N_8PdO_6S_2$ anal. calcd.: C 37.30; H 3.85; N 13.39; S 7.66.
found: C 37.28; H 3.84; N 13.16; S 7.69.

5.3.16 Calix[4](4,5-dimethylimidazoyl)-platinum(II) triflate (**XIV**)

This synthesis was conducted in accordance to literature for similar compounds.[240]

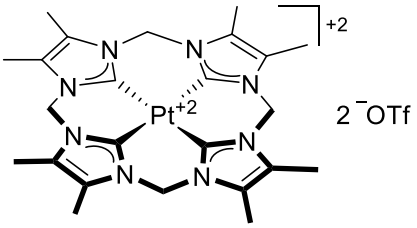

XIV

Calix[4](4,5-dimethylimidazolium) triflate (281.2 mg, 193.6 µmol, 1.0 eq.) is dissolved in 10 mL dry DMSO together with $PtCl_2(MeCN)_2$ (68.3 mg, 196.2 µmol, 1.01 eq.) and NaOAc (158.8 mg, 1.94 mmol, 10.0 eq.). The mixture is stirred at 70 °C for 19 h. The DMSO is removed *via* vacuum distillation, 4 mL MeCN is added to precipitate an orange crude product upon addition of 40 mL Et_2O. The solid is suspended in 10 mL MeCN, centrifuged and the liquid phase is filtered through a plug of alkaline aluminum oxide and eluted with 100 mL MeCN. The solvent is reduced to 5 mL volume and 20 mL Et_2O is added to precipitate a white solid. The solid is isolated *via* centrifugation and washed two times with 5 mL Et_2O. After drying in *vacuo* the product is obtained as a white solid in 29% yield (51.6 mg, 55.7 µmol).

^{1}H NMR (400 MHz, DMSO-d_6) δ(ppm) = 6.41 (s, 8H, -CH_2-), 2.41 (s, 24H, -CH_3).

^{13}C NMR (101 MHz, DMSO-d_6) δ(ppm) = 155.45 (N-*C*-N), 125.80 (N-*C*-CH_3), 60.80 (-*C*H_2-), 8.03 (-*C*H_3).

ESI-MS: m/z [**XIV** -2OTf^-]$^{2+}$ calc: 313.62, found: 313.64; [**XIII** -1OTf^-]$^+$ calc: 776.19, found: 776.19

Elemental analysis: for $C_{26}H_{32}F_6N_8PtO_6S_2$ anal. calcd.: C 33.73; H 3.48; N 12.10; S 6.93

found: C 33.66; H 3.49; N 11.94; S 6.75.

5.3.17 Calix[4](4,5-dimethylimidazoyl)-silver(I) hexafluorophosphate (**XV**)

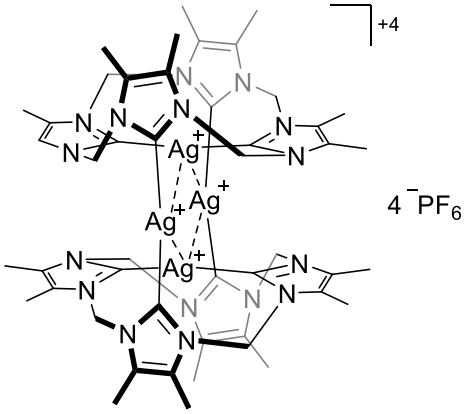

XV

Calix[4](4,5-dimethylimidazolium) hexafluorophosphate (150.0 mg, 147.6 µmol, 1.0 eq.) is dissolved in 15 mL dry MeCN and stirred with Ag_2O (213.7 mg, 922.3 µmol, 6.25 eq.) for 16 h at room temperature under exclusion of light. The mixture is centrifuged and Whatman filtered. The solvent is removed and the residue washed three times with MeCN (1.5 mL, 0.5 mL, 0.5 mL). The off-white solid is dissolved in 7 mL MeCN and reprecipitated *via* addition of 24 mL Et_2O. The solid is isolated *via* centrifugation and washed two times with 3 mL Et_2O. After drying in vacuum the product is obtained as a white solid in 82% yield (113.5 mg, 60.5 µmol).

^{1}H NMR (400 MHz, DMSO-d_6) δ(ppm) = 6.65 - 6.07 (m, 16H, -CH_2-), 2.33 (s, 24H, -CH_3), 1.74 (s, 24H, -CH_3).

^{13}C NMR (101 MHz, DMSO-d_6) δ(ppm) = 176.08 (d, $^1J_{109Ag\text{-}13C}$ = 211.8 Hz; d, $^1J_{107Ag\text{-}13C}$ = 182.9 Hz, N-*C*-N) 128.66 (d, $^3J_{Ag\text{-}13C}$ = 4.2 Hz, N-*C*-CH_3), 126.32 (d, $^3J_{Ag\text{-}13C}$ = 4.6 Hz, N-*C*-CH_3), 59.78 (-*C*H_2-), 8.34 (-*C*H_3), 7.18 (-*C*H_3).

ESI-MS: m/z [**XV** -4PF_6^-]$^{4+}$ calc: 324.04, found: 324.15; [**XV** -4PF_6^- +F^-]$^{3+}$ calc: 438.39, found: 438.32; [**XV**-3PF_6^-]$^{3+}$ calc: 480.38, found: 480.19; [**XV** -2PF_6^-]$^{2+}$ calc: 793.05, found: 792.86; [**XV** -1PF_6^-]$^+$ calc: 1731.06, found: 1730.29.

Elemental analysis: for $C_{48}H_{64}Ag_4F_{24}N_{16}P_4$ anal. calcd.: C 30.72; H 3.44; N 11.94; S 0.00.
found: C 30.42; H 3.38; N 11.62; S 0.00.

5.3.18 Calix[4](4,5-dimethylimidazoyl)-gold(I) hexafluorophosphate (**XVI**)

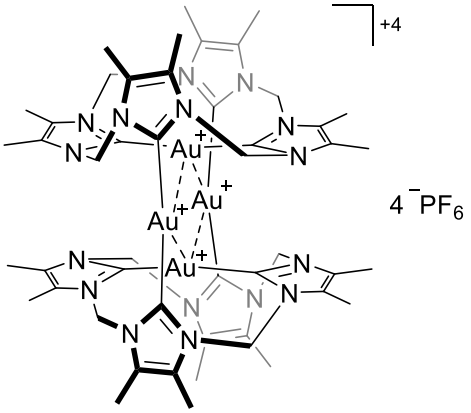

XVI

Calix[4](4,5-dimethylimidazolium) hexafluorophosphate (100.5 mg, 98.4 µmol, 2.0 eq.) is suspended in 12 mL dry DMSO together with AuCl(THT) (64.0 mg, 199.0 µmol, 4.04 eq.) and NaOAc (40.8 mg, 492 µmol, 10.0 eq.) and stirred for 16 h at 70 °C. The solvent is removed *via* vacuum distillation and 20 mL MeOH are added and the mixture is stirred for 1 h at room temperature. The suspension is centrifuged, the solid is washed two times with 1 mL MeOH. The solid is dissolved in 8 mL MeCN, Whatman filtered and reprecipitated *via* addition of 40 mL Et_2O. The white solid is washed two times with 3 mL Et_2O. The crude product is dissolved in 8 mL MeCN and filtered through a plug of alkaline aluminum oxide and eluted with 200 mL MeCN. The solvent is reduced to 5 mL and a white solid precipitated upon addition of 30 mL Et_2O, which is washed one time with 5 mL Et_2O. After drying in *vacuo* the product is obtained as a white solid in 64% yield (69.8 mg, 31.3 µmol).

^{1}H NMR (400 MHz, CD_3CN) δ(ppm) = 6.35 - 6.15 (m, 16H, -C*H*$_2$-), 2.35 (s, 24H, -C*H*$_3$), 1.82 (s, 24H, -C*H*$_3$).

^{13}C NMR (101 MHz, CD_3CN) δ(ppm) = 184.53 (N-*C*-N), 175.36 (N-*C*-N), 129.96 (N-*C*-CH_3), 128.36 (N-*C*-CH_3), 60.29 (-*C*H_2-), 9.40 (-*C*H_3), 8.32 (-*C*H_3).

ESI-MS: m/z [**XVI** -4PF_6^-]$^{4+}$ calc: 413.10, found: 413.52.

Elemental analysis: for $C_{48}H_{64}Au_4F_{24}N_{16}P_4$ anal. calcd.: C 25.82; H 2.89; N 10.04; S 0.00.
found: C 25.07; H 2.71; N 9.71; S 0.00.

5.3.19 Calix[4](4,5-dimethylimidazoyl)-copper(III) hexafluorophosphate (XVII)

This synthesis was conducted in accordance to literature for a similar compound.[241]

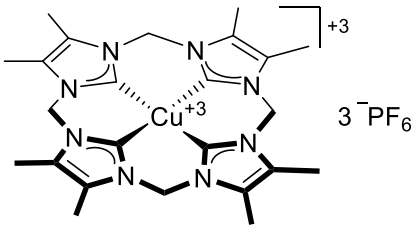

XVII

Calix[4](4,5-dimethylimidazolium) hexafluorophosphate (100.4 mg, 98.4 µmol, 1.0 eq.) is dissolved with $Cu(OAc)_2 \cdot H_2O$ (40.6 mg, 203.7 µmol, 2.1 eq.) in 5 mL DMSO. The mixture is stirred in an open vessel for 16 h at 40 °C. To the cyan solution 7 mL DCM is added and an off-white solid precipitated upon addition of 30 mL Et_2O. The solid is 5 times consecutively dissolved in 1.0 mL MeCN and reprecipitated *via* addition of 10 mL DCM. After drying in vacuum the product is obtained as white solid in 61% yield (60.4 mg, 64.9 µmol).

^{1}H NMR (500 MHz, CD_3CN) δ(ppm) = 6.12 (s, 8H, -C*H*$_2$-), 2.48 (s, 24H, -C*H*$_3$).

^{13}C NMR (101 MHz, CD_3CN) δ(ppm) = 129.62 (N-*C*-CH_3), 59.92 (-*C*H_2-), 9.31 (-*C*H_3).

ESI-MS: m/z [**XVII** -3PF_6^-]$^{3+}$ calc: 165.07, found: 165.12; [**XVII** -1PF_6^-]$^+$ calc: 785.13, found: 784.77.

Elemental analysis: for $C_{24}H_{32}CuF_{18}N_8P_3 \cdot {}^1/_9$ DMSO anal. calcd.: C 30.96; H 3.50; N 11.92; S 0.38.
found: C 30.79; H 3.51; N 11.85; S 0.38.

5.3.20 Calix[4](4,5-dimethylimidazoyl)-copper(III) hexafluorophosphate (XVIII)

This synthesis was conducted in accordance to literature for a similar compound.[239]

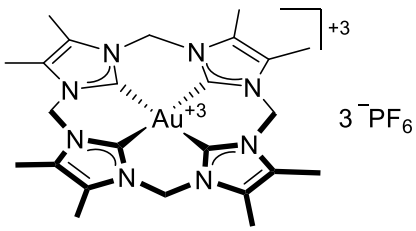

XVIII

Calix[4](4,5-dimethylimidazolium) triflate (177.8 mg, 172.1 µmol, 1.0 eq.) is suspended in 5 mL dry DMSO together with $Au(OAc)_3$ (64.6 mg, 172.1 µmol, 1.0 eq.), NaOAc (21.3 mg, 258.2 µmol, 1.5 eq.) and NaCl (10.4 mg, 172.1 µmol, 1.0 eq.). The mixture is stirred for 5 h at 100 °C. The brown suspension is filtered and 6 mL MeCN is added to the filtrate. A white solid is precipitated upon addition of 30 mL Et_2O. The solid is separated *via* centrifugation, washed three times with 10 mL MeCN and two times with 10 mL DCM. After drying in vacuum the solid is dissolved in 5 mL H_2O and slowly added to NH_4PF_6 (130 mg, 798 µmol, 4.6 eq.) dissolved in H_2O. The resulting white precipitate is centrifuged and washed three times with 10 mL H_2O. After drying in vacuo the product is obtained as a white solid in 5% yield (9.8 mg, 9.2 µmol).

^{1}H NMR (500 MHz, CD_3CN) δ(ppm) = 6.34 (s, 8H, -C*H*$_2$-), 2.50 (s, 24H, -C*H*$_3$).

^{13}C NMR (126 MHz, CD_3CN) δ(ppm) = 142.82 (N-*C*-N), 130.37 (N-*C*-CH_3), 62.91 (-*C*H_2-), 9.17 (-*C*H_3).

^{19}F NMR (471 MHz, CD_3CN) δ(ppm) = -72.91 (d, $^1J_{31P\text{-}19F}$ = 706.9 Hz, PF_6^-).

ESI-MS: m/z [**XVII** -3PF_6^-]$^{3+}$ calc: 209.75, found: 209.91; [**XVII** -2PF_6^-]$^{2+}$ calc: 387.10, found: 387.12; [**XVII** -1PF_6^-]$^+$ calc: 919.70, found: 918.89.

Elemental analysis: for $C_{24}H_{32}AuF_{18}N_8P_3$ anal. calcd.: C 27.08; H 3.03; N 10.53; S 0.00.
found: C 26.16; H 3.36; N 9.92; S 0.00.

6 Reprint Permissions

6.1 Elsevier

"Tuning the electronic properties of tetradentate iron-NHC complexes: Towards stable and selective epoxidation catalysts"

Marco A. Bernd, Florian Dyckhoff, Benjamin J. Hofmann, Alexander D. Böth, Jonas F. Schlagintweit, Jens Oberkofler, Robert M. Reich and Fritz E. Kühn

Journal of Catalysis **2020**, *391*, 548–561

DOI: 10.1016/j.jcat.2020.08.037

Reproduced with the permission from Elsevier.

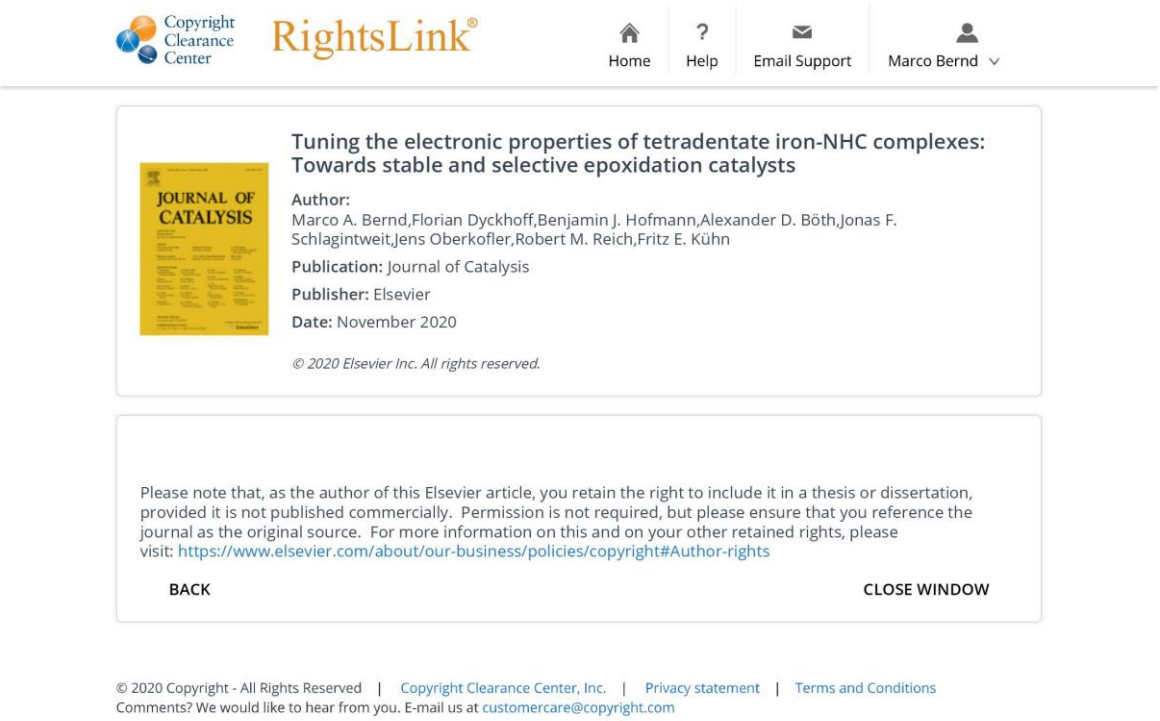

6.2 Royal Society of Chemistry, publications with authorship

"Synthesis, characterization, and biological studies of multidentate gold(I) and gold(III) NHC complexes"

E. B. Bauer, M. A. Bernd, M. Schütz, J. Oberkofler, A. Pöthig, R. M. Reich and F. E. Kühn

Dalton Transactions **2019**, *48*, 16615-16625

DOI: 10.1039/C9DT03183A

"Macrocyclic NHC complexes of group 10 elements with enlarged aromaticity for biological studies"

M. A. Bernd, E. B. Bauer, J. Oberkofler, A. Bauer, R. M. Reich and F. E. Kühn

Dalton Transactions **2020**, *49*, 14106-14114

DOI: 10.1039/D0DT02598D

Both reproduced with the permission from the Royal Society of Chemistry

(…)

Authors contributing to RSC publications (journal articles, books or book chapters) do not need to formally request permission to reproduce material contained in this article provided that the correct acknowledgement is given with the reproduced material.

(…)

If you are the author of this article you do not need to formally request permission to reproduce figures, diagrams etc. contained in this article in third party publications or in a thesis or dissertation provided that the correct acknowledgement is given with the reproduced material.

(…)

If you are the author of this article you still need to obtain permission to reproduce the whole article in a third party publication with the exception of reproduction of the whole article in a thesis or dissertation.

6.3 American Chemical Society

Figure 14, Reference [176]: Browning, R. J., Reardon, P. J. T., Parhizkar, M., Pedley, R. B., Edirisinghe, M., Knowles, J. C., Stride, E., *ACS Nano* **2017,** *11* (9), 8560-8578.

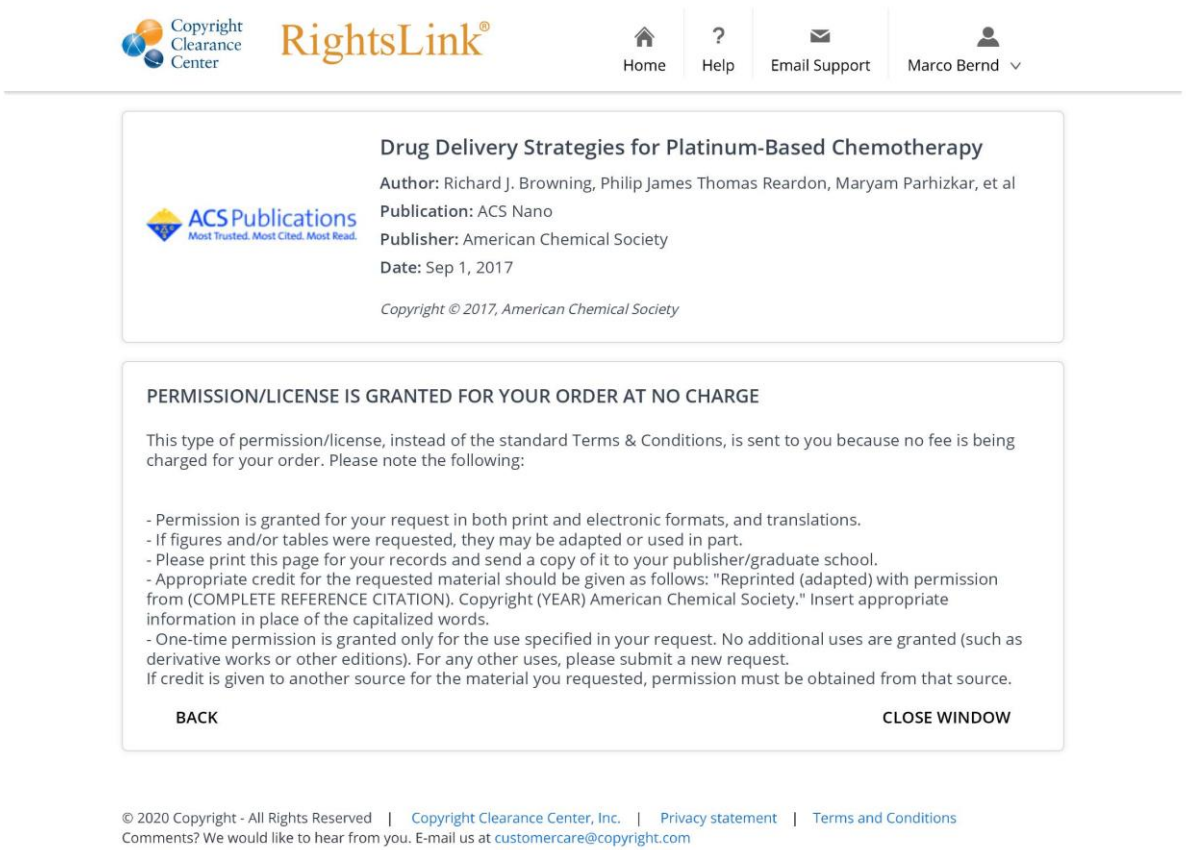

6.4 Royal Society of Chemistry

Figure 15, Reference [170]: R. Todd and S. Lippard, *Metallomics*, **2009**, *1* (4), 280-291.

Copyright Clearance Center Marketplace™

Royal Society of Chemistry - License Terms and Conditions

This is a License Agreement between Marco Bernd ("You") and Royal Society of Chemistry ("Publisher") provided by Copyright Clearance Center ("CCC"). The license consists of your order details, the terms and conditions provided by Royal Society of Chemistry, and the CCC terms and conditions.

All payments must be made in full to CCC.

Order Date	06-Oct-2020	Type of Use	Republish in a thesis/dissertation
Order license ID	1068150-1		
ISSN	1756-591X	Publisher	RSC Pub
		Portion	Image/photo/illustration

LICENSED CONTENT

Publication Title	Metallomics : integrated biometal science	Country	United Kingdom of Great Britain and Northern Ireland
Author/Editor	Royal Society of Chemistry (Great Britain)	Rightsholder	Royal Society of Chemistry
Date	01/01/2009	Publication Type	e-Journal
Language	English	URL	http://www.rsc.org/Publishing/Journals/MT/Index.asp

REQUEST DETAILS

Portion Type	Image/photo/illustration	Distribution	Worldwide
Number of images / photos / illustrations	1	Translation	Original language of publication
Format (select all that apply)	Print, Electronic	Copies for the disabled?	No
		Minor editing privileges?	Yes
Who will republish the content?	Academic institution	Incidental promotional use?	Yes
Duration of Use	Life of current edition	Currency	EUR
Lifetime Unit Quantity	Up to 499		
Rights Requested	Main product		

NEW WORK DETAILS

Title	Macrocyclic Tetra-dentate NHC Complexes for Catalysis and Medicinal Chemistry	Institution name	Technical University Munich
		Expected presentation date	2020-12-31
Instructor name	Marco Bernd		

ADDITIONAL DETAILS

Order reference number	N/A	The requesting person / organization to appear on the license	Marco Bernd

REUSE CONTENT DETAILS

Title, description or numeric reference of the portion(s)	Figure 2	Title of the article/chapter the portion is from	Inhibition of transcription by platinum antitumor compounds
Editor of portion(s)	N/A	Author of portion(s)	Royal Society of Chemistry (Great Britain)
Volume of serial or monograph	4	Issue, if republishing an article from a serial	N/A
Page or page range of portion	280-291	Publication date of portion	2009-05-26

CCC Republication Terms and Conditions

1. Description of Service; Defined Terms. This Republication License enables the User to obtain licenses for republication of one or more copyrighted works as described in detail on the relevant Order Confirmation (the "Work(s)"). Copyright Clearance Center, Inc. ("CCC") grants licenses through the Service on behalf of the rightsholder identified on the Order Confirmation (the "Rightsholder"). "Republication", as used herein, generally means the inclusion of a Work, in whole or in part, in a new work or works, also as described on the Order Confirmation. "User", as used herein, means the person or entity making such republication.

2. The terms set forth in the relevant Order Confirmation, and any terms set by the Rightsholder with respect to a particular Work, govern the terms of use of Works in connection with the Service. By using the Service, the person transacting for a republication license on behalf of the User represents and warrants that he/she/it (a) has been duly authorized by the User to accept, and hereby does accept, all such terms and conditions on behalf of User, and (b) shall inform User of all such terms and conditions. In the event such person is a "freelancer" or other third party independent of User and CCC, such party shall be deemed jointly a "User" for purposes of these terms and conditions. In any event, User shall be deemed to have accepted and agreed to all such terms and conditions if User republishes the Work in any fashion.

3. Scope of License; Limitations and Obligations.

   3.1. All Works and all rights therein, including copyright rights, remain the sole and exclusive property of the Rightsholder. The license created by the exchange of an Order Confirmation (and/or any invoice) and payment by User of the full amount set forth on that document includes only those rights expressly set forth in the Order Confirmation and in these terms and conditions, and conveys no other rights in the Work(s) to User. All rights not expressly granted are hereby reserved.

   3.2. General Payment Terms: You may pay by credit card or through an account with us payable at the end of the month. If you and we agree that you may establish a standing account with CCC, then the following terms apply: Remit Payment to: Copyright Clearance Center, 29118 Network Place, Chicago, IL 60673-1291. Payments Due: Invoices are payable upon their delivery to you (or upon our notice to you that they are available to you for downloading). After 30 days, outstanding amounts will be subject to a service charge of 1-1/2% per month or, if less, the maximum rate allowed by applicable law. Unless otherwise specifically set forth in the Order Confirmation or in a separate written agreement signed by CCC, invoices are due and payable on "net 30" terms. While User may exercise the rights licensed immediately upon issuance of the Order Confirmation, the license is automatically revoked and is null and void, as if it had never been issued, if complete payment for the license is not received on a timely basis either from User directly or through a payment agent, such as a credit card company.

   3.3. Unless otherwise provided in the Order Confirmation, any grant of rights to User (i) is "one-time" (including the editions and product family specified in the license), (ii) is non-exclusive and non-transferable and (iii) is subject to any and all limitations and restrictions (such as, but not limited to, limitations on duration of use or circulation) included in the Order Confirmation or invoice and/or in these terms and conditions. Upon completion of the licensed use, User shall either secure a new permission for further use of the Work(s) or immediately cease any new use of the Work(s) and shall render inaccessible (such as by deleting or by removing or severing links or other locators) any further copies of the Work (except for copies printed on paper in accordance with this license and still in User's stock at the end of such period).

   3.4. In the event that the material for which a republication license is sought includes third party materials (such as photographs, illustrations, graphs, inserts and similar materials) which are identified in such material as having been used by permission, User is responsible for identifying, and seeking separate licenses (under this Service or otherwise) for, any of such third party materials; without a separate license, such third party materials may not be used.

   3.5. Use of proper copyright notice for a Work is required as a condition of any license granted under the Service. Unless otherwise provided in the Order Confirmation, a proper copyright notice will read substantially as follows: "Republished with permission of [Rightsholder's name], from [Work's title, author, volume, edition number and year of copyright]; permission conveyed through Copyright Clearance Center, Inc. " Such notice must be provided in a reasonably legible font size and must be placed either immediately adjacent to the Work as used (for example, as part of a by-line or footnote but not as a separate electronic link) or in the place where substantially all other credits or notices for the new work containing the republished Work are located. Failure to include the required notice results in loss to the Rightsholder and CCC, and the User shall be liable to pay liquidated damages for each such failure equal to twice the use fee specified in the Order Confirmation, in addition to the use fee itself and any other fees and charges specified.

   3.6. User may only make alterations to the Work if and as expressly set forth in the Order Confirmation. No Work may be used in any way that is defamatory, violates the rights of third parties (including such third parties' rights of copyright, privacy, publicity, or other tangible or intangible property), or is otherwise illegal, sexually explicit or obscene. In addition, User may not conjoin a Work with any other material that may result in damage to the reputation of the Rightsholder. User agrees to inform CCC if it becomes aware of any infringement of any rights in a Work and to cooperate with any reasonable request of CCC or the Rightsholder in connection therewith.

4. Indemnity. User hereby indemnifies and agrees to defend the Rightsholder and CCC, and their respective employees and directors, against all claims, liability, damages, costs and expenses, including legal fees and expenses, arising out of any use of a Work beyond the scope of the rights granted herein, or any use of a Work which has been altered in any unauthorized way by User, including claims of defamation or infringement of rights of copyright, publicity, privacy or other tangible or intangible property.

5. Limitation of Liability. UNDER NO CIRCUMSTANCES WILL CCC OR THE RIGHTSHOLDER BE LIABLE FOR ANY DIRECT, INDIRECT, CONSEQUENTIAL OR INCIDENTAL DAMAGES (INCLUDING WITHOUT LIMITATION DAMAGES FOR LOSS OF BUSINESS PROFITS OR INFORMATION, OR FOR BUSINESS INTERRUPTION) ARISING OUT OF THE USE OR INABILITY TO USE A WORK, EVEN IF ONE OF THEM HAS BEEN ADVISED OF THE POSSIBILITY OF SUCH DAMAGES. In any event, the total liability of the Rightsholder and CCC (including their respective employees and directors) shall not exceed the total amount actually paid by User for this license. User assumes full liability for the actions and omissions of its principals, employees, agents, affiliates, successors and assigns.

6. Limited Warranties. THE WORK(S) AND RIGHT(S) ARE PROVIDED "AS IS". CCC HAS THE RIGHT TO GRANT TO USER THE RIGHTS GRANTED IN THE ORDER CONFIRMATION DOCUMENT. CCC AND THE RIGHTSHOLDER DISCLAIM ALL OTHER WARRANTIES RELATING TO THE WORK(S) AND RIGHT(S), EITHER EXPRESS OR IMPLIED, INCLUDING WITHOUT LIMITATION IMPLIED WARRANTIES OF MERCHANTABILITY OR FITNESS FOR A PARTICULAR PURPOSE. ADDITIONAL RIGHTS MAY BE REQUIRED TO USE ILLUSTRATIONS, GRAPHS, PHOTOGRAPHS, ABSTRACTS, INSERTS OR OTHER PORTIONS OF THE WORK (AS OPPOSED TO THE ENTIRE WORK) IN A MANNER CONTEMPLATED BY USER; USER UNDERSTANDS AND AGREES THAT NEITHER CCC NOR THE RIGHTSHOLDER MAY HAVE SUCH ADDITIONAL RIGHTS TO GRANT.

7. Effect of Breach. Any failure by User to pay any amount when due, or any use by User of a Work beyond the scope of the license set forth in the Order Confirmation and/or these terms and conditions, shall be a material breach of the license created by the Order Confirmation and these terms and conditions. Any breach not cured within 30 days of written notice thereof shall result in immediate termination of such license without further notice. Any unauthorized (but licensable) use of a Work that is terminated immediately upon notice thereof may be liquidated by payment of the Rightsholder's ordinary license price therefor; any unauthorized (and unlicensable) use that is not terminated immediately for any reason (including, for example, because materials containing the Work cannot reasonably be recalled) will be subject to all remedies available at law or in equity, but in no event to a payment of less than three times the Rightsholder's ordinary license price for the most closely analogous licensable use plus Rightsholder's and/or CCC's costs and expenses incurred in collecting such payment.

8. Miscellaneous.

   8.1. User acknowledges that CCC may, from time to time, make changes or additions to the Service or to these terms and conditions, and CCC reserves the right to send notice to the User by electronic mail or otherwise for the purposes of notifying User of such changes or additions; provided that any such changes or additions shall not apply to permissions already secured and paid for.

   8.2. Use of User-related information collected through the Service is governed by CCC's privacy policy, available online here:https://marketplace.copyright.com/rs-ui-web/mp/privacy-policy

   8.3. The licensing transaction described in the Order Confirmation is personal to User. Therefore, User may not assign or transfer to any other person (whether a natural person or an organization of any kind) the license created by the Order Confirmation and these terms and conditions or any rights granted hereunder; provided, however, that User may assign such license in its entirety on written notice to CCC in the event of a transfer of all or substantially all of User's rights in the new material which includes the Work(s) licensed under this Service.

   8.4. No amendment or waiver of any terms is binding unless set forth in writing and signed by the parties. The Rightsholder and CCC hereby object to any terms contained in any writing prepared by the User or its principals, employees, agents or affiliates and purporting to govern or otherwise relate to the licensing transaction described in the Order Confirmation, which terms are in any way inconsistent with any terms set forth in the Order Confirmation and/or in these terms and conditions or CCC's standard operating procedures, whether such writing is prepared prior to, simultaneously with or subsequent to the Order Confirmation, and whether such writing appears on a copy of the Order Confirmation or in a separate instrument.

   8.5. The licensing transaction described in the Order Confirmation document shall be governed by and construed under the law of the State of New York, USA, without regard to the principles thereof of conflicts of law. Any case, controversy, suit, action, or proceeding arising out of, in connection with, or related to such licensing transaction shall be brought, at CCC's sole discretion, in any federal or state court located in the County of New York, State of New York, USA, or in any federal or state court whose geographical jurisdiction covers the location of the Rightsholder set forth in the Order Confirmation. The parties expressly submit to the personal jurisdiction and venue of each such federal or state court.If you have any comments or questions about the Service or Copyright Clearance Center, please contact us at 978-750-8400 or send an e-mail to support@copyright.com.

v 1.1

6.5 Creative Commons Attribution License [Attribution 4.0 International (CC BY 4.0)]

Figure 17, Reference [198]: Fernández, L., Silva, V., Domínguez-González, T., Claudio-Betancourt, S., Toro-Maldonado, R., Maso, L., Sanabria, K., Pérez-Verdejo, J., González, J., Rosado-Fraticelli, G., Meléndez, F., Santiago, F., Rivera-Rivera, D., Navarro, C., Chardón, A., Vera, A., Tinoco, A., *Inorganics* **2020,** *8*, 10.

License accessible *via*: https://creativecommons.org/licenses/by/4.0/legalcode

Creative Commons Legal Code

Attribution 4.0 International

Official translations of this license are available in other languages.
Creative Commons Corporation ("Creative Commons") is not a law firm and does not provide legal services or legal advice. Distribution of Creative Commons public licenses does not create a lawyer-client or other relationship. Creative Commons makes its licenses and related information available on an "as-is" basis. Creative Commons gives no warranties regarding its licenses, any material licensed under their terms and conditions, or any related information. Creative Commons disclaims all liability for damages resulting from their use to the fullest extent possible.

Using Creative Commons Public Licenses

Creative Commons public licenses provide a standard set of terms and conditions that creators and other rights holders may use to share original works of authorship and other material subject to copyright and certain other rights specified in the public license below. The following considerations are for informational purposes only, are not exhaustive, and do not form part of our licenses.

Considerations for licensors: Our public licenses are intended for use by those authorized to give the public permission to use material in ways otherwise restricted by copyright and certain other rights. Our licenses are irrevocable. Licensors should read and understand the terms and conditions of the license they choose before applying it. Licensors should also secure all rights necessary before applying our licenses so that the public can reuse the material as expected. Licensors should clearly mark any material not subject to the license. This includes other CC-licensed material, or material used under an exception or limitation to copyright.

Considerations for the public: By using one of our public licenses, a licensor grants the public permission to use the licensed material under specified terms and conditions. If the licensor's permission is not necessary for any reason–for example, because of any applicable exception or limitation to copyright–then that use is not regulated by the license. Our licenses grant only permissions under copyright and certain other rights that a licensor has authority to grant. Use of the licensed material may still be restricted for other reasons, including because others have copyright or other rights in the material. A licensor may make special requests, such as asking that all changes be marked or described. Although not required by our licenses, you are encouraged to respect those requests where reasonable.

Creative Commons Attribution 4.0 International Public License

By exercising the Licensed Rights (defined below), You accept and agree to be bound by the terms and conditions of this Creative Commons Attribution 4.0 International Public License ("Public License"). To the extent this Public License may be interpreted as a contract, You are granted the Licensed Rights in consideration of Your acceptance of these terms and conditions, and the Licensor grants You such rights in consideration of benefits the Licensor receives from making the Licensed Material available under these terms and conditions.

Section 1 – Definitions.

a. **Adapted Material** means material subject to Copyright and Similar Rights that is derived from or based upon the Licensed Material and in which the Licensed Material is translated, altered, arranged, transformed, or otherwise modified in a manner requiring permission under the Copyright and Similar Rights held by the Licensor. For purposes of this Public License, where the Licensed Material is a musical work, performance, or sound recording, Adapted Material is always produced where the Licensed Material is synched in timed relation with a moving image.
b. **Adapter's License** means the license You apply to Your Copyright and Similar Rights in Your contributions to Adapted Material in accordance with the terms and conditions of this Public License.
c. **Copyright and Similar Rights** means copyright and/or similar rights closely related to copyright including, without limitation, performance, broadcast, sound recording, and Sui Generis Database Rights, without regard to how the rights are labeled or categorized. For purposes of this Public License, the rights specified in Section 2(b)(1)-(2) are not Copyright and Similar Rights.
d. **Effective Technological Measures** means those measures that, in the absence of proper authority, may not be circumvented under laws fulfilling obligations under Article 11 of the WIPO Copyright Treaty adopted on December 20, 1996, and/or similar international agreements.
e. **Exceptions and Limitations** means fair use, fair dealing, and/or any other exception or limitation to Copyright and Similar Rights that applies to Your use of the Licensed Material.
f. **Licensed Material** means the artistic or literary work, database, or other material to which the Licensor applied this Public License.
g. **Licensed Rights** means the rights granted to You subject to the terms and conditions of this Public License, which are limited to all Copyright and Similar Rights that apply to Your use of the Licensed Material and that the Licensor has authority to license.
h. **Licensor** means the individual(s) or entity(ies) granting rights under this Public License.
i. **Share** means to provide material to the public by any means or process that requires permission under the Licensed Rights, such as reproduction, public display, public performance, distribution, dissemination, communication, or importation, and to make material available to the public including in ways that members of the public may access the material from a place and at a time individually chosen by them.
j. **Sui Generis Database Rights** means rights other than copyright resulting from Directive 96/9/EC of the European Parliament and of the Council of 11 March 1996 on the legal protection of databases, as amended and/or succeeded, as well as other essentially equivalent rights

anywhere in the world.

k. **You** means the individual or entity exercising the Licensed Rights under this Public License. **Your** has a corresponding meaning.

Section 2 – Scope.

a. **License grant**.

1. Subject to the terms and conditions of this Public License, the Licensor hereby grants You a worldwide, royalty-free, non-sublicensable, non-exclusive, irrevocable license to exercise the Licensed Rights in the Licensed Material to:
   A. reproduce and Share the Licensed Material, in whole or in part; and
   B. produce, reproduce, and Share Adapted Material.
2. Exceptions and Limitations. For the avoidance of doubt, where Exceptions and Limitations apply to Your use, this Public License does not apply, and You do not need to comply with its terms and conditions.
3. Term. The term of this Public License is specified in Section 6(a).
4. Media and formats; technical modifications allowed. The Licensor authorizes You to exercise the Licensed Rights in all media and formats whether now known or hereafter created, and to make technical modifications necessary to do so. The Licensor waives and/or agrees not to assert any right or authority to forbid You from making technical modifications necessary to exercise the Licensed Rights, including technical modifications necessary to circumvent Effective Technological Measures. For purposes of this Public License, simply making modifications authorized by this Section 2(a)(4) never produces Adapted Material.
5. Downstream recipients.
   A. Offer from the Licensor – Licensed Material. Every recipient of the Licensed Material automatically receives an offer from the Licensor to exercise the Licensed Rights under the terms and conditions of this Public License.
   B. No downstream restrictions. You may not offer or impose any additional or different terms or conditions on, or apply any Effective Technological Measures to, the Licensed Material if doing so restricts exercise of the Licensed Rights by any recipient of the Licensed Material.
6. No endorsement. Nothing in this Public License constitutes or may be construed as permission to assert or imply that You are, or that Your use of the Licensed Material is, connected with, or sponsored, endorsed, or granted official status by, the Licensor or others designated to receive attribution as provided in Section 3(a)(1)(A)(i).

b. **Other rights**.

1. Moral rights, such as the right of integrity, are not licensed under this Public License, nor are publicity, privacy, and/or other similar personality rights; however, to the extent possible, the Licensor waives and/or agrees not to assert any such rights held by the Licensor to the limited extent necessary to allow You to exercise the Licensed Rights, but not otherwise.
2. Patent and trademark rights are not licensed under this Public License.
3. To the extent possible, the Licensor waives any right to collect royalties from You for the exercise of the Licensed Rights, whether directly or through a collecting society under any voluntary or waivable statutory or compulsory licensing scheme. In all other cases the Licensor expressly reserves any right to collect such royalties.

Section 3 – License Conditions.

Your exercise of the Licensed Rights is expressly made subject to the following conditions.

a. **Attribution**.

1. If You Share the Licensed Material (including in modified form), You must:
   A. retain the following if it is supplied by the Licensor with the Licensed Material:
      i. identification of the creator(s) of the Licensed Material and any others designated to receive attribution, in any reasonable manner requested by the Licensor (including by pseudonym if designated);
      ii. a copyright notice;
      iii. a notice that refers to this Public License;
      iv. a notice that refers to the disclaimer of warranties;
      v. a URI or hyperlink to the Licensed Material to the extent reasonably practicable;
   B. indicate if You modified the Licensed Material and retain an indication of any previous modifications; and
   C. indicate the Licensed Material is licensed under this Public License, and include the text of, or the URI or hyperlink to, this Public License.
2. You may satisfy the conditions in Section 3(a)(1) in any reasonable manner based on the medium, means, and context in which You Share the Licensed Material. For example, it may be reasonable to satisfy the conditions by providing a URI or hyperlink to a resource that includes the required information.
3. If requested by the Licensor, You must remove any of the information required by Section 3(a)(1)(A) to the extent reasonably practicable.
4. If You Share Adapted Material You produce, the Adapter's License You apply must not prevent recipients of the Adapted Material from complying with this Public License.

Section 4 – Sui Generis Database Rights.

Where the Licensed Rights include Sui Generis Database Rights that apply to Your use of the Licensed Material:

a. for the avoidance of doubt, Section 2(a)(1) grants You the right to extract, reuse, reproduce, and Share all or a substantial portion of the contents of the database;
b. if You include all or a substantial portion of the database contents in a database in which You have Sui Generis Database Rights, then the database in which You have Sui Generis Database Rights (but not its individual contents) is Adapted Material; and
c. You must comply with the conditions in Section 3(a) if You Share all or a substantial portion of the contents of the database.

For the avoidance of doubt, this Section 4 supplements and does not replace Your obligations under this Public License where the Licensed Rights include other Copyright and Similar Rights.

Section 5 – Disclaimer of Warranties and Limitation of Liability.

a. **Unless otherwise separately undertaken by the Licensor, to the extent possible, the Licensor offers the Licensed Material as-is and as-available, and makes no representations or warranties of any kind concerning the Licensed Material, whether express, implied, statutory, or other. This includes, without limitation, warranties of title, merchantability, fitness for a particular purpose, non-infringement, absence of latent or other defects, accuracy, or the presence or absence of errors, whether or not known or discoverable. Where disclaimers of warranties are not allowed in full or in part, this disclaimer may not apply to You.**

b. **To the extent possible, in no event will the Licensor be liable to You on any legal theory (including, without limitation, negligence) or otherwise for any direct, special, indirect, incidental, consequential, punitive, exemplary, or other losses, costs, expenses, or damages arising out of this Public License or use of the Licensed Material, even if the Licensor has been advised of the possibility of such losses, costs, expenses, or damages. Where a limitation of liability is not allowed in full or in part, this limitation may not apply to You.**

c. The disclaimer of warranties and limitation of liability provided above shall be interpreted in a manner that, to the extent possible, most closely approximates an absolute disclaimer and waiver of all liability.

Section 6 – Term and Termination.

a. This Public License applies for the term of the Copyright and Similar Rights licensed here. However, if You fail to comply with this Public License, then Your rights under this Public License terminate automatically.
b. Where Your right to use the Licensed Material has terminated under Section 6(a), it reinstates:

1. automatically as of the date the violation is cured, provided it is cured within 30 days of Your discovery of the violation; or
2. upon express reinstatement by the Licensor.

For the avoidance of doubt, this Section 6(b) does not affect any right the Licensor may have to seek remedies for Your violations of this Public License.

c. For the avoidance of doubt, the Licensor may also offer the Licensed Material under separate terms or conditions or stop distributing the Licensed Material at any time; however, doing so will not terminate this Public License.
d. Sections 1, 5, 6, 7, and 8 survive termination of this Public License.

Section 7 – Other Terms and Conditions.

a. The Licensor shall not be bound by any additional or different terms or conditions communicated by You unless expressly agreed.
b. Any arrangements, understandings, or agreements regarding the Licensed Material not stated herein are separate from and independent of the terms and conditions of this Public License.

Section 8 – Interpretation.

a. For the avoidance of doubt, this Public License does not, and shall not be interpreted to, reduce, limit, restrict, or impose conditions on any use of the Licensed Material that could lawfully be made without permission under this Public License.
b. To the extent possible, if any provision of this Public License is deemed unenforceable, it shall be automatically reformed to the minimum extent necessary to make it enforceable. If the provision cannot be reformed, it shall be severed from this Public License without affecting the enforceability of the remaining terms and conditions.
c. No term or condition of this Public License will be waived and no failure to comply consented to unless expressly agreed to by the Licensor.
d. Nothing in this Public License constitutes or may be interpreted as a limitation upon, or waiver of, any privileges and immunities that apply to the Licensor or You, including from the legal processes of any jurisdiction or authority.

Creative Commons is not a party to its public licenses. Notwithstanding, Creative Commons may elect to apply one of its public licenses to material it publishes and in those instances will be considered the “Licensor.” The text of the Creative Commons public licenses is dedicated to the public domain under the CC0 Public Domain Dedication. Except for the limited purpose of indicating that material is shared under a Creative Commons public license or as otherwise permitted by the Creative Commons policies published at creativecommons.org/policies, Creative Commons does not authorize the use of the trademark “Creative Commons” or any other trademark or logo of Creative Commons without its prior written consent including, without limitation, in connection with any unauthorized modifications to any of its public licenses or any other arrangements, understandings, or agreements concerning use of licensed material. For the avoidance of doubt, this paragraph does not form part of the public licenses.

Creative Commons may be contacted at creativecommons.org.

6.6 John Wiley and Sons

Figure 18, Reference [215]: Georgiades, S. N., Abd Karim, N. H., Suntharalingam, K., Vilar, R., *Angewandte Chemie International Edition* **2010,** *49* (24), 4020-4034.

JOHN WILEY AND SONS LICENSE
TERMS AND CONDITIONS

Oct 19, 2020

This Agreement between Tecnical Univrsity of Munich -- Marco Bernd ("You") and John Wiley and Sons ("John Wiley and Sons") consists of your license details and the terms and conditions provided by John Wiley and Sons and Copyright Clearance Center.

License Number	4932480304909
License date	Oct 19, 2020
Licensed Content Publisher	John Wiley and Sons
Licensed Content Publication	Angewandte Chemie International Edition
Licensed Content Title	Interaction of Metal Complexes with G-Quadruplex DNA
Licensed Content Author	Ramon Vilar, Kogularamanan Suntharalingam, Nurul H. Abd Karim, et al
Licensed Content Date	May 26, 2010
Licensed Content Volume	49
Licensed Content Issue	24
Licensed Content Pages	15
Type of use	Dissertation/Thesis
Requestor type	University/Academic
Format	Print and electronic

1 von 6

Portion	Figure/table
Number of figures/tables	1
Will you be translating?	No
Title	Macrocyclic Tetra-Dentate NHC Complexes For Catalysis And Medicinal Chemistry
Institution name	Technical University Munich
Expected presentation date	Dec 2020
Portions	Figure 1
Requestor Location	Technical University of Munich Arcisstraße 21 Munich, Bavaria 80333 Germany Attn: Technical University of Munich
Publisher Tax ID	EU826007151
Total	0.00 EUR

Terms and Conditions

TERMS AND CONDITIONS

This copyrighted material is owned by or exclusively licensed to John Wiley & Sons, Inc. or one of its group companies (each a"Wiley Company") or handled on behalf of a society with which a Wiley Company has exclusive publishing rights in relation to a particular work (collectively "WILEY"). By clicking "accept" in connection with completing this licensing transaction, you agree that the following terms and conditions apply to this transaction (along with the billing and payment terms and conditions established by the Copyright Clearance Center Inc., ("CCC's Billing and Payment terms and conditions"), at the time that you opened your RightsLink account (these are available at any time at http://myaccount.copyright.com).

Terms and Conditions

2 von 6

- The materials you have requested permission to reproduce or reuse (the "Wiley Materials") are protected by copyright.
- You are hereby granted a personal, non-exclusive, non-sub licensable (on a stand-alone basis), non-transferable, worldwide, limited license to reproduce the Wiley Materials for the purpose specified in the licensing process. This license, **and any CONTENT (PDF or image file) purchased as part of your order,** is for a one-time use only and limited to any maximum distribution number specified in the license. The first instance of republication or reuse granted by this license must be completed within two years of the date of the grant of this license (although copies prepared before the end date may be distributed thereafter). The Wiley Materials shall not be used in any other manner or for any other purpose, beyond what is granted in the license. Permission is granted subject to an appropriate acknowledgement given to the author, title of the material/book/journal and the publisher. You shall also duplicate the copyright notice that appears in the Wiley publication in your use of the Wiley Material. Permission is also granted on the understanding that nowhere in the text is a previously published source acknowledged for all or part of this Wiley Material. Any third party content is expressly excluded from this permission.
- With respect to the Wiley Materials, all rights are reserved. Except as expressly granted by the terms of the license, no part of the Wiley Materials may be copied, modified, adapted (except for minor reformatting required by the new Publication), translated, reproduced, transferred or distributed, in any form or by any means, and no derivative works may be made based on the Wiley Materials without the prior permission of the respective copyright owner.**For STM Signatory Publishers clearing permission under the terms of the STM Permissions Guidelines only, the terms of the license are extended to include subsequent editions and for editions in other languages, provided such editions are for the work as a whole in situ and does not involve the separate exploitation of the permitted figures or extracts,** You may not alter, remove or suppress in any manner any copyright, trademark or other notices displayed by the Wiley Materials. You may not license, rent, sell, loan, lease, pledge, offer as security, transfer or assign the Wiley Materials on a stand-alone basis, or any of the rights granted to you hereunder to any other person.
- The Wiley Materials and all of the intellectual property rights therein shall at all times remain the exclusive property of John Wiley & Sons Inc, the Wiley Companies, or their respective licensors, and your interest therein is only that of having possession of and the right to reproduce the Wiley Materials pursuant to Section 2 herein during the continuance of this Agreement. You agree that you own no right, title or interest in or to the Wiley Materials or any of the intellectual property rights therein. You shall have no rights hereunder other than the license as provided for above in Section 2. No right, license or interest to any trademark, trade name, service mark or other branding ("Marks") of WILEY or its licensors is granted hereunder, and you agree that you shall not assert any such right, license or interest with respect thereto
- NEITHER WILEY NOR ITS LICENSORS MAKES ANY WARRANTY OR REPRESENTATION OF ANY KIND TO YOU OR ANY THIRD PARTY, EXPRESS, IMPLIED OR STATUTORY, WITH RESPECT TO THE MATERIALS OR THE ACCURACY OF ANY INFORMATION CONTAINED IN THE MATERIALS, INCLUDING, WITHOUT LIMITATION, ANY IMPLIED WARRANTY OF MERCHANTABILITY, ACCURACY, SATISFACTORY QUALITY, FITNESS FOR A PARTICULAR PURPOSE, USABILITY, INTEGRATION OR NON-INFRINGEMENT AND ALL SUCH WARRANTIES ARE HEREBY EXCLUDED BY WILEY AND ITS LICENSORS AND WAIVED

3 von 6

BY YOU.

- WILEY shall have the right to terminate this Agreement immediately upon breach of this Agreement by you.
- You shall indemnify, defend and hold harmless WILEY, its Licensors and their respective directors, officers, agents and employees, from and against any actual or threatened claims, demands, causes of action or proceedings arising from any breach of this Agreement by you.
- IN NO EVENT SHALL WILEY OR ITS LICENSORS BE LIABLE TO YOU OR ANY OTHER PARTY OR ANY OTHER PERSON OR ENTITY FOR ANY SPECIAL, CONSEQUENTIAL, INCIDENTAL, INDIRECT, EXEMPLARY OR PUNITIVE DAMAGES, HOWEVER CAUSED, ARISING OUT OF OR IN CONNECTION WITH THE DOWNLOADING, PROVISIONING, VIEWING OR USE OF THE MATERIALS REGARDLESS OF THE FORM OF ACTION, WHETHER FOR BREACH OF CONTRACT, BREACH OF WARRANTY, TORT, NEGLIGENCE, INFRINGEMENT OR OTHERWISE (INCLUDING, WITHOUT LIMITATION, DAMAGES BASED ON LOSS OF PROFITS, DATA, FILES, USE, BUSINESS OPPORTUNITY OR CLAIMS OF THIRD PARTIES), AND WHETHER OR NOT THE PARTY HAS BEEN ADVISED OF THE POSSIBILITY OF SUCH DAMAGES. THIS LIMITATION SHALL APPLY NOTWITHSTANDING ANY FAILURE OF ESSENTIAL PURPOSE OF ANY LIMITED REMEDY PROVIDED HEREIN.
- Should any provision of this Agreement be held by a court of competent jurisdiction to be illegal, invalid, or unenforceable, that provision shall be deemed amended to achieve as nearly as possible the same economic effect as the original provision, and the legality, validity and enforceability of the remaining provisions of this Agreement shall not be affected or impaired thereby.
- The failure of either party to enforce any term or condition of this Agreement shall not constitute a waiver of either party's right to enforce each and every term and condition of this Agreement. No breach under this agreement shall be deemed waived or excused by either party unless such waiver or consent is in writing signed by the party granting such waiver or consent. The waiver by or consent of a party to a breach of any provision of this Agreement shall not operate or be construed as a waiver of or consent to any other or subsequent breach by such other party.
- This Agreement may not be assigned (including by operation of law or otherwise) by you without WILEY's prior written consent.
- Any fee required for this permission shall be non-refundable after thirty (30) days from receipt by the CCC.
- These terms and conditions together with CCC's Billing and Payment terms and conditions (which are incorporated herein) form the entire agreement between you and WILEY concerning this licensing transaction and (in the absence of fraud) supersedes all prior agreements and representations of the parties, oral or written. This Agreement may not be amended except in writing signed by both parties. This Agreement shall be binding upon and inure to the benefit of the parties' successors, legal representatives, and authorized assigns.
- In the event of any conflict between your obligations established by these terms and

4 von 6

conditions and those established by CCC's Billing and Payment terms and conditions, these terms and conditions shall prevail.

- WILEY expressly reserves all rights not specifically granted in the combination of (i) the license details provided by you and accepted in the course of this licensing transaction, (ii) these terms and conditions and (iii) CCC's Billing and Payment terms and conditions.
- This Agreement will be void if the Type of Use, Format, Circulation, or Requestor Type was misrepresented during the licensing process.
- This Agreement shall be governed by and construed in accordance with the laws of the State of New York, USA, without regards to such state's conflict of law rules. Any legal action, suit or proceeding arising out of or relating to these Terms and Conditions or the breach thereof shall be instituted in a court of competent jurisdiction in New York County in the State of New York in the United States of America and each party hereby consents and submits to the personal jurisdiction of such court, waives any objection to venue in such court and consents to service of process by registered or certified mail, return receipt requested, at the last known address of such party.

WILEY OPEN ACCESS TERMS AND CONDITIONS

Wiley Publishes Open Access Articles in fully Open Access Journals and in Subscription journals offering Online Open. Although most of the fully Open Access journals publish open access articles under the terms of the Creative Commons Attribution (CC BY) License only, the subscription journals and a few of the Open Access Journals offer a choice of Creative Commons Licenses. The license type is clearly identified on the article.

The Creative Commons Attribution License

The Creative Commons Attribution License (CC-BY) allows users to copy, distribute and transmit an article, adapt the article and make commercial use of the article. The CC-BY license permits commercial and non-

Creative Commons Attribution Non-Commercial License

The Creative Commons Attribution Non-Commercial (CC-BY-NC)License permits use, distribution and reproduction in any medium, provided the original work is properly cited and is not used for commercial purposes.(see below)

Creative Commons Attribution-Non-Commercial-NoDerivs License

The Creative Commons Attribution Non-Commercial-NoDerivs License (CC-BY-NC-ND) permits use, distribution and reproduction in any medium, provided the original work is properly cited, is not used for commercial purposes and no modifications or adaptations are made. (see below)

Use by commercial "for-profit" organizations

Use of Wiley Open Access articles for commercial, promotional, or marketing purposes requires further explicit permission from Wiley and will be subject to a fee.

Further details can be found on Wiley Online Library http://olabout.wiley.com/WileyCDA/Section/id-410895.html

Other Terms and Conditions:

v1.10 Last updated September 2015

Questions? customercare@copyright.com or +1-855-239-3415 (toll free in the US) or +1-978-646-2777.

7 Bibliographic Data of Complete Publications

7.1 Tuning the electronic properties of tetradentate iron-NHC complexes: Towards stable and selective epoxidation catalysts

Marco A. Bernd,[‡] Florian Dyckhoff,[‡] Benjamin J. Hofmann, Alexander D. Böth, Jonas F. Schlagintweit, Jens Oberkofler, Robert M. Reich and Fritz E. Kühn*

Department of Chemistry and Catalysis Research Center, Molecular Catalysis, Technische Universität München, Lichtenbergstr. 4, D-85747 Garching bei München, Germany

[‡] equally contributing authors

[*] corresponding author

Journal of Catalysis **2020**, *391*, 548–561

DOI: 10.1016/j.jcat.2020.08.037

Direct link: https://doi.org/10.1016/j.jcat.2020.08.037

7.2 Synthesis, characterization, and biological studies of multidentate gold(I) and gold(III) NHC complexes

Elisabeth B. Bauer,[a,‡] Marco A. Bernd,[a,‡] Max Schütz,[a,b] Jens Oberkofler,[a] Alexander Pöthig,[c] Robert M. Reich[a] and Fritz E. Kühn[a,*]

[a] Department of Chemistry and Catalysis Research Center, Molecular Catalysis, Technische Universität München, Lichtenbergstr. 4, D-85747 Garching bei München, Germany.

[b] Department of Chemistry and Catalysis Research Center, Chair of Inorganic and Metal-Organic Chemistry, Technische Universität München, Lichtenbergstr. 4, D-85747 Garching bei München, Germany.

[c] Single Crystal XRD Laboratory of the Catalysis Research Center, Technische Universität München, Ernst-Otto-Fischer-Str. 1, 85747 Garching bei München, Germany.

[‡] equally contributing authors

[*] corresponding author

Dalton Transactions **2019**, *48*, 16615–16625

DOI: 10.1039/C9DT03183A

Direct link: https://doi.org/10.1039/C9DT03183A

7.3 Macrocyclic NHC complexes of group 10 elements with enlarged aromaticity for biological studies

Marco A. Bernd,[a,‡] Elisabeth B. Bauer,[a,‡] Jens Oberkofler,[a] Andreas Bauer,[b] Robert M. Reich[a] and Fritz E. Kühn[a,*]

[a] Department of Chemistry and Catalysis Research Center, Molecular Catalysis, Technische Universität München, Lichtenbergstr. 4, D-85747 Garching bei München, Germany.

[b] Department of Chemistry and Catalysis Research Center, Chair of Organic Chemistry I, Technische Universität München, Lichtenbergstr. 4, D-85747 Garching bei München, Germany.

[‡] equally contributing authors

[*] corresponding author

Dalton Transactions **2020**, *49*, 14106-14114

DOI: 10.1039/D0DT02598D

Direct link: https://doi.org/10.1039/D0DT02598D

8 References

[1] Díez-González, S., Nolan, S. P., *Coordin. Chem. Rev.* **2007,** *251* (5), 874-883.
[2] Fischer, E. O., Maasböl, A., *Angew. Chem. Int. Ed.* **1964,** *3* (8), 580-581.
[3] Frenking, G., Solà, M., Vyboishchikov, S. F., *J. Organomet. Chem.* **2005,** *690* (24), 6178-6204.
[4] de Frémont, P., Marion, N., Nolan, S. P., *Coordin. Chem. Rev.* **2009,** *253* (7), 862-892.
[5] Bourissou, D., Guerret, O., Gabbaï, F. P., Bertrand, G., *Chem. Rev.* **2000,** *100* (1), 39-92.
[6] Díez-González, S., Marion, N., Nolan, S. P., *Chem. Rev.* **2009,** *109* (8), 3612-3676.
[7] Vyboishchikov, S. F., Frenking, G., *Chem. Eur. J.* **1998,** *4* (8), 1428-1438.
[8] Schrock, R. R., *J. Am. Chem. Soc.* **1974,** *96* (21), 6796-6797.
[9] Dötz, K. H., Stendel, J., *Chem. Rev.* **2009,** *109* (8), 3227-3274.
[10] Chauvin, Y., *Angew. Chem. Int. Ed.* **2006,** *45* (23), 3740-3747.
[11] Grubbs, R. H., *Angew. Chem. Int. Ed.* **2006,** *45* (23), 3760-3765.
[12] Schrock, R. R., *Angew. Chem. Int. Ed.* **2006,** *45* (23), 3748-3759.
[13] Wanzlick, H. W., Kleiner, H. J., *Angew. Chem.* **1961,** *73* (14).
[14] Wanzlick, H. W., *Angew. Chem. Int. Ed.* **1962,** *1* (2), 75-80.
[15] Wanzlick, H.-W., Schönherr, H.-J., *Angew. Chem. Int. Ed.* **1968,** *7* (2), 141-142.
[16] Öfele, K., *J. Organomet. Chem.* **1968,** *12* (3), P42-P43.
[17] Sommer, W. J., Weck, M., *Coordin. Chem. Rev.* **2007,** *251* (5), 860-873.
[18] Cetinkaya, B., Cetinkaya, E., Lappert, M. F., *J. Chem. Soc., Dalton Trans* **1973,** (9), 906-912.
[19] Cardin, D. J., Cetinkaya, B., Cetinkaya, E., Lappert, M. F., Randall, E. W., Rosenberg, E., *J. Chem. Soc., Dalton Trans* **1973,** (19), 1982-1985.
[20] Cetinkaya, B., Dixneuf, P., Lappert, M. F., *J. Chem. Soc., Chem. Commun.* **1973,** (6), 206-206.
[21] Arduengo, A. J., Harlow, R. L., Kline, M., *J. Am. Chem. Soc.* **1991,** *113* (1), 361-363.
[22] Arduengo, A. J., Davidson, F., Dias, H. V. R., Goerlich, J. R., Khasnis, D., Marshall, W. J., Prakasha, T. K., *J. Am. Chem. Soc.* **1997,** *119* (52), 12742-12749.
[23] Arduengo, A. J., *Acc. Chem. Res.* **1999,** *32* (11), 913-921.
[24] Arduengo, A. J., Krafczyk, R., Schmutzler, R., Craig, H. A., Goerlich, J. R., Marshall, W. J., Unverzagt, M., *Tetrahedron* **1999,** *55* (51), 14523-14534.
[25] Hopkinson, M. N., Richter, C., Schedler, M., Glorius, F., *Nature* **2014,** *510* (7506), 485-496.
[26] Radius, U., Bickelhaupt, F. M., *Coordin. Chem. Rev.* **2009,** *253* (5), 678-686.
[27] Frison, G., Sevin, A., *J. Chem. Soc., Perkin Trans. 2* **2002,** (10), 1692-1697.
[28] Arduengo, A. J., Dias, H. V. R., Davidson, F., Harlow, R. L., *J. Organomet. Chem.* **1993,** *462* (1), 13-18.
[29] Schumann, H., Gottfriedsen, J., Glanz, M., Dechert, S., Demtschuk, J., *J. Organomet. Chem.* **2001,** *617-618*, 588-600.
[30] Kuhn, N., Henkel, G., Kratz, T., Kreutzberg, J., Boese, R., Maulitz, A. H., *Chem. Ber.* **1993,** *126* (9), 2041-2045.
[31] Arduengo, A. J., Dias, H. V. R., Calabrese, J. C., Davidson, F., *J. Am. Chem. Soc.* **1992,** *114* (24), 9724-9725.
[32] Li, X.-W., Su, J., Robinson, G. H., *Chem. Commun.* **1996,** (23), 2683-2684.
[33] Nakai, H., Tang, Y., Gantzel, P., Meyer, K., *Chem. Commun.* **2003,** (1), 24-25.
[34] Schäfer, A., Weidenbruch, M., Saak, W., Pohl, S., *J. Chem. Soc., Chem. Commun.* **1995,** (11), 1157-1158.
[35] Arduengo, A. J., Tamm, M., McLain, S. J., Calabrese, J. C., Davidson, F., Marshall, W. J., *J. Am. Chem. Soc.* **1994,** *116* (17), 7927-7928.
[36] Zinn, F. K., Viciu, M. S., Nolan, S. P., *Annu. Rep. Prog. Chem., Sect. B: Org. Chem.* **2004,** *100* (0), 231-249.
[37] Jacobsen, H., Correa, A., Poater, A., Costabile, C., Cavallo, L., *Coordin. Chem. Rev.* **2009,** *253* (5), 687-703.
[38] Öfele, K., Herrmann, W. A., Mihalios, D., Elison, M., Herdtweck, E., Priermeier, T., Kiprof, P., *J. Organomet. Chem.* **1995,** *498* (1), 1-14.
[39] Herrmann, W. A., Köcher, C., *Angew. Chem. Int. Ed.* **1997,** *36* (20), 2162-2187.

[40] Herrmann, W. A., *Angew. Chem. Int. Ed.* **2002,** *41* (8), 1290-1309.
[41] Hahn, F. E., Jahnke, M. C., *Angew. Chem. Int. Ed.* **2008,** *47* (17), 3122-3172.
[42] Pugh, D., Danopoulos, A. A., *Coordin. Chem. Rev.* **2007,** *251* (5), 610-641.
[43] Mata, J. A., Poyatos, M., Peris, E., *Coordin. Chem. Rev.* **2007,** *251* (5), 841-859.
[44] Gusev, D. G., *Organometallics* **2009,** *28* (22), 6458-6461.
[45] Henrique Teles, J., Melder, J.-P., Ebel, K., Schneider, R., Gehrer, E., Harder, W., Brode, S., Enders, D., Breuer, K., Raabe, G., *Helv. Chim. Acta* **1996,** *79* (1), 61-83.
[46] Kücükbay, H., Cetinkaya, B., Guesmi, S., Dixneuf, P. H., *Organometallics* **1996,** *15* (10), 2434-2439.
[47] Enders, D., Gielen, H., Raabe, G., Runsink, J., Teles, J. H., *Chem. Ber.* **1996,** *129* (12), 1483-1488.
[48] Herrmann, W. A., Elison, M., Fischer, J., Köcher, C., Artus, G. R. J., *Angew. Chem. Int. Ed.* **1995,** *34* (21), 2371-2374.
[49] Hu, X., Tang, Y., Gantzel, P., Meyer, K., *Organometallics* **2003,** *22* (4), 612-614.
[50] Aggarwal, V. K., Badine, D. M., Moorthie, V. A., Yudin, A. K., Asymmetric Synthesis of Epoxides and Aziridines from Aldehydes and Imines. In *Aziridines and Epoxides in Organic Synthesis*, WILEY-VCH: Weinheim, **2006**; 1-35.
[51] Weissermel, K., Arpe, H. J., *Industrielle Organische Chemie. Bedeutende Vor- und Zwischenprodukte*. 5 ed.; Wiley-VCH: Weinheim, **1998**.
[52] Liu, Y., Deng, K., Wang, S., Xiao, M., Han, D., Meng, Y., *Polym. Chem.* **2015,** *6* (11), 2076-2083.
[53] Moon, S. J., Kang, T. J., *Text. Res. J.* **2000,** *70* (12), 1063-1069.
[54] Jin, K., Maalouf, J. H., Lazouski, N., Corbin, N., Yang, D., Manthiram, K., *J. Am. Chem. Soc.* **2019,** *141* (15), 6413-6418.
[55] Kilty, P. A., Sachtler, W. M. H., *Catal. Rev.* **1974,** *10* (1), 1-16.
[56] Nijhuis, T. A., Makkee, M., Moulijn, J. A., Weckhuysen, B. M., *Ind. Eng. Chem. Res.* **2006,** *45* (10), 3447-3459.
[57] Choi, W. J., Choi, C. Y., *Biotechnol. Bioprocess Eng.* **2005,** *10* (3), 167.
[58] Zviely, M., Aroma Chemicals II: Heterocycles. In *Chemistry and Technology of Flavors and Fragrances*, Rowe, D. J., Ed. WILEY-VCH: Weinheim, **2004**; 85-115.
[59] Bernhard, M., Anton, J., Schmidt, F., Sandkaulen, F., Pascaly, M., *Chem. Unserer Zeit* **2017,** *51* (3), 198-209.
[60] Buijink, J. K. F., Lange, J.-P., Bos, A. N. R., Horton, A. D., Niele, F. G. M., Chapter 13 - Propylene Epoxidation via Shell's SMPO Process: 30 Years of Research and Operation. In *Mechanisms in Homogeneous and Heterogeneous Epoxidation Catalysis*, Oyama, S. T., Ed. Elsevier: Amsterdam, **2008**; 355-371.
[61] Russo, V., Tesser, R., Santacesaria, E., Di Serio, M., *Ind. Eng. Chem. Res.* **2013,** *52* (3), 1168-1178.
[62] Clerici, M. G. In *TS-1 and propylene oxide, 20 years later* Oxidation and functionalization: classical and alternative routes and sources, Milan (Italy), Proceedings of the DGMK/SCI-conference: Milan (Italy), **2005**.
[63] Weissermel, K., Arpe, H.-J., *Industrielle Organische Chemie*. Wiley-VCH: Weinheim, **1998**.
[64] Hauser, S. A., Cokoja, M., Kühn, F. E., *Catal. Sci. Technol.* **2013,** *3* (3), 552-561.
[65] Altmann, P., Cokoja, M., Kühn, F. E., *Eur. J. Inorg. Chem.* **2012,** *2012* (19), 3235-3239.
[66] Kühn, F. E., Santos, A. M., Roesky, P. W., Herdtweck, E., Scherer, W., Gisdakis, P., Yudanov, I. V., Di Valentin, C., Rösch, N., *Chem. Eur. J.* **1999,** *5* (12), 3603-3615.
[67] Romão, C. C., Kühn, F. E., Herrmann, W. A., *Chem. Rev.* **1997,** *97* (8), 3197-3246.
[68] Schmidt, A., Grover, N., Zimmermann, T. K., Graser, L., Cokoja, M., Pöthig, A., Kühn, F. E., *J. Catal.* **2014,** *319*, 119-126.
[69] Dyckhoff, F., Li, S., Reich, R. M., Hofmann, B. J., Herdtweck, E., Kühn, F. E., *Dalton Trans.* **2018,** *47* (29), 9755-9764.
[70] Hofmann, B. J., Huber, S., Reich, R. M., Drees, M., Kühn, F. E., *J. Organomet. Chem.* **2019,** *885*, 32-38.
[71] Beattie, I. R., Jones, P. J., *Inorg. Chem.* **1979,** *18* (8), 2318-2319.
[72] Al-Ajlouni, A. M., Espenson, J. H., *J. Org. Chem.* **1996,** *61* (12), 3969-3976.

[73] Herrmann, W. A., Fischer, R. W., Scherer, W., Rauch, M. U., *Angew. Chem. Int. Ed.* **1993,** *32* (8), 1157-1160.
[74] Adam, W., Mitchell, C. M., *Angew. Chem. Int. Ed.* **1996,** *35* (5), 533-535.
[75] Kück, J. W., Reich, R. M., Kühn, F. E., *Chem. Rec.* **2016,** *16* (1), 349-64.
[76] Kühn, F. E., Scherbaum, A., Herrmann, W. A., *J. Organomet. Chem.* **2004,** *689* (24), 4149-4164.
[77] Deuss, P. J., den Heeten, R., Laan, W., Kamer, P. C. J., *Chem. Eur. J.* **2011,** *17* (17), 4680-4698.
[78] Cavani, F., Teles, J. H., *ChemSusChem* **2009,** *2* (6), 508-534.
[79] Enthaler, S., Junge, K., Beller, M., *Angew. Chem. Int. Ed.* **2008,** *47* (18), 3317-3321.
[80] Chen, M. S., White, M. C., *Science* **2010,** *327* (5965), 566.
[81] Hölzl, S. M., Altmann, P. J., Kück, J. W., Kühn, F. E., *Coord. Chem. Rev.* **2017,** *352*, 517-536.
[82] Que Jr, L., Tolman, W. B., *Nature* **2008,** *455*, 333.
[83] Lindhorst, A. C., Haslinger, S., Kühn, F. E., *Chem. Commun.* **2015,** *51* (97), 17193-17212.
[84] Baik, M.-H., Newcomb, M., Friesner, R. A., Lippard, S. J., *Chem. Rev.* **2003,** *103* (6), 2385-2420.
[85] Tinberg, C. E., Lippard, S. J., *Acc. Chem. Res.* **2011,** *44* (4), 280-288.
[86] Lipscomb, J. D., *Annu. Rev. Microbiol.* **1994,** *48* (1), 371-399.
[87] Banerjee, R., Jones, J. C., Lipscomb, J. D., *Annu. Rev. Biochem.* **2019,** *88* (1), 409-431.
[88] Denisov, I. G., Makris, T. M., Sligar, S. G., Schlichting, I., *Chem. Rev.* **2005,** *105* (6), 2253-2278.
[89] Meunier, B., de Visser, S. P., Shaik, S., *Chem. Rev.* **2004,** *104* (9), 3947-3980.
[90] Guengerich, F. P., *J. Biochem. Mol. Toxicol.* **2007,** *21* (4), 163-168.
[91] Ortiz de Montellano, P. R., *Chem. Rev.* **2010,** *110* (2), 932-948.
[92] Poulos, T. L., *Chem. Rev.* **2014,** *114* (7), 3919-3962.
[93] Austin, R. N., Groves, J. T., *Metallomics* **2011,** *3* (8), 775-787.
[94] Groves, J. T., Kruper, W. J., *J. Am. Chem. Soc.* **1979,** *101* (25), 7613-7615.
[95] Groves, J. T., McClusky, G. A., *J. Am. Chem. Soc.* **1976,** *98* (3), 859-861.
[96] Groves, J. T., Nemo, T. E., Myers, R. S., *J. Am. Chem. Soc.* **1979,** *101* (4), 1032-1033.
[97] Bryliakov, K. P., Talsi, E. P., *Coordin. Chem. Rev.* **2014,** *276*, 73-96.
[98] Jin, S., Makris, T. M., Bryson, T. A., Sligar, S. G., Dawson, J. H., *J. Am. Chem. Soc.* **2003,** *125* (12), 3406-3407.
[99] McQuarters, A. B., Wolf, M. W., Hunt, A. P., Lehnert, N., *Angew. Chem. Int. Ed.* **2014,** *53* (19), 4750-4752.
[100] Rittle, J., Green, M. T., *Science* **2010,** *330* (6006), 933-937.
[101] Yosca, T. H., Rittle, J., Krest, C. M., Onderko, E. L., Silakov, A., Calixto, J. C., Behan, R. K., Green, M. T., *Science* **2013,** *342* (6160), 825-829.
[102] Bhuyan, J., Sarkar, R., Sarkar, S., *Angew. Chem. Int. Ed.* **2011,** *50* (45), 10603-10607.
[103] Asakura, T., [47] Hemoglobin porphyrin modification. In *Methods in Enzymology*, Fleischer, S.; Packer, L., Eds. Academic Press: **1978**; Vol. 52, 447-455.
[104] Yonetani, T., Asakura, T., *J. Biol. Chem.* **1969,** *244* (17), 4580-4588.
[105] Nam, W., *Acc. Chem. Res.* **2007,** *40* (7), 522-531.
[106] Nam, W., Oh, S.-Y., Sun, Y. J., Kim, J., Kim, W.-K., Woo, S. K., Shin, W., *J. Org. Chem.* **2003,** *68* (20), 7903-7906.
[107] Nam, W., Ryu, Y. O., Song, W. J., *J. Biol. Inorg. Chem.* **2004,** *9* (6), 654-660.
[108] Costas, M., *Coordin. Chem. Rev.* **2011,** *255* (23), 2912-2932.
[109] Feng, Y., England, J., Que, L., *ACS Catal.* **2011,** *1* (9), 1035-1042.
[110] Chen, K., Costas, M., Kim, J., Tipton, A. K., Que, L., *J. Am. Chem. Soc.* **2002,** *124* (12), 3026-3035.
[111] McDonald, A. R., Que, L., *Coord. Chem. Rev.* **2013,** *257* (2), 414-428.
[112] Hadian-Dehkordi, L., Hosseini-Monfared, H., *Green Chem.* **2016,** *18* (2), 497-507.
[113] Kück, J. W., Anneser, M. R., Hofmann, B., Pöthig, A., Cokoja, M., Kühn, F. E., *ChemSusChem* **2015,** *8* (23), 4056-4063.
[114] Mas-Ballesté, R., Que, L., *J. Am. Chem. Soc.* **2007,** *129* (51), 15964-15972.
[115] Hill, C. L., *Nature* **1999,** *401* (6752), 436-437.
[116] Noyori, R., Aoki, M., Sato, K., *Chem. Commun.* **2003,** (16), 1977-1986.
[117] Murch, B. P., Bradley, F. C., Que, L., *J. Am. Chem. Soc.* **1986,** *108* (16), 5027-5028.

[118] Wonwoo, N. A. M., Ho, R., Selverstone Valentine, J., *J. Am. Chem. Soc.* **1991,** *113* (18), 7052-7054.
[119] Chen, M. S., White, M. C., *Science* **2007,** *318* (5851), 783-787.
[120] Cussó, O., Garcia-Bosch, I., Ribas, X., Lloret-Fillol, J., Costas, M., *J. Am. Chem. Soc.* **2013,** *135* (39), 14871-14878.
[121] Fingerhut, A., Serdyuk, O. V., Tsogoeva, S. B., *Green Chem.* **2015,** *17* (4), 2042-2058.
[122] Rohde, J.-U., In, J.-H., Lim, M. H., Brennessel, W. W., Bukowski, M. R., Stubna, A., Münck, E., Nam, W., Que, L., *Science* **2003,** *299* (5609), 1037-1039.
[123] Lim, M. H., Rohde, J.-U., Stubna, A., Bukowski, M. R., Costas, M., Ho, R. Y. N., Münck, E., Nam, W., Que, L., *Proc. Natl. Acad. Sci. U.S.A.* **2003,** *100* (7), 3665-3670.
[124] Fujita, M., Costas, M., Que, L., *J. Am. Chem. Soc.* **2003,** *125* (33), 9912-9913.
[125] Kaizer, J., Klinker, E. J., Oh, N. Y., Rohde, J.-U., Song, W. J., Stubna, A., Kim, J., Münck, E., Nam, W., Que, L., *J. Am. Chem. Soc.* **2004,** *126* (2), 472-473.
[126] Rohde, J.-U., Torelli, S., Shan, X., Lim, M. H., Klinker, E. J., Kaizer, J., Chen, K., Nam, W., Que, L., *J. Am. Chem. Soc.* **2004,** *126* (51), 16750-16761.
[127] Mas-Ballesté, R., Costas, M., van den Berg, T., Que Jr., L., *Chem. Eur. J.* **2006,** *12* (28), 7489-7500.
[128] Bukowski, M. R., Comba, P., Lienke, A., Limberg, C., Lopez de Laorden, C., Mas-Ballesté, R., Merz, M., Que Jr., L., *Angew. Chem. Int. Ed.* **2006,** *45* (21), 3446-3449.
[129] Oloo, W. N., Fielding, A. J., Que, L., *J. Am. Chem. Soc.* **2013,** *135* (17), 6438-6441.
[130] Costas, M., Chen, K., Que, L., *Coordin. Chem. Rev.* **2000,** *200-202*, 517-544.
[131] Kal, S., Xu, S., Que Jr., L., *Angew. Chem. Int. Ed.* **2019,** *59* (19), 7332-7349.
[132] Kück, J. W., Raba, A., Markovits, I. I. E., Cokoja, M., Kühn, F. E., *ChemCatChem* **2014,** *6* (7), 1882-1886.
[133] Kal, S., Xu, S., Que Jr., L., *Angew. Chem. Int. Ed.* **2020,** *59* (19), 7332-7349.
[134] Kal, S., Draksharapu, A., Que, L., *J. Am. Chem. Soc.* **2018,** *140* (17), 5798-5804.
[135] Fukuzumi, S., Morimoto, Y., Kotani, H., Naumov, P., Lee, Y.-M., Nam, W., *Nat. Chem.* **2010,** *2* (9), 756-759.
[136] Kal, S., Que Jr., L., *Angew. Chem. Int. Ed.* **2019,** *58* (25), 8484-8488.
[137] Zhang, J., Wei, W.-J., Lu, X., Yang, H., Chen, Z., Liao, R.-Z., Yin, G., *Inorg. Chem.* **2017,** *56* (24), 15138-15149.
[138] Karlin, K. D., *Nat. Chem.* **2010,** *2* (9), 711-712.
[139] Swart, M., *Chem. Commun.* **2013,** *49* (59), 6650-6652.
[140] Pfaff, F. F., Kundu, S., Risch, M., Pandian, S., Heims, F., Pryjomska-Ray, I., Haack, P., Metzinger, R., Bill, E., Dau, H., Comba, P., Ray, K., *Angew. Chem. Int. Ed.* **2011,** *50* (7), 1711-1715.
[141] Ingleson, M. J., Layfield, R. A., *Chem. Commun.* **2012,** *48* (30), 3579-3589.
[142] Riener, K., Haslinger, S., Raba, A., Högerl, M. P., Cokoja, M., Herrmann, W. A., Kühn, F. E., *Chem. Rev.* **2014,** *114* (10), 5215-5272.
[143] Connelly, N. G., Geiger, W. E., *Chem. Rev.* **1996,** *96* (2), 877-910.
[144] Cramer, S. A., Jenkins, D. M., *J. Am. Chem. Soc.* **2011,** *133* (48), 19342-19345.
[145] Meyer, S., Klawitter, I., Demeshko, S., Bill, E., Meyer, F., *Angew. Chem. Int. Ed.* **2013,** *52* (3), 901-905.
[146] Raba, A., Cokoja, M., Ewald, S., Riener, K., Herdtweck, E., Pöthig, A., Herrmann, W. A., Kühn, F. E., *Organometallics* **2012,** *31* (7), 2793-2800.
[147] Anneser, M. R., Haslinger, S., Pöthig, A., Cokoja, M., Basset, J.-M., Kühn, F. E., *Inorg. Chem.* **2015,** *54* (8), 3797-3804.
[148] Weiss, D. T., Anneser, M. R., Haslinger, S., Pöthig, A., Cokoja, M., Basset, J.-M., Kühn, F. E., *Organometallics* **2015,** *34* (20), 5155-5166.
[149] Anneser, M. R., Haslinger, S., Pöthig, A., Cokoja, M., D'Elia, V., Högerl, M. P., Basset, J.-M., Kühn, F. E., *Dalton Trans.* **2016,** *45* (15), 6449-6455.
[150] Xu, J., Murphy, S. L., Kochanek, K. D., Arias, E., Mortality in the United States, 2018. National Center for Health Statistics: Hyattsville, MD, **2020**.

[151] Siegel, R. L., Miller, K. D., Jemal, A., *CA Cancer J. Clin.* **2019,** *69* (1), 7-34.
[152] Weinberg, R. A., *The biology of cancer*. 2nd ed.; Garland Science: New York, **2014**.
[153] Avendaño, C., Menendez, J. C., *Medicinal chemistry of anticancer drugs*. 2nd ed.; Elsevier: Amsterdam, **2015**.
[154] Deman, J., Van Larebeke, N., *Tumor Biol.* **2001,** *22* (3), 191-202.
[155] Doenecke, D., Koolman, J., Fuchs, G., Gerok, W., Karlsons Biochemie und Pathobiochemie. 15th ed.; Georg Thieme Verlag: Stuttgart, New York, **2005**.
[156] Hanahan, D., Weinberg, R. A., *Cell* **2000,** *100* (1), 57-70.
[157] Hanahan, D., Weinberg, Robert A., *Cell* **2011,** *144* (5), 646-674.
[158] Zhang, X., Marjani, S. L., Hu, Z., Weissman, S. M., Pan, X., Wu, S., *Cancer Res.* **2016,** *76* (6), 1305-1312.
[159] Chabner, B. A., Roberts, T. G., *Nat. Rev. Cancer* **2005,** *5* (1), 65-72.
[160] Gilman, A., *Am. J. Surg.* **1963,** *105* (5), 574-578.
[161] Christakis, P., *Yale J. Biol. Med.* **2011,** *84* (2), 169-172.
[162] Qin, Z., Li, X., Zhang, J., Tang, J., Han, P., Xu, Z., Yu, Y., Yang, C., Wang, C., Xu, T., Xu, Z., Zou, Q., *Medicine* **2016,** *95* (39), e4801.
[163] Shang, M., Ren, M., Zhou, C., *Chem. Res. Toxicol.* **2019,** *32* (12), 2517-2525.
[164] Haddow, A., Kon, G., Ross, W., *Nature* **1948,** *162* (4125), 824-825.
[165] Goldacre, R., Loveless, A., Ross, W., *Nature* **1949,** *163* (4148), 667-669.
[166] Panasci, L., Xu, Z.-Y., Bello, V., Aloyz, R., *Anti-Cancer Drugs* **2002,** *13* (3).
[167] Wiltshaw, E., *Platin. Met. Rev.* **1979,** *23* (3), 90-98.
[168] Rosenberg, B., Van Camp, L., Krigas, T., *Nature* **1965,** *205* (4972), 698-699.
[169] Rosenberg, B., Vancamp, L., Trosko, J. E., Mansour, V. H., *Nature* **1969,** *222* (5191), 385-386.
[170] Todd, R. C., Lippard, S. J., *Metallomics* **2009,** *1* (4), 280-291.
[171] Gleason, J. L., White, J. H., Chapter 89 - Bifunctional Vitamin D Hybrid Molecules. In *Vitamin D*, 4th ed.; Feldman, D., Ed. Academic Press: London, **2018**; Vol. 2, 647-655.
[172] Seroka, B., Łotowski, Z., Hryniewicka, A., Rárová, L., Sicinski, R., Tomkiel, A., Morzycki, J., *Molecules* **2020,** *25* (3), 655.
[173] Galluzzi, L., Senovilla, L., Vitale, I., Michels, J., Martins, I., Kepp, O., Castedo, M., Kroemer, G., *Oncogene* **2012,** *31* (15), 1869-1883.
[174] Holleman, A. F., Wiberg, E., Wiberg, N., *Lehrbuch der anorganischen Chemie*. 102. ed.; de Gruyter: Berlin, **2007**.
[175] Johnstone, T. C., Suntharalingam, K., Lippard, S. J., *Chem. Rev.* **2016,** *116* (5), 3436-3486.
[176] Browning, R. J., Reardon, P. J. T., Parhizkar, M., Pedley, R. B., Edirisinghe, M., Knowles, J. C., Stride, E., *ACS Nano* **2017,** *11* (9), 8560-8578.
[177] Marullo, R., Werner, E., Degtyareva, N., Moore, B., Altavilla, G., Ramalingam, S. S., Doetsch, P. W., *PLOS ONE* **2013,** *8* (11), e81162.
[178] Oun, R., Moussa, Y. E., Wheate, N. J., *Dalton Trans.* **2018,** *47* (19), 6645-6653.
[179] Dasari, S., Bernard Tchounwou, P., *Eur. J. Pharmacol.* **2014,** *740*, 364-378.
[180] Siddik, Z. H., *Oncogene* **2003,** *22* (47), 7265-7279.
[181] Sutton, B. M., *Gold Bull.* **1986,** *19* (1), 15-16.
[182] Berners-Price, S. J., Filipovska, A., *Metallomics* **2011,** *3* (9), 863-873.
[183] Kean, W. F., Forestier, F., Kassam, Y., Buchanan, W. W., Rooney, P. J., *Semin. Arthritis Rheum.* **1985,** *14* (3), 180-186.
[184] Sutton, B. M., McGusty, E., Walz, D. T., DiMartino, M. J., *J. Med. Chem.* **1972,** *15* (11), 1095-1098.
[185] Simon, T. M., Kunishima, D. H., Vibert, G. J., Lorber, A., *Cancer* **1979,** *44* (6), 1965-1975.
[186] Mirabelli, C. K., Johnson, R. K., Sung, C. M., Faucette, L., Muirhead, K., Crooke, S. T., *Cancer Res.* **1985,** *45* (1), 32-39.
[187] Marzano, C., Gandin, V., Folda, A., Scutari, G., Bindoli, A., Rigobello, M. P., *Free Radic. Biol. Med.* **2007,** *42* (6), 872-881.

[188] Debnath, A., Parsonage, D., Andrade, R. M., He, C., Cobo, E. R., Hirata, K., Chen, S., García-Rivera, G., Orozco, E., Martínez, M. B., Gunatilleke, S. S., Barrios, A. M., Arkin, M. R., Poole, L. B., McKerrow, J. H., Reed, S. L., *Nat. Med.* **2012,** *18* (6), 956-960.
[189] Lewis, M. G., DaFonseca, S., Chomont, N., Palamara, A. T., Tardugno, M., Mai, A., Collins, M., Wagner, W. L., Yalley-Ogunro, J., Greenhouse, J., Chirullo, B., Norelli, S., Garaci, E., Savarino, A., *AIDS* **2011,** *25* (11), 1347-1356.
[190] Harbut, M. B., Vilchèze, C., Luo, X., Hensler, M. E., Guo, H., Yang, B., Chatterjee, A. K., Nizet, V., Jacobs, W. R., Schultz, P. G., Wang, F., *Proc. Natl. Acad. Sci. U.S.A.* **2015,** *112* (14), 4453-4458.
[191] Rothan, H. A., Stone, S., Natekar, J., Kumari, P., Arora, K., Kumar, M., *Virology* **2020,** *547*, 7-11.
[192] Sztandera, K., Gorzkiewicz, M., Klajnert-Maculewicz, B., *Mol. Pharm.* **2019,** *16* (1), 1-23.
[193] Sun, R. W.-Y., Che, C.-M., *Coordin. Chem. Rev.* **2009,** *253* (11), 1682-1691.
[194] Tiekink, E. R. T., *Crit. Rev. Oncol. Hematol.* **2002,** *42* (3), 225-248.
[195] Tiekink, E. R. T., *Inflammopharmacology* **2008,** *16* (3), 138-142.
[196] McKeage, M. J., Maharaj, L., Berners-Price, S. J., *Coordin. Chem. Rev.* **2002,** *232* (1), 127-135.
[197] Bindoli, A., Rigobello, M. P., Scutari, G., Gabbiani, C., Casini, A., Messori, L., *Coordin. Chem. Rev.* **2009,** *253* (11), 1692-1707.
[198] Fernández, L., Silva, V., Domínguez-González, T., Claudio-Betancourt, S., Toro-Maldonado, R., Maso, L., Sanabria, K., Pérez-Verdejo, J., González, J., Rosado-Fraticelli, G., Meléndez, F., Santiago, F., Rivera-Rivera, D., Navarro, C., Chardón, A., Vera, A., Tinoco, A., *Inorganics* **2020,** *8*, 10.
[199] Hickey, J. L., Ruhayel, R. A., Barnard, P. J., Baker, M. V., Berners-Price, S. J., Filipovska, A., *J. Am. Chem. Soc.* **2008,** *130* (38), 12570-12571.
[200] Gromer, S., Arscott, L. D., Williams, C. H., Schirmer, R. H., Becker, K., *J. Biol. Chem.* **1998,** *273* (32), 20096-20101.
[201] John, K., Alla, V., Meier, C., Pützer, B. M., *Cell Death Differ.* **2011,** *18* (5), 874-886.
[202] Yu, B., Ma, L., Jin, J., Jiang, F., Zhou, G., Yan, K., Liu, Y., *Toxicol. Res.* **2018,** *7* (6), 1081-1090.
[203] Tan, C.-P., Lu, Y.-Y., Ji, L.-N., Mao, Z.-W., *Metallomics* **2014,** *6* (5), 978-995.
[204] Nagakannan, P., Eftekharpour, E., *Free Radic. Biol. Med.* **2017,** *108*, 819-831.
[205] Fujino, G., Noguchi, T., Matsuzawa, A., Yamauchi, S., Saitoh, M., Takeda, K., Ichijo, H., *Mol. Cell. Biol.* **2007,** *27* (23), 8152-8163.
[206] Saitoh, M., Nishitoh, H., Fujii, M., Takeda, K., Tobiume, K., Sawada, Y., Kawabata, M., Miyazono, K., Ichijo, H., *EMBO J.* **1998,** *17* (9), 2596-2606.
[207] Cheng, X., Holenya, P., Can, S., Alborzinia, H., Rubbiani, R., Ott, I., Wölfl, S., *Mol. Cancer* **2014,** *13* (1), 221.
[208] Fiskus, W., Saba, N., Shen, M., Ghias, M., Liu, J., Gupta, S. D., Chauhan, L., Rao, R., Gunewardena, S., Schorno, K., Austin, C. P., Maddocks, K., Byrd, J., Melnick, A., Huang, P., Wiestner, A., Bhalla, K. N., *Cancer Res.* **2014,** *74* (9), 2520-2532.
[209] Zou, P., Chen, M., Ji, J., Chen, W., Chen, X., Ying, S., Zhang, J., Zhang, Z., Liu, Z., Yang, S., Liang, G., *Oncotarget* **2015,** *6* (34), 36505-36521.
[210] Oehninger, L., Rubbiani, R., Ott, I., *Dalton Trans.* **2013,** *42* (10), 3269-3284.
[211] Mora, M., Gimeno, M. C., Visbal, R., *Chem. Soc. Rev.* **2019,** *48* (2), 447-462.
[212] Modica-Napolitano, J. S., Aprille, J. R., *Adv. Drug Deliv. Rev.* **2001,** *49* (1), 63-70.
[213] Chen, L. B., *Annu. Rev. Cell Biol.* **1988,** *4* (1), 155-181.
[214] Pipier, A., De Rache, A., Modeste, C., Amrane, S., Mothes-Martin, E., Stigliani, J.-L., Calsou, P., Mergny, J.-L., Pratviel, G., Gomez, D., *Dalton Trans.* **2019,** *48* (18), 6091-6099.
[215] Georgiades, S. N., Abd Karim, N. H., Suntharalingam, K., Vilar, R., *Angew. Chem. Int. Ed.* **2010,** *49* (24), 4020-4034.
[216] Guarra, F., Marzo, T., Ferraroni, M., Papi, F., Bazzicalupi, C., Gratteri, P., Pescitelli, G., Messori, L., Biver, T., Gabbiani, C., *Dalton Trans.* **2018,** *47* (45), 16132-16138.
[217] Bazzicalupi, C., Ferraroni, M., Papi, F., Massai, L., Bertrand, B., Messori, L., Gratteri, P., Casini, A., *Angew. Chem. Int. Ed.* **2016,** *55* (13), 4256-4259.
[218] Wragg, D., de Almeida, A., Bonsignore, R., Kühn, F. E., Leoni, S., Casini, A., *Angew. Chem. Int. Ed.* **2018,** *57* (44), 14524-14528.

[219] Kim, N. W., Piatyszek, M. A., Prowse, K. R., Harley, C. B., West, M. D., Ho, P. L., Coviello, G. M., Wright, W. E., Weinrich, S. L., Shay, J. W., *Science* **1994,** *266* (5193), 2011.
[220] Ma, D.-L., Che, C.-M., Yan, S.-C., *J. Am. Chem. Soc.* **2009,** *131* (5), 1835-1846.
[221] Lipps, H. J., Rhodes, D., *Trends Cell Biol.* **2009,** *19* (8), 414-422.
[222] De Cian, A., Lacroix, L., Douarre, C., Temime-Smaali, N., Trentesaux, C., Riou, J.-F., Mergny, J.-L., *Biochimie* **2008,** *90* (1), 131-155.
[223] Wu, G., Chen, L., Liu, W., Yang, D., *Molecules* **2019,** *24* (8).
[224] Chaires, J. B., *FEBS J.* **2010,** *277* (5), 1098-1106.
[225] Wheelhouse, R. T., Sun, D., Han, H., Han, F. X., Hurley, L. H., *J. Am. Chem. Soc.* **1998,** *120* (13), 3261-3262.
[226] Romera, C., Bombarde, O., Bonnet, R., Gomez, D., Dumy, P., Calsou, P., Gwan, J.-F., Lin, J.-H., Defrancq, E., Pratviel, G., *Biochimie* **2011,** *93* (8), 1310-1317.
[227] Boschi, E., Davis, S., Taylor, S., Butterworth, A., Chirayath, L. A., Purohit, V., Siegel, L. K., Buenaventura, J., Sheriff, A. H., Jin, R., Sheardy, R., Yatsunyk, L. A., Azam, M., *J. Phys. Chem. B* **2016,** *120* (50), 12807-12819.
[228] Che, C. M., Siu, F. M., *Curr. Opin. Chem. Biol.* **2010,** *14* (2), 255-61.
[229] Pratviel, G., *Coordin. Chem. Rev.* **2016,** *308*, 460-477.
[230] Tsolekile, N., Nelana, S., Oluwafemi, O. S., *Molecules* **2019,** *24* (14), 2669.
[231] Wei, C., Jia, G., Zhou, J., Han, G., Li, C., *Phys. Chem. Chem. Phys.* **2009,** *11* (20), 4025-32.
[232] Bruijnincx, P. C. A., Sadler, P. J., *Curr. Opin. Chem. Biol.* **2008,** *12* (2), 197-206.
[233] Altmann, P. J., Weiss, D. T., Jandl, C., Kühn, F. E., *Chem. Asian J.* **2016,** *11* (10), 1597-1605.
[234] Wu, Y., Wu, S.-X., Li, H.-B., Geng, Y., Su, Z.-M., *Dalton Trans.* **2011,** *40* (17), 4480-4488.
[235] Bernd, M. A., Dyckhoff, F., Hofmann, B. J., Böth, A. D., Schlagintweit, J. F., Oberkofler, J., Reich, R. M., Kühn, F. E., *J. Catal.* **2020,** *391*, 548-561.
[236] Liu, W., Bensdorf, K., Hagenbach, A., Abram, U., Niu, B., Mariappan, A., Gust, R., *Eur. J. Med. Chem.* **2011,** *46* (12), 5927-5934.
[237] Bass, H. M., Cramer, S. A., Price, J. L., Jenkins, D. M., *Organometallics* **2010,** *29* (15), 3235-3238.
[238] Dyckhoff, F., Schlagintweit, J. F., Reich, R. M., Kühn, F. E., *Catal. Sci. Technol.* **2020,** *10* (11), 3532-3536.
[239] Bauer, E. B., Bernd, M. A., Schütz, M., Oberkofler, J., Pöthig, A., Reich, R. M., Kühn, F. E., *Dalton Trans.* **2019,** *48* (44), 16615-16625.
[240] Bernd, M. A., Bauer, E. B., Oberkofler, J., Bauer, A., Reich, R. M., Kühn, F. E., *Dalton Trans.* **2020,** *49* (40), 14106-14114.
[241] Ghavami, Z. S., Anneser, M. R., Kaiser, F., Altmann, P. J., Hofmann, B. J., Schlagintweit, J. F., Grivani, G., Kühn, F. E., *Chem. Sci.* **2018,** *9* (43), 8307-8314.
[242] Bertrand, B., Williams, M. R. M., Bochmann, M., *Chem. Eur. J.* **2018,** *24* (46), 11840-11851.
[243] Olmstead, M. M., Power, P. P., Shoner, S. C., *Inorg. Chem.* **1991,** *30* (11), 2547-2551.
[244] Shine, H. J., Zhao, B.-J., Marx, J. N., Ould-Ely, T., Whitmire, K. H., *J. Org. Chem.* **2004,** *69* (26), 9255-9261.
[245] *APEX suite of crystallographic software*, 2015-5.2; Bruker AXS Inc.: Madison, Wisconsin, USA, 2014/2015.
[246] *SAINT*, 8.32B, 8.34A, 8.38A; Bruker AXS Inc.: Madison, Wisconsin, USA, 2012/2014/2017.
[247] *SADABS*, 2012/1, 2014/5, 2016/2 Bruker AXS Inc.: Madison, Wisconsin, USA, 2012/2014/2016.
[248] Sheldrick, G., *Acta Crystallogr. A* **2015,** *71* (1), 3-8.
[249] Sheldrick, G., *Acta Crystallogr. C* **2015,** *71* (1), 3-8.
[250] Hubschle, C. B., Sheldrick, G. M., Dittrich, B., *J. Appl. Crystallogr.* **2011,** *44* (6), 1281-1284.
[251] International Tables for Crystallography. Vol. C (Ed.: A. J. Wilson) ed.; Tables 6.1.1.4 (pp. 500-502), p., 4.2.4.2 (pp. 193–199). Ed. Kluwer Academic Publishers,: Dordrecht, The Netherlands, **1992**.
[252] Spek, A., *Acta Crystallogr. D* **2009,** *65* (2), 148-155.
[253] Sniekers, J., Verguts, K., Brooks, N. R., Schaltin, S., Phan, T. H., Trung Huynh, T. M., Van Meervelt, L., De Feyter, S., Seo, J. W., Fransaer, J., Binnemans, K., *Chem. Eur. J.* **2016,** *22* (3), 1010-1020.

9 Eidesstattliche Erklärung

Ich erkläre an Eides statt, dass ich die bei der promotionsführenden Einrichtung Fakultät Chemie der TUM zur Promotionsprüfung vorgelegte Arbeit mit dem Titel:

“Macrocyclic Tetra-dentate NHC Complexes for Catalysis and Medicinal Chemistry”

an der Fakultät für Chemie, Professur für Molekulare Katalyse unter der Anleitung und Betreuung durch Prof. Dr. Fritz E. Kühn ohne sonstige Hilfe erstellt und bei der Abfassung nur die gemäß § 6 Abs. 6 und 7 Satz 2 angegebenen Hilfsmittel benutzt habe.

Ich habe keine Organisation eingeschaltet, die gegen Entgelt Betreuerinnen und Betreuer für die Anfertigung von Dissertationen sucht, oder die mir obliegenden Pflichten hinsichtlich der Prüfungsleistungen für mich ganz oder teilweise erledigt.

Ich habe die Dissertation in dieser oder ähnlicher Form in keinem anderen Prüfungsverfahren als Prüfungsleistung vorgelegt.

Ich habe den angestrebten Doktorgrad noch nicht erworben und bin nicht in einem früheren Promotionsverfahren für den angestrebten Doktorgrad endgültig gescheitert.

Die öffentlich zugängliche Promotionsordnung der TUM ist mir bekannt, insbesondere habe ich die Bedeutung von § 28 (Nichtigkeit der Promotion) und § 29 (Entzug des Doktorgrades) zur Kenntnis genommen. Ich bin mir der Konsequenzen einer falschen Eidesstattlichen Erklärung bewusst.

Mit der Aufnahme meiner personenbezogenen Daten in die Alumni-Datei bei der TUM bin ich einverstanden.

_____

Garching, 10.03.2021

10 Complete List of Publications

10.1 Journal Articles

Tuning the electronic properties of tetradentate iron-NHC complexes: Towards stable and selective epoxidation catalysts

M. A. Bernd,‡ F. Dyckhoff,‡ B. J. Hofmann, A. D. Böth, J. F. Schlagintweit, J. Oberkofler, R. M. Reich and F. E. Kühn*

Journal of Catalysis **2020**, *391*, 548–561

Synthesis, characterization, and biological studies of multidentate gold(I) and gold(III) NHC complexes

E. B. Bauer,‡ M. A. Bernd,‡ M. Schütz, J. Oberkofler, A. Pöthig, R. M. Reich and F. E. Kühn*

Dalton Transactions **2019**, *48*, 16615-16625

Macrocyclic NHC complexes of group 10 elements with enlarged aromaticity for biological studies

M. A. Bernd,‡ E. B. Bauer,‡ J. Oberkofler, A. Bauer, R. M. Reich and F. E. Kühn*

Dalton Transactions **2020**, *49*, 14106-14114

10.2 Conference Contribution

Backbone Modified Macrocyclic Tetra-NHC Iron Complexes Applied in Epoxidation Catalysis

M. A. Bernd, F. Dyckhoff, F. E. Kühn

Poster, IV International Conference on Catalysis and Chemical Engineering (CCE-2020)

Los Angeles, USA, February 2020

Backbone Modified Macrocyclic Tetra-NHC Iron Complexes Applied in Epoxidation Catalysis

Marco A. Bernd, Florian Dyckhoff and Fritz E. Kühn

Chair of Inorganic Chemistry & Molecular Catalysis, Catalysis Research Center, Technical University of Munich, Ernst-Otto-Fischer-Straße 1, 85748 Garching, Germany

E-Mail: marco.bernd@tum.de

1. Introduction

In recent years a lot of effort has been directed to develop effective methods for the selective oxidation of olefins. Most efficient homogeneous catalysts for this reaction are based on transition metals, which are either scarce and/or toxic.[1] Therefore, efforts have been made to development catalysts based on cheaper, abundant and non-toxic metals. For a long time iron, being cheap, abundant and non-toxic, has been in the focus of catalyst development. Utilizing iron and mimicking the active site of proteins like cytochrome P450 has led to the development of various bio inspired iron catalysts and their investigation in oxidation catalysis.[1-2]

Recently, we have shown that the NHC-based (*N*-heterocyclic carbene) heme inspired complexes **3a** and **3b** show a remarkably high activity in epoxidation catalysis, using H_2O_2 as oxygen source.[3-6]

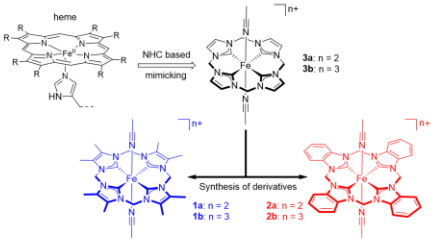

2. Aim

To gain a further understanding of the catalytic performance, two derivatives of the tetra-NHC ligand, one with electron donating and one with electron accepting properties, have been used to synthesize the iron(II) (**1a** & **2a**) and iron(III) (**1b** & **2b**) complexes, respectively. These new components were characterized by various methods. Cyclic voltammetry is used to evaluate the electronic properties of the ligand systems. The different electronic properties influence the catalytic performance to either higher activity or higher stability of the catalyst.

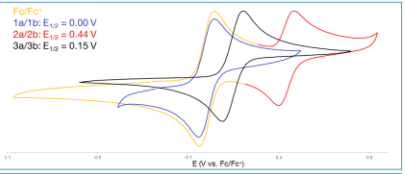

3. Synthesis of Iron complexes

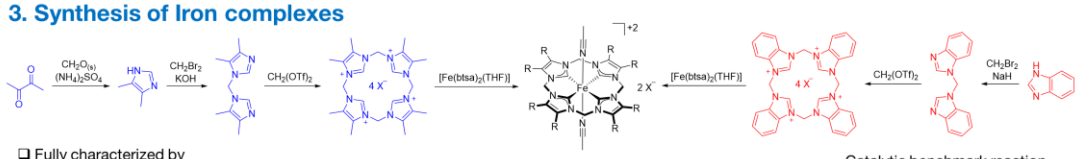

- Fully characterized by ^{1}H-, ^{13}C-NMR, ESI-MS, elemental analysis
- SC-XRD of **1b**, **2a**, **2b**
  SC-XRD of **1a** could not be performed due to inherent twinning

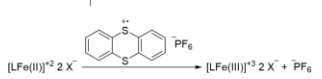

Catalytic benchmark reaction

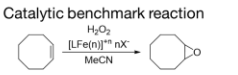

4. Catalytic evaluation

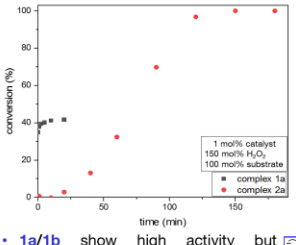

- **1a**/**1b** show high activity but degradades before full conversion.
- **2a**/**2b** reaches full conversion after an induction period at lower activity, broader substrate and temperature tolerance.

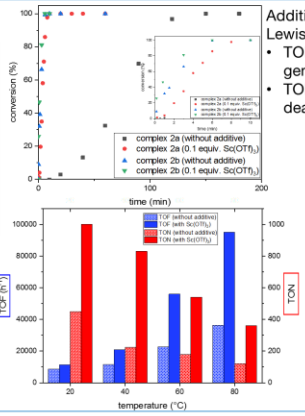

Addition of $Sc(OTf)_3$, being a Lewis acid, results in higher:

- TOF due to acceleration of generating the active species
- TON due to reactivating a deactivated dead end species

2a/**2b** offer higher conversion rates for substrates with functional groups

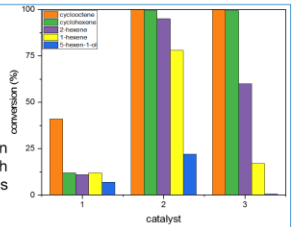

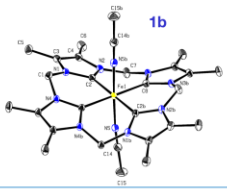

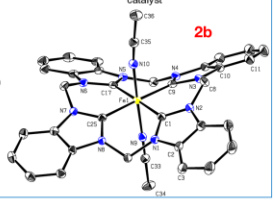

5. Summary and Outlook

- Two new macrocyclic tetra-NHC-Fe(II) complexes and their respective Fe(III) derivates have been synthesized and fully characterized.
- Successful application in epoxidation catalysis.
- Synthesis of deuterated derivatives of **3a** and **3b** are ongoing.
  - Investigation of degradation pathway

6. References

[1] S.A. Hauser, M. Cokoja, F.E. Kühn; *Catal. Sci. Technol.*, 3, **2013**, 552-561.
[2] S.M. Hölzl, P.J. Altmann, J.W. Kück, F.E. Kühn; *Coord. Chem. Rev.*, 352, **2017**, 517-536.
[3] M.R. Anneser, S. Haslinger, A. Pöthig, M. Cokoja, J.-M. Basset, F.E. Kühn; *Inorg. Chem.*, 54, **2015**, 3797-3804.
[4] J.W. Kück, M.R. Anneser, B. Hofmann, A. Pöthig, M. Cokoja, F.E. Kühn; *ChemSusChem*, 8, **2015**, 4056-4063.
[5] J.F. Schlagintweit, F. Dyckhoff, L. Nguyen, C.H.G. Jakob, R.M. Reich, F.E. Kühn; *J. Catal.*, 383, **2020**, 144-152.
[6] A.R. McDonald, L. Que; *Coord. Chem. Rev.*, 257, **2013**, 414-428.

Acknowledgements

TUM Graduate School

11 APPENDIX

11.1 Crystallographic data

Table 1: Crystallographic data and refinement parameters.

Compound	**VIII**	**XII**	**XIII**
formula	$C_{70}H_{54}F_6FeN_{10}O_6S_2$	$C_{26}H_{32}F_6NiN_8O_6S_2$	$C_{26}H_{32}F_6PdN_8O_6S_2$
CCDC number	---	---	---
fw	1365.22	789.4	837.12
color/habit	yellow block	clear yellow needle	clear colourless fragment
Cryst. Dimens. [mm^3]	0.152 x 0.190 x 0.350	0.038 x 0.098 x 0.235	0.063 x 0.078 x 0.103
Cryst. Syst.	triclinic	tetragonal	triclinic
space group	P -1	P 42/n	P -1
a [Å]	10.1114(16)	21.126(12)	6.6625(11)
b [Å]	17.227(3)	21126	10.7400(19)
c [Å]	21.140(3)	8.149(6)	11.169(2)
α [deg]	82.629(5)	90	75.199(5)
β [deg]	84.356(5)	90	88.343(5)
γ [deg]	87.600(5)	90	89.969(5)
V [$Å^3$]	3632.6(9)	3637.0(5)	772.3(2)
Z	2	4	1
T [K]	100(2)	293(2)	100(2)
D_{calcd} [g/cm^{-3}]	1.187	1.592	1.800
μ [mm^{-1}]	0.297	0.737	0.829
F(000)	1350	1800	424
ϑ range [deg]	2.16 to 25.35	2.68 to 25.64	2.35 to 25.68
index range (h, k, l)	-12 ≤ h ≤ +12 -20 ≤ k ≤ +20 -24 ≤ l ≤ +25	-25 ≤ h ≤ +25 -25 ≤ k ≤ +25 -9 ≤ l ≤ +9	-7 ≤ h ≤ +8 -13 ≤ k ≤ +13 -13 ≤ l ≤ +13
Reflections collected	148581	136797	30265
no. of indep refIns/R_{int}	13309/0.0337	3438/0.0491	2918/0.0497
no. of data/ restraints/params	13309/42/843	3438/0/254	2918/114/264
R1/wR2 ($I>2\sigma(I)$)	0.0533/0.1318	0.0400/0.1059	0.0279/0.0687
R1/wR2 (*all data*)	0.0564/0.1342	0.0426/0.1082	0.0280/0.0688
GOF (on F^2)	1.062	1.089	1.037
Largest diff peak and hole [e $Å^{-3}$]	2.081/-0.865	1.983/-0.534	1.192/-0.508

Table 2: Crystallographic data and refinement parameters.

Compound	**XIV**	**XV**	**XVII**
formula	$C_{26}H_{32}F_6PtN_8O_6S_2$	$C_{48}H_{64}F_{24}Ag_4N_{16}P_4$	$C_{24}H_{32}F_{18}CuN_8P_3$
CCDC number	---	---	---
fw	925.79	1876.48	931.01
color/habit	clear colourless block	clear colourless fragment	clear yellow fragment
Cryst. Dimens. [mm^3]	0.218 x 0.332 x 0.429	0.180 x 0.247 x 0.776	0.097 x 0.134 x 0.195
Cryst. Syst.	triclinic	orthorhombic	tetragonal
space group	P -1	A m a 2	I 4/m
a [Å]	6.6115(5)	27.754(9)	27.332(17)
b [Å]	10.6491(6)	14.332(4)	27.332(17)
c [Å]	11.2958(8)	24.060(8)	12.910(8)
α [deg]	105.321(29	90	90
β [deg]	91.799(2)	90	90
γ [deg]	90.759(2)	90	90
V [$Å^3$]	766.46(9)	9570.0(5)	9644.0(14)
Z	1	8	12
T [K]	100(2)	100(2)	103(2)
D_{calcd} [g/cm^{-3}]	2.006	1.426	1.239
μ [mm^{-1}]	4807	1042	0.62
F(000)	456	4168	3644
ϑ range [deg]	2.34 to 25.34	1.81 to 25.35	2.29 to 26.36
index range (h, k, l)	-7 ≤ h ≤ +7 -12 ≤ k ≤ +12 -13 ≤ l ≤ +13	-33 ≤ h ≤ +33 -17 ≤ k ≤ +17 -28 ≤ l ≤ +28	-34 ≤ h ≤ +34 -34 ≤ k ≤ +34 -16 ≤ l ≤ +16
Reflections collected	28983	100028	201665
no. of indep refIns/R_{int}	2779/0.0256	8794/0.0226	5149/0.0374
no. of data/ restraints/params	2779/259/300	8794/103/541	5149/69/313
R1/wR2 (I>2σ(I))	0.0126/0.0323	0.0333/0.0907	0.0487/0.1480
R1/wR2 (*all data*)	0.0126/0.0323	0.0340/0.0914	0.0532/0.1527
GOF (on F^2)	1.047	1.043	1.063
Largest diff peak and hole [e $Å^{-3}$]	0.599/-0.866	1.914/-1.121	0.816/-1.992

11.2 NMR spectra

11.2.1 1,1'-Methylenebis(4,5-diphenylimidazole) ($^{Ph}Im_2Me$)

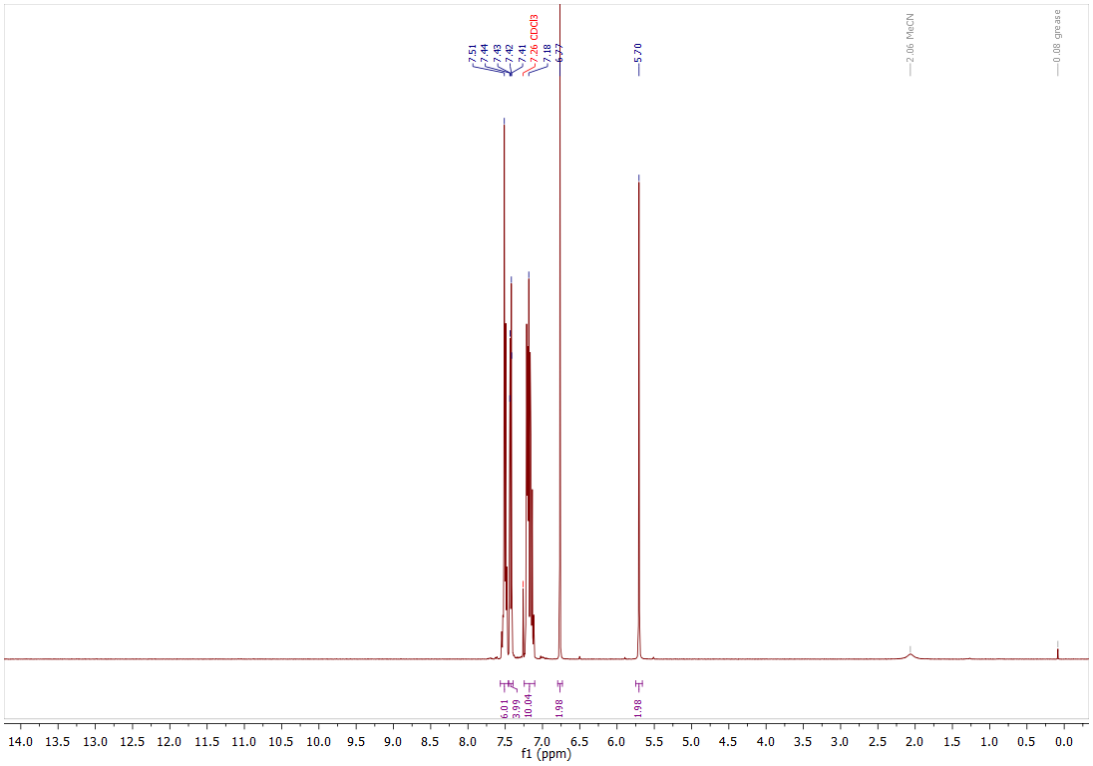

Figure 32: ^{1}H NMR spectrum of $^{Ph}Im_2Me$ in $CDCl_3$.

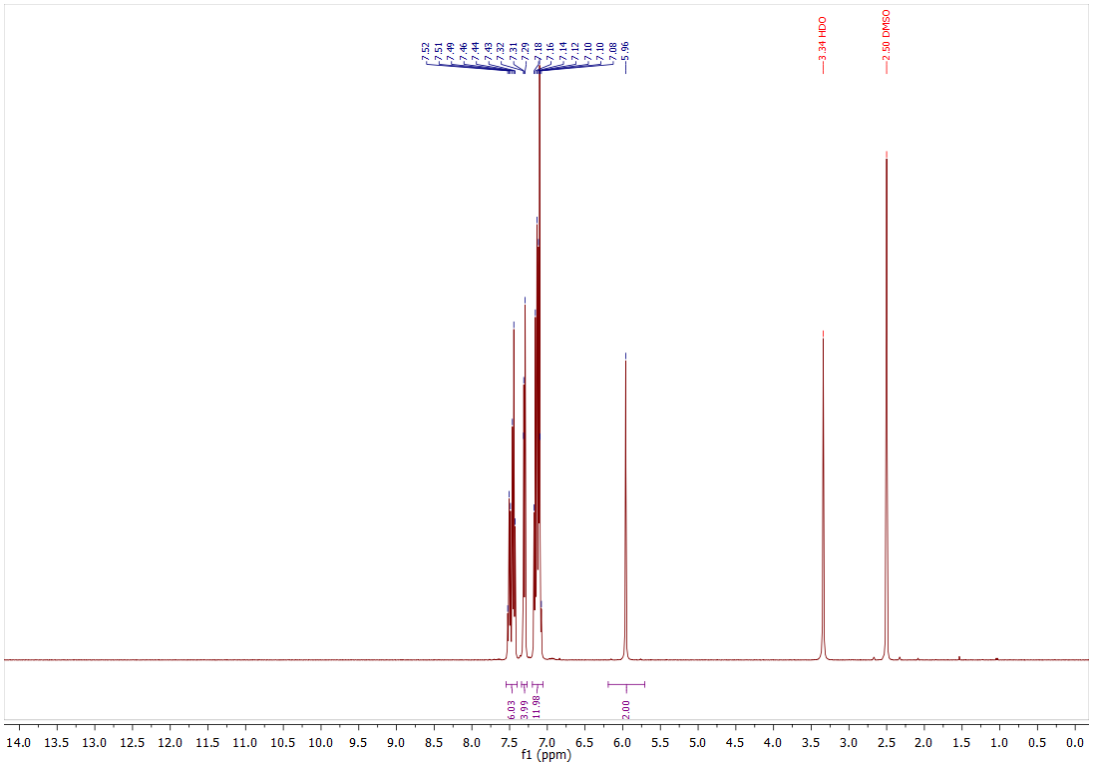

Figure 33: ^{1}H NMR spectrum of $^{Ph}Im_2Me$ in DMSO-d_6.

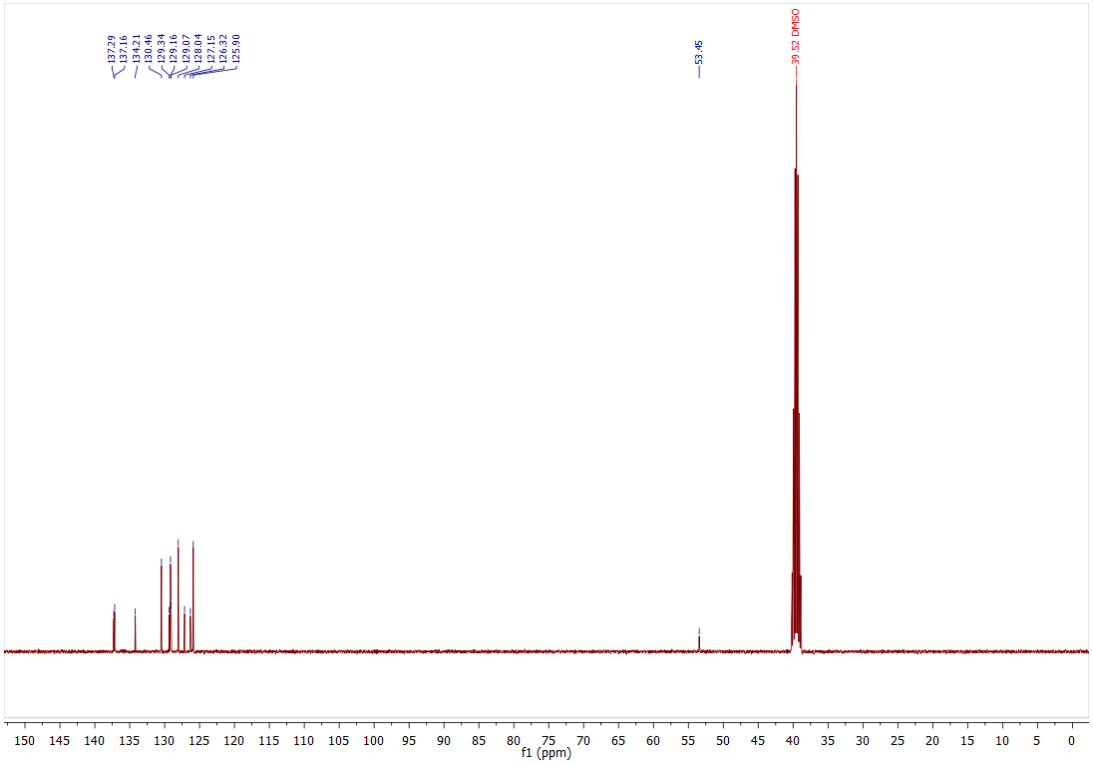

Figure 34: ^{13}C NMR spectrum of ^{Ph}**Im$_2$Me** in DMSO-d_6.

11.2.2 *trans*-Diacetonitrile[calix[4](4,5-diphenylimidazoyl)]iron(II) triflate (VIII)

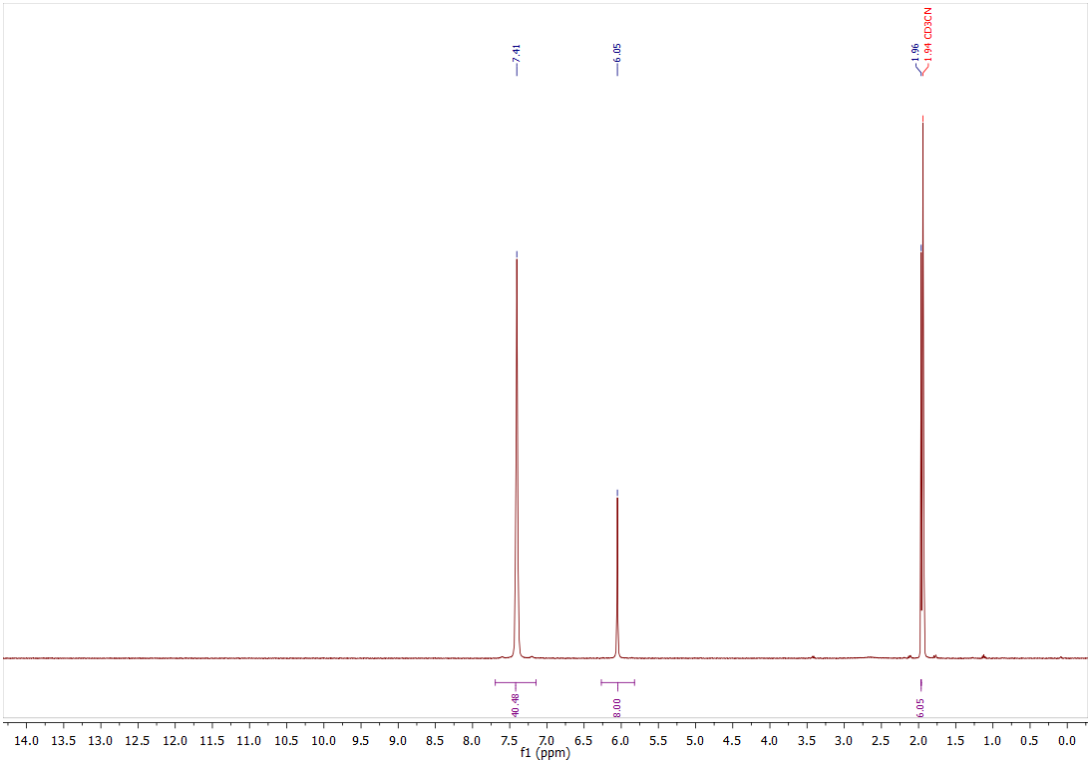

Figure 35: ^{1}H NMR spectrum of complex **VIII** in CD_3CN.

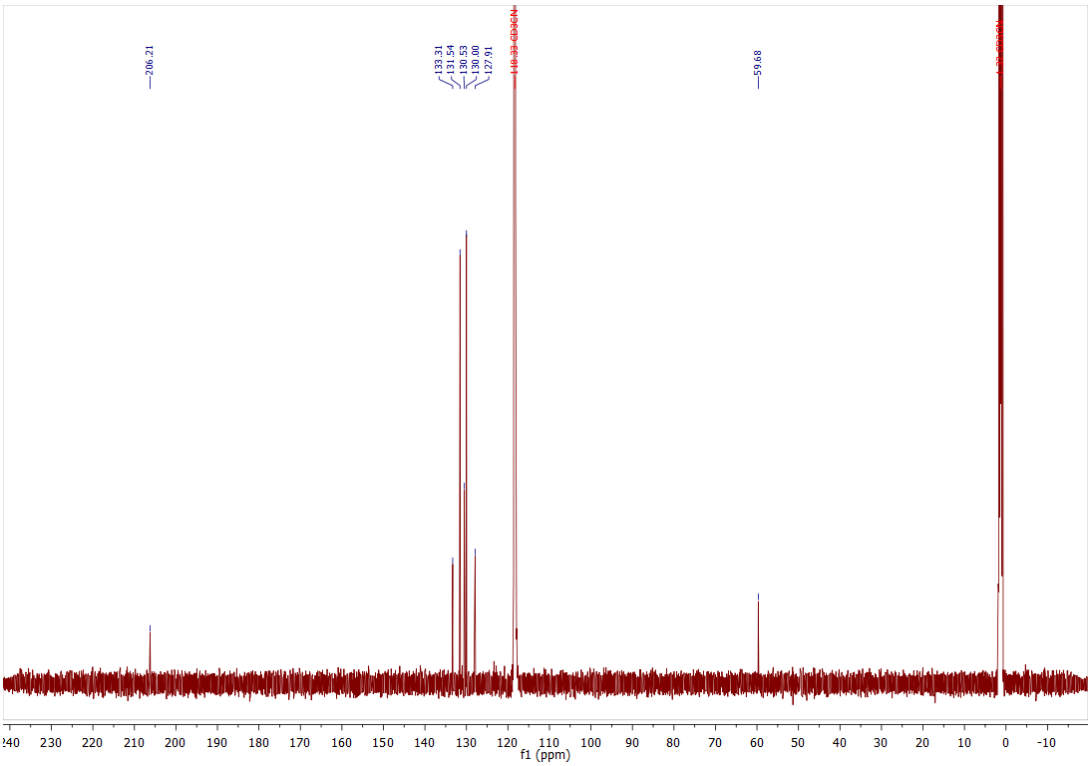

Figure 36: ^{13}C NMR spectrum of complex **VIII** in CD_3CN.

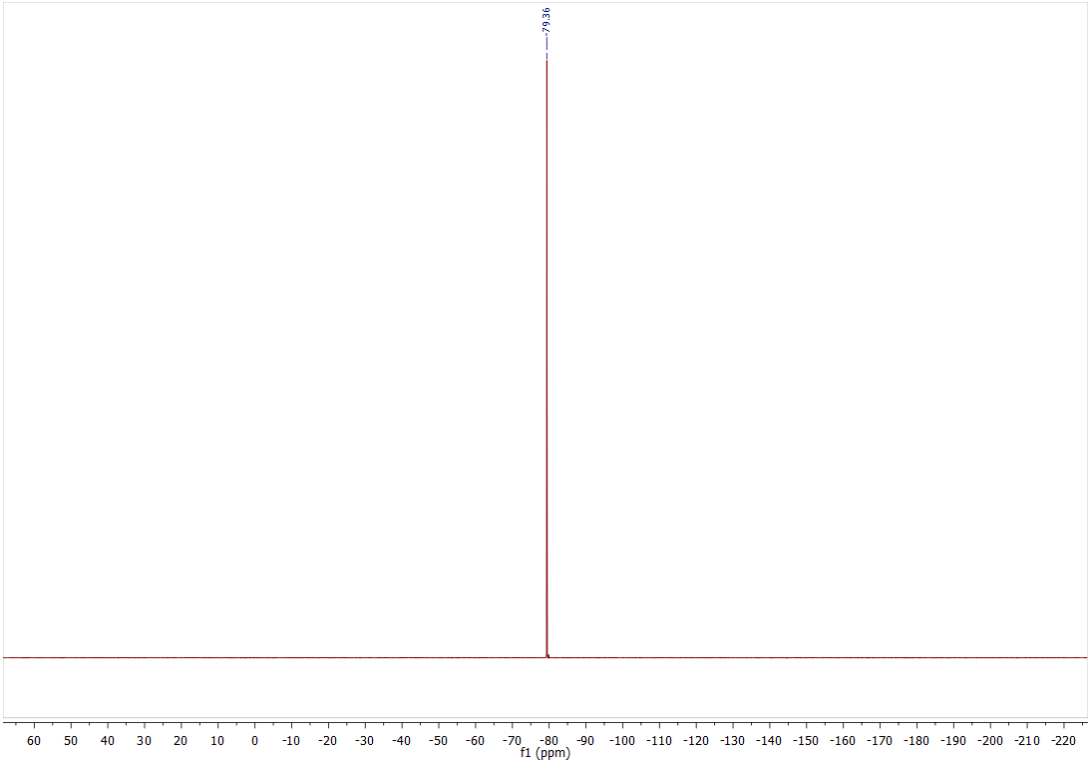

Figure 37: ^{19}F NMR spectrum of complex **VIII** in CD_3CN.

11.2.3 4,5-bis(*para*-fluorophenyl)imidazole (*p*-F-PhIm)

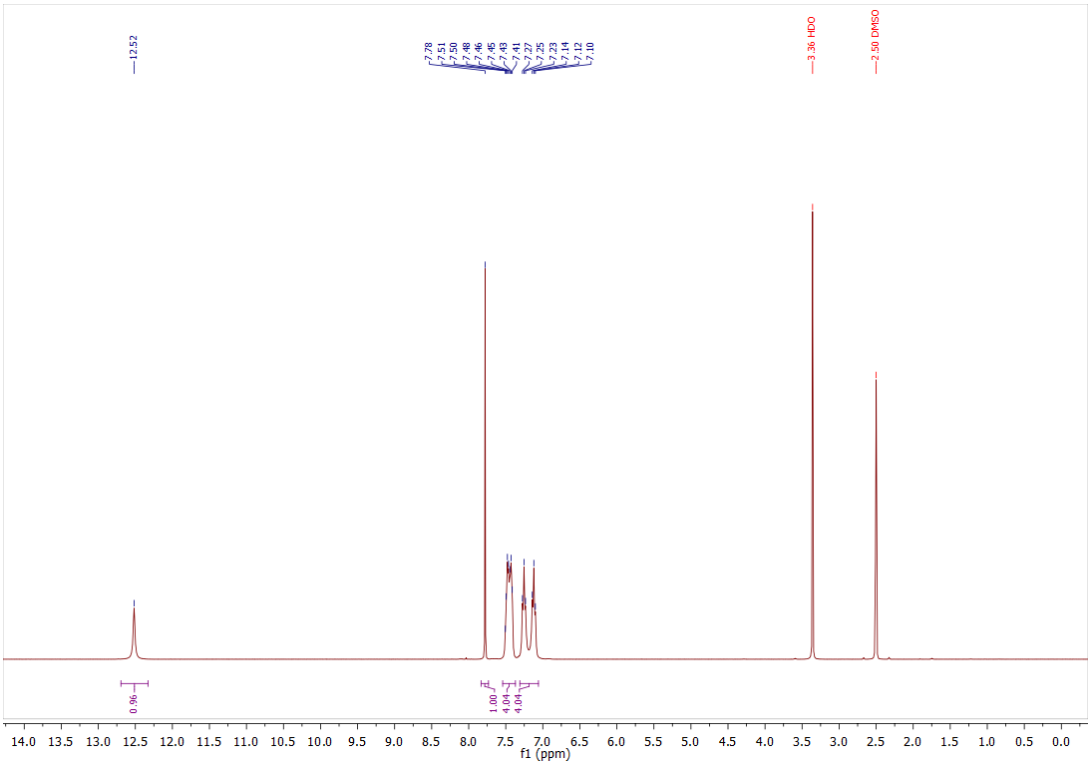

Figure 38: ^{1}H NMR spectrum of *p*-F-PhIm in DMSO-d_6.

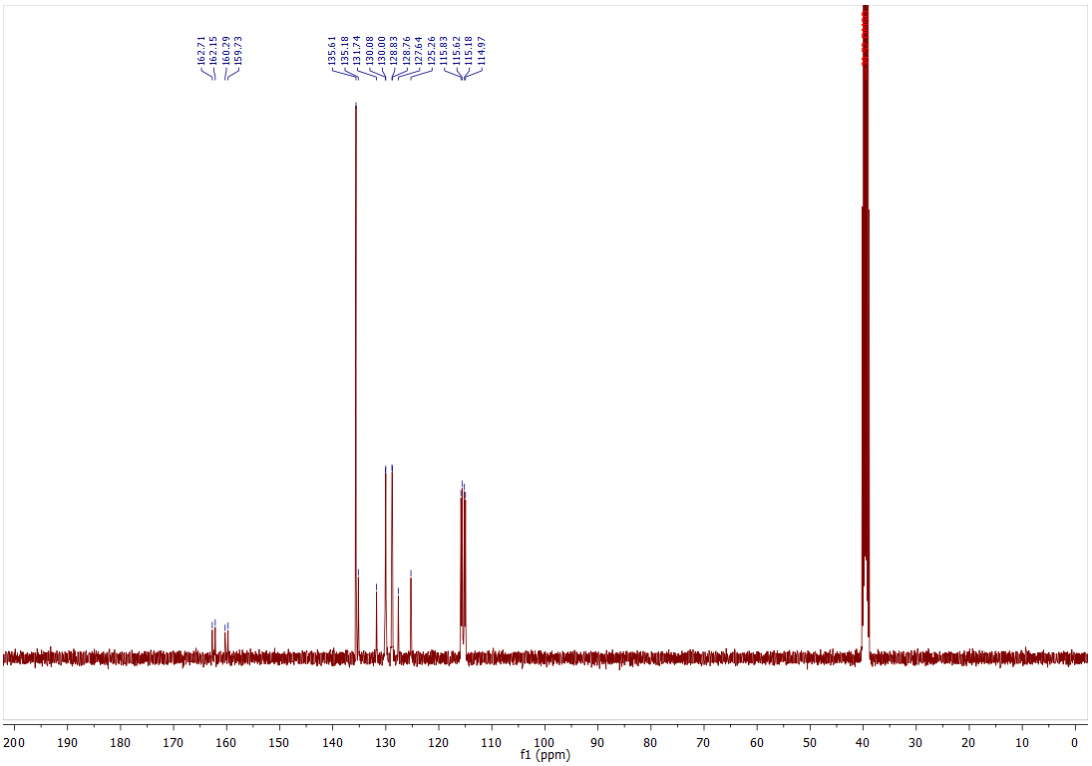

Figure 39: ^{13}C NMR spectrum of *p*-F-PhIm in DMSO-d_6.

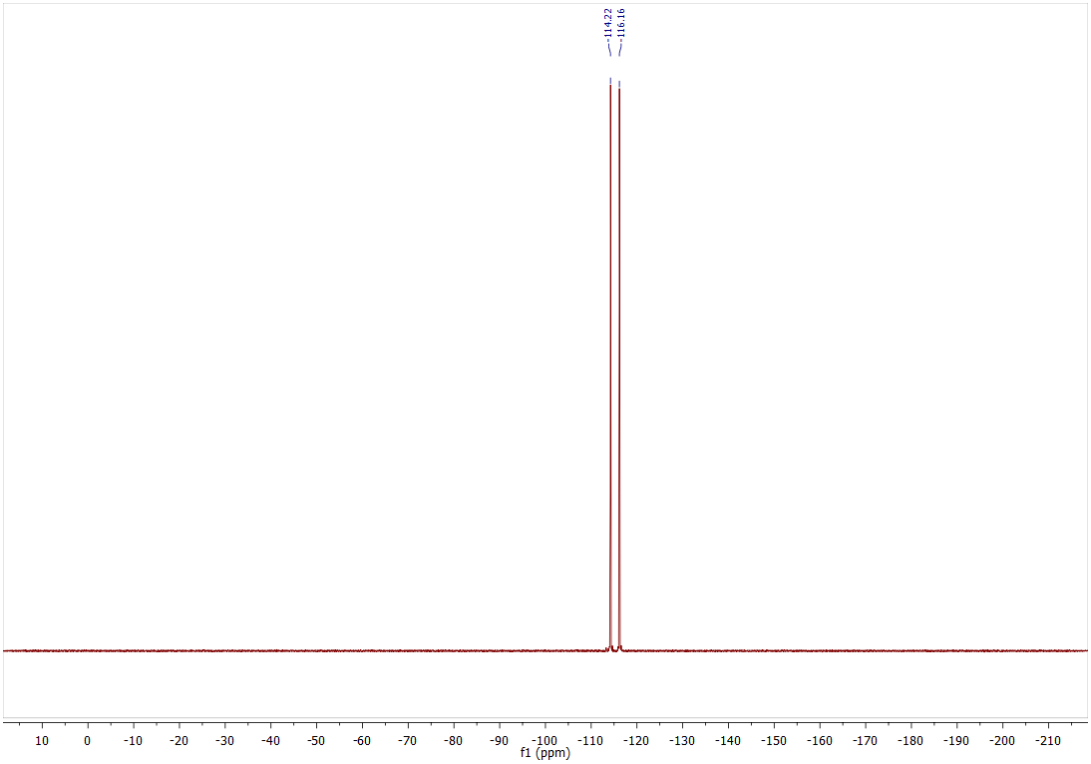

Figure 40: ^{19}F NMR spectrum of ***p*-F-Ph**$\mathbf{Im}$ in DMSO-d_6.

11.2.4 1,1'-Methylenebis(4,5-bis(*para*-fluorophenyl)-imidazole) (*p*-F-PhIm_2Me)

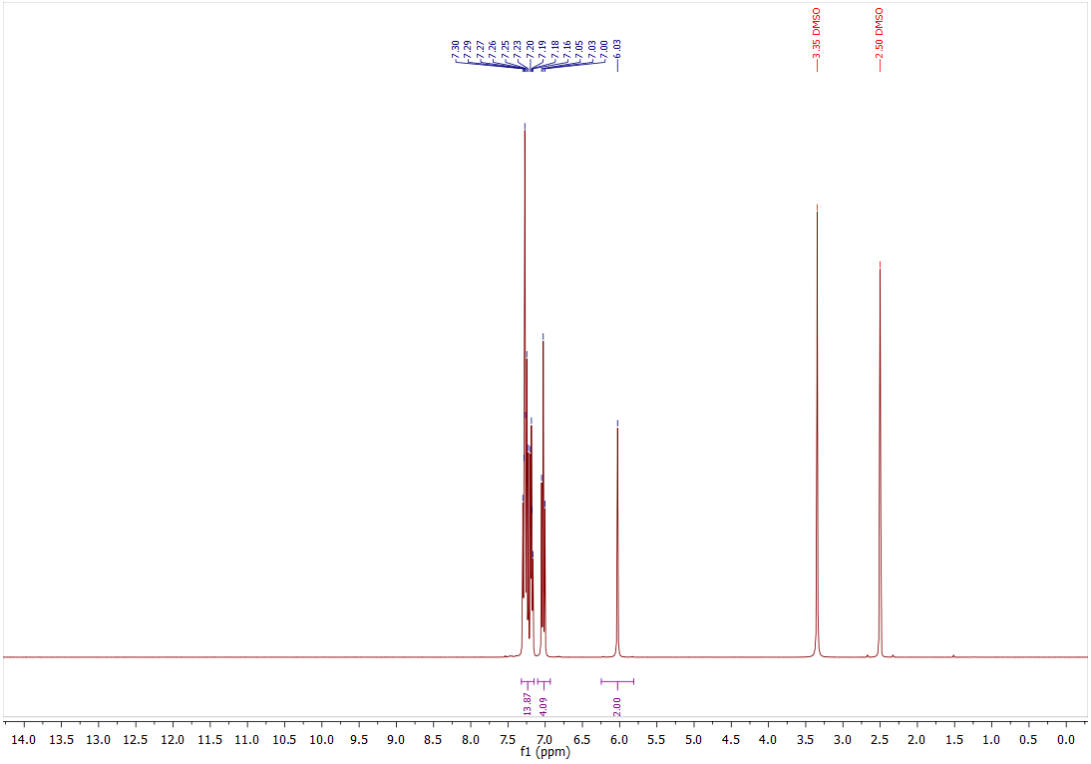

Figure 41: ^{1}H NMR spectrum of ***p*-F-Ph**$\mathbf{Im_2Me}$ in DMSO-d_6.

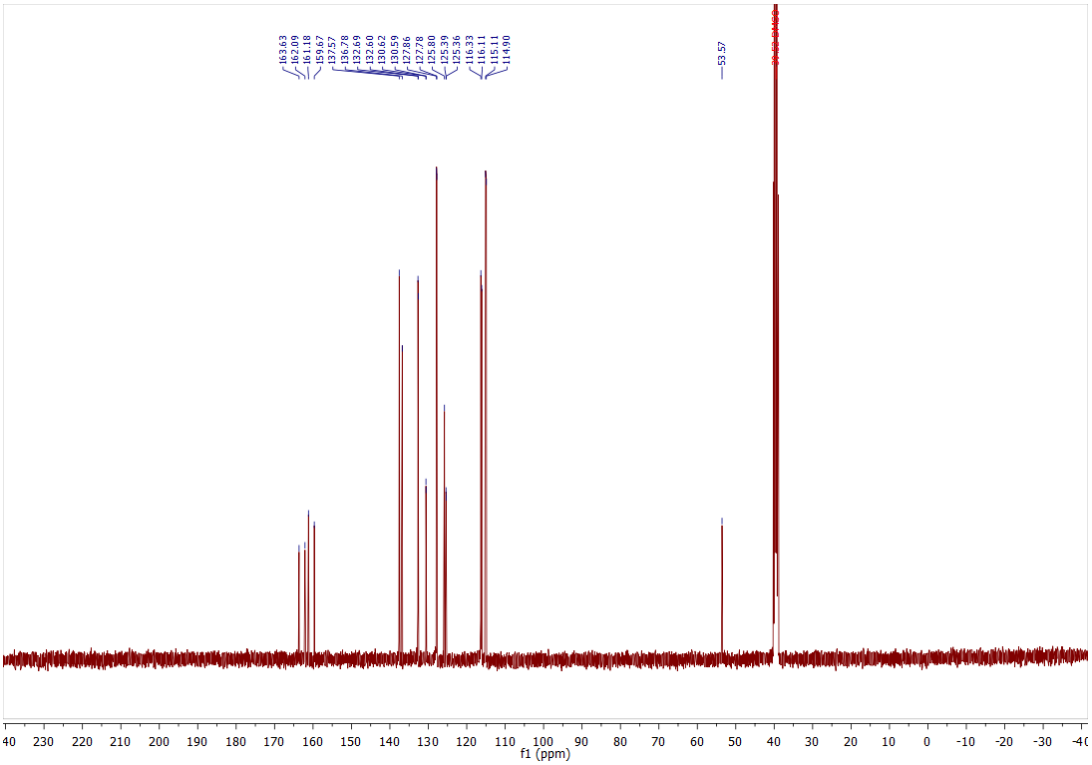

Figure 42: ^{13}C NMR spectrum of ***p*-F-PhIm_2Me** in DMSO-d_6.

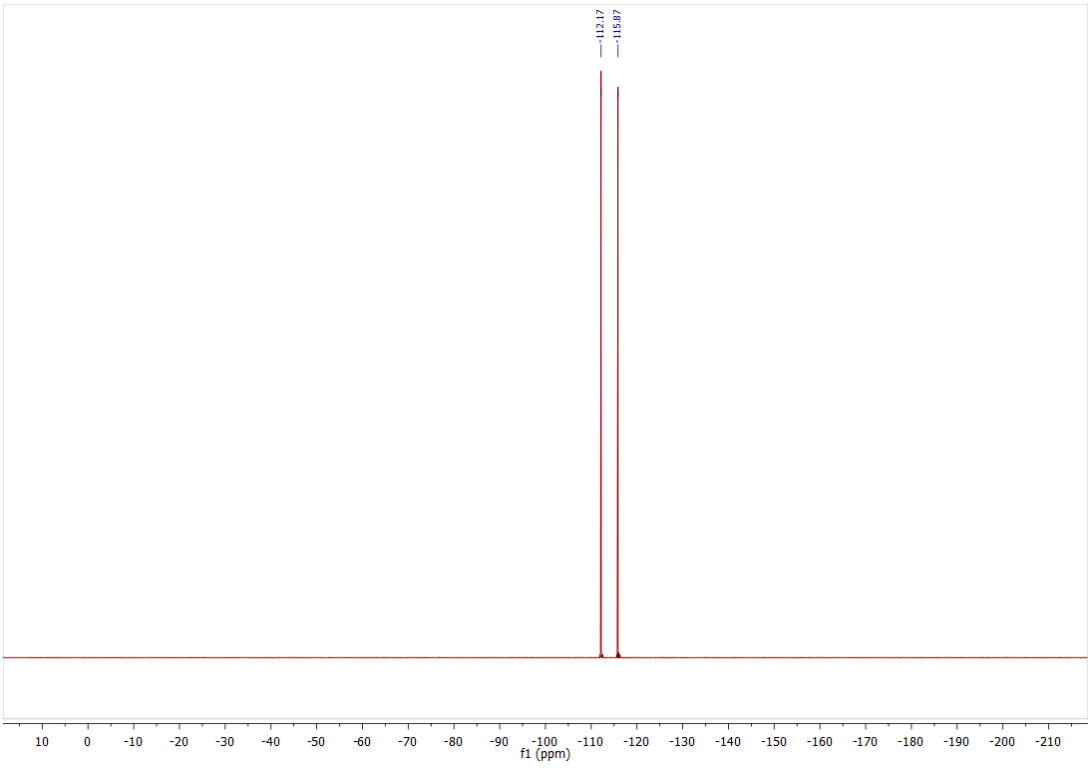

Figure 43: ^{19}F NMR spectrum of ***p*-F-PhIm_2Me** in DMSO-d_6.

11.2.5 *trans*-Diacetonitrile[calix[4](4,5-bis(*para*-fluorophenyl)imidazoyl] iron(II) triflate (**IX**)

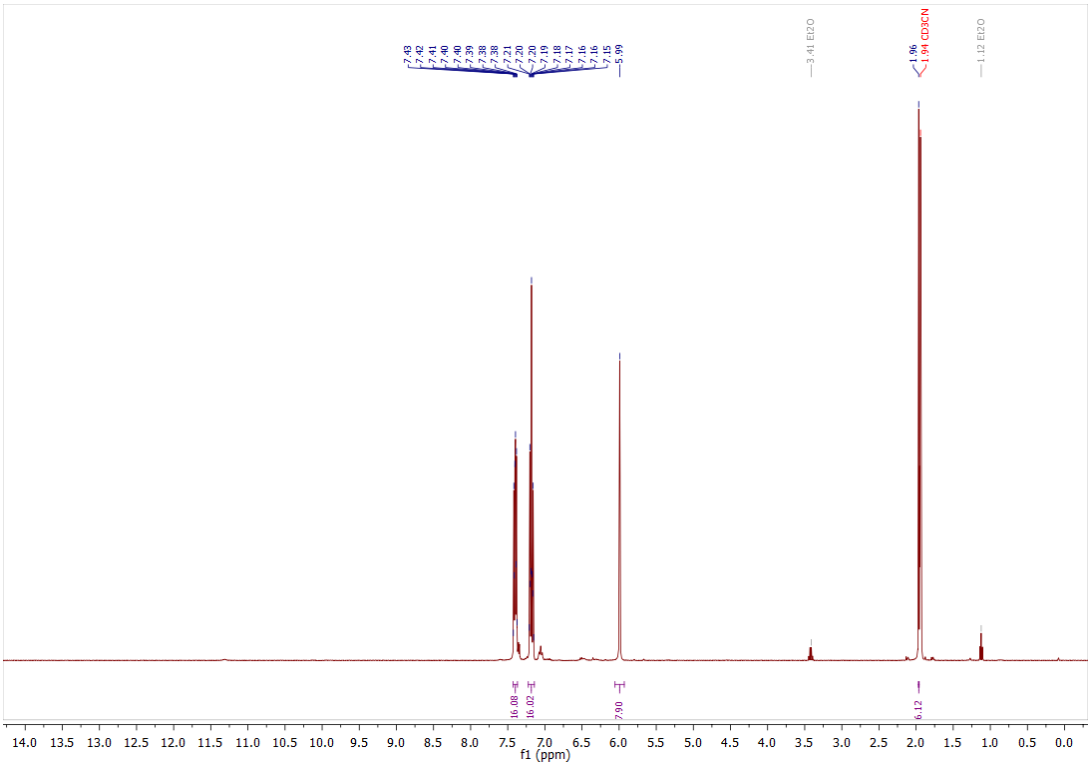

Figure 44: ^{1}H NMR spectrum of **IX** in CD_3CN.

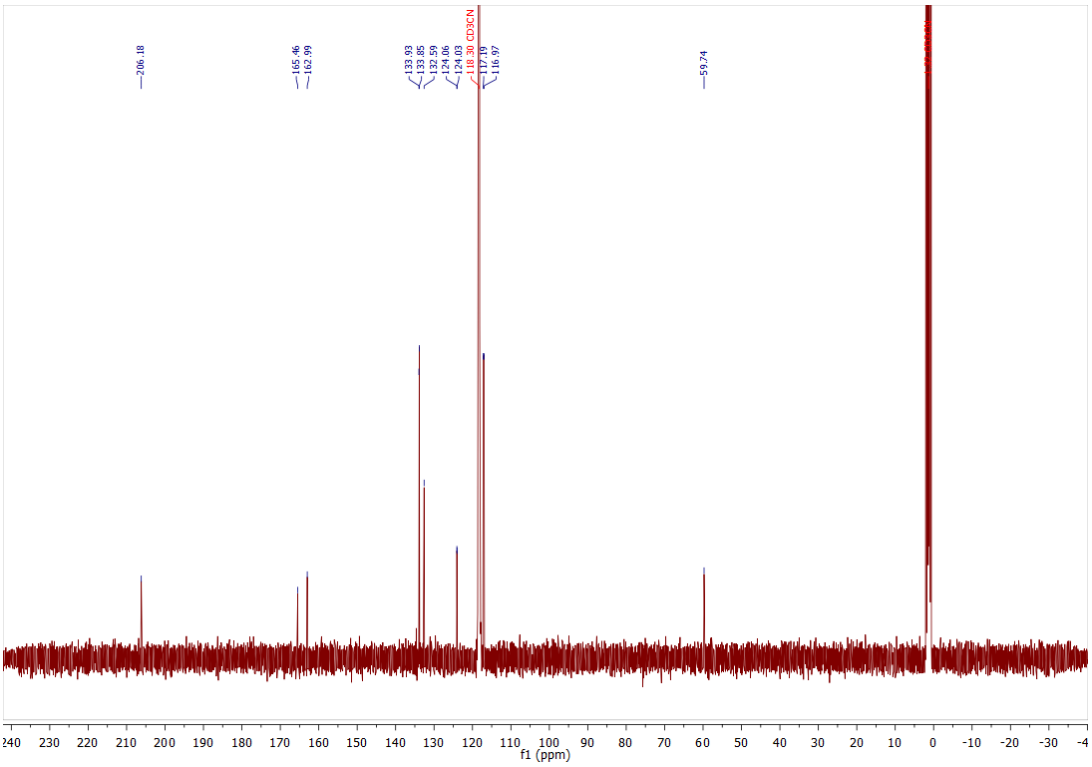

Figure 45: ^{13}C NMR spectrum of **IX** in CD_3CN.

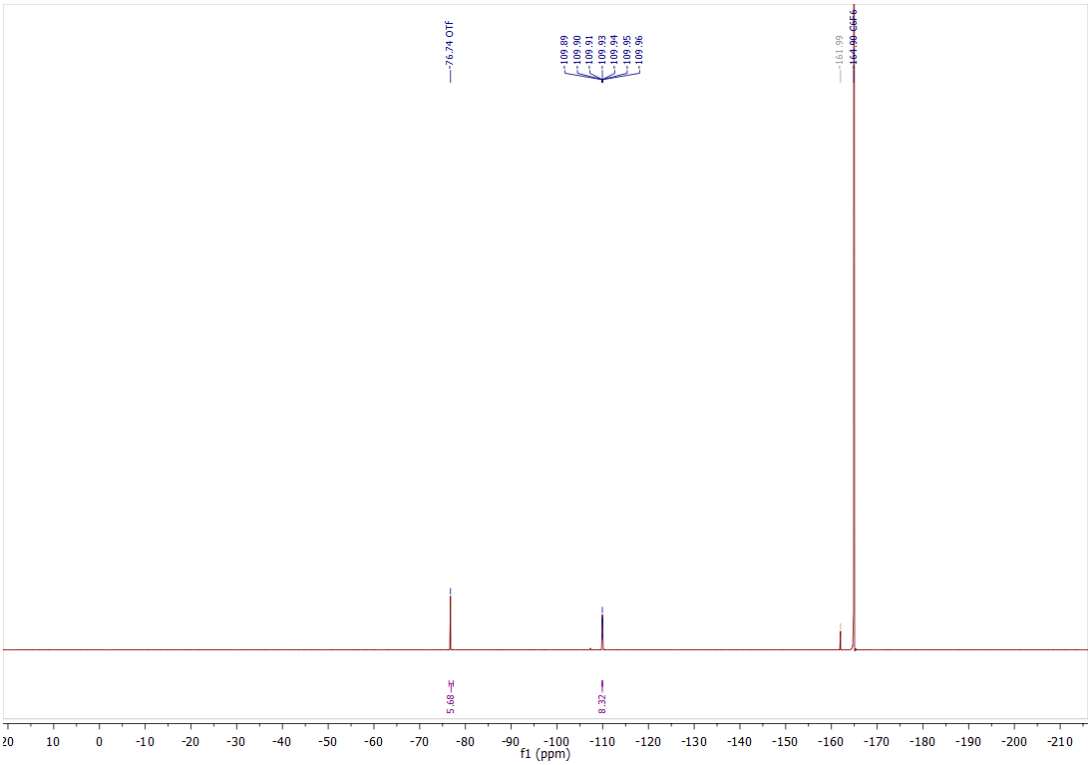

Figure 46: ^{19}F NMR spectrum of **IX** in CD_3CN with C_6F_6 present in an external canula as internal reference. The signal at -161.99 ppm derives from the utilized C_6F_6.

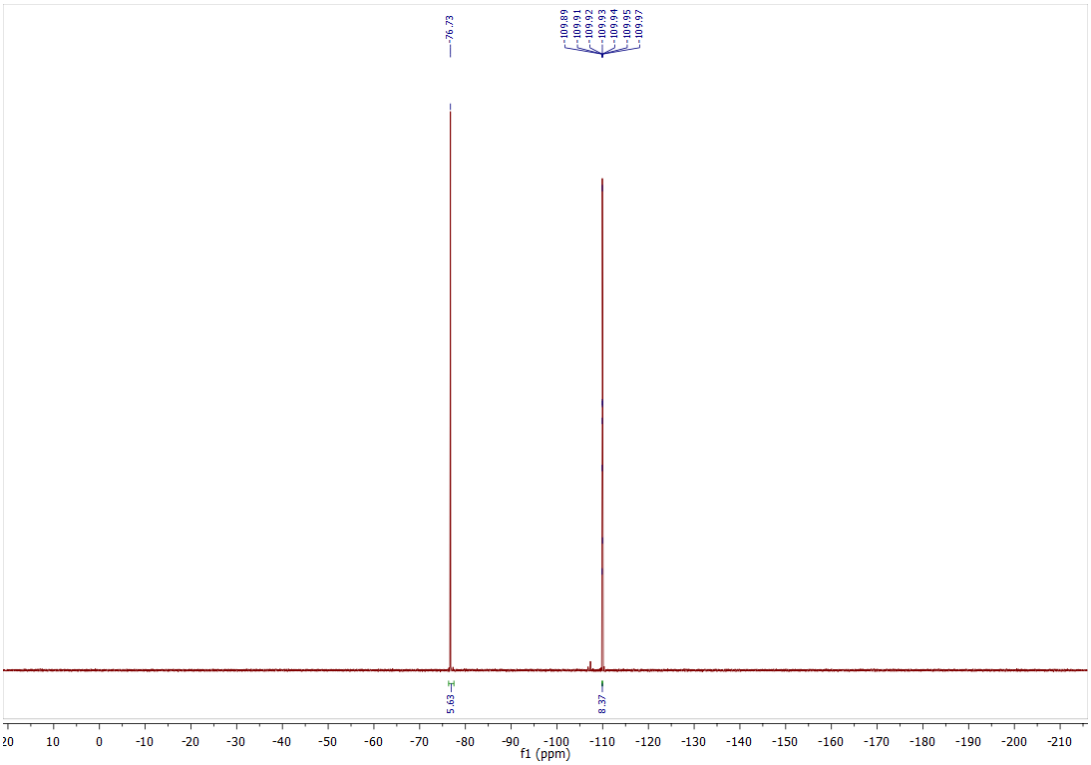

Figure 47: ^{19}F NMR spectrum of **IX** in CD_3CN without internal reference.

11.2.6 Sodium imidazolide

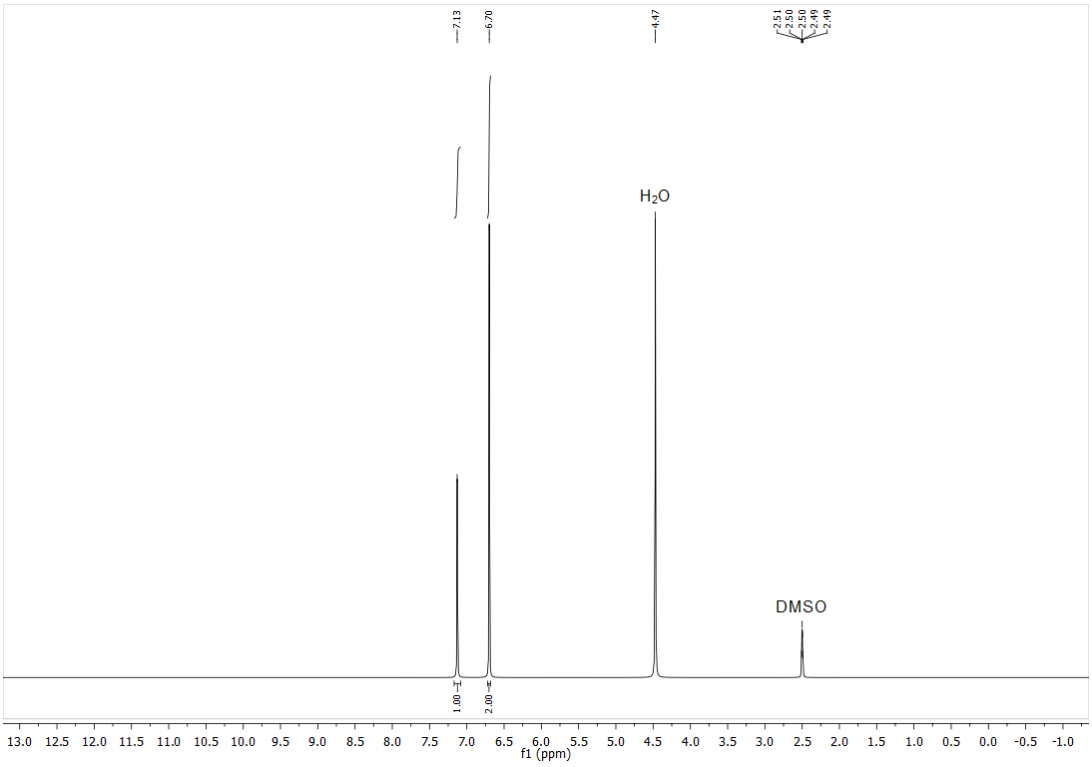

Figure 48: ^{1}H NMR spectrum of sodium imidazolide in DMSO-d_6. The water signal is downfield shifted due to the alkaline character of the imidazolide.

11.2.7 Di(imidazol-1-yl)methane-d$_2$ (**Im$_2$Me-*d$_2$***)

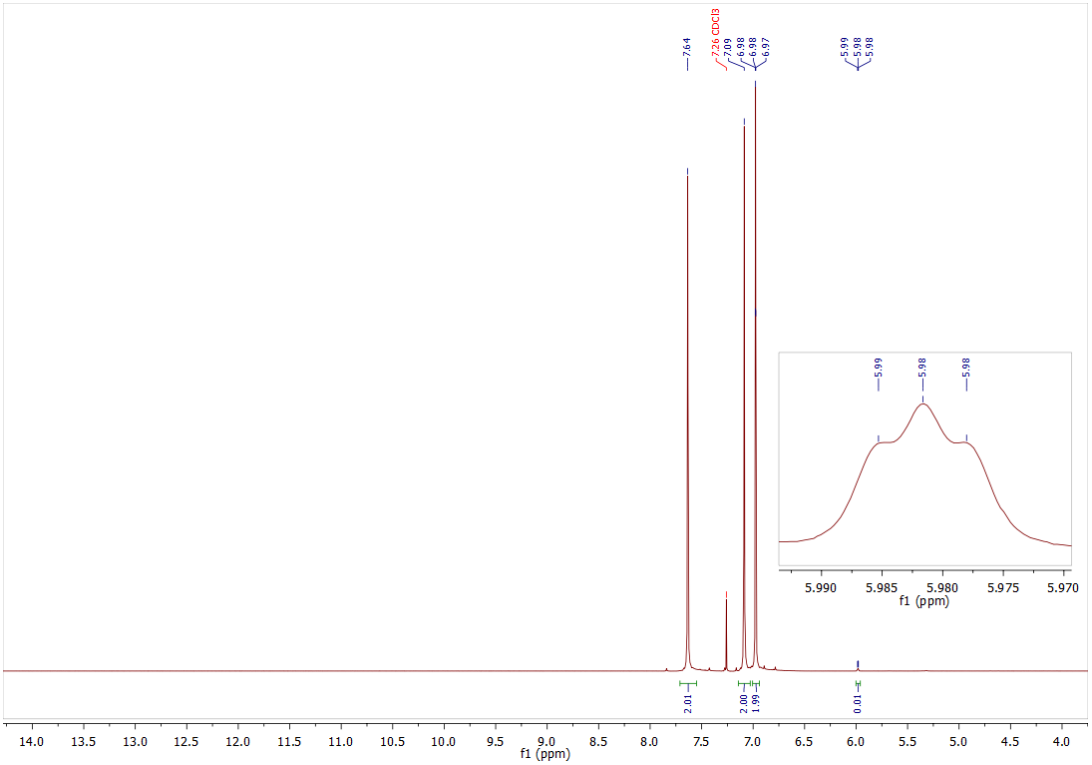

Figure 49: ^{1}H NMR of **Im$_2$Me-*d$_2$*** in $CDCl_3$, signals for non-deuterated regions are in alignment with literature, no loss of deuterium content is visible.

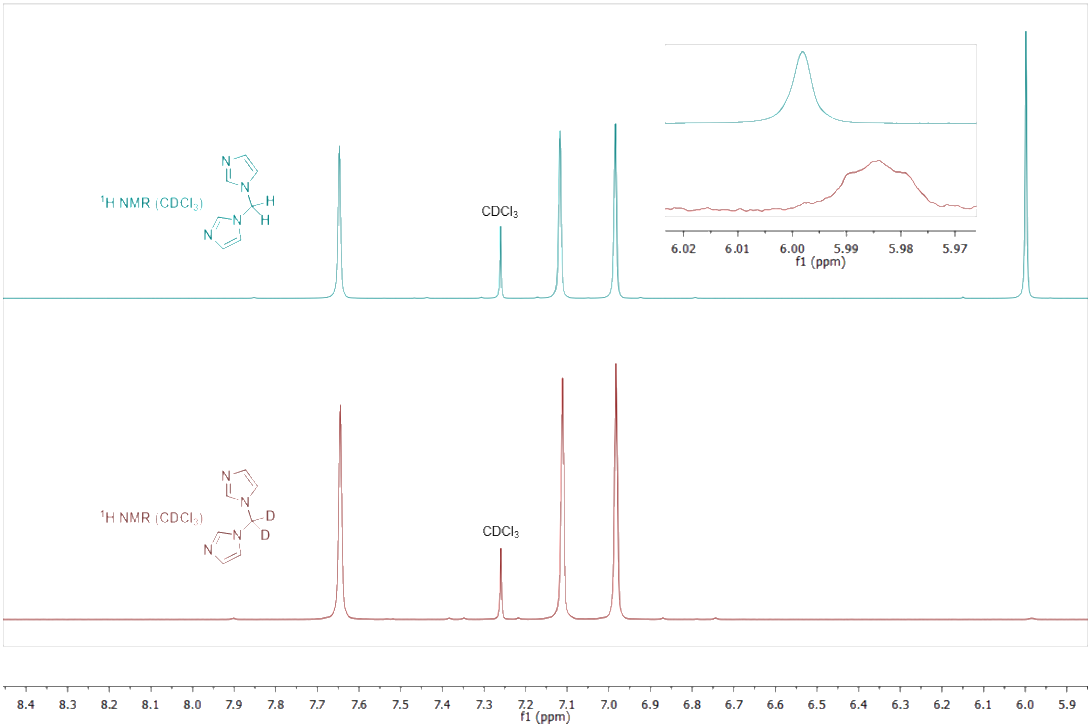

Figure 50: Comparative ^{1}H and ^{2}H NMR spectra of **Im_2Me-*d*$_2$** in and its non-deuterated analogue in $CDCl_3$.

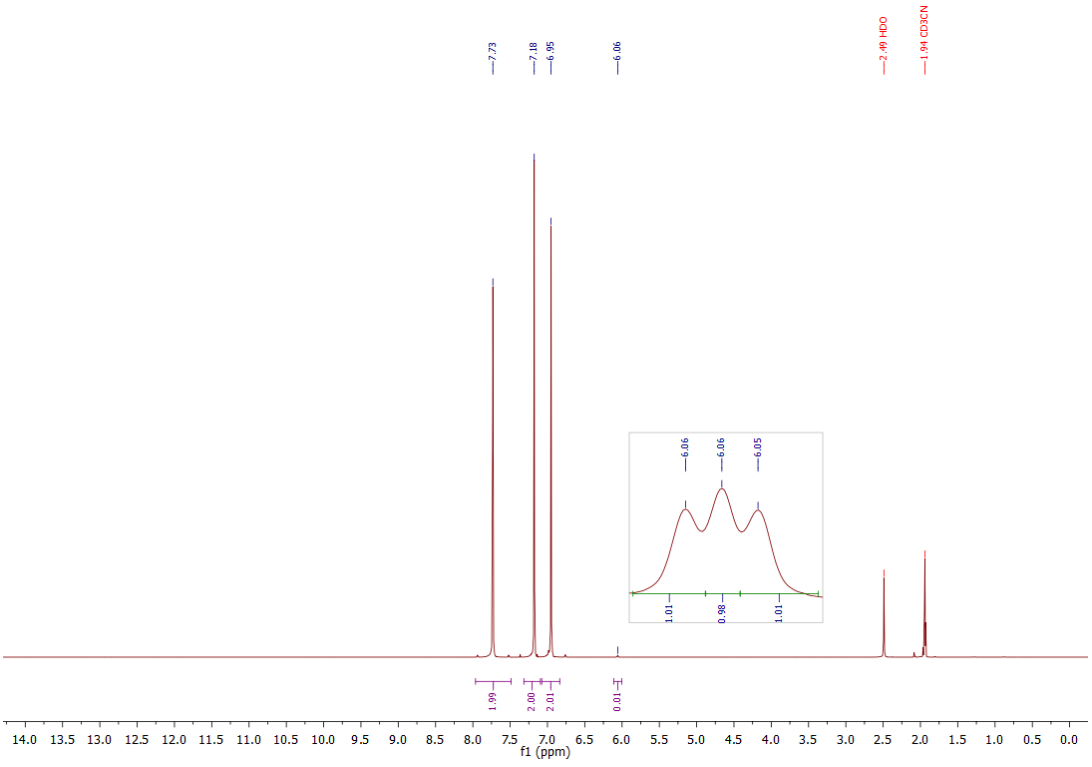

Figure 51: ^{1}H NMR of **Im_2Me-*d*$_2$** in CD_3CN, no loss of deuterium content is visible.

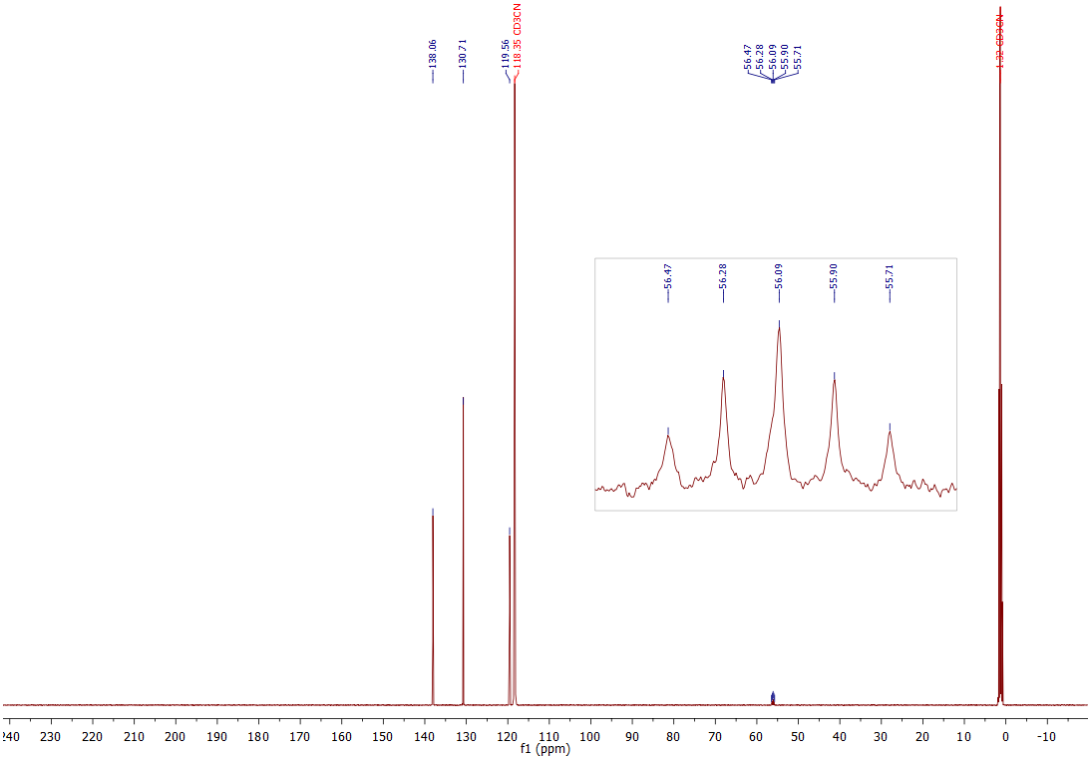

Figure 52: ^{13}C NMR of **Im_2Me-d_2** in CD_3CN, the presence of two deuterium atoms is visible due to the $^{1}J_{D\text{-}13C}$ coupling (tt, 23.6 Hz) of the corresponding signal.

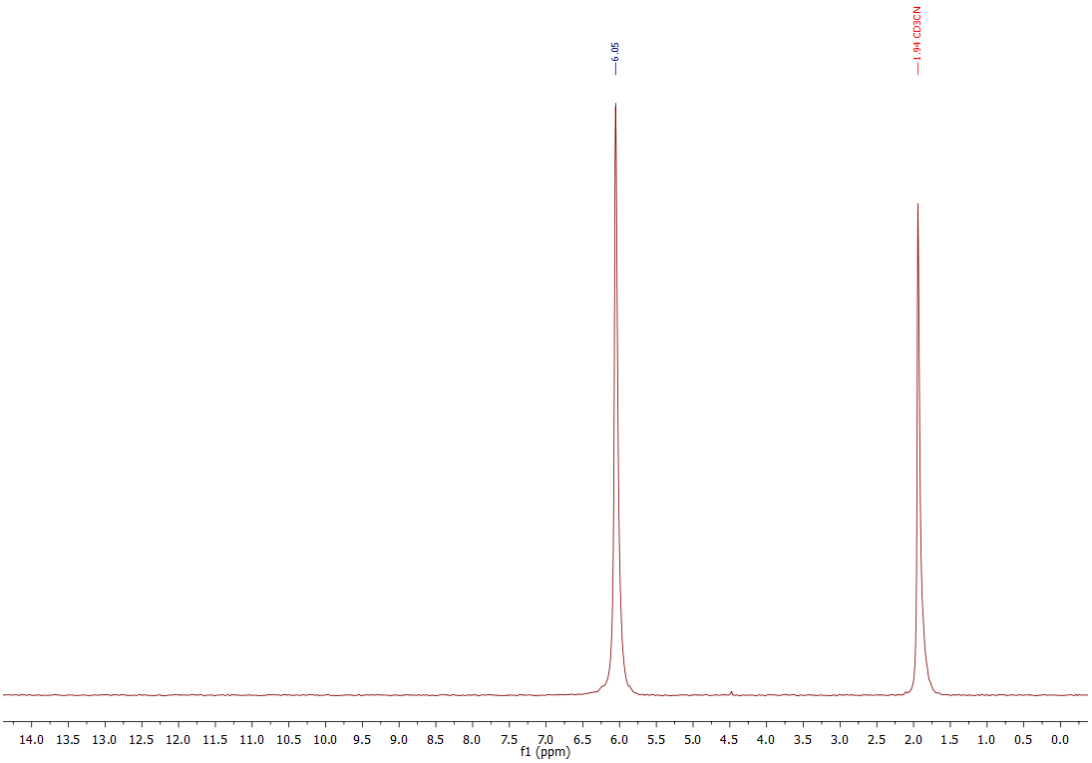

Figure 53: ^{2}H NMR of **Im_2Me-d_2** in CH_3CN. The chemical shift of the deuterated methylene bridge is in alignment with literature values of a ^{1}H NMR spectrum for the corresponding chemical environment of a non-deuterated species. CD_3CN is added as reference.

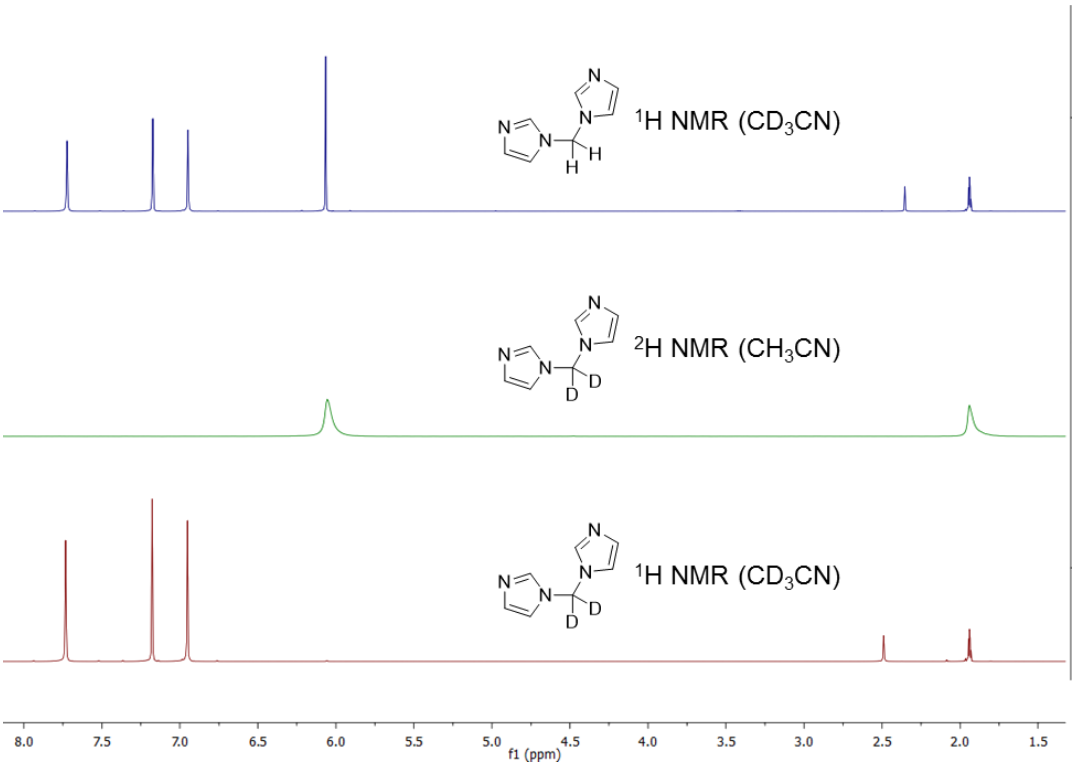

Figure 54: Comparative ^{1}H and ^{2}H NMR spectra of **Im_2Me-*d_2*** and its non-deuterated analogue.

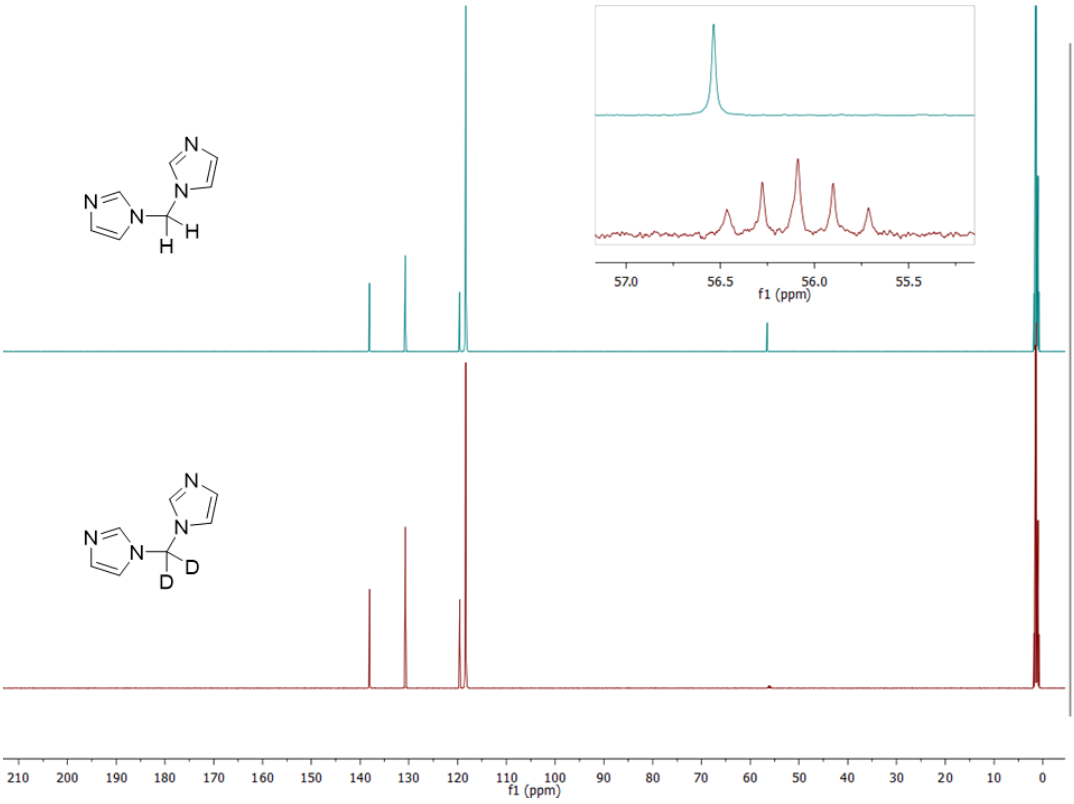

Figure 55: Comparative ^{13}C NMR spectra of **Im_2Me-*d_2*** and its non-deuterated analogue.

11.2.8 Calix[4]imidazolium-d_8 triflate (**L-*d*$_8$ OTf**)

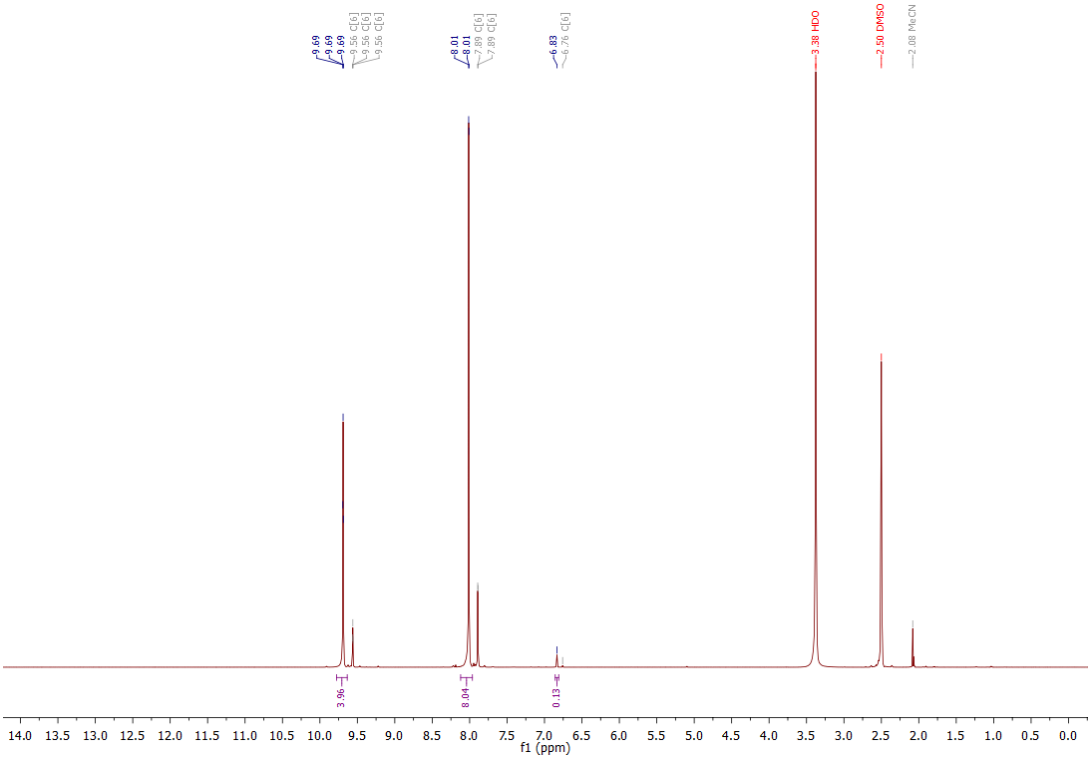

Figure 56: ^{1}H NMR spectrum of **L-*d*$_8$ OTf** in DMSO-*d*$_6$. No loss in deuterium content is visible.

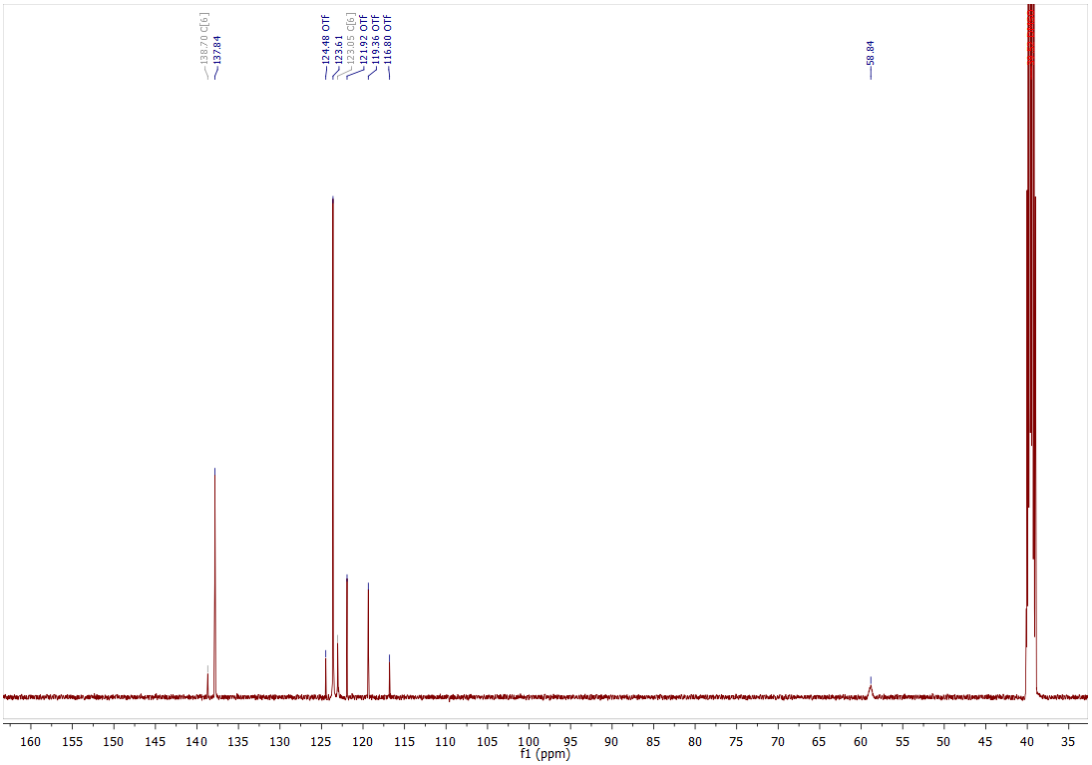

Figure 57: ^{13}C NMR of **L-*d*$_8$ OTf** in DMSO-*d*$_6$, the presence of deuterium atoms is suggested by the multiplet present at the methylene bridge, due to $^{1}J_{D\text{-}13C}$ coupling of the corresponding signal.

11.2.9 Calix[4]imidazolium-d$_8$ hexafluorophosphate (**L-*d*$_8$ PF$_6$**)

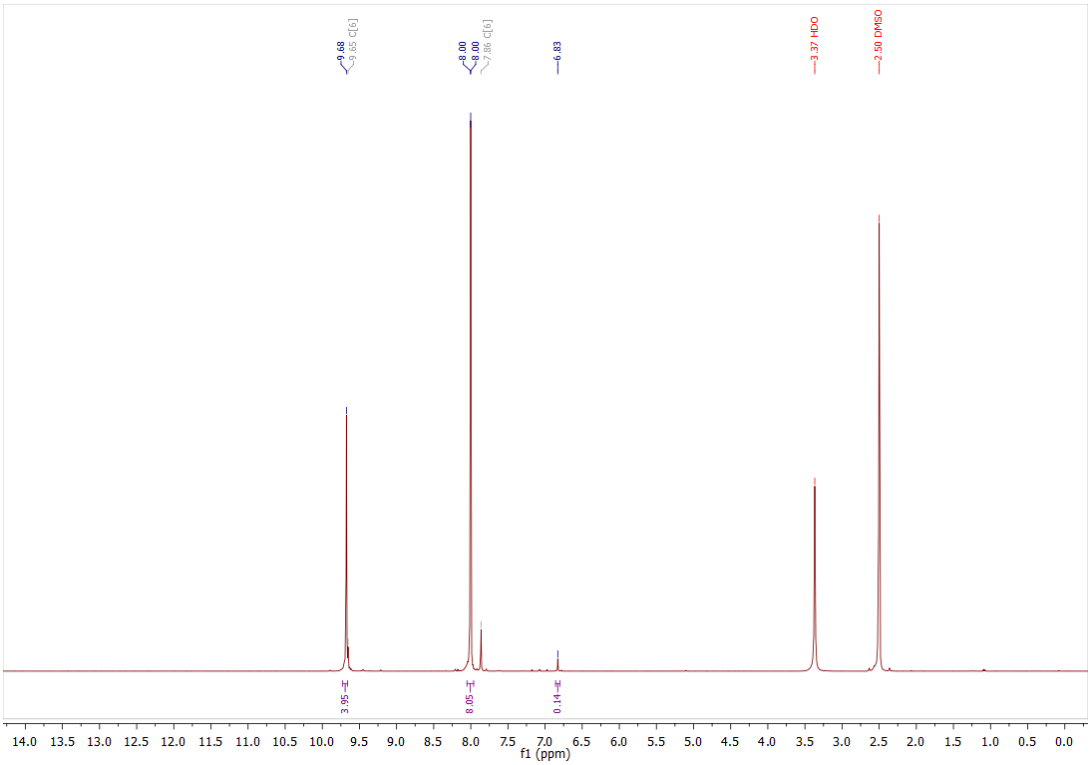

Figure 58: ^{1}H NMR spectrum of **L-*d*$_8$ PF$_6$** in DMSO-*d*$_6$. No loss in deuterium content is visible.

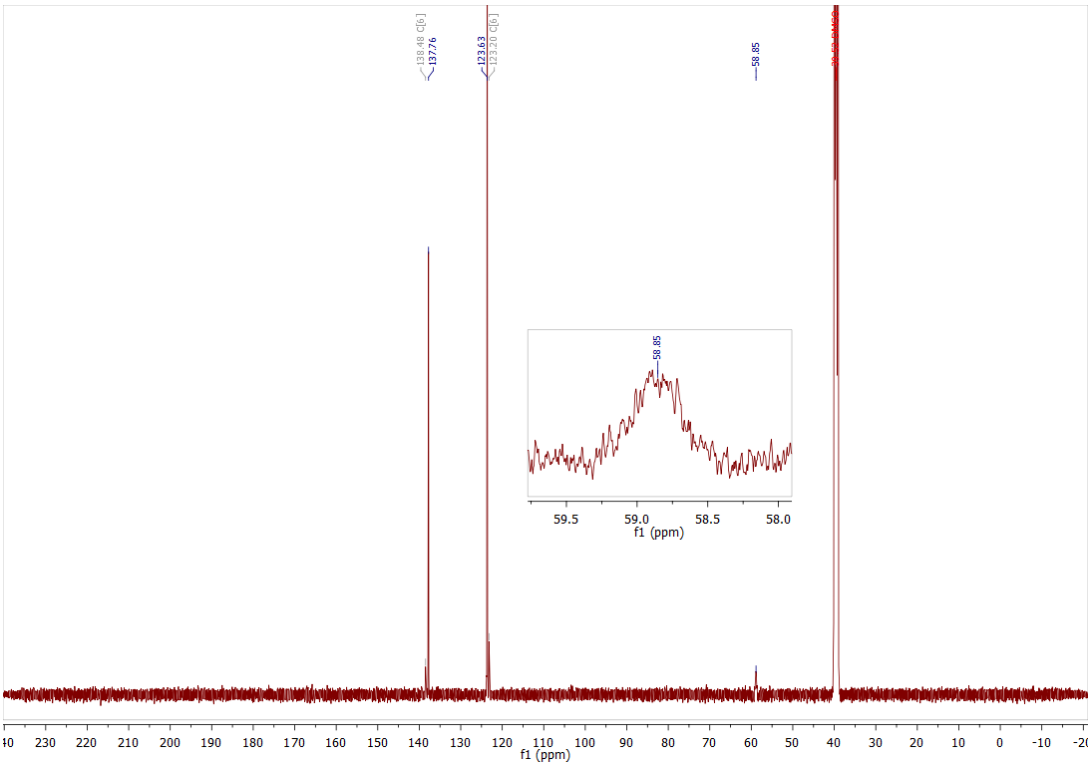

Figure 59: ^{13}C NMR of **L-*d*$_8$ PF$_6$** in DMSO-*d*$_6$, the multiplet at the methylene bridge (58.85 ppm) is due to $^{1}J_{D\text{-}13C}$ coupling of the corresponding signal.

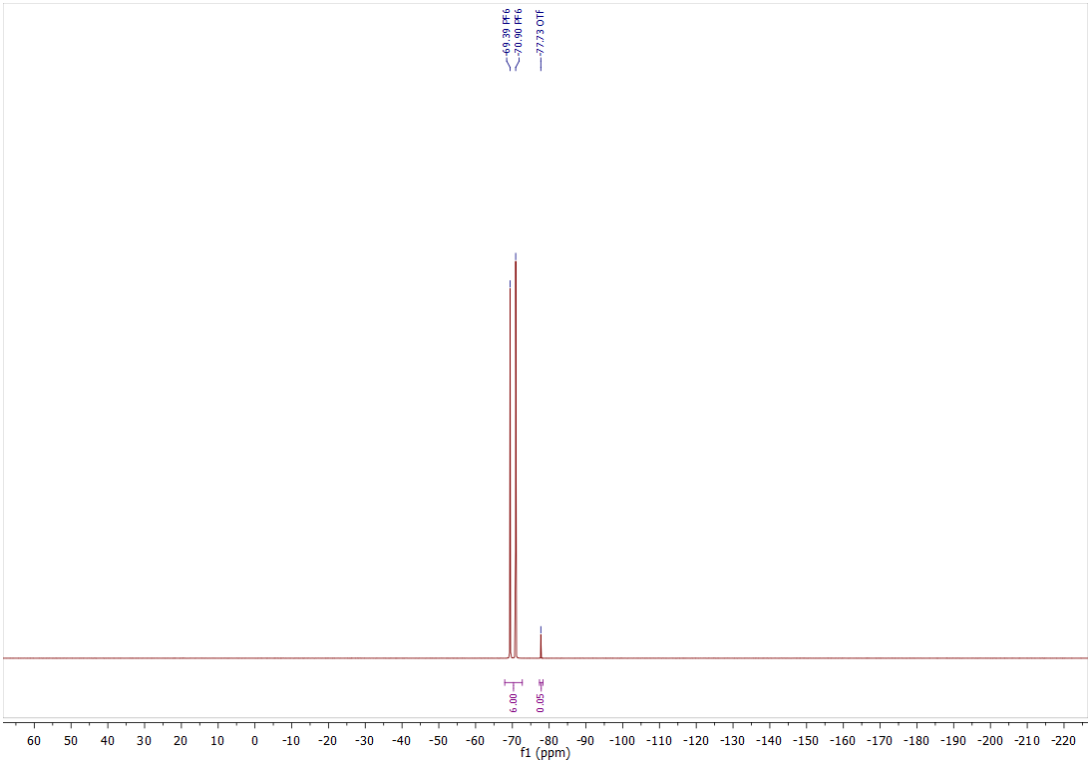

Figure 60: ^{19}F NMR of **L-d_8 PF_6** in DMSO-d_6, no reference standard is added, as only the integral ration is of interest.

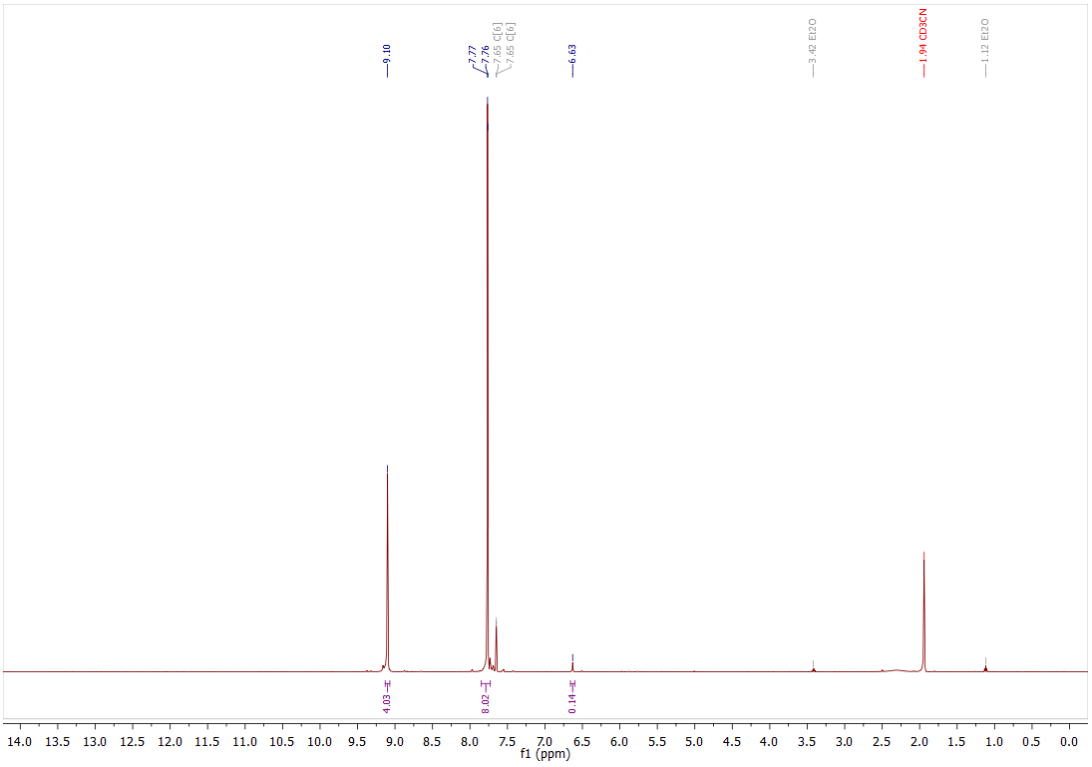

Figure 61: ^{1}H NMR spectrum of **L-d_8 PF_6** in CD_3CN. No loss in deuterium content is visible.

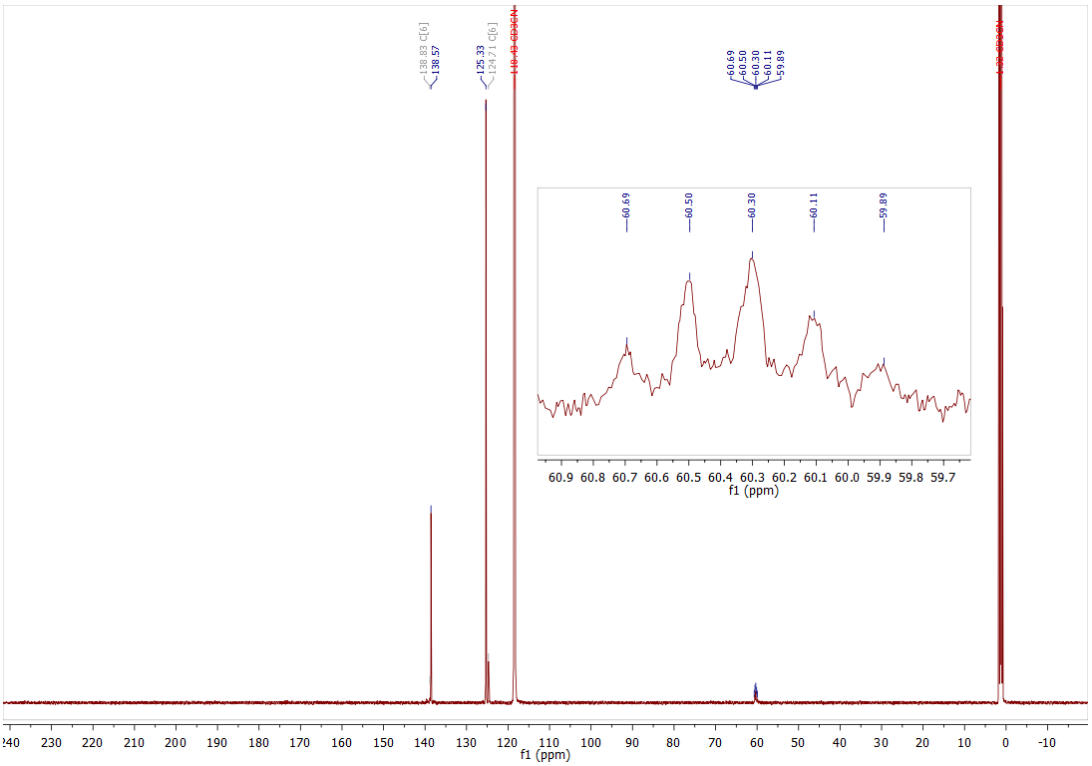

Figure 62: ^{13}C NMR of **L-*d*$_8$ PF$_6$** in CD_3CN, the methylene bridge (60.30 ppm) shows a triplet of triplet multiplicity due to $^{1}J_{D\text{-}13C}$ coupling of two deuterium atoms with the ^{13}C at the corresponding location.

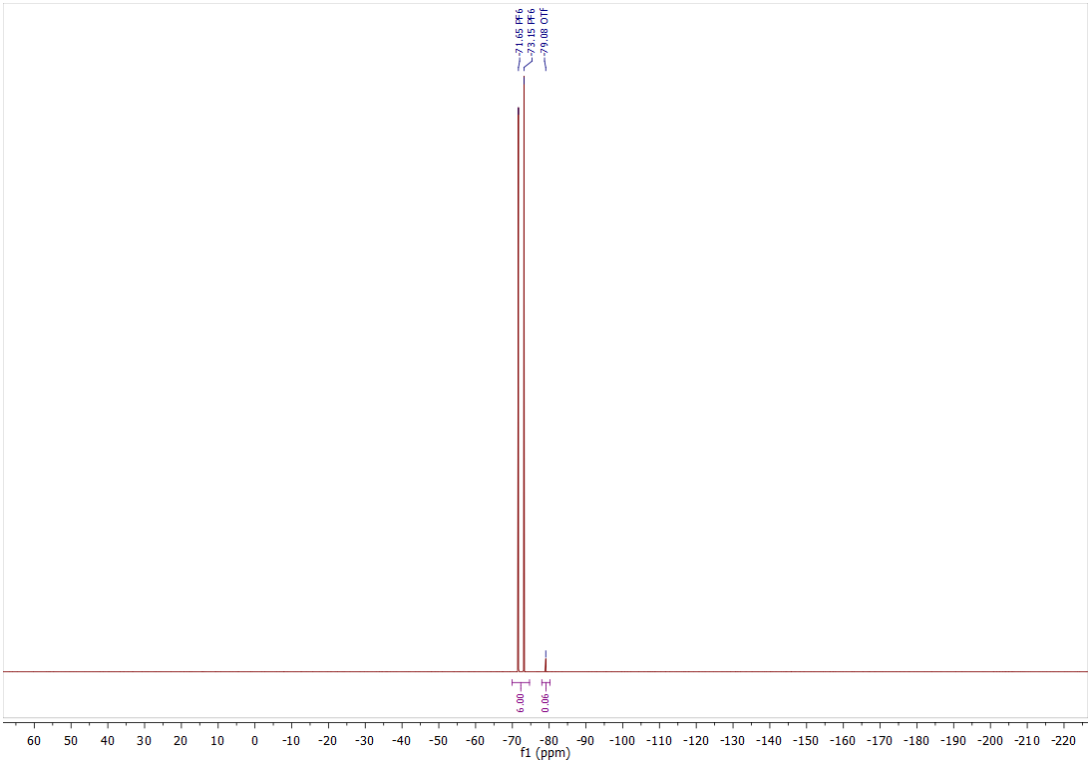

Figure 63: ^{19}F NMR of **L-*d*$_8$ PF$_6$** in CD_3CN, no reference standard is added, as only the integral ration is of interest.

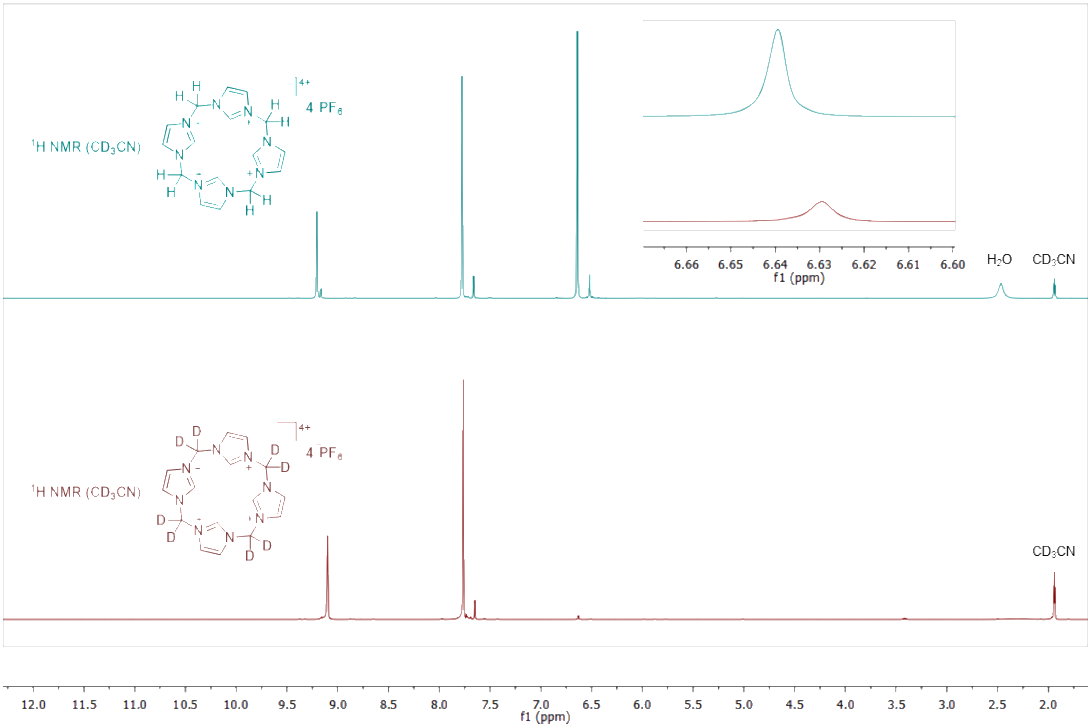

Figure 64: Comparative ^{1}H NMR spectra of **L-*d*$_8$ PF$_6$** and its non-deuterated analogue, both in CD_3CN.

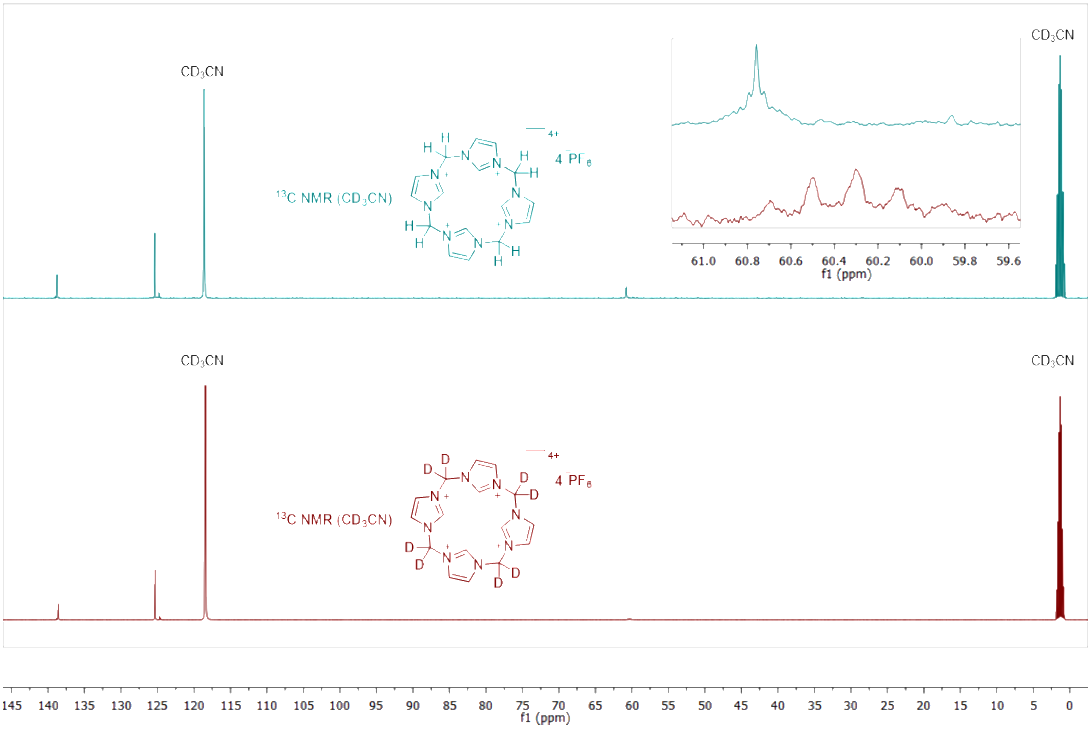

Figure 65: Comparative ^{13}C NMR spectra of **L-*d*$_8$ PF$_6$** and its non-deuterated analogue, both in CD_3CN.

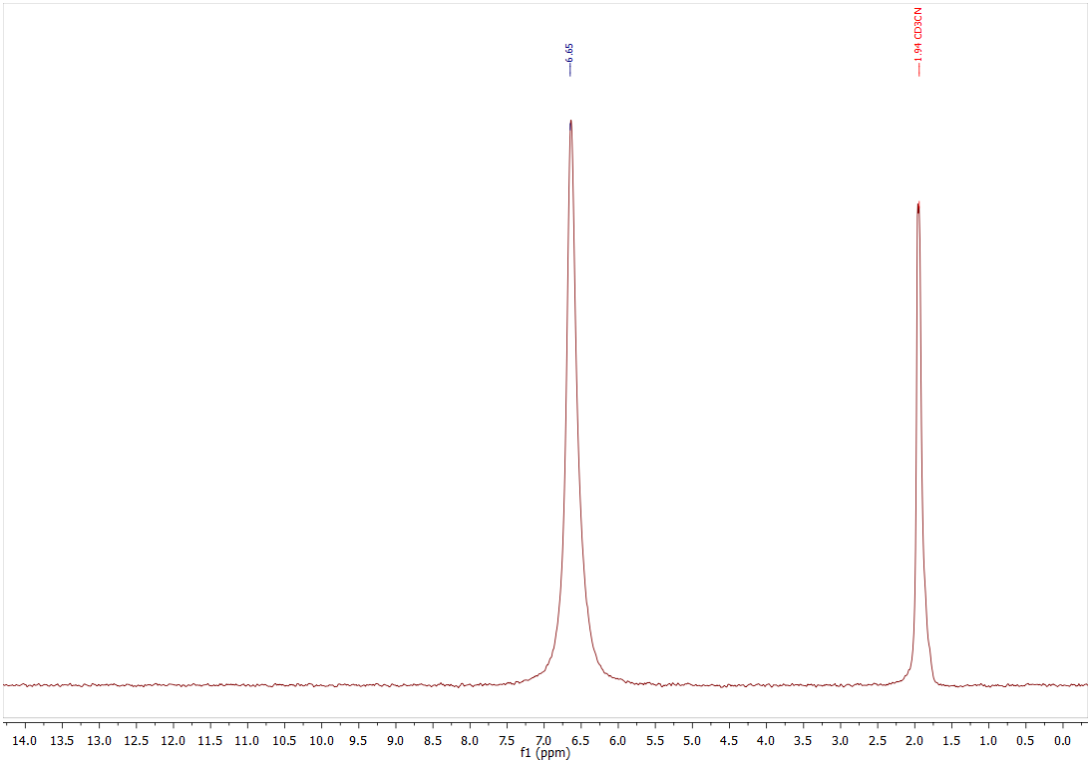

Figure 66: ^{2}H NMR of **L-*d*$_8$ PF$_6$** in CH_3CN, the chemical shift of the deuterated methylene bridge is in alignment with literature values of a ^{1}H NMR spectrum for the corresponding chemical environment of a non-deuterated species. CD_3CN is added for referencing.

11.2.10 trans-Diacetonitrile[calix[4]imidazoyl-d$_8$]iron(II) hexafluorophosphate (X)

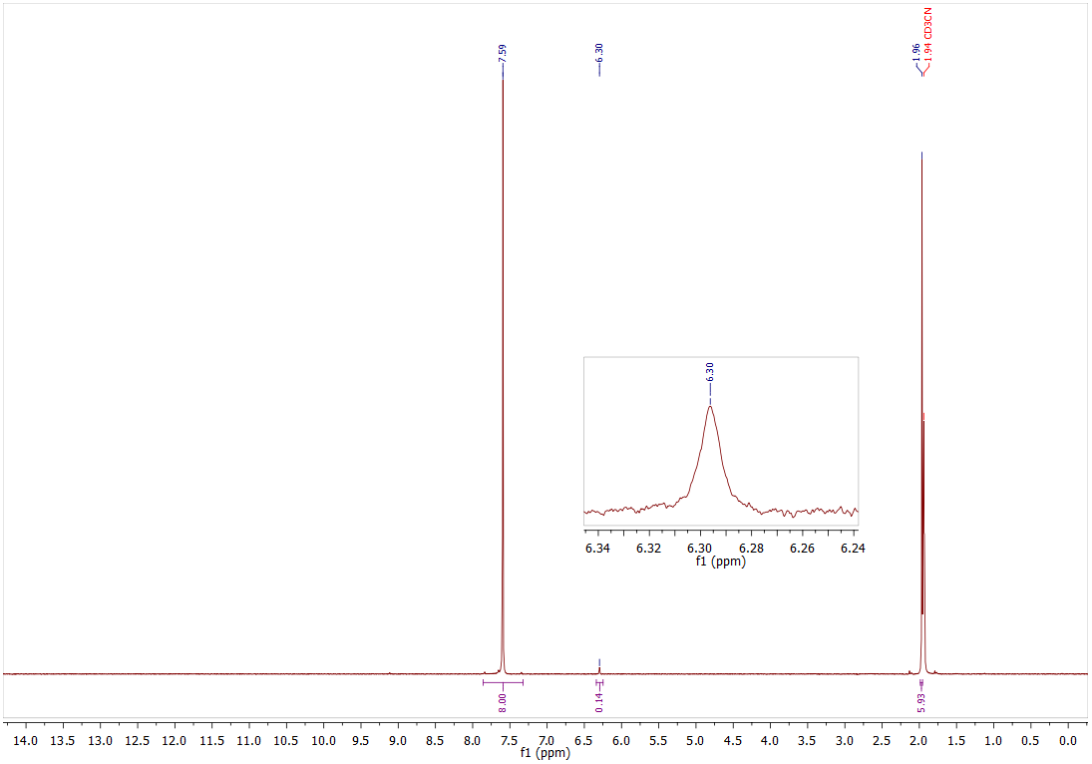

Figure 67: ^{1}H NMR spectrum of **X** in CD_3CN. No loss in deuterium content is visible.

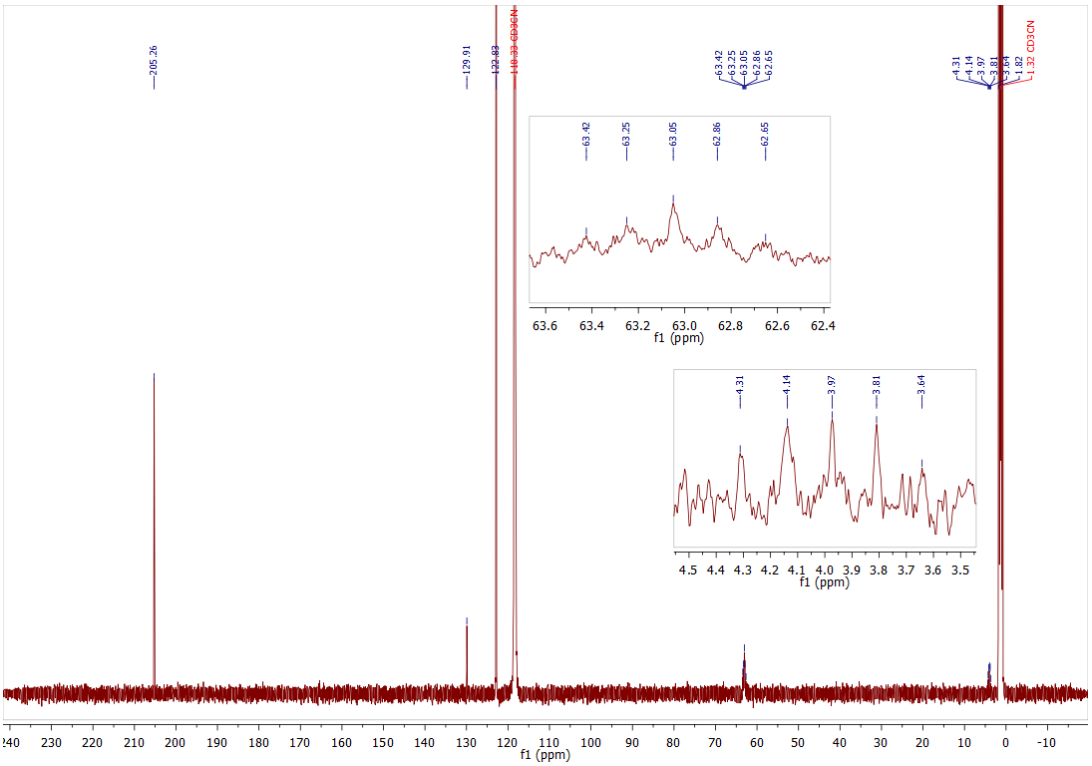

Figure 68: ^{13}C NMR of **X** in CD_3CN, the methylene bridge (63.05 ppm) still shows a triplet of triplet multiplicity due to $^{1}J_{D\text{-}13C}$ coupling of two deuterium atoms with the ^{13}C at the corresponding location, but cannot be resolved fully. Interestingly, signals for the coordinating acetonitrile are found at 129.91 and 3.97 ppm. The multiplet at 3.97 ppm, which should be a *ttt* but cannot be resolved completely, suggests that deuterated acetonitrile is coordinating as axial ligands.

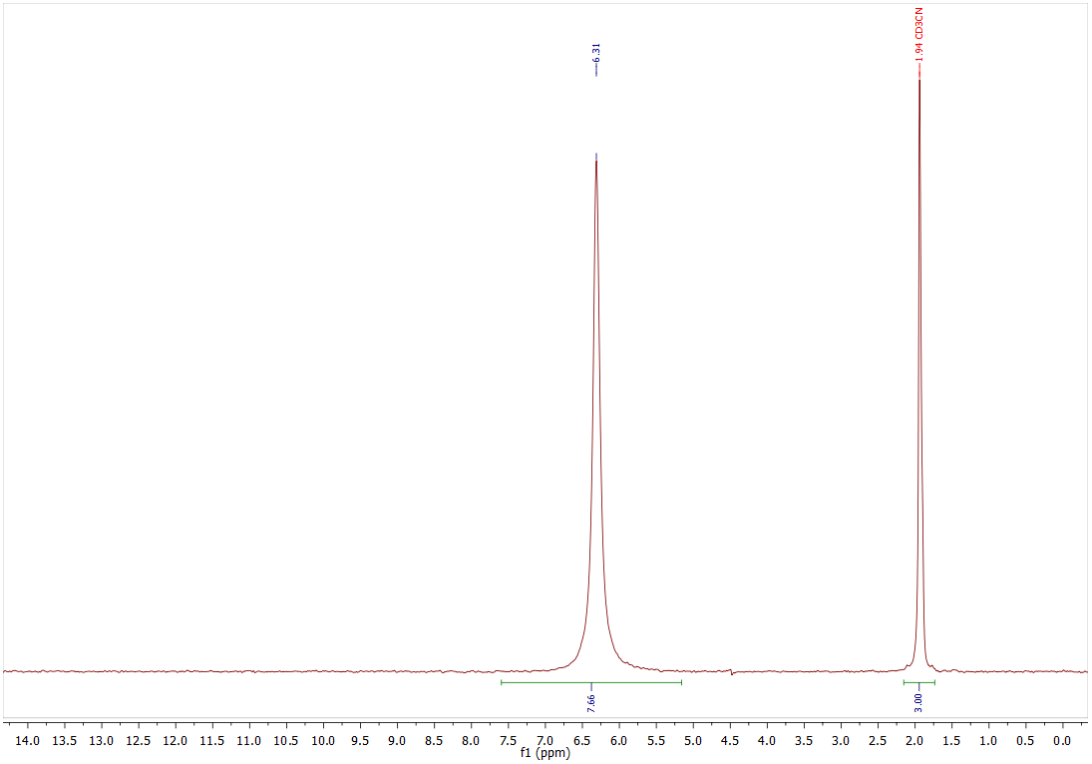

Figure 69: ^{2}H NMR spectrum of **X** in CH_3CN, the chemical shift of the deuterated methylene bridge is in alignment with literature values of a ^{1}H NMR spectrum for the corresponding chemical environment of a non-deuterated species. An equimolar amount of CD_3CN was added to the sample as internal standard.

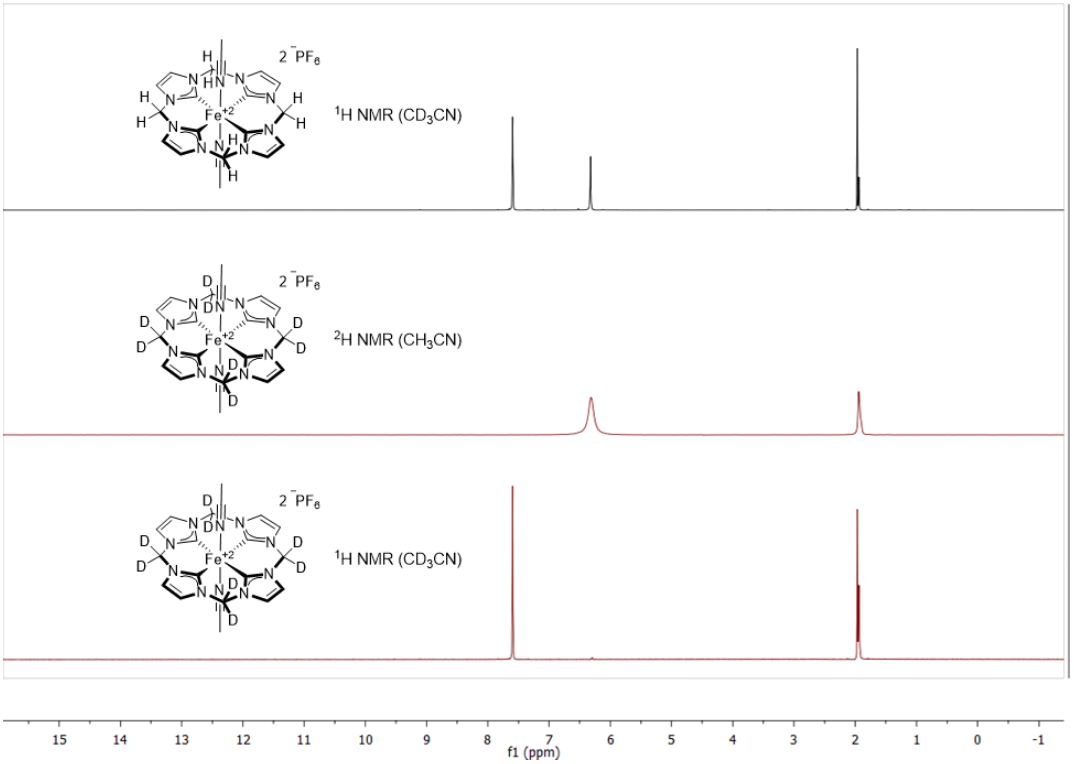

Figure 70: Comparative ^{1}H and ^{2}H NMR spectra of **X** and its non-deuterated species.

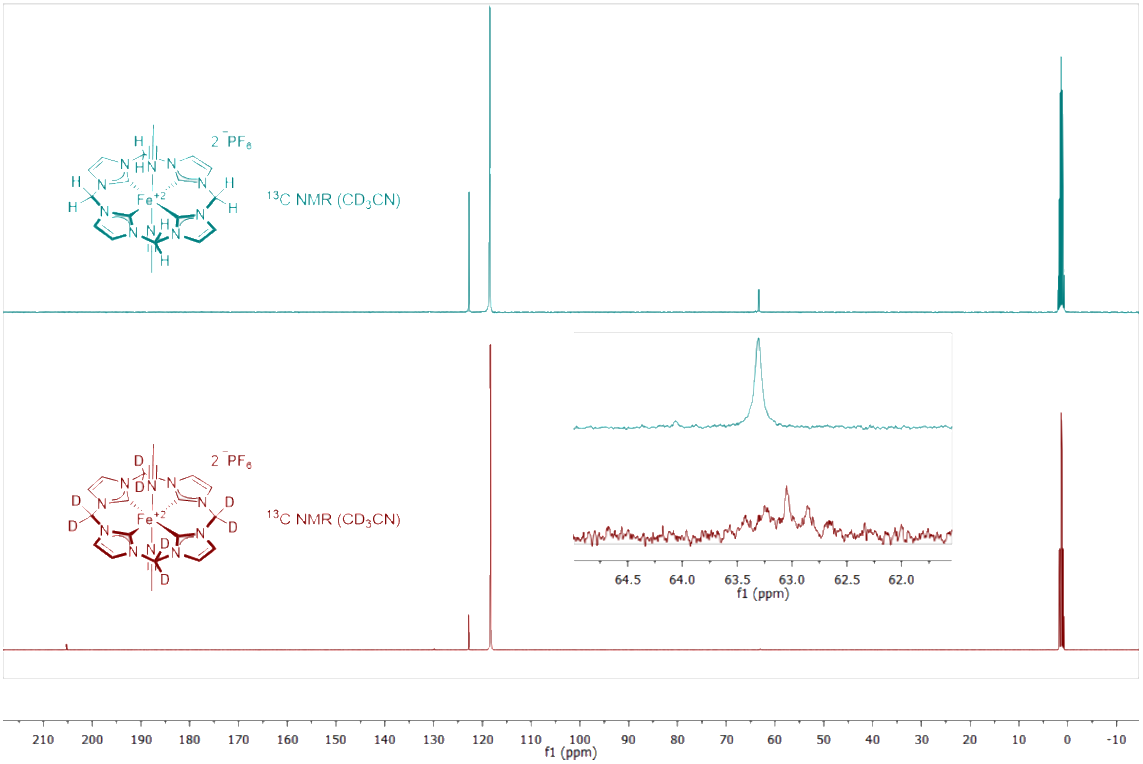

Figure 71: Comparative ^{13}C NMR spectra of **X** and deuterated species. The carbene signal in the non-deuterated analogue could not be resolved.

11.2.11 trans-Diacetonitrile[calix[4]imidazoyl-d_8]iron(III) hexafluorophosphate (**XI**)

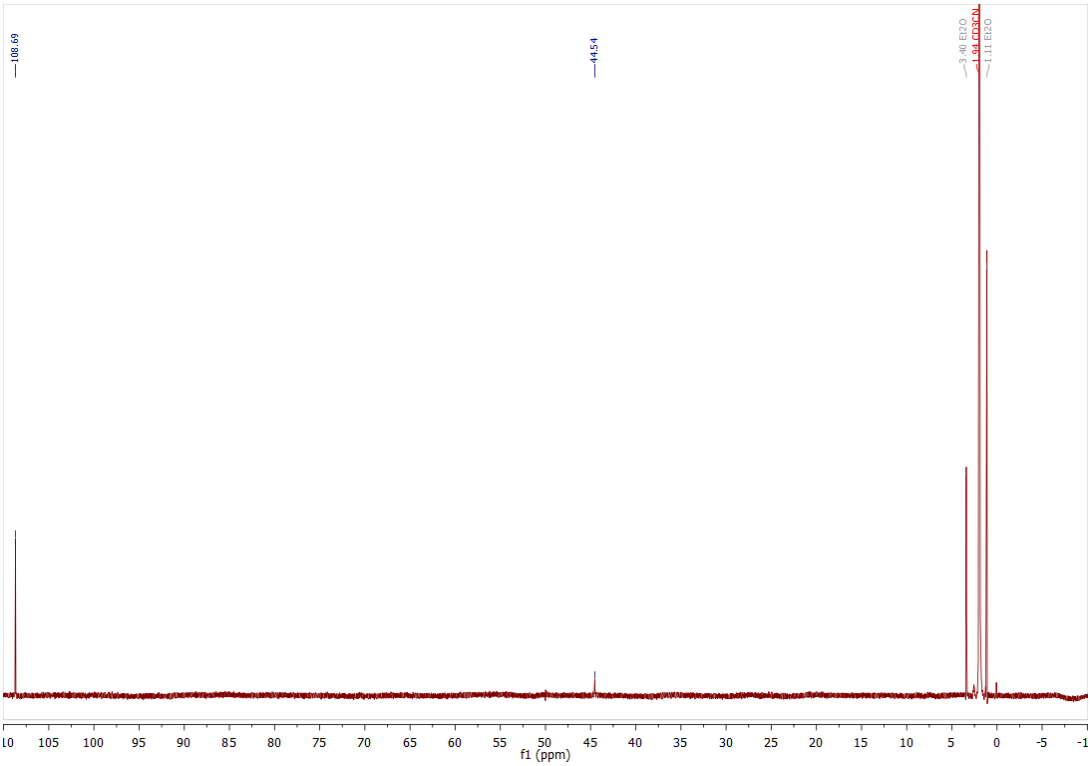

Figure 72: ^{1}H NMR spectrum of **XI** in CD_3CN. Signal integration was not performed due to the paramagnetic nature of the signals.

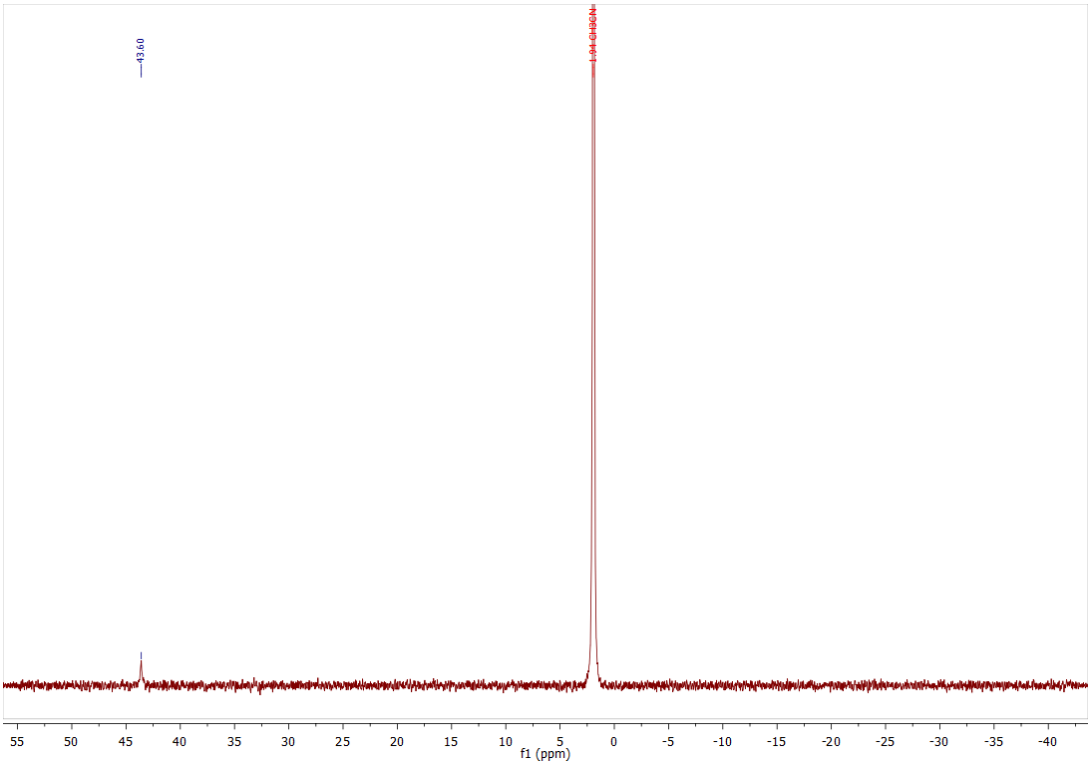

Figure 73: ^{2}H NMR spectrum of **XI** in CH_3CN, CD_3CN is added as referencing standard.

11.2.12 Calix[4](4,5-dimethylimidazoyl)-nickel(II) triflate (**XII**)

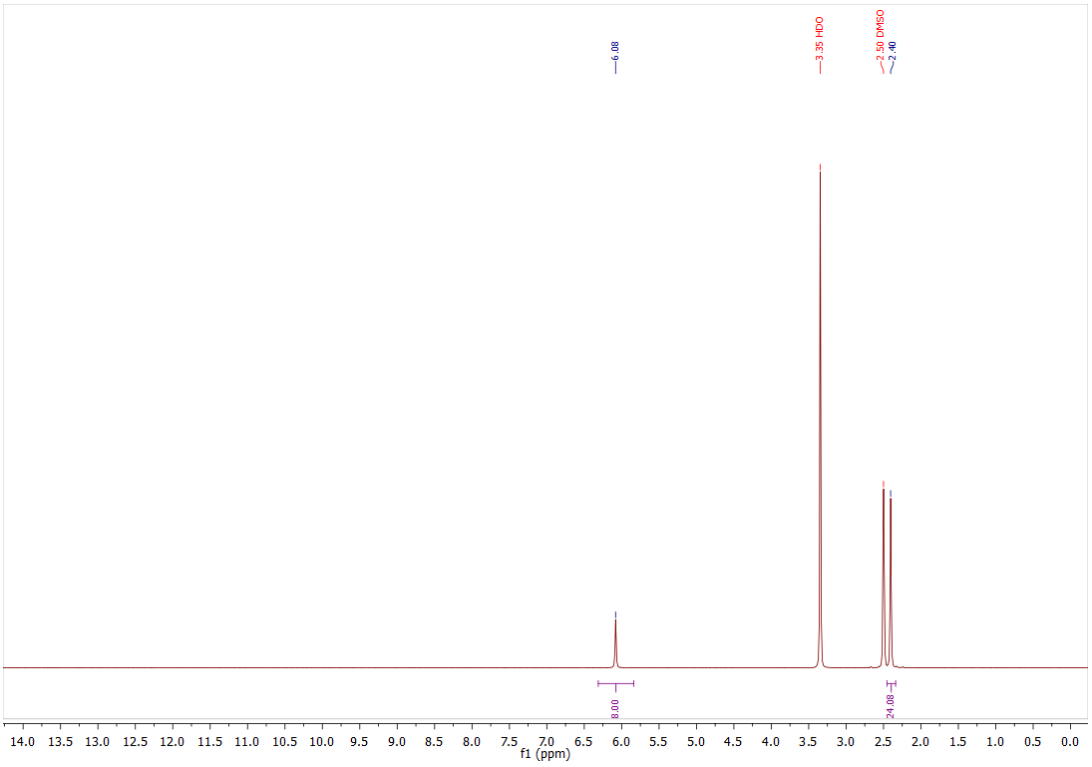

Figure 74: ^{1}H NMR spectrum of **XII** in DMSO-d_6.

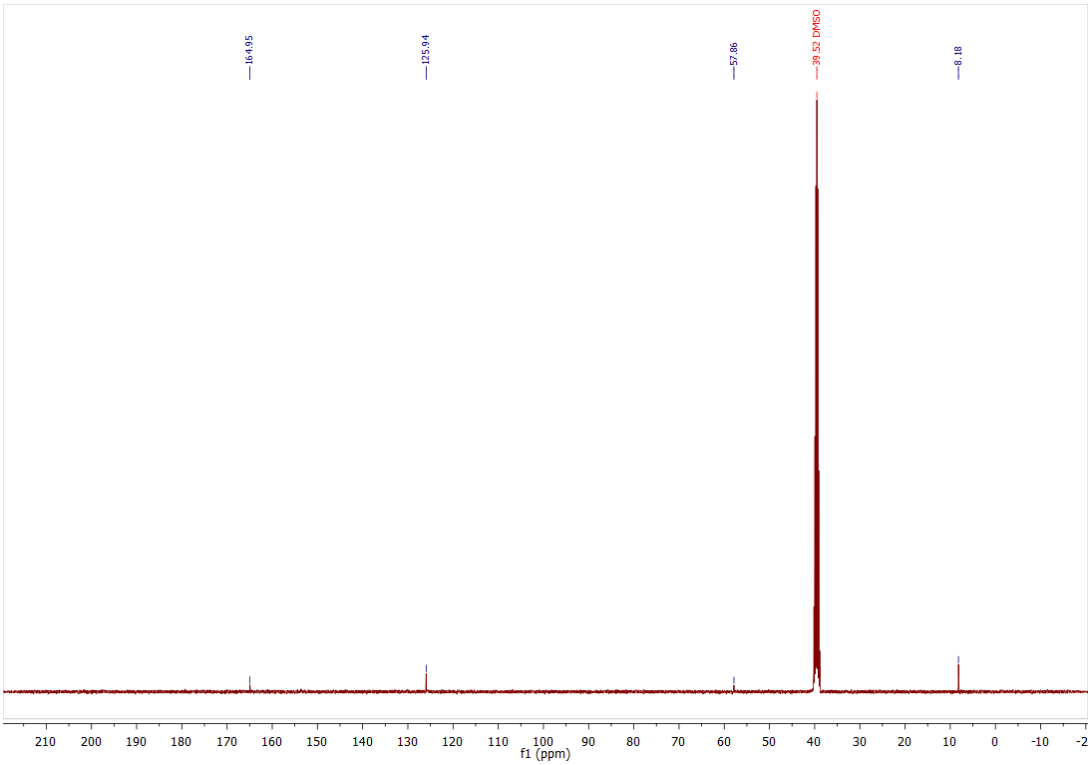

Figure 75: ^{13}C NMR spectrum of **XII** in DMSO-d_6.

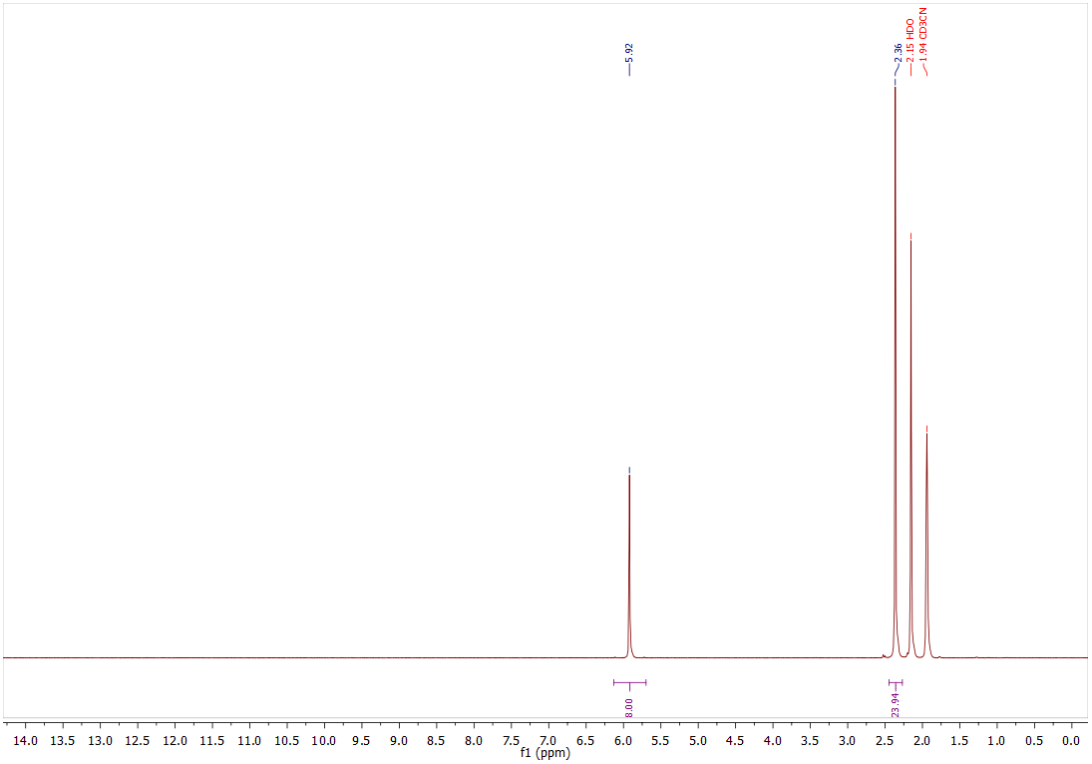

Figure 76: ^{1}H NMR spectrum of **XII** in CD_3CN.

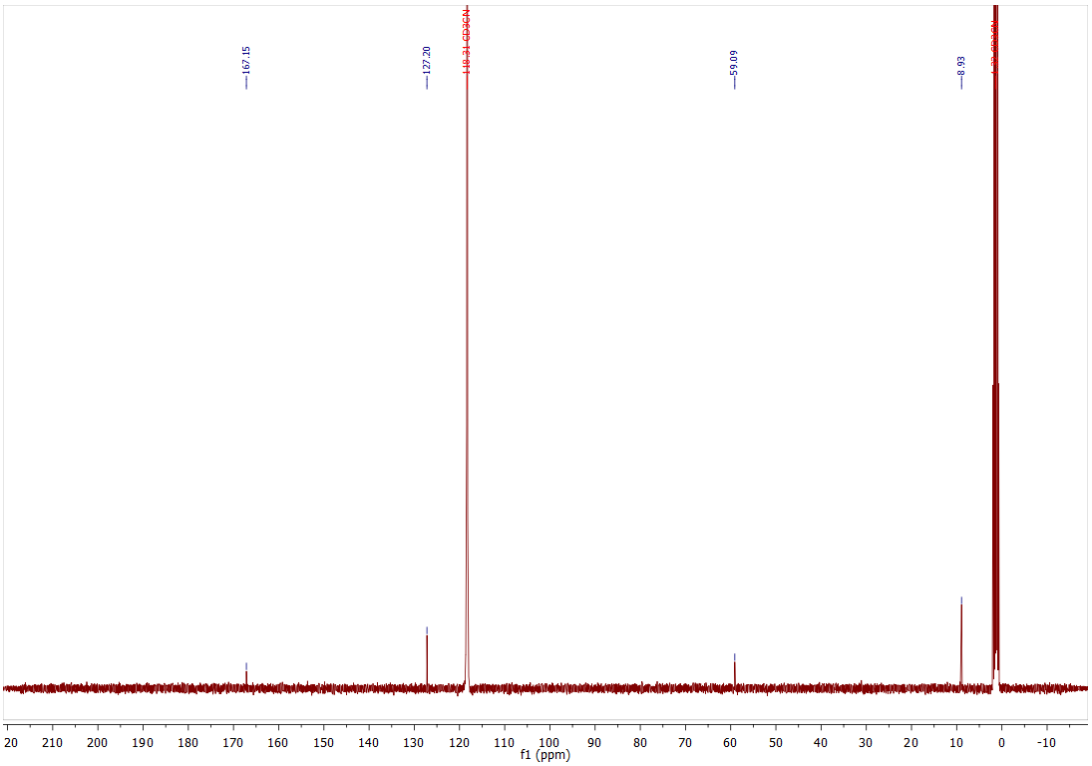

Figure 77: ^{13}C NMR spectrum of **XII** in CD_3CN.

11.2.13 Calix[4](4,5-dimethylimidazoyl)-palladium(II) triflate (**XIII**)

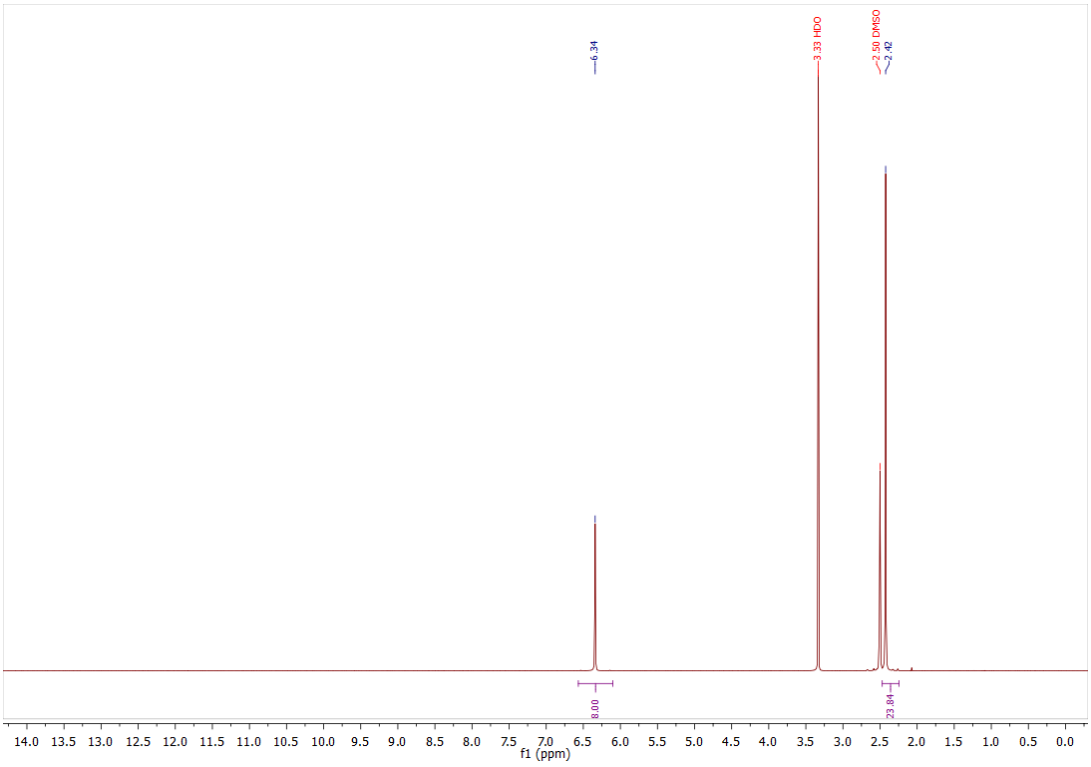

Figure 78: ^{1}H NMR spectrum of **XIII** in DMSO-d_6.

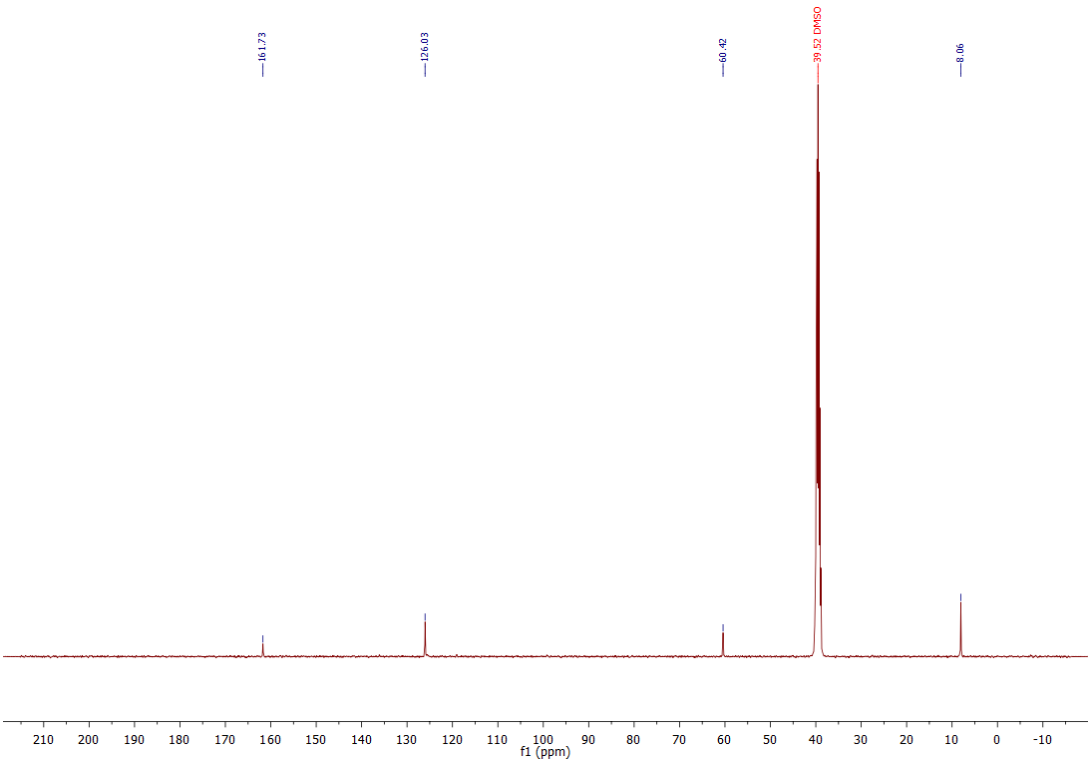

Figure 79: ^{13}C NMR spectrum of **XIII** in DMSO-d_6.

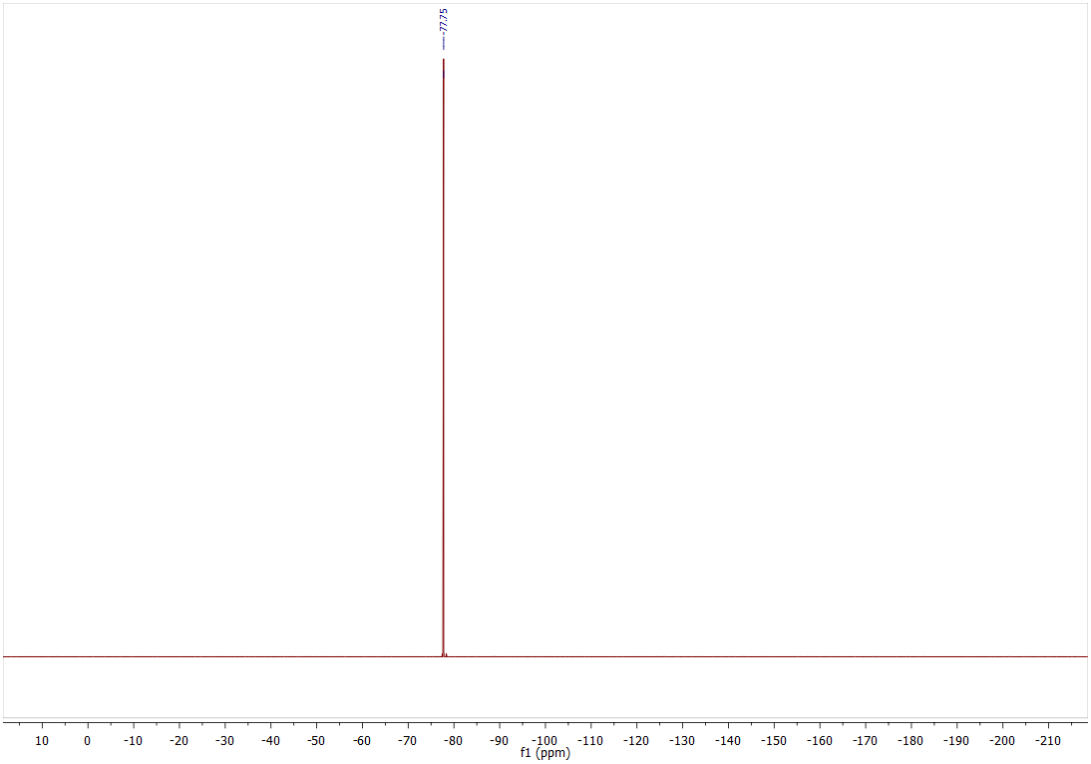

Figure 80: ^{19}F NMR spectrum of **XIII** in DMSO-d_6.

11.2.14 Calix[4](4,5-dimethylimidazoyl)-platinum(II) triflate (**XIV**)

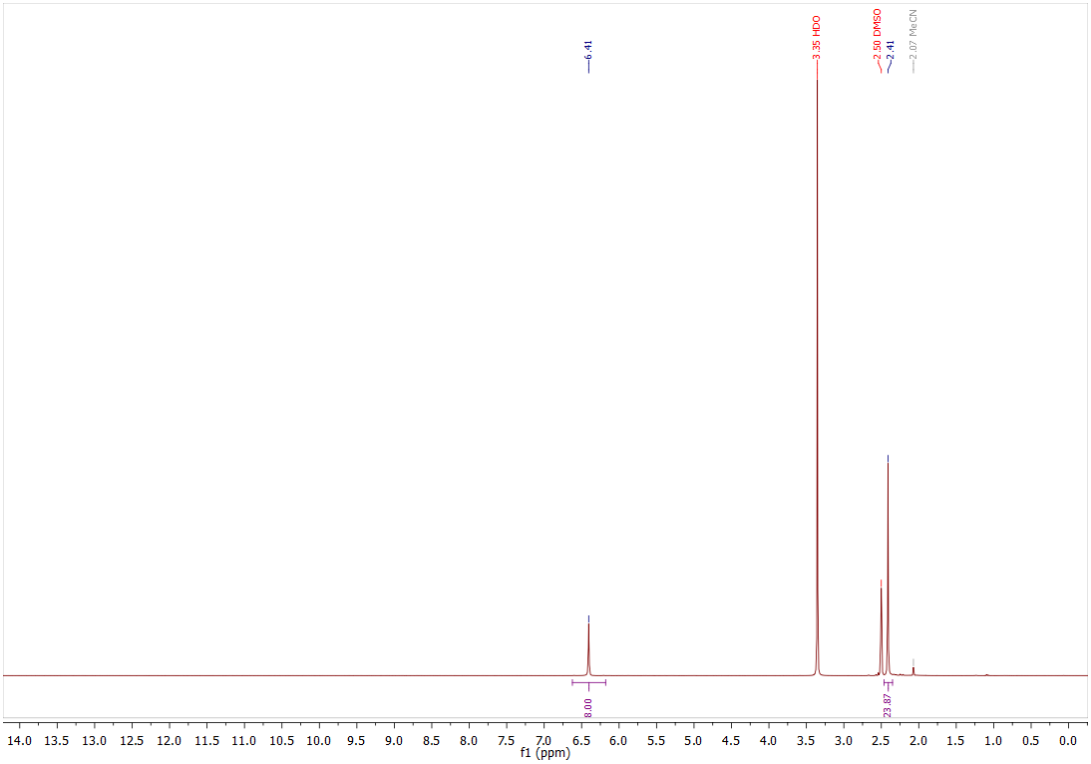

Figure 81: ^{1}H NMR spectrum of **XIV** in DMSO-d_6.

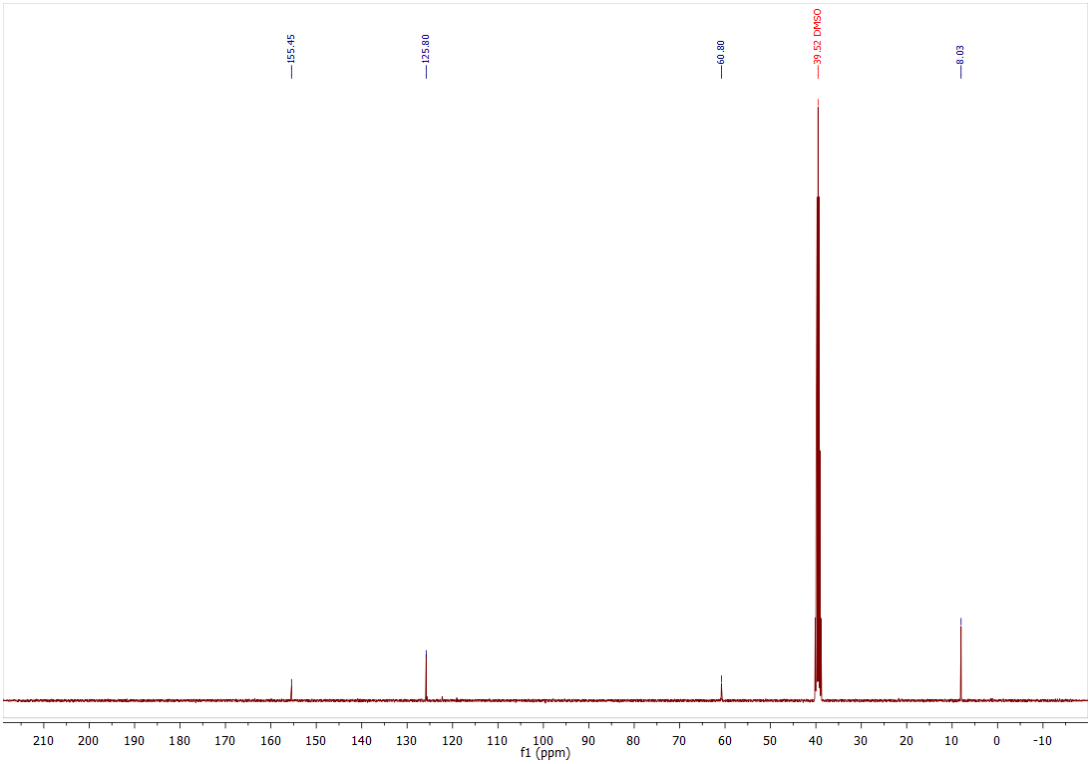

Figure 82: ^{13}C NMR spectrum of **XIV** in DMSO-d_6.

11.2.15 Calix[4](4,5-dimethylimidazoyl)-silver(I) hexafluorophosphate (**XV**)

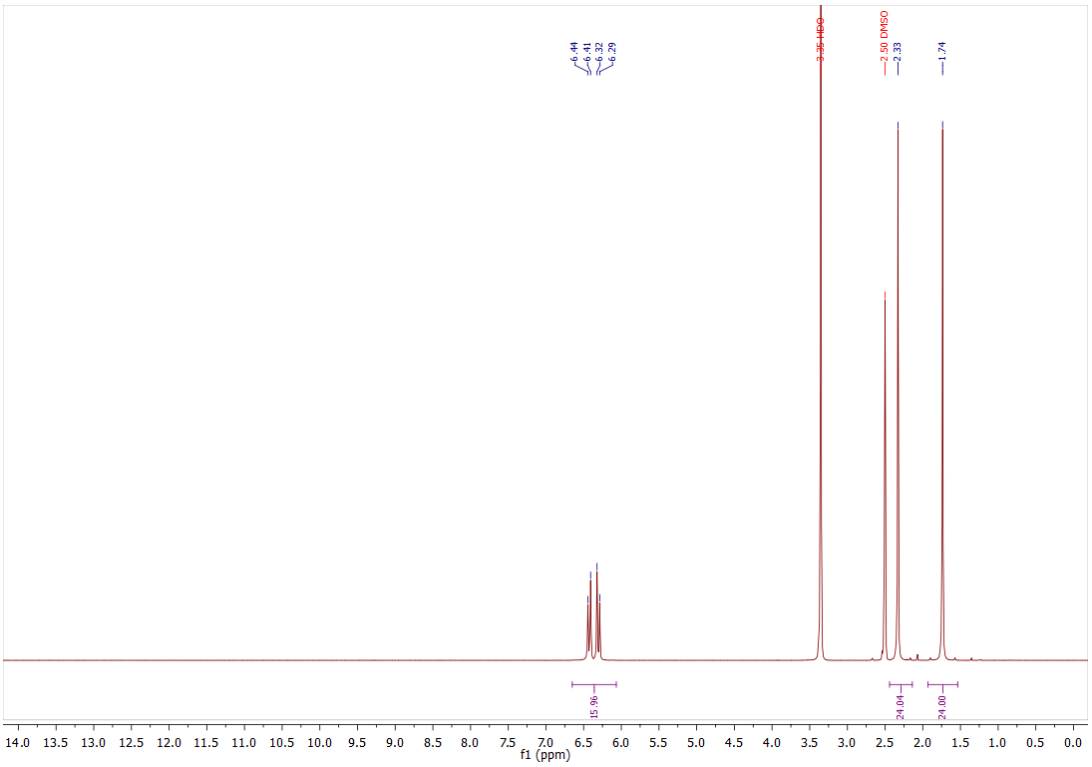

Figure 83: ^{1}H NMR spectrum of **XV** in DMSO-d_6. Comparable chemical regions show multiplicity due to the lower symmetry induced by the structure.

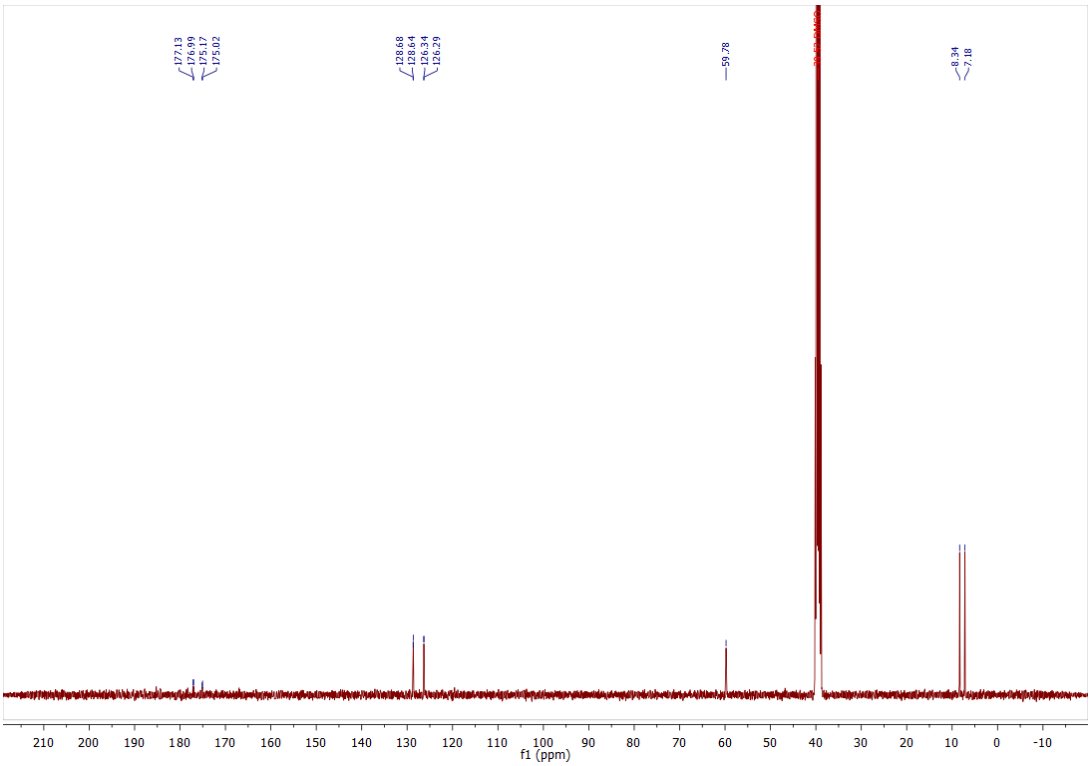

Figure 84: ^{13}C NMR spectrum of **XV** in DMSO-d_6. The carbene signal is split into 4 signals due to coupling with ^{109}Ag and ^{107}Ag. The imidazolyl backbone and methyl groups show multiplicity due to the lower symmetry induced by the structure.

11.2.16 Calix[4](4,5-dimethylimidazoyl)-gold(I) hexafluorophosphate (**XVI**)

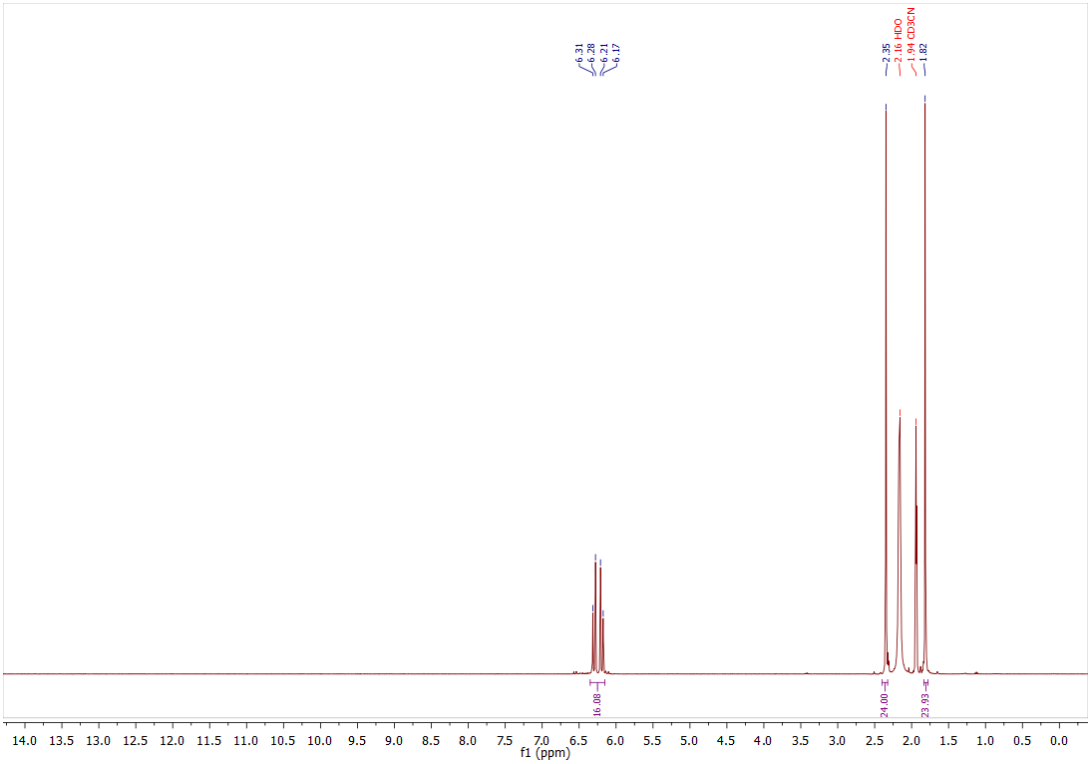

Figure 85: ^{1}H NMR spectrum of **XVI** in CD_3CN. Comparable chemical regions show multiplicity due to symmetry break induced by the structure.

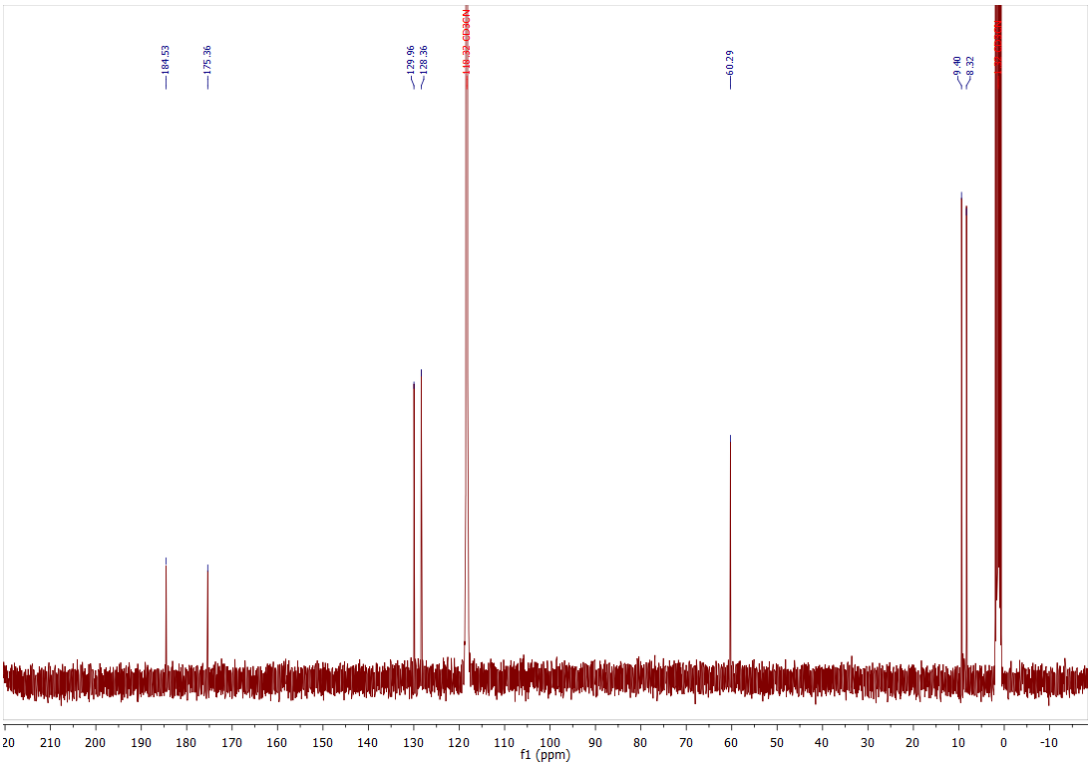

Figure 86: ^{13}C NMR spectrum of **XVI** in CD_3CN. The signal splitting for all chemical regions except the methylene bridges is due to the complexes structure, which can be assumed to be similar to the corresponding Ag(I) complex.

11.2.17 Calix[4](4,5-dimethylimidazoyl)-copper(III) hexafluorophosphate (XVII)

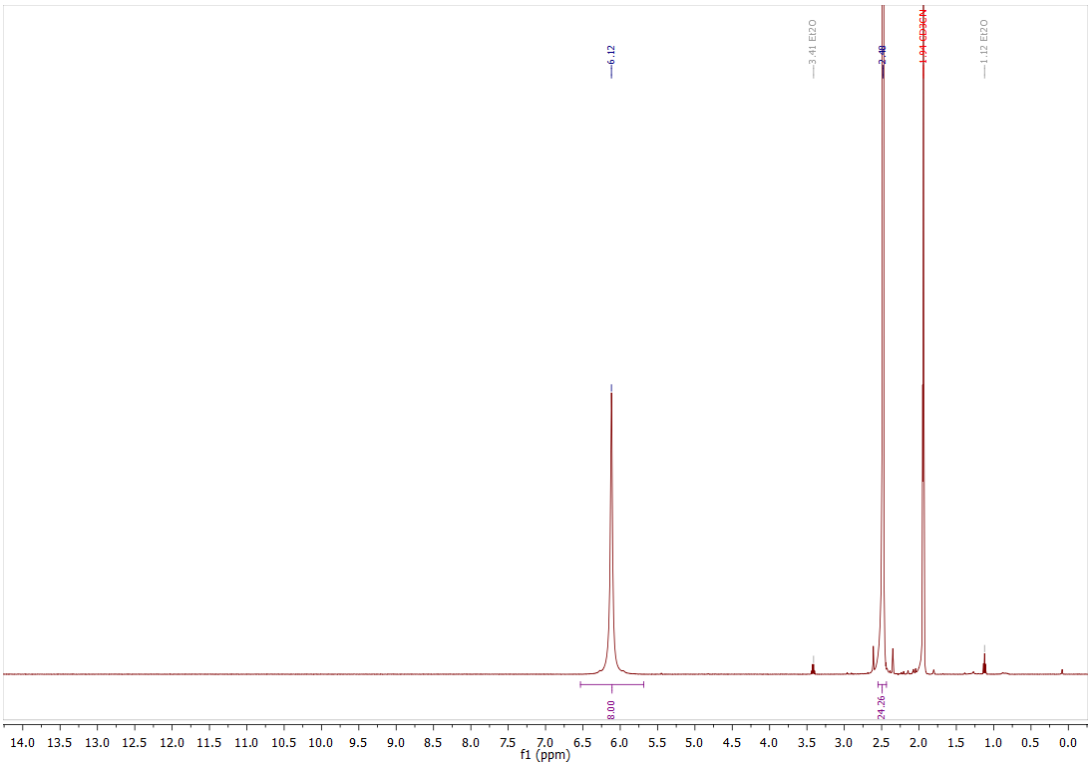

Figure 87: ^{1}H NMR spectrum of **XVII** in CD_3CN.

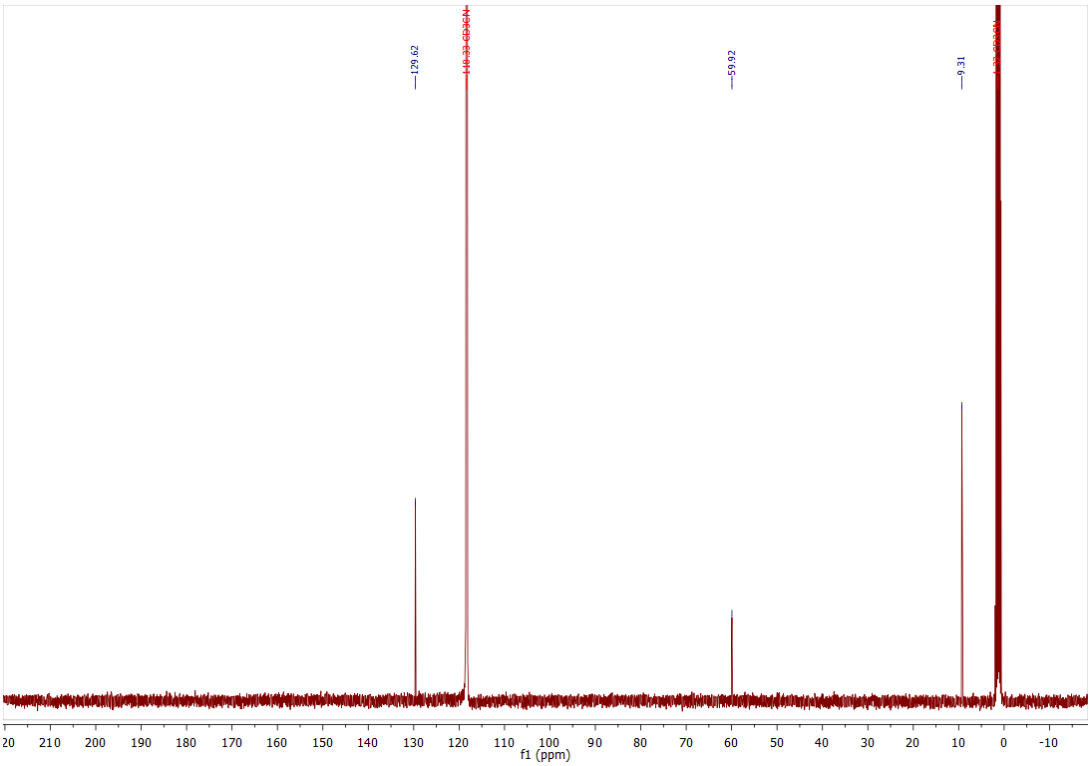

Figure 88: ^{13}C NMR spectrum of **XVII** in CD_3CN. The carbene carbon signal could not be resolved.

11.2.18 Calix[4](4,5-dimethylimidazoyl)-gold(III) hexafluorophosphate (XVIII)

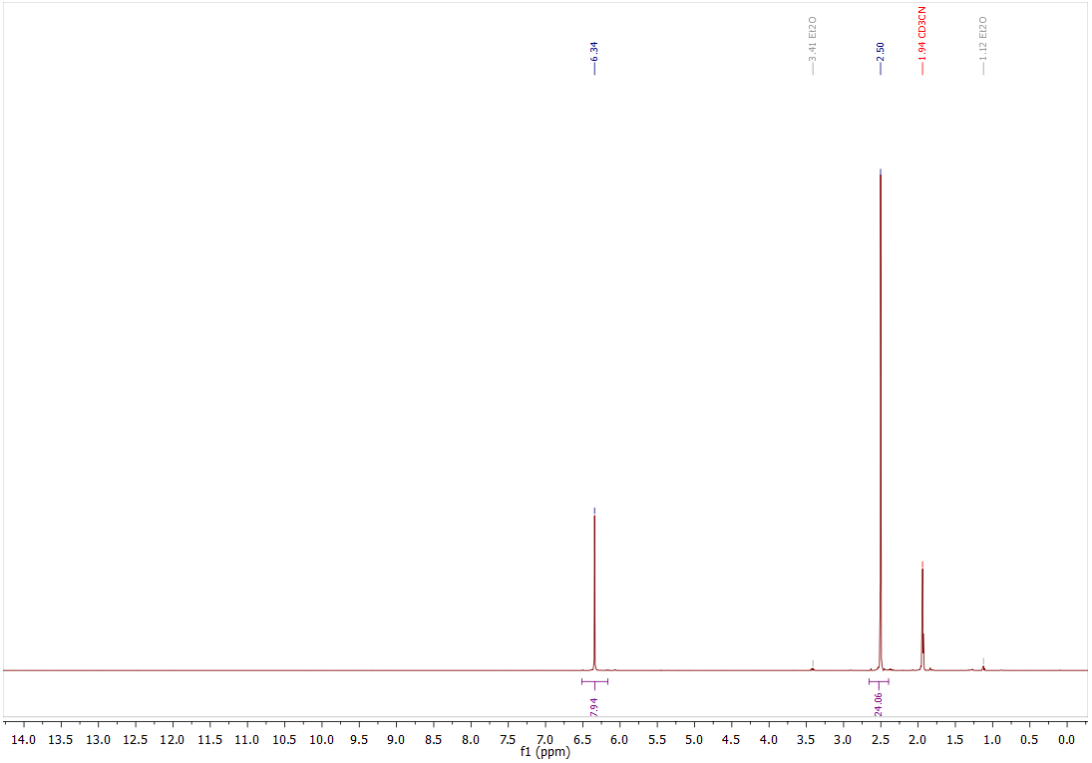

Figure 89: ^{1}H NMR spectrum of **XVIII** in CD_3CN.

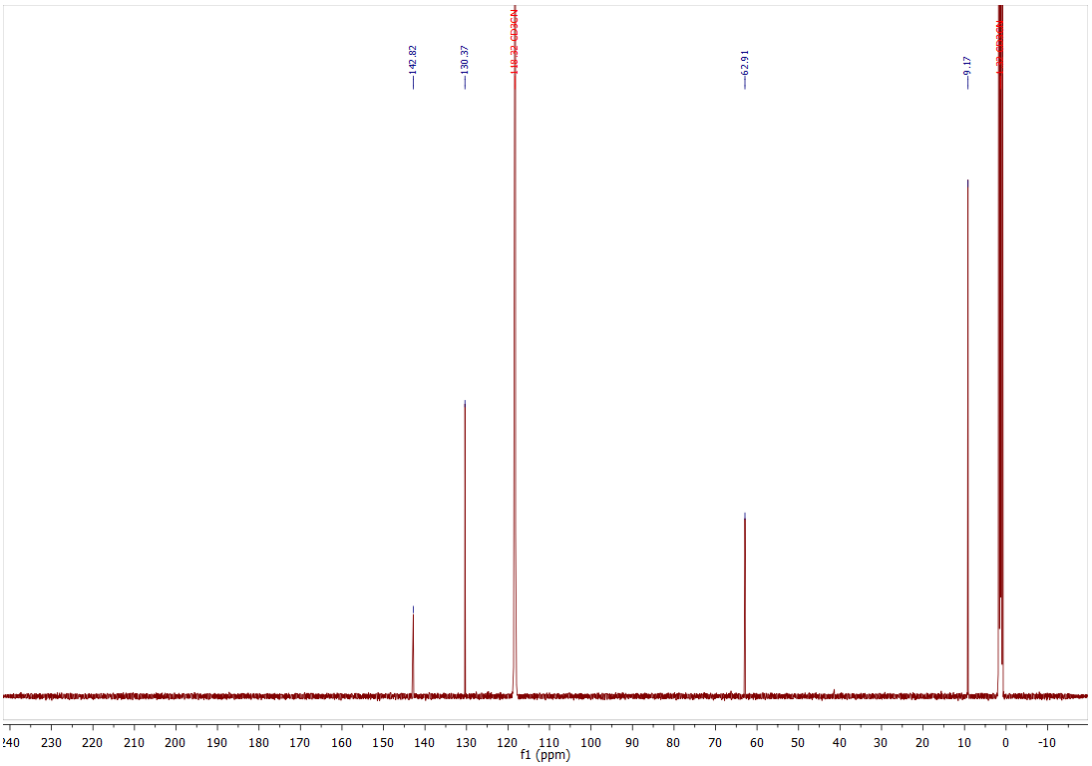

Figure 90: ^{13}C NMR spectrum of **XVIII** in CD_3CN.

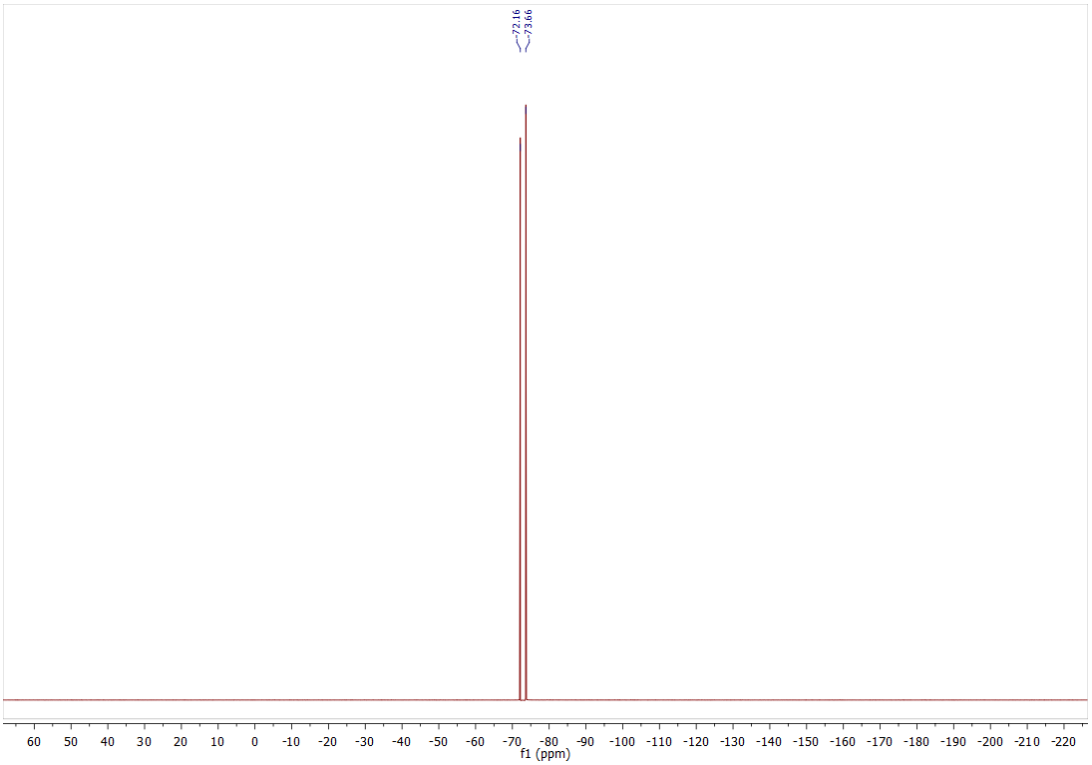

Figure 91: ^{19}F NMR spectrum of **XVIII** in CD_3CN.

11.3 Cyclic voltammetry

11.3.1 Phenyl/aryl substituted macrocyclic iron(II) complexes

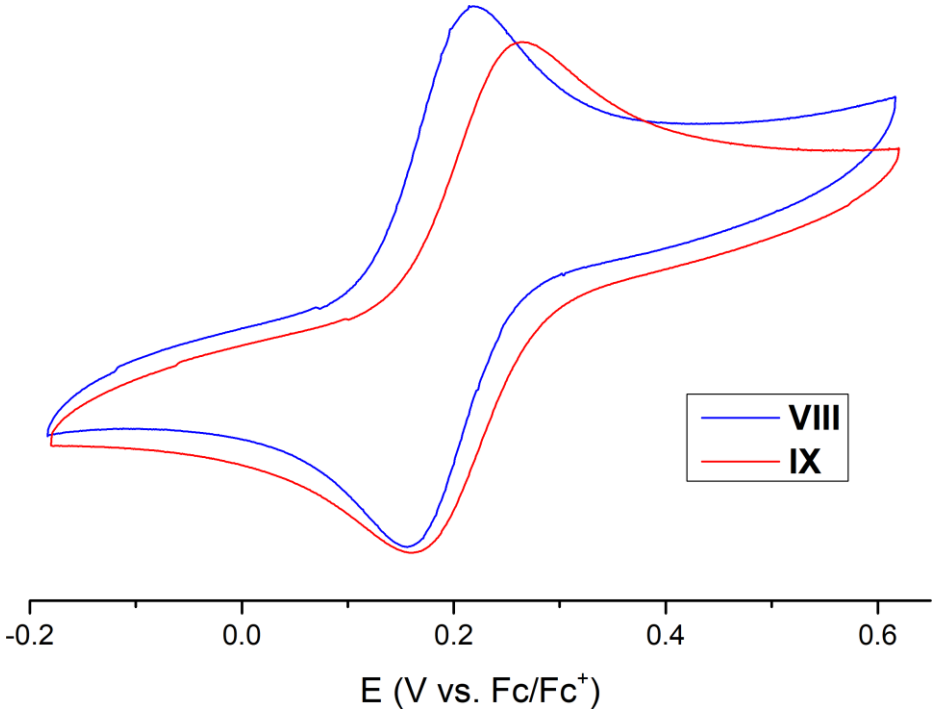

Figure 92: CV of complexes **VIII** and **IX**. The half-cell potential of **VIII** is determined to be $E_{1/2}$ = 0.19 V, with an oxidation potential $E_{ox.}$ = 0.21 V and a reduction potential $E_{red.}$ = 0.16 V. The half-cell potential of **IX** is determined to be $E_{1/2}$ = 0.21 V, with an oxidation potential $E_{ox.}$ = 0.27 V and a reduction potential $E_{red.}$ = 0.16 V.

11.3.2 trans-Diacetonitrile[calix[4]imidazoyl-d_8]iron(II) hexafluorophosphate (**X**)

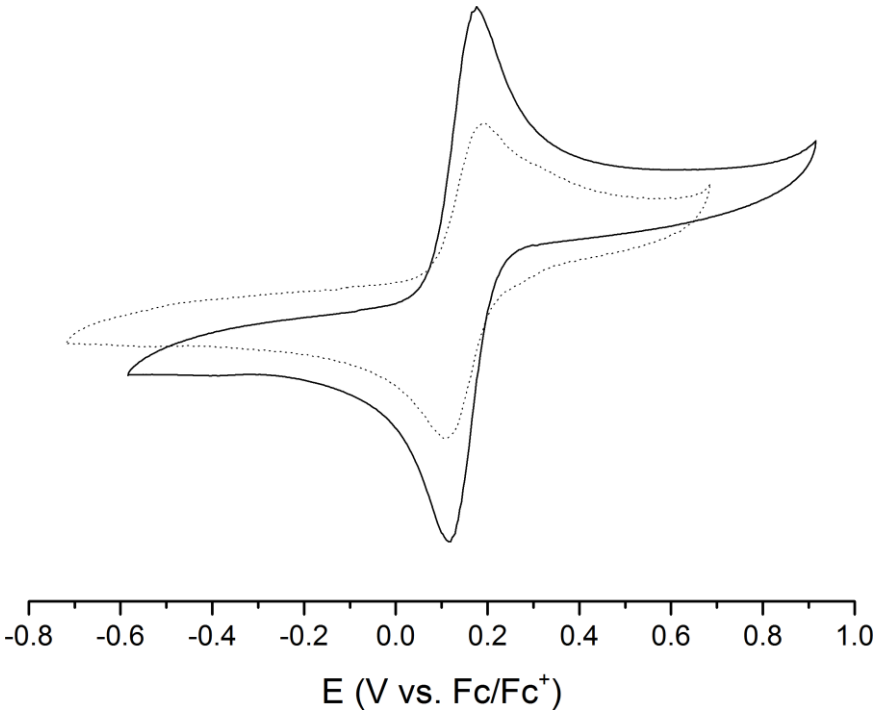

Figure 93: Cyclic voltammogram of complex **X** (solid line). The half-cell potential is determined to be $E_{1/2}$ = 0.15 V, with an oxidation potential $E_{ox.}$ = 0.18 V and a reduction potential $E_{red.}$ = 0.12 V, referenced towards the half-cell potential of the Fc/Fc^+ redox couple. With regard to the measuring inaccuracy, the determined half-cell potential is identical to the non-deuterated derivative (dotted line).[147]